Preferential hydrodynamic, geomorphological, and vegetation ecology conditions for turtle nesting

Al Wajh Bank, Saudi Arabia

Supriya Thadi

Delft University of Technology

TU Delft

Preferential hydrodynamic, geomorphological, and vegetation ecology conditions for turtle nesting

Al Wajh Bank, Saudi Arabia

by

Supriya Thadi

Student Name	Student Number
Supriya Thadi	4776976

Thesis committee:	Prof. Dr. Ir. Stefan Aarninkhof, TU Delft, Chair
	Prof. Dr. Ir. Ad Reniers, Supervisor
	Dr. Ir. J A Alvarez Antolinez, Supervisor
	Ir. M.H.K. Hassan Niazi, Supervisor
Institution:	Delft University of Technology
Place:	Faculty of Civil Engineering, Delft
Project Duration:	May, 2020 - September, 2021

Cover Image: Turtle crawling towards the ocean [92]

TU Delft

Preface

This document presents the master thesis " Preferential hydrodynamic, geomorphological, and vegetation ecology conditions for turtle nesting, Al Wajh Bank, Saudi Arabia". The thesis is an attempt to find the preferential coastal features and conditions for turtle nesting at Al Wajh bank, Saudi Arabia to protect the endangered species. It was written as the final assignment to obtain the graduation requirements for the master Hydraulic Engineering at Delft, University of Technology. The research and writing of the thesis took place between May 2020 and September 2021.

First of all, I want to thank my supervisor Prof. dr. ir. Stefan Aarninkhof for giving me this project. I am also thankful to my daily supervisor Ir. Hassan Niazi who helped me to start and gave direction to this project. I appreciate the positive feedback you both gave and your flexibility with regard to planning of meetings. I am also thankful that both of you always understood my situation and supported me during tough times. I would also like to show my gratitude to Prof. dr. ir. Ad Reniers for sharing his expertise as well as his critical advice on the project. Further, I would like to thank Dr. ir. Jose Alvarez Antolinez for his valuable advice in the final phase of my project which helped to make this report more presentable and for his guidance which helped me to think critically about every step of the project.

Last, but not least, I am grateful to my father, Nagendra Thadi; mother, Jayalakshmi Thadi; and sister, Anusha Thadi, for supporting me throughout my masters. This project wouldn't have been possible without their support. Graduating is a long process with ups and downs and graduating during the Covid-19 pandemic came with challenges. Thank you for putting up with me and for your unconditional love and support, which made me confident in life. My friend, Vivek, also deserves a word of thanks for cheering me up and pulling me through and always being there when I needed it.

I hope you will enjoy reading it.

Supriya Thadi
Delft, September 2021

Summary

Sea turtles are a popular tourist attraction that offer travelers a unique nature experience. As a part of Saudi Arabia's 2030 vision an unprecedented amount of tourism development is being carried out under the 'Red Sea Development Project'. The aim is to develop hyper - luxury islands in a sustainable and ecologically friendly way by closely following 'Building with Nature' principles. The tourism development site at Al Wajh Bank encompasses an archipelago of more than 90 islands and some of the sandy islands provide nesting grounds for Hawksbill and Green turtles. The thesis is a component of a broad study on investigating the preferential conditions for the sea turtle nesting and conservation where TU Delft is collaborating with NIOZ and KAUST. The present study makes a preliminary assessment of the preferential conditions for sea turtle nesting of wave hydrodynamics and geomorphological conditions based on available data and numerical wave model simulations. The study is expected to provide information and guidance for future research for the conservation of sea turtle nesting at Al Wajh Bank.

The coral reefs provide breeding grounds for sea turtles in the gently sloping sandy beaches along the raised islands where the sand has ideal conditions of moisture, temperature, and distribution of sediment size for successful nesting and hatching of eggs at an optimum distance from the highwater line to avoid inundation by wave runup. In general, the foreshore at the turtle nesting site has a fore reef with steep slope followed by wide and shallow reef flat having high bottom roughness for dissipation of wave energy. The Al Wajh Bank spread over an area of 2880 km^2 has a very large and complex barrier reef system at the outer edge in the deep sea enclosing a massive lagoon with several islands. These islands have sandy beaches on the up wave (windward) side and mud flats with sand and vegetation in the sheltered zones. The vegetation is dominated by mangroves in the mud flats and sea grass in the shallow lagoon beds.

The study used the Delft3D WAVE stand alone phase averaging spectral wave model for transforming waves from offshore to nearshore and to examine the energy dissipation characteristics of the reef system. The high resolution bathymetry data for the Al Wajh Banks was obtained from GCC and a relatively coarse resolution data for the offshore from GEBCO. The model simulated offshore wind and wave data validated using satellite altimetry, SAR and Buoy measurements was obtained from BMT ARGOSS online services website "waveclimate.com". The normal and extreme wave conditions were derived using this data. The data on GPS coordinates at the location of turtle nesting sites was provided by a survey undertaken by KAUST. A limited data on sediment size distribution at four islands south of Al Wajh Bank was made available by KAUST collected by ALS Arabia. The data on beach slopes, distance of nests from HWL, geomorphology, vegetation was derived from secondary sources or in an indirect manner using bathymetry data.

The wave model results were analysed for the nearshore wave heights and distribution of energy density at the fore reef and inside the lagoon. The wave model results revealed that the extensive barrier reef on the seaward side of the Al Wajh Bank is able to completely prevent and dissipate the energy of the offshore waves providing ideal conditions for turtle nesting at seaside islands. Further, the results show that the offshore waves do not have any role in the production and dissipation of wave energy inside the lagoon. The study confirmed that the waves inside the lagoon are exclusively local wind generated waves. The wave climate inside the lagoon during storm conditions is only influenced

by the prevailing strong winds and not dependent on the storm generated extreme waves from the offshore.

Most of the sea turtle nests have been found on the up wave or windward side of beaches with flat and wide reefs or fringing reefs between the reef crest and the high-water line. The wave model demonstrated the large energy dissipation rates under these geo-morphological conditions. In the absence of relevant data on sediments for the nesting and non-nesting beaches no specific conclusions could be drawn. The beach slopes where sea turtle nests were abundant had slopes in the range of 1:10 and 1:20. The study indicated that the non-nesting sites inside the lagoon are in the sheltered zones of inner reef shelfs and behind the islands where mud flats with mangrove and other vegetation are abundant.

The wave runup is estimated using the HyCReWW metamodel at the nesting and non-nesting sites. The metamodel estimates indicated that the wave runup is of comparable magnitude both for the nesting and non-nesting sites. The comparison of runup distance along the beach indicated that the turtle nesting sites are located sufficiently away from the runup computed for 1 in 100 year wave height

A satellite imagery based global shoreline data source (Shoreline Monitor, Deltares/TUDelft) was used to examine the erosion and accretion trends at Al Wajh Bank. The data identified two of the islands as having chronic erosion which have a small percentage of nesting sites. The analysis of the data identified that the turtle nesting sites are located on beaches with stable erosion / accretion rates.

The study confirmed the limitations of the Delft3D WAVE (SWAN) model used in simulating IG waves. Due to very large domain and the course grid adopted in the present study the wave setup aspects have not been covered. The present study was useful in providing a range of information and guidance for further hydrodynamic and geomorphological data inputs at a regional scale and application of models like X-Beach or SWASH for a more comprehensive and detailed analysis on the influence of the surf and swash zone dynamics including IG waves on the sea turtle nesting sites. A systematic data acquisition on geomorphological and sediment characteristics will be useful for logistic regression analysis to study the dominant factors influencing the turtle nesting and non-nesting sites.

Contents

Nomenclature

Abbreviations

Abbreviation	Definition
ALS	Australian Laboratory Services
AMM	Annual Maxima Method
ANOVA	Analysis of Variance
CFSR	Climate Forecast System Reanalysis
DIA	Discrete Interaction Approximation
ECMWF	European Centre for Medium Range Weather
EVA	Extreme Value Analysis
GCS	General Commission of Survey
GEBCO	General Bathymetric Chart of the Oceans
GEV	General Extreme Value
GPD	General Pareto Distribution
HW	High Water
IG	Infragravity waves
LAT	Lowest Astronomical Tide
LTA	Lumped Triad Approximation
LW	Low Water
POT	Peak Over Threshold
ppt	Parts per thousand
RMSE	Root Mean Square Error
SAR	Synthetic Aperture Radar
SWAN	Simulating Waves Nearshore
WAM	Wave Modelling
WRF	Weather Research and Forecasting

List of Figures

List of Tables

1

Introduction

1.1. Background

The Al Wajh Bank, located along the east coast of Red Sea in Saudi Arabia's Tabuk region, has been in the news due to an ambitious tourism development project proposed by Saudi Crown Prince Mohammed bin Salman in July 2017 as part of the Red Sea Project (RSP). The project is expected to incorporate eco-engineering methods while also promoting large-scale tourism. A study supported by RSP used conservation planning tools to develop Marine Spatial Planning for the region, which resulted in conservation zoning to prioritise and protect the area from present and future impacts [18].

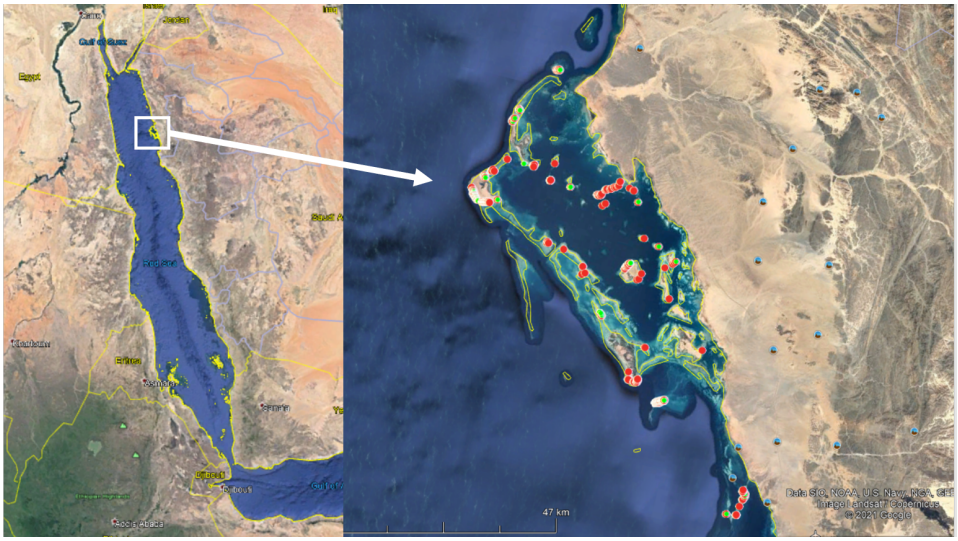

Figure 1.1: Red Sea development project site location with Red and Green dots representing turtle nesting areas

The Al Wajh Bank is spread over an area of approximately 2880 km^2 in the northern part of Red Sea ($25^\circ\ 5'N$, $36^\circ\ 45'E$) from Al Wajh town in the north to Umluj in the south. The location is of high ecological importance, including a large central lagoon, a complex reef system, and about 90 pristine islands. The outer boundary of the Al Wajh Bank stretches between 26-40 km from the mainland, with a length of around 76 km along the coastline. The lagoon and the islands harbor a diverse range of

fish, corals, and marine organisms, as well as shallow grass beds, algal communities, and mangrove ecosystems [12]. Some of the islands on the rim of the reef barrier system and inside the lagoon have favorable breeding grounds for Hawksbill and Green Turtles. A survey conducted by KAUST in 2018 under the Red Sea Project revealed a total of 37 islands having turtle nests. Most of the nests were found on Birrim island located on the northern rim of archipelago which had 660 nests of Green turtle and 125 nests of Hawksbill turtle. The other island with most nests is Al Waqadi located south of the archipelago with 397 nests of Hawksbill Turtle and 37 nests of Green Turtle. The Al Wajh Bank with the Turtle nests is shown in Figure 1.1. The distribution of Hawksbill and Green Turtle nests on various islands as per the survey is given in Table A.1 at Appendix A.

The Hawksbill and Green Turtles are two of the seven turtle species that are critically endangered. These two turtles are members of the Cheloniidae family of sea turtles, which are known for their hard shells. Nesting is typically seasonal lasting between two and six months of the year. The name hawksbill turtle comes from its narrow, elongated jaw, which resembles a hawk's beak. Grown - up hawksbill turtles weigh between 40 and 80 kg and have shell length ranging from 50 to 90 cm. The sharp beak is well adapted to a diet of sponges, marine plants, tunicates, sea anemone, and mollusks marine plants. Hawksbill turtles can be found in shallow-water coral reefs in tropical areas. Hawksbill turtles have been subjected to extensive harvesting for the beauty of their carapace all throughout the world. Tortoiseshell hair combs and eyeglass frames were once manufactured from their shell scutes. Green turtles weigh 65 to 200 kg and has straight-line carapace length (SCL) of 80 to 120 cm. Green turtles are herbivores that live in shallow tropical waters. They visit more temperate locations on a seasonal basis. The turtle gets its name from the thick, close to green colour fat deposit present behind the carapace, which is used to make turtle soup.[81]

Observing nesting sea turtles has become a popular tourism attraction for visitors to the coastal areas. Participation in this activity is important because it improves people's understanding of sea turtles, raising public awareness and increasing the number of people who conserve and care for sea turtles in general. This activity also generates a substantial amount of revenue and jobs in the neighbourhood. However, if nesting females are disturbed, the presence of humans on the beach can cause them to abandon their nesting process [61]. Natural disasters such as floods during storms and rising sea levels can result in nesting habitats being eroded and destroyed. Sea turtle nesting habitats are becoming increasingly threatened as a result of human infrastructure and coastal changes, and knowing how this will directly effect sea turtle species is critical for sustainable management and conservation of nesting sites [60].

It is clearly established by various investigations that the sea turtles look for a set of unique geomorphological and microclimatic conditions in their nesting habitats on sandy beaches which decide the hatching success of the eggs and safe return of the hatchlings to the sea. The islands of coral atolls and barrier reef systems have been known for providing safe havens for millennia with these unique features for sea turtle breeding. The reef systems exposed to the waves and the tidal fluctuations transform and dissipate the wave energy which in turn aid in the morphological and ecological evolution of the reef Islands and sandy coastlines. The hydrodynamics related to wave propagation and transformation along with tidal fluctuations in the reef environment are the primary drivers in shaping the conditions for safe turtle nesting habitats. Modeling hydrodynamics of nesting areas is therefore necessary for understanding the nesting preference. Nesting behaviour would vary in the future as a result of changes in the coastal ecosystem caused by climate change, sea level rise, and human interference.

1.2. Preferential Conditions for Sea Turtle Nesting

It is unclear why or how turtles chose a specific nesting location. The physical characteristics that female turtles use to choose a nesting area are not well understood. The microclimate of the beach sediments [72], which impacts egg survival, hatching, and the male-to-female ratio [63], will have an impact on the nest placement. The temperature of the nest determines the sex of sea turtle hatchlings [86]. The nest microclimate is shaped by the general climate of the beach, the location of the nest in respect to the vegetation, and shoreline [47]. Beach slope, salinity, temperature, beach width, and distance to vegetation and high water line are all important characteristics to consider while choosing a nesting site.[99, 97]. Although it has been established that natal location influences beach selection, the specific location of the nest varies by species and circumstances at each nesting site with respect to slope, elevation and distance from the vegetation and high water line [97].

Coastal developments is typically unsuitable for sea turtle nesting locations at the critical stage of their lives. Seawalls on the beach or in the surrounding zones, beach nourishment or sand extraction, and the removal of vegetation cover on dunes, to name a few examples, all contribute to erosion and have a direct influence on sea turtle habitat. The sand temperature, on the other hand, influences the hatchlings' gender. Depending on the species and beach temperature, the eggs take 45 to 70 days to develop [44]. At higher temperatures, females are produced, whereas males are generated at lower temperatures. The crucial temperature, which yields an equivalent number of males and females, is between $28°C$ to $31°C$ [1]. Building large structures or eliminating natural flora near the shore may change sand temperature, resulting in an unequal sex ratio of hatchlings. There have been several issues raised about the impact of global warming on sea turtles, ranging from a change in sand temperature to a faster rate of coastal erosion.

The hatchlings emerge from the nests by moving the sand upwards to the surface. The temperature of the surface sand is important when the hatchlings emerge from the nest. When hatchlings come into contact with hot sand during the day, they become inactive; but, when temperatures drop at night, they become active again [81]. Predators such as crabs, dogs, birds, lizards, and raccoons may prey on the hatchlings, causing many of them to die. To reach the ocean, the hatchlings crawl towards the brighter seaward horizon [58]. Unlit beaches are generally lighted by the reflection of light from the moon and stars at night, and by the rising sun at dawn. Artificial lights from buildings or streetlights on developed beaches may cause hatchlings to become disoriented and die before reaching the sea due to dehydration. As a result, any artificial light shining on the shore might confuse the hatchlings by interfering with natural sea-finding cues, preventing them from finding the ocean [90].

The movement of coastal sediments and the formation of beaches and backshore dunes are influenced significantly by nearshore sea and swell waves, as well as associated currents and the wind. These are some of the places preferred by turtles for nesting,. Unlike the beaches of the mainland shoreline, coral reef coasts feature substantial physical differences as well as unique hydrodynamic processes. Reef dynamics are influenced by waves and wave-generated currents, and the friction effects of fringing and barrier reefs which dissipate energy, altering how much wave energy reaches the shoreline and the lagoon behind the reefs. The large variations in wave energy and exposure to severe storms can explain the reef formation. The change of energy gradients with depth in the forereef zone and over the reef crest is widely acknowledged as having a major impact on both coral reef biological zonation and sediment dispersal and deposition [24]. Wind and wave-generated currents are also known to impact sediment movement over the reef and reef flats, as well as having major control over the availability of nutrients and food for corals and other reef species. Wave energy levels and storm occurrence have been found to have broad relationships with reef zonation and wave climatology, of

coral reefs [36]. Wave breaking or bottom friction, in principle, raises the mean water level, providing a pressure gradient that aids flow over the reef along the wave propagation direction [98].

1.3. Coral Reefs and Wave Hydrodynamics

The three distinct zones of coral reef system are: the fore-reef, reef crest, and back reef. The back reef comprises the shallow lagoon between the shore and coral reef. The lagoon habitat includes small patches of corals, sea grass beds, and sand plains. The back reef waters are generally warm due to the shallow depth, reduced water flow, and protection from waves. The reefs act as barrier for transmission of wave energy to the back reef, thus protecting the coastline. Dissipation of wave energy over coral reefs has a major role on reef morphology, stability of island shoreline, distribution of marine organisms and nutrient uptake. The back reef salinity can change due to inputs of freshwater. Rainfall and runoff can transport sediments from coast causing increase turbidity in this zone. The fore reef is the steep sloping section at the ocean side of the reef and extends down in depth to a sand plain. The fore reef is less influenced by the wave hydrodynamics due to the steep slope along with large depths and provides conditions ideal for coral growth compared to other zones. The highest diversity of corals is found in the fore reef at 15–20 m depth due to light accessibility and transport of nutrients for coral reef communities from deeper waters by internal waves and currents.

The reef crest is the pinnacle of the reef and can be exposed during extreme low tides. The reef crest encounters harsh environment and breaking waves limit the diversity of marine organisms including corals to only a few species that can survive in this high-energy zone. Waves undergo dramatic changes when they encounter coral reef environment. The geometrical features of coral reefs generate hydrodynamic environments different from those of beach systems along the coasts. The steep fore reef slope and sudden transition from relatively deep to shallow water between the fore reef and outer reef flat leads to wave transformation involving shoaling, refraction, diffraction, and dissipation by wave-breaking and enhancement of bottom frictional effects. The evolution of beach geometry and sediment distribution due to the transport of sediments by wave induced runup and currents has a significant impact on sea turtle nesting sites.

Winds acting on the water surface off the coast transfer energy and produce waves that leave the generating area and move towards the shoreline. These waves propagate and are transformed by various processes such as wave diffraction, refraction, and shoaling, and superimpose locally generated wind waves. Wave energy is dissipated when waves encounters a nearshore zone with shallow and complicated bathymetry in the presence of islands or reef flats. Wave refraction is one of the most visible characteristics of wave crests entering shallow water at an angle. Because various sections of the wave crest are in different depths of water, these lines do not break at the same time. Waves are affected by depth; as they feel the bottom, they change, and waves traveling towards the coast at an angle align their crests parallel to the coastline. After propagating across the rough reef terrain, waves may be dampened on the shallow reef flats owing to frictional dissipation. In the presence of sufficiently shallow depths, the dissipation of wave energy will take place due to wave breaking along the relatively steep forereef [98, 70]. Coastal areas are thus protected by coral reef banks against wave and storm hazards such as flooding, overtopping, wave runup, and erosion.

Complex systems of fringing and barrier reefs characterize the littoral areas along the Red Sea shoreline. The shoreline and backreef lagoons are effectively protected by these coral reefs, which substantially dissipate wave energy. Despite the numerous studies on the Red Sea reef hydrodynamics and ecosystems, no research on the wave climates of reef-protected areas has been undertaken.

The wave climate of such an environment is important to study because it influences not only the processes that lead to morphological changes in coastal reefs and the coastline, but also the washover and inundation of turtle nesting areas, especially when high-energy waves are present.

The energy in water waves is made up of two components:

1. Kinetic energy (E_k) associated with the orbital motion of the water particles.
2. Potential energy (E_p) resulting from displacement of the water surface away from the still water level (SWL).

According to Airy wave theory, the potential energy computed with reference to the still water level and assuming all waves propagate in the same direction, the two energies are equal, and the total energy per unit crest width is given by:

$$E = E_k + E_p = \frac{\rho g H^2 L}{16} + \frac{\rho g H^2 L}{16} = \frac{\rho g H^2 L}{8}$$

Where H is the wave height, g gravitational acceleration, ρ is the density of sea water and L is the wavelength. The energy per unit area or energy density $\bar{E}$ is given by:

$$\bar{E} = \frac{E}{L} = \frac{\rho g H^2}{8}$$

The rate at which energy is transmitted in the direction of wave propagation is the flux of wave energy or the wave power (Ec_g), the product of wave energy (E) and group celerity (c_g).

$$Ec_g = \frac{1}{8}\rho g H^2 \frac{g}{\omega} \tanh{(kh)} \frac{1}{2}\left(1 + \frac{2kh}{\sinh 2kh}\right)$$

Where h is the mean water depth, ω is the angular frequency, k is the wave number and Cg is the group velocity. With some simplification it can be shown that in deep water the energy is propagated at one half of the celerity of an individual wave whereas in shallow water the rate of energy propagation is equal to the celerity of the wave.

As waves travel outside the area of generation some loss of energy takes place in the deep sea as the wave steepness exceeds the Miche (1944) breaking criteria [66]. The primary mechanism for energy dissipation as wave growth takes place is turbulence due to white capping as a portion of a wave crest becomes over steepened and breaks, dissipating energy due to turbulence as well as pressure effects on the front of the wave. The second most important wave energy sink is dissipation because of the transformation of waves due to wave breaking. Wave energy loss can be accounted for by both background turbulence and turbulence caused by wave breaking. [28, 4].

Wave energy dissipation on coral reefs is dominated by wave breaking and bottom friction and the change in energy flux (Ec_g), the product of wave energy (E) and group celerity (c_g) i.e. wave power [23] can be described (in one dimension) as:

$$\frac{\partial Ec_g}{\partial x} = -\varepsilon_f - \varepsilon_b$$

where ε_f and ε_b are rates of dissipation due to friction and breaking, respectively.

It is established that the energy dissipation due to bottom friction may be of the order of a few Watts per square meter, which is comparable to the energy input by moderate winds [3]. The time rate of energy density loss due to bottom friction $S_{bf}(k)$, at wave number k can be written as [69]:

$$S_{bf}(k) = -\langle \tau_0 u_{bn} \rangle$$

where τ_0 is the bottom shear stress and u_{bn} is the orbital velocity of the wave component with wave number k. [37, 20, 25, 64] have all done extensive work on the bottom boundary layer structure in order to obtain τ_0, u_{bn}, and other quantities as a function of wave and current velocities away from the boundary [69].

Similar to the effect of benthic vegetation on the dissipation of wave energy the three-dimensional structure of coral reef cause conditions for altering the hydrodynamics of wave transformation and energy dissipation. The reefs present a complex structure with high hydraulic roughness causing substantial frictional energy dissipation. The carbonate reef bottom and the colonies of benthic organisms including corals induce turbulent shear stress resulting in rough boundary layer resulting in dissipation of wave energy [79, 74].

In shallow water as wave height increases and the depth decreases the wave crest becomes unstable and starts breaking as the particle velocity exceeds the velocity of the wave crest. The breaking condition corresponds to crest angle of $120°$. Using solitary wave and non-linear wave theory the breaking index which is the ratio of the breaking wave height to the water depth gives a value of 0.78 [66]. This index is worked out for horizontal bottom. A sloping bottom is encountered in reality which will modify the index. The angle of the bed slope in relation to the wave steepness modifies the process of breaking in various different ways and depends on the Iribarren parameter ξ [6]. The analogy of individual wave crests with turbulent bores is used in majority of the models for the breaking of random waves. [5, 89].

1.4. Terminology

The terminology used in this thesis is defined in this section. This research focuses on the wave hydrodynamics and coastal geomorphology along the Al Wajh bank, with a focus on sea turtle nesting sites. The coastal zone terminology used in this report is shown in Figure 1.2. The Figure 1.3 depicts an idealized crossshore profile of an island shoreline, with the major elements of the backshore and foreshore indicated. The reef geomorphological aspects discussed in this study are depicted in Figure 1.3. The reef flat level can be below or above the nearshore tidal elevation.

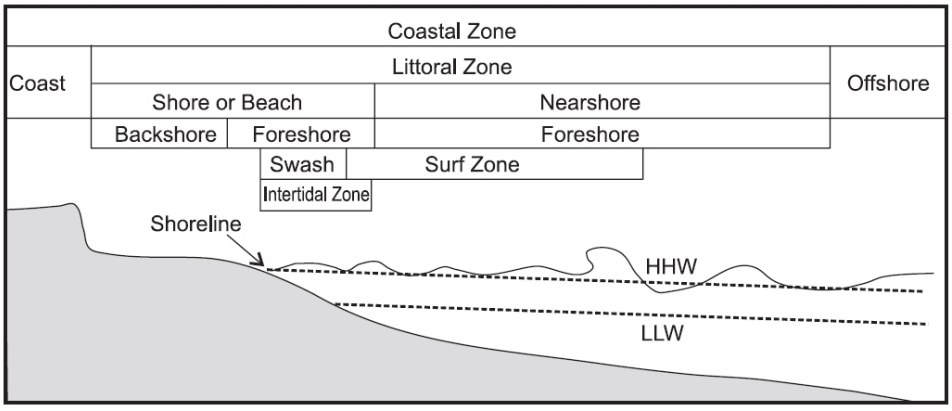

Figure 1.2: Coastal Zone Terminology, taken from [24]

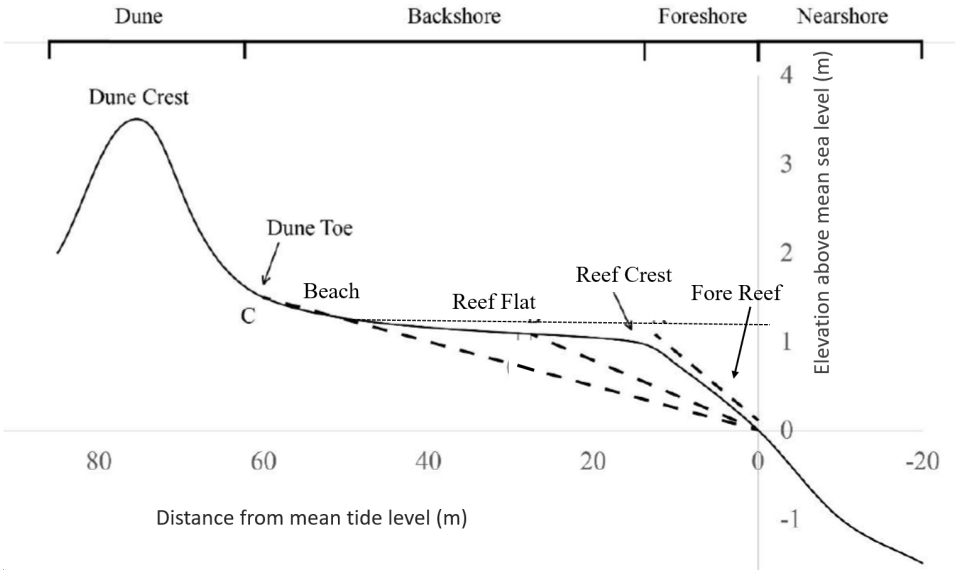

Figure 1.3: Features of Backshore and Foreshore, taken from [93]

The study deals with wave transformation from offshore to nearshore. Sea and swell are two terms that are commonly used to describe the wave field. Wind sea refers to the wave field that is directly connected to the wind. Swell occurs when waves travel away from the source of generation and are no longer influenced by the wind forcing that formed them. Wind seas are short-period waves that are still being formed by winds. Waves that have moved away from the generating region are referred to as swell. Swells are waves that are more regular in form, with well-defined long crests and relatively long periods. Sea and swell waves have the ability to transport not only a large amount of energy, but also momentum.

1.5. Scope and Objective of the study

As explained above, the Al Wajh bank has a number of sea turtle nesting grounds and a need is felt in the context of the Red Sea Project to understand the hydrodynamic and geomorphological features favouring the preference of turtle nesting sites on the various Islands at the rim of the coral reef and inside the lagoon. There is no study available in literature examining this aspect for the Al Wajh bank. A number of studies on the modelling of wave and wind climate at the scale of Red Sea are available but there are very few close to the reef banks along the Red Sea coastline. There is no systematic data available on waves and tidal circulation for the Al Wajh banks.

This thesis will focus on the coral reef banks and the lagoon and is a first step in understanding primarily the wave hydrodynamics and to a limited extant the geomorphological features at the turtle nesting sites using available data on topography, bathymetry wind and wave using the Delft3D Wave standalone model. The current study focuses on the spectral wave hydrodynamic processes in the two-dimensional domain for the Al Wajh Bank. In the absence of wave data in the nearshore and inside the lagoon for calibration and validation of the model, a qualitative approach has been adopted in this study for a relative assessment of the wave dynamics at Al Wajh Bank. The study identifies the gaps in the data and also future strategies for modelling and understanding the “Preferential hydrodynamic conditions for Turtle Nesting at Al Wajh Bank”.

1.6. Research questions

The primary research question is:

What are the preferential hydrodynamic, geomorphologic and vegetation features influencing the selection of turtle nesting at Al Wajh Bank?

The following secondary objectives have been defined in order to achieve the primary goal:

1. How is the wave propagation taking place near the seaward end islands and the islands in the lagoon?
2. How are the different conditions (hydrodynamic, vegetation and beach features) influencing the turtle nesting sites at Al Wajh banks?
3. Why are turtle choosing one beach over the other in this area?

1.7. Approach and Methodology

A research on habitat preference of the Hawksbill and Green Turtles at Al Wajh Bank is proposed. The present study will provide initial assessment of the habitats to guide further detailed research under the broad study to provide information for conservation of turtle nesting sites. The goal is to identify the hydrodynamic and geomorphological conditions favouring turtle nesting at the islands of the coral reef system at Al Wajh Bank. The study will use numerical modeling techniques and analysis of the available geomorphological data at the nesting and non-nesting sites.

Based on available literature on habitat preferences for sea turtle nesting the favourable and not so favourable conditions will be identified. A detailed survey by KAUST will provide data on the locations of nesting sites with exact GPS based coordinates. Spatial data on various parameters including island topography, reef and nearshore bathymetry, wind and wave data, data on sediments and beach slopes will be obtained from several sources. The data will be analysed to prepare the necessary hydrodynamic and geometrical inputs for the numerical wave model simulations and analysis of geomorphological parameters. Numerical wave model will be used to transform wave from offshore to nearshore to provide inputs for wave run up computations. The model will also be used to examine the wave energy dissipation across the barrier reef at Al Wajh Bank for normal and extreme wave conditions. The Geomorphological features will be identified and analysed with the available data.

The coastline of the area was divided into cross sections, 500 m apart, which resulted in 378 cross sections covering large and small islands inside and outside the lagoon). In this study a filtering process is applied based on marine habitat assessment for these sections using information available in ‘ATLAS of Saudi Arabian Red Sea Marine Habitat’. After this assessment it was concluded that the turtles prefer sandy beaches having adequate beach width and do not prefer areas having mangroves and nearshore vegetation. Therefore, the cross sections in which mangroves and vegetation was present were not considered for further study. The second filtering of the cross sections was done based on the wave model grid limitations. Some islands were not properly resolved due to grid size resolution of 100 m. Therefore, the main 5 larger islands of this archipelago were selected for this study which were having higher number of nests on their beaches. Of these, three islands are on the seaside and two inside the lagoon. Thus, 66 cross sections shown in Table 1.1 will be discussed further in this study: 31 nesting and 35 non-nesting.

Table 1.1: Location details of the cross-sections analysed in this study. N, NN, SS, and LS represents nesting site, non-nesting site, seaside, and lagoon-side respectively

Cross-section No.	Island Name	Easting	Northing	N or NN	SS or LS
7	Um Rumah 1 Island	257059.91	2844793.52	NN	LS
8	Um Rumah 1 Island	257440.91	2844513.45	NN	LS
9	Um Rumah 1 Island	257882.73	2844720.05	NN	LS
21	Um Rumah 1 Island	259444.21	2844914.30	N	LS
22	Um Rumah 1 Island	259359.96	2844489.15	N	LS
47	Ghawar Island	253320.02	2853347.81	N	SS
48	Ghawar Island	253117.15	2852892.03	N	SS
49	Ghawar Island	253068.40	2852453.75	N	SS
50	Ghawar Island	253123.55	2851965.61	NN	SS
51	Ghawar Island	253208.16	2851480.25	NN	SS
52	Ghawar Island	253343.86	2851005.80	NN	SS
53	Ghawar Island	253368.18	2850524.25	NN	SS
54	Ghawar Island	253380.82	2850027.54	NN	SS
55	Ghawar Island	253310.76	2849538.59	NN	SS
56	Ghawar Island	253259.22	2849049.23	NN	SS
57	Ghawar Island	253411.29	2848601.39	NN	SS
58	Ghawar Island	253712.85	2848207.53	NN	SS
59	Ghawar Island	254105.10	2847900.90	NN	SS
63	Birrim Island	249592.58	2835341.88	N	SS
64	Birrim Island	249238.86	2835694.13	N	SS
65	Birrim Island	248925.32	2836072.92	N	SS
66	Birrim Island	248572.50	2836402.42	N	SS
67	Birrim Island	248489.52	2836894.14	N	SS
68	Birrim Island	248183.85	2837266.43	N	SS
69	Birrim Island	247883.24	2837653.42	N	SS
70	Birrim Island	247618.29	2838027.06	NN	SS
71	Birrim Island	247444.59	2838441.47	NN	SS
72	Birrim Island	247265.54	2838794.85	NN	SS
73	Birrim Island	247395.37	2839251.10	NN	SS
74	Birrim Island	247646.57	2839673.95	NN	SS
75	Birrim Island	248032.77	2839980.49	NN	SS
76	Birrim Island	248381.67	2840326.77	NN	SS
77	Birrim Island	248774.49	2840632.96	NN	SS
78	Birrim Island	249228.42	2840726.64	NN	SS
79	Birrim Island	249695.19	2840674.10	NN	LS
80	Birrim Island	250067.12	2840402.94	N	LS
81	Birrim Island	250319.16	2839975.03	N	LS
95	Birrim Island	253647.55	2836342.50	N	LS
97	Birrim Island	252612.42	2835651.06	NN	LS
98	Birrim Island	252173.24	2835429.99	N	SS
99	Birrim Island	251673.98	2835444.57	N	SS
100	Birrim Island	251197.05	2835305.32	N	SS
101	Birrim Island	250702.87	2835250.36	N	SS
102	Birrim Island	250215.64	2835178.50	NN	SS
232	Quman Island	285283.50	2826864.94	N	LS
236	Quman Island	285605.39	2828110.23	N	LS
243	Quman Island	283168.23	2829900.10	NN	LS
244	Quman Island	282798.52	2829594.37	N	LS
245	Quman Island	282613.45	2829182.46	N	LS
246	Quman Island	282302.81	2828799.74	N	LS
247	Quman Island	282110.45	2828348.48	N	LS
250	Quman Island	281822.41	2827083.48	NN	LS

Cross-section No.	Island Name	Easting	Northing	N or NN	SS or LS
251	Quman Island	282158.15	2826732.95	NN	LS
252	Quman Island	282485.05	2826364.75	NN	LS
253	Quman Island	282822.52	2826006.80	NN	LS
323	Sheybarah South Island	289077.71	2806534.46	N	SS
325	Sheybarah South Island	289677.26	2807264.94	N	SS
326	Sheybarah South Island	289734.85	2806772.42	N	SS
327	Sheybarah South Island	289485.18	2806371.03	N	SS
338	Sheybarah South Island	288299.85	2808836.87	NN	SS
339	Sheybarah South Island	287768.86	2806753.34	N	SS
340	Sheybarah South Island	287732.37	2807248.60	NN	SS
341	Sheybarah South Island	287663.20	2807739.63	NN	SS
342	Sheybarah South Island	287535.17	2808220.62	N	SS
343	Sheybarah South Island	287323.83	2808671.89	NN	SS
344	Sheybarah South Island	287238.57	2809155.31	NN	SS

1.8. Thesis outline

This thesis describes the study broadly in three parts: Al Wajh Bank and Red Sea data analysis (Chapter 2), geomorphology and vegetation ecology of Al Wajh Bank sea turtle nesting and non-nesting sites Chapter 3 and numerical modelling of hydrodynamics of Al Wajh Bank and results of spectral wave transformation from offshore to nearshore Chapter 4.

Chapter 2 describes the analysis of the available Al Wajh Bank data on island topography, reef and lagoon bathymetry, turtle nesting location survey and analysis of sediment data for providing input to the numerical model and geomorphological analysis. The analysis of data on wind, waves, geomorphological features, vegetation, beach profiles is also given in this chapter.

Chapter 3 describes the analysis on the preferential conditions of turtle nesting at Al Wajh Bank for the available data related to foreshore geomorphology, beach slopes, sediment characteristics, vegetation and Al Wajh Bank erosion and accretion trends.

In Chapter 4 the numerical model setup for the offshore and nearshore region of Al Wajh Bank including the details of grid nesting, boundary conditions, parameters for various wave transformation processes are described. This chapter also describes the Delft3D WAVE numerical model, and the physical background of the SWANmodel used by Delft3D WAVE including the brief information on model implementation This is followed by the analysis of results for nearshore wave distribution; distribution of spectral energy density across the barrier reef and lagoon; wave heights and energy dissipation in the fore reef zone including wave run up and sensitivity analysis for the model.

Chapter 5 presents a discussion and limitation on Numerical model and geomorphological analysis results. Finally, Chapter 6 and Chapter 7 contain the conclusions and recommendations, respectively.

2

Al Wajh Bank and Red Sea Data

2.1. Introduction

The Al Wajh Bank is located in the northern half of the Red sea along its eastern coastline. The Red Sea, which stretches over 1900 km is formed by a narrow and relatively deep marine trough, lying between 13° and 28° N latitude. It is connected to the Mediterranean Sea in the north by the Suez Canal, and to the Indian Ocean in the south by the Bab Al Mandab strait in the Gulf of Aden. It is home to the world's most extensive and richest marine ecosystem. The Red Sea is the world's most salty (up to 46 ppt) seawater, with temperatures exceeding $35^\circ C$. This is primarily due to the lack of streams and rivers that flow into the sea, insufficient precipitation or runoff, and high evaporation levels. During the winter, however, there are sporadic flash floods, particularly near the Red Sea's eastern coast. The occurrence of frequent flash floods, combined with plenty of sunlight, clear vision, deep light penetration, and warm water, encourages coral growth [29]. The Red Sea coast of western Saudi Arabia is characterized by narrow coastal fringing reefs that span tens of kilometers from the coast before plummeting into deep water. Saudi Arabia is home to vast seagrass beds, offshore reef ecosystems, mangroves, and algal flats. These regions are home to a diverse range of coral ecosystems and reef morphologies. [12]

The Khaled bin Sultan Living Ocean Foundation has brought out an "Atlas of the Saudi Arabian Red Sea Marine Habitats" which gives comprehensive information on selected coral reef ecosystems including Al Wajh bank. The west coast of Saudi Arabia comprises the Al Wajh Bank; an archipelago of 6 large and more than 80 small islands, with the larger islands spanning an area of approximately $11km^2$. This group of islands are mainly flat and made of sand with only a few islands such as Al Shaykh Marbat being rocky with less than 5 m high cliffs. Some of the flat, sand islands include Shurayrat, Suwayhil, and Abu Lahiq. The sandy shorelines of the main islands contain alluvial deposits and well characterized wadis or drainage systems [12].

As shown in Figure 2.1, Al Wajh bank archipelago is bordered on the coast by barrier reefs and has marine ecosystems as well as a central lagoon. Complex barrier reef systems are found on coastal edge of the following islands; Jazirat Umm Rumah, Jazirat Birrim, and Jazirat Shaybarah. Intriguingly, these barrier reefs are the only coral barrier reef systems found in Red Sea and a sudden fall to depths of more than 500 m in these reefs on the coastal edge can be observed. The average distance between the outer edge of the barrier reef and shore is 20 km. Barrier reefs are home for a multitude of coral

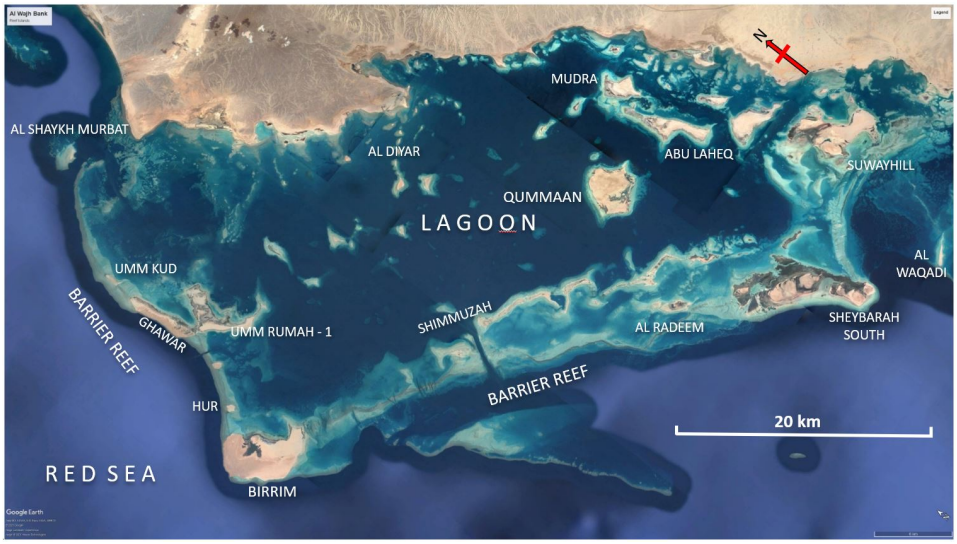

Figure 2.1: Al Wajh Banks with island names and important features

colonies which run along the Al Wajh Bank coastline for approximately 50 km. Furthermore, southern and northern ends of these barrier reefs merge into the islands. On the other hand, shallow fringing reefs can be found stretching along the coastline of Qummaan. Other types of reef systems found on the Al Wajh bank include 1. platform, 2. reticulate , 3. submerged patch , 4. submerged ribbon reef systems and 5. lagoon pinnacles.

Islands such as Qummaan, Mudra, Abu Laheq, Al Diyar are seated in the central lagoon with Qummaan being the largest in area amongst them. Depth of the central lagoon can be up to 40 m and near shore areas of the lagoon are shallow. Mudflats and large seagrass covered areas are commonly seen in southern banks and they are shallower than northern parts of the bank. There are several narrow channels found in the lagoon with depths > 5 m and widths < 900 m. Additionally, strong water currents are observed in the narrow openings between the banks and open ocean despite minimal tidal amplitudes of less than 1m. Northern lagoon contains several other atolls and supports different mangroves and grass beds.

2.2. Bathymetry

A general idea of the sub sea and land features at Al Wajh Bank was given in Section 2.1. A detailed information on the bathymetry of the Red Sea in and around Al Wajh Bank is essential to set up wave hydrodynamic models. Data on bathymetry was made available by KAUST sourced from Kingdom of Saudi Arabia General Commission of Survey (GCS). A 50 cm grid high resolution bathymetry data was made available for the Al Wajh Bank covering the area shown in Figure 2.2 (A). The sounding data outside the lagoon was supplied for the area shown in Figure 2.2 (B). The bathymetry data was referenced to the Lowest Astronomical Tide (LAT).

The mathematical model domain for the study will need bathymetry data in a larger area as the spectral waves will be transformed from offshore to nearshore for the Northern Red Sea. The offshore wave data was taken from http://www.waveclimate.com at $25.5°N$ latitude and $36.25°E$ longitude where the sea depths are of the order of 1500 m. The GCS survey data does not cover this area. Therefore, additional bathymetry covering the offshore region of available wave data was obtained from General Bathymetric Chart of the Oceans (GEBCO) using Deltares Delft Dashboard Tool.

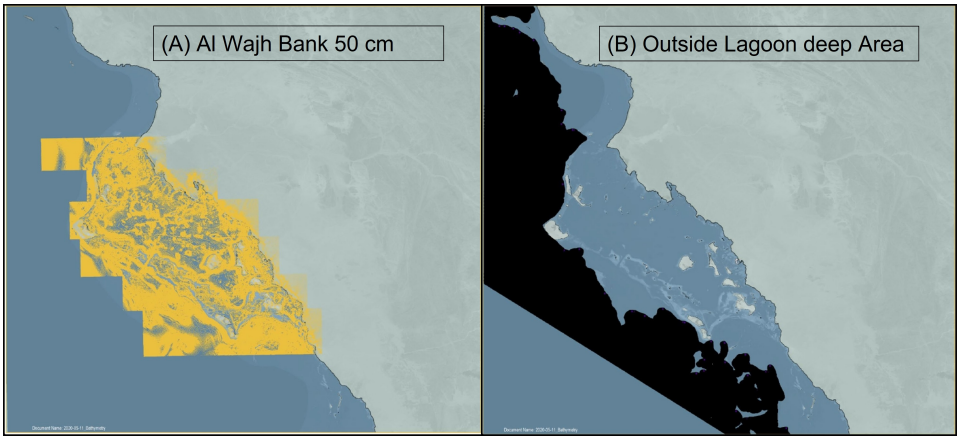

Figure 2.2: Area covered by GCS Bathymetric Data. Yellow represents nearshore bathymetry, Black represents offshore bathymetry, Grey represents land and Bule represents water

The bathymetry and topography data with reference to the LAT for the Al Wajh Bank and outside the reef is shown in Figure 2.3. The +ve values are depths below LAT and the -ve values are elevations above LAT. The enlarged bathymetry of the northern and southern part of the Al Wajh Bank is shown in Figure 2.4 and Figure 2.5. The depths inside the lagoon are in the range of 10 m to 40 m with deeper depths prevailing more in the northern part. The southern part of the lagoon is relatively shallow with depths in the range of 10 m to 25 m. The shallow reef flats on the seaside are having depths in the range of 1 m to 10 m. The outside border of the reef has a sudden drop in depths to over 50 metres, with a sharp gradient in the seabed. The depth increases to more than 500 m within 2 km from the reef edge.

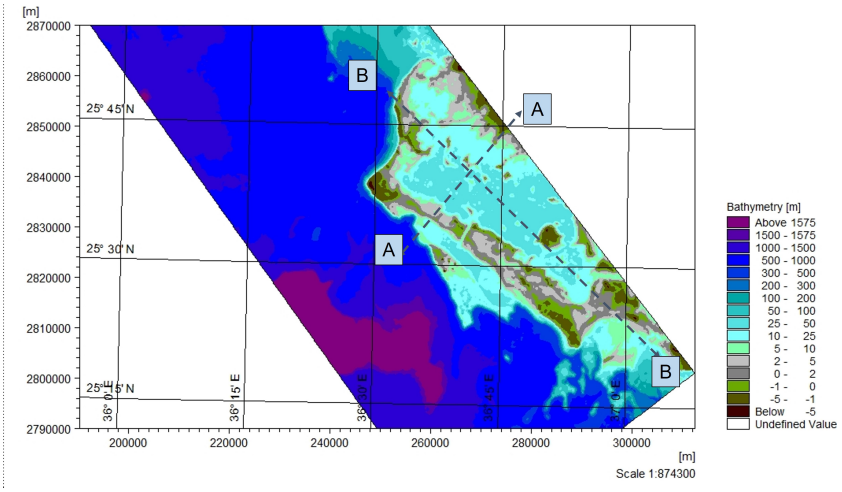

Figure 2.3: Detailed bathymetry at the Al Wajh Bank. Cross shore section A-A represented in Figure 2.6 and alongshore section B-B represented in Figure 2.7

There are several Islands emerging to the surface from the reef peaks with exposed dry land where the elevation above the LAT is in the range of 1 m to 3 m. Some of the Islands have elevations above 5 m with supposedly rocky terrain.

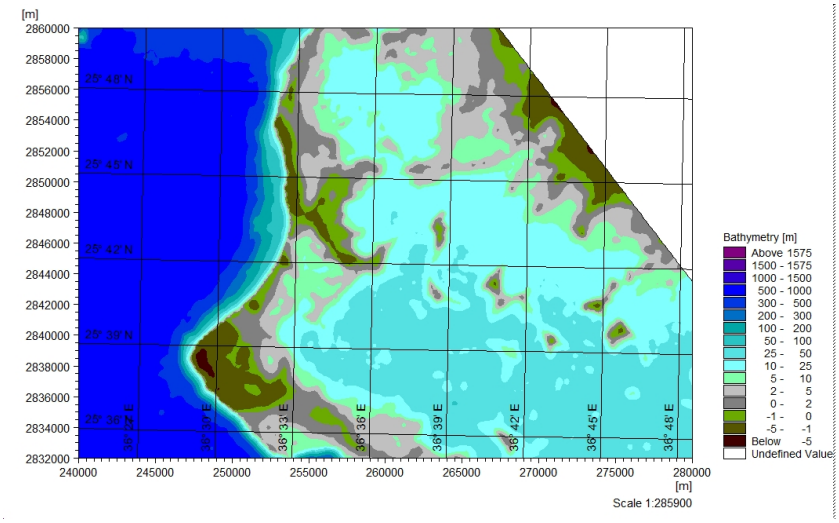

Figure 2.4: Bathymetry in the north of Al Wajh Bank

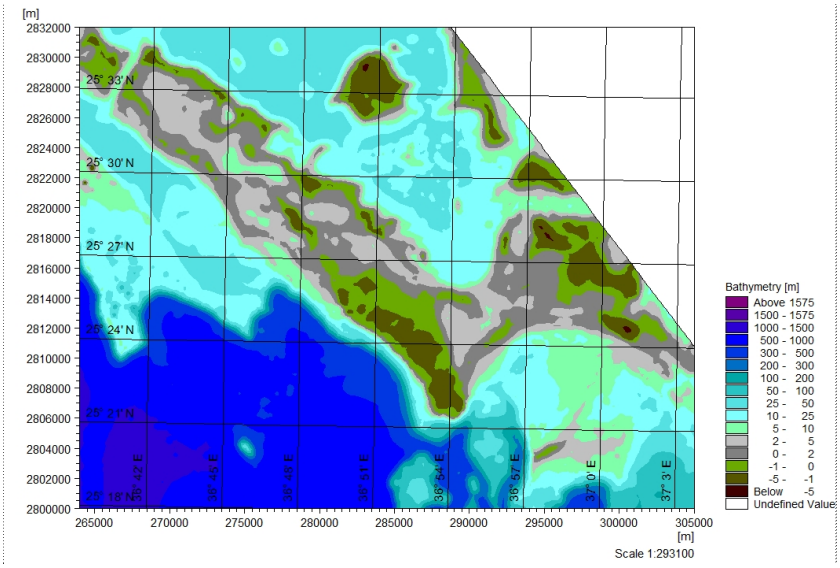

Figure 2.5: Bathymetry in the south of Al Wajh Bank

Transects showing the profile of the lagoon bottom and topography of the Islands are also shown Figure 2.6 to Figure 2.9. Steep gradient in the bathymetry is observed at the edge of the reefs. For the Al Wajh bank reef, two transects are taken in the cross shore (Figure 2.6) and longshore direction (Figure 2.7). Profiles across the Birrim and Qummaan Islands are also shown in Figure 2.8 and Figure 2.9.

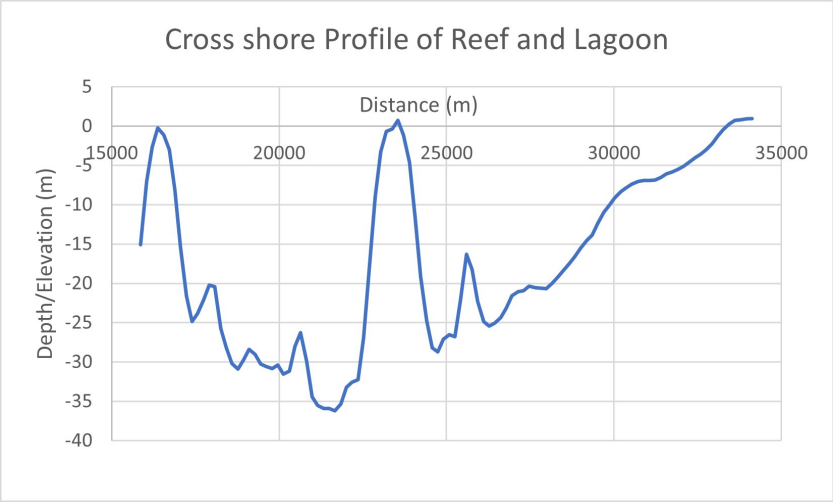

Figure 2.6: Cross shore profile at the Al Wajh Bank

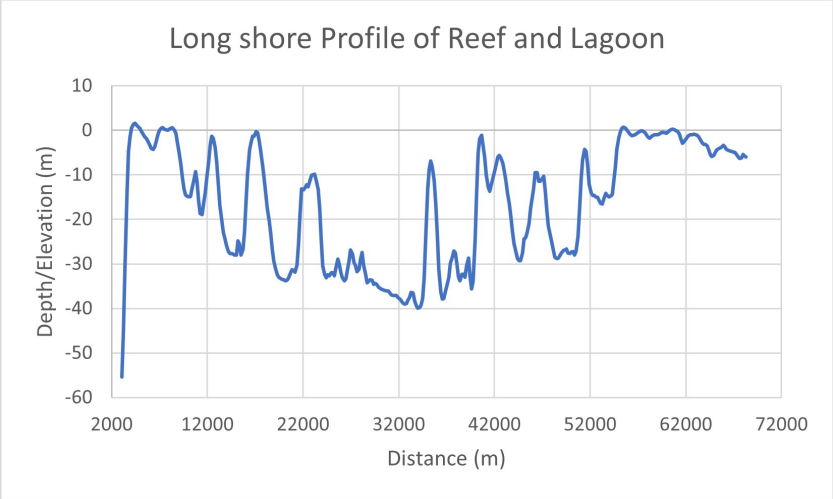

Figure 2.7: Alongshore profile for Al Wajh Bank

Figure 2.8: Cross shore profile across Birrim Island located at the northwest side of the Al Wajh Bank archipelago.

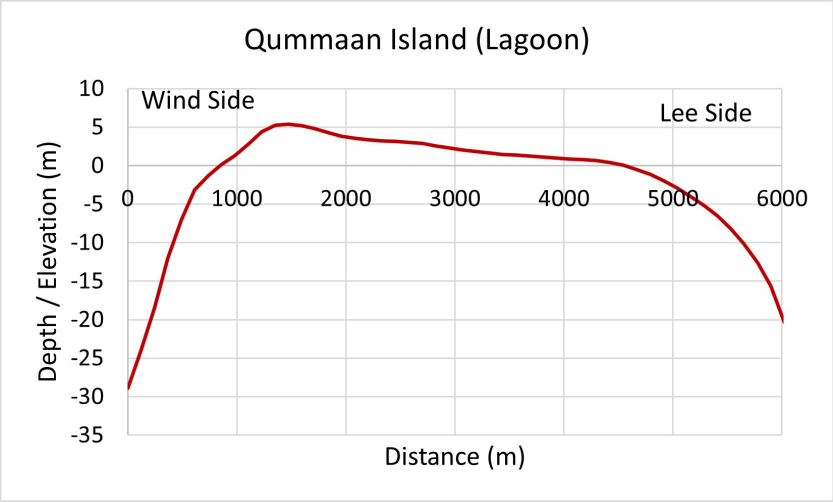

Figure 2.9: Profile across Qummaan Island located at the center of Al Wajh Bank lagoon.

2.3. Wind and Wave Data for Red Sea

The Red Sea is a 3000 km long and 300 km wide closed basin formed by a rift valley between the Africa continent and Arabian Peninsula. The predominant topographic relief of mountains and hills on the east and west sides of the Red Sea has a major effect on wind circulation [78]. Under the influence of the Mediterranean the northern half of Red Sea has winds blowing from northwest throughout the year with some influence of westerly flowing winds from mountain gaps along the Arabian coast. In contract the southern half of Red Sea is influenced by both the Mediterranean and Indian Ocean circulation especially during the South West Monsoon. The winds in southern Red Sea are from South East and North West. Thus, the central part has opposing winds from north and south but also influenced by jets of high speed wind from the Tomar Gap. The waves generation and propagation in the Red sea is influenced by the changing wind pattern in the north, centre and the south. This condition complicates modelling and prediction of the precise wave field in Red sea [55].

A number of studies are available in literature for the Red Sea on the analysis of the wind and wave climate which cover the entire Red Sea but have limited focus on the nearshore and the coastline. The data from Global and regional climatological models ECMWF, WRF are applied to wave hindcast models WAVEWATCH, WAM, SWAN with calibration and validation using a few Buoy based field observations in the South Red Sea particularly near Jeddah [53, 51, 52].

The wind and wave data used in this study were obtained from the BMT ARGOSS online services website ”waveclimate.com,” which offers model simulated and validated data for the global grid (0.5°x0.5°) for the Mediterranean, the Black Sea, the Red Sea and the Persian Gulf (1/4°x1/4°). The BMT ARGOSS ’waveclimate.com’ sources the data from the agencies shown in Table 2.1.

The ’waveclimate.com’ provides calibrated and validated data and it can be used directly without further processing. The data is more suitable for preliminary engineering applications and is useful, especially, in fully exposed deep water conditions. Satellite Altimeter and SAR measurements are periodically calibrated and validated using Buoy measurements. The altimeter and scatterometer data are calibrated separately with Buoy data and the error is reported to be 12% for wave data and 15% for wind data. The website has the relevant documents detailing the calibration and validation process for the wave and wind data [38].

Table 2.1: The BMT ARGOSS 'waveclimate.com' sources the wind and wave data from the following agencies:

Name of Supplier	Nature of Data
Albatros Flow Research	Development of offshore to nearshore transformation models
The Delft Institute of Earth Oriented Space Research (DEOS)	Satellite Altimeter Data
European Centre for Medium-Range Weather Forecast (ECMWF)	Collocated ERS SAR imagettes and WAM data
The European Space Agency (ESA)	Low bite rate ERS data
The French Processing and Archiving Facility (CERSAT)	ERS Scatterometer data
The National Data Buoy Centre (NDBC)	NOAA Buoy data

2.3.1. Wind Data

The processed online wind data was extracted from 'waveclimate.com' in the Red Sea, offshore of Al Wajh Bank at $25.5°N$ latitude and $36.25°E$ longitude. The information on wind speed (U10) and wind direction was obtained with a time step of 3 hours for the period 1st January 1992 to 31st December 2018. The 27-year data was analysed to compute the annual daily and monthly mean values for magnitude and direction. The directional distribution of wind from January to December is given in Appendix B. The monthly data on daily distribution of mean wind speed with monthly standard deviation from January to December is shown Appendix C. The predominant wind direction is consistently from North West for all the months. The annual wind rose diagram is shown in Figure 2.10. The annual distribution of the daily mean wind speed and direction are shown in Figure 2.11 and Figure 2.12. The wind direction is in general from the North -West throughout the year. The mean wind speed is between 4 m/s to 7 m/s which matches with the previous analysis of data for the North Red Sea. The higher magnitude of winds are observed in the and around June and September. A distinct change in the wind direction for summer (May to September) and winter (October to December) is observed.

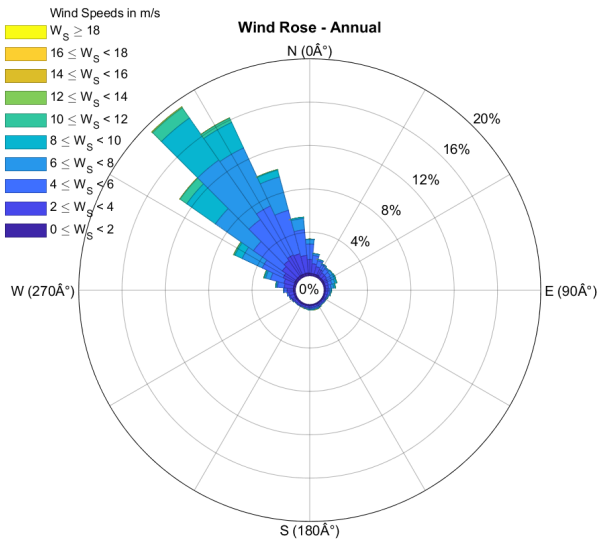

Figure 2.10: Annual Wind Rose offshore of Al Wajh Bank at location $25.5°N$ latitude and $36.25°E$ longitude

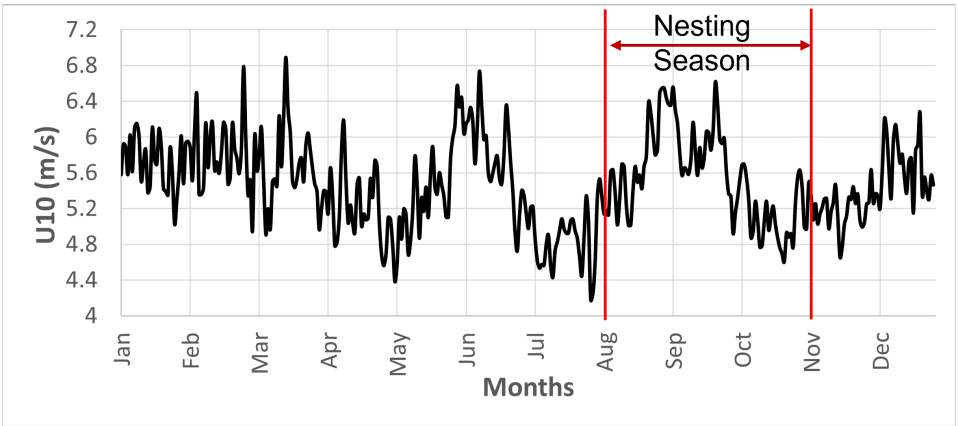

Figure 2.11: Daily Mean Wind Speed of 27 years data (1992-2018)

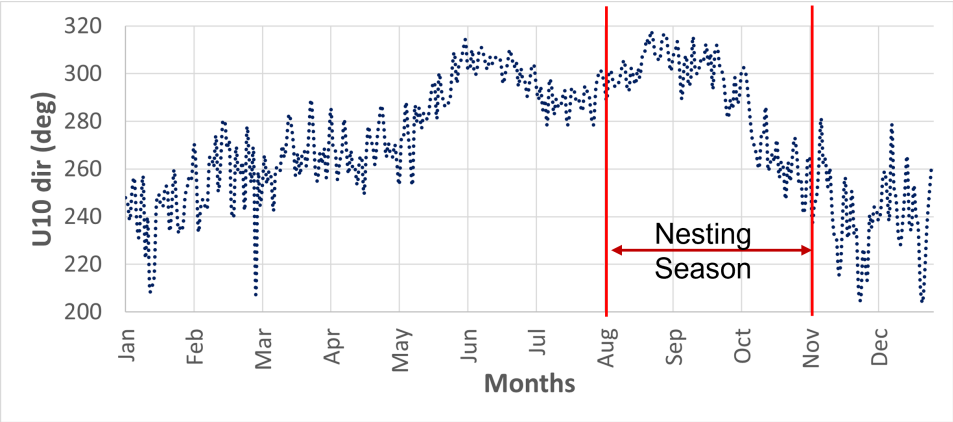

Figure 2.12: Daily Mean Wind Direction of 27 years data (1992-2018)

2.3.2. Wave Data

Like wind data the offshore wave data was extracted at $25.5°N$ latitude and $36.25°E$ longitude from 'Waveclimate.com' in the Red Sea for modelling the wave conditions near Al Wajh Bank. The data are based on spectral wave data and the wave parameters covered are significant wave height, principle wave direction including mean, zero crossing and peak wave periods. The data are obtained with a time step of 3 hours for the period 1st January 1992 to 31st December 2018. The 27-year data are analysed to compute the daily, monthly and annual mean values for the wave parameters. The directional distribution of waves from January to December is given in Appendix C. The monthly data on daily distribution of mean of Significant wave heights with monthly standard deviation from January to December is given in the Tables at Appendix C. The predominant wave direction is consistently from North West for all the months. The annual wave rose diagram is shown in Figure 2.13.

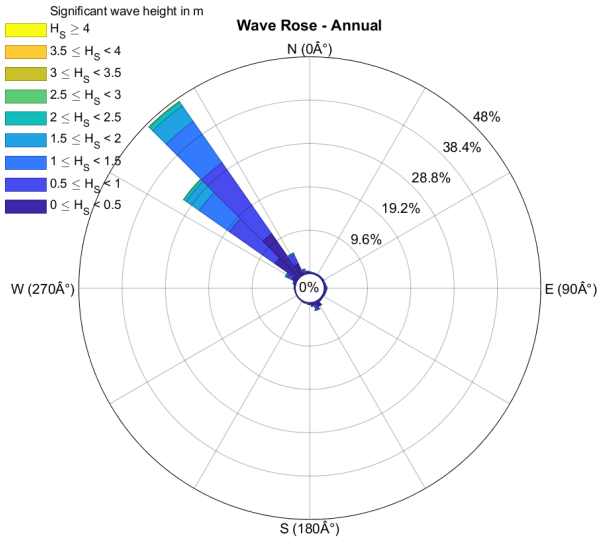

Figure 2.13: Wave Rose Diagram offshore of Al Wajh at location $25.5° N$ latitude and $36.25° E$ longitude

The annual distribution of the daily mean Hs, Tp and direction are shown in Figure 2.14 to Figure 2.16. The wave direction is in general from the North West throughout the year. The mean significant wave height is between 0.6 m to 1.2 m which matches with the previous analysis of data for the North Red Sea. The higher magnitude of waves are observed in and around June and September which coincides with peak wind conditions occurring during these months. A distinct change in the wave direction for summer (May to September) and winter (October to December) is observed and similar trend was observed for the wind.

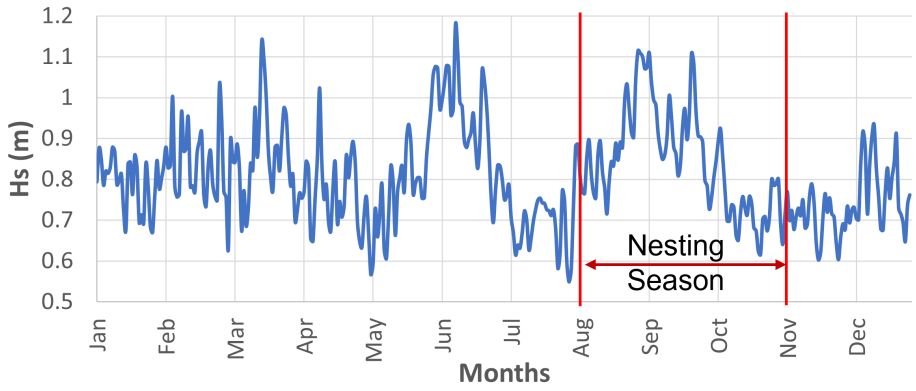

Figure 2.14: Daily mean significant wave height from January to December of 27 years data (1992-2018)

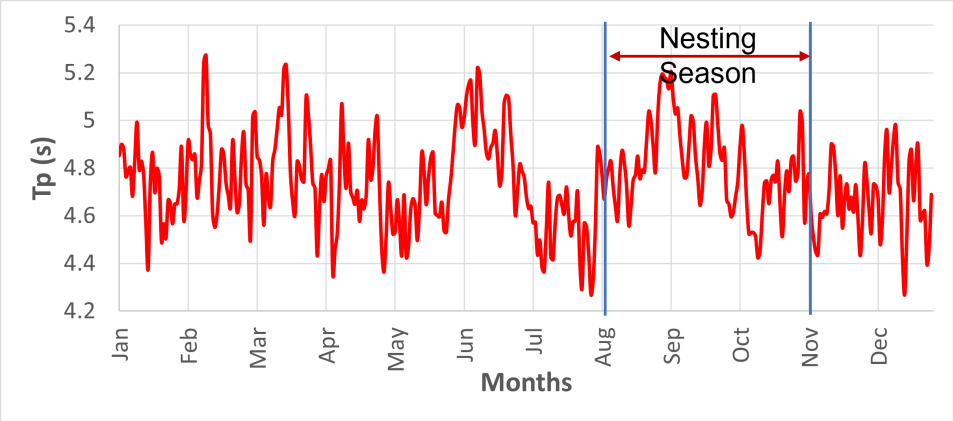

Figure 2.15: Daily mean peak wave period from January to December of 27 years data (1992-2018)

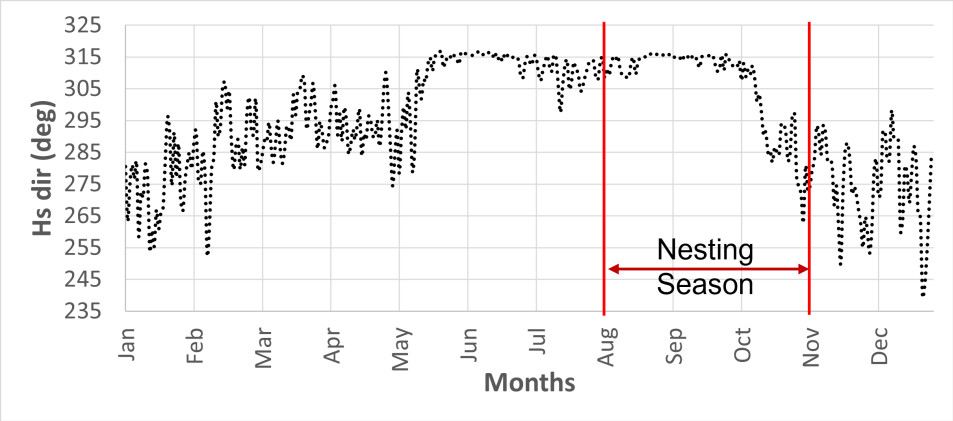

Figure 2.16: Daily mean Wave Direction from January to December of 27 years data (1992-2018)

2.3.3. Extreme Value Analysis

The estimation of extreme wave heights is carried out for the offshore wave data for the assessment of the impact on the nesting areas around the islands, the reefs and the lagoon. The modelled and verified data for 27 years obtained from 'waveclimate.com' was used for this analysis. This data is generally not recommended for use in EVA, especially, for design of structures as the data is modelled for spatial resolution of 0.25^o and may miss some of the storm peaks [38]. In the present study due to limitations in obtaining high resolution model or observed data the available 'waveclimate.com' data is considered to be adequate for the assessment of the impact on turtle nesting sites near Al Wajh Bank in particular and the reef system in general.

Extreme value theory is used for the estimation of the one in 'm' year return value (H_s), the value which is exceeded on an average once every 'm' years. A sample of measured data is used to determine the probability distribution function (PDF), $P_x(x)$ that may adequately represent the data [40]. The purpose is to estimate the probability of extreme events and therefore the focus is generally limited to the extreme tail of the distribution. Three methods are commonly mentioned for the modelling of extreme value of wave data to obtain the return value estimates: the initial distribution method (IDM), the annual maxima method (AMM), and the peaks over threshold method (POT). The IDM is a predecessor of the AMM and POT techniques which is not very popular or advisable for the extreme value analysis of waves. This method uses all available data for fitting the cumulative distribution functions (CDF) and

has limitations and lacks proper scientific basis.

To obtain a valid distribution, the observations need to be independent and identically distributed [40]. For general variable data averages, maximum values, and exceedance over thresholds, it is recommended to use normal, generalised extreme value (GEV) and generalised Pareto distributions (GPD) respectively for which statistical theory provides a proper scientific basis. The H_s data is not independent and hence only the maximum or the exceedance over a threshold are used for modelling the extreme values in the tail. The AMM which is based on block maxima (commonly annual) uses the GEV distributions. The AMM uses the maximum value in a year and tries to address the assumption of independence of observations. In this method the focus is on the extreme tail of the distribution which uses the largest value in a 12-month period, and it has been shown that the maxima will adhere to a generalized extreme value distribution [17]. The AMM suffers due to limited sample size (only one observation in each year) and the CDF cannot be fitted accurately, despite having a sound theoretical basis. Due to small size of the samples the model estimates for return values have large uncertainties. Thus, AMM has some limitations for oceanographic applications where the data is not available for a large number of years.

These shortcomings can be overcome in the POT method which separates the moderate conditions from the storm events by defining an arbitrary threshold. This permits the selection of a number of peak values above the threshold from the observations i.e., one observation from each storm. It can be shown using the extreme value theory that these extremes will follow the generalised Pareto distribution (GPD). The only drawback is the selection of an arbitrary threshold which will influence the estimation of the extreme values. The sampling frequency also has an affect on the capturing of storm events e.g., satellite altimeter observations where sampling interval could be separated by a few days. The availability of longer time series gives better results using the POT method.

It is assumed that the peak excesses over a high threshold u of a time series are independently distributed and occur in time according to a Poisson process with rate λu and independently distributed as a GPD. The distribution function for the GPD is given by

$$F_u(y) = \begin{cases} 1 - \left(1 + \xi \frac{y}{\sigma_u}\right)^{\frac{-1}{\xi}}, for\, \xi \neq 0 \\ 1 - exp\left(\frac{-y}{\sigma_u}\right),\ for\, \xi = 0 \end{cases}$$

where 0 < y < ∞, σ_u > 0 and −∞ < ξ < ∞. The two parameters of the GPD are called the scale (σ_u) and shape (ξ) parameters. When ξ = 0 the GPD is said to have a type I tail and amounts to the exponential distribution with mean σ_u; when ξ > 0 it has a type II tail, and it is the Pareto distribution.

The 1 in m year return value zm based on a POT/GPD analysis is given by:

$$z_m = \begin{cases} u + \frac{\sigma_u}{\xi}\left\{(\lambda_u m)^{\xi},\ for\, \xi \neq 0\right\} \\ u + \sigma_u log(\lambda_u m),\ for\, \xi = 0 \end{cases}$$

Distribution fitting involves estimation of the parameters that define the distribution. The location tells where the distribution will lie along the x-axis. The scale talks about the spread of the distribution. Th shape parameters determines the shape of the distribution, and the threshold talks about the minimum value along the x-axis. The GPD is generally specified by three parameters: location μ, scale α and shape ξ and often specified by only scale and shape. Numerical methods are used for the estimation of parameters and the methods of moment (MOM) and maximum likelihood (ML) methods are, generally, the preferred methods. The estimates of return values in the extreme value analysis also includes the estimate of the uncertainty and several methods are used to compute the confidence intervals

(uncertainty). The popular method for estimating uncertainty is the bootstrap method which offers a simple and reliable method for computing standard error of estimators but exhibits inconsistency for extreme value problems. An ad hoc method is used to correct and adjust the bootstrap estimates [21] and the computed confidence intervals are referred as adjusted bootstrap.

In the present study, the extreme value analysis of the significant wave heights (H_s) has been carried out using the POT/GPD method. The threshold was chosen to have at least two or more peak values in a year. The threshold value of H_s = 2.5 m was chosen which gave a sample of 59 extreme values for the 27 years data. The details of the storms selected for the analysis of extreme values is given in Appendix D. The initial estimate of the parameters for the GPD was attempted using the ML method but this method failed to give a solution. Therefore, the MOM was used to estimate the parameters which gave ξ=0.0001, σ_u=0.2193 and θ=2.4818. The shape parameter $\xi \sim 0$ and thus the fitted GPD is close to exponential distribution. The estimated return value plot of the GPD model fitted to H_s and associated adjusted bootstrap 95% confidence intervals are shown in Figure 2.17. The estimated wave heights for return periods of 1, 10, 50 and 100 years are given in Table 2.2.

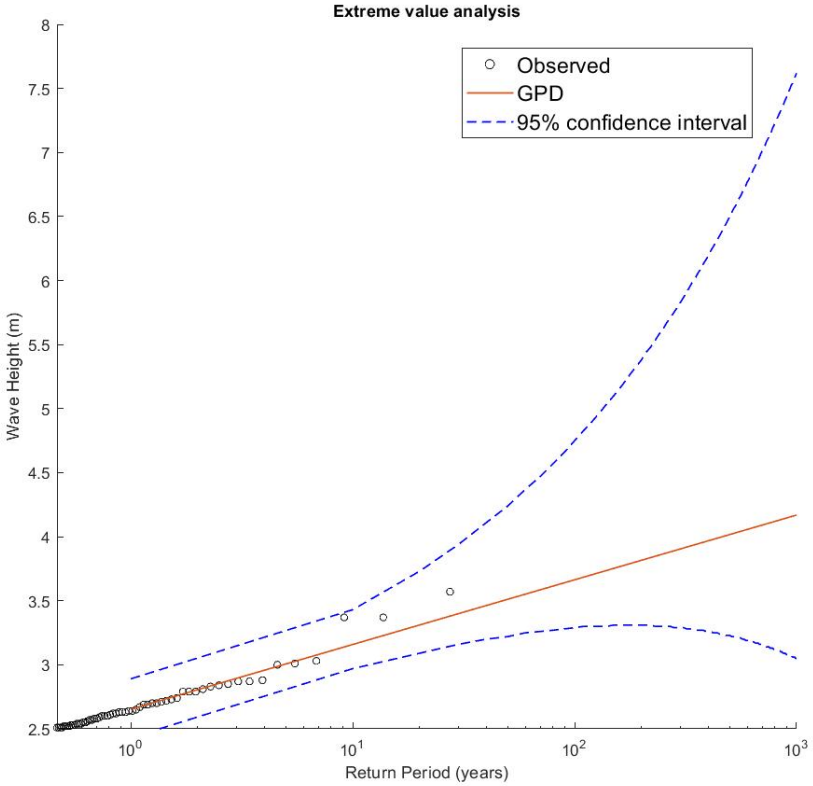

Figure 2.17: Return value plot of the GPD model fitted to the H_s obtained with the MOM method (solid red line) and associated adjusted bootstrap 95% confidence intervals (dashed blue line). The POT data are represented by black circles

Table 2.2: H_s for different Return Periods with 95% confidence values

Sr. No.	Return Period (years)	Significant Wave Height (m)
1	1	2.65 (2.54,2.78)
2	10	3.16 (3.02,3.39)
3	50	3.51 (3.36,4.15)
4	100	3.66 (3.49,4.62)

2.4. Tide Data

The tides at Al Wajh can be classified as micro tides with spring tidal range of 0.59 m and neap tidal range of 0.33 m. Tides are semi diurnal with tidal period of 12 hours 25 minutes and have no diurnal inequality. The tidal levels at Al Wajh are as follows:

Highest Astronomical Tide (HAT)	1.11 m
Mean High Water Spring (MHWS)	0.89 m
Mean Sea Level (MSL)	0.58 m
Mean Low Water Neaps (MLWN)	0.43 m
Mean Low Water Spring (MLWS)	0.30 m
Lowest Astronomical Tide (LAT)	0.00 m

2.5. Sediment Data

Particle size analysis was carried out for sediments samples taken from a few Islands in the south of Al Wajh Bank. The sampling locations are shown in Figure 2.18.

Figure 2.18: Sediment Sample Sites (yellow triangles). These samples were collected by KAUST

The data was provided by KAUST and the analysis was carried out by ALS Arabia. A total of 52

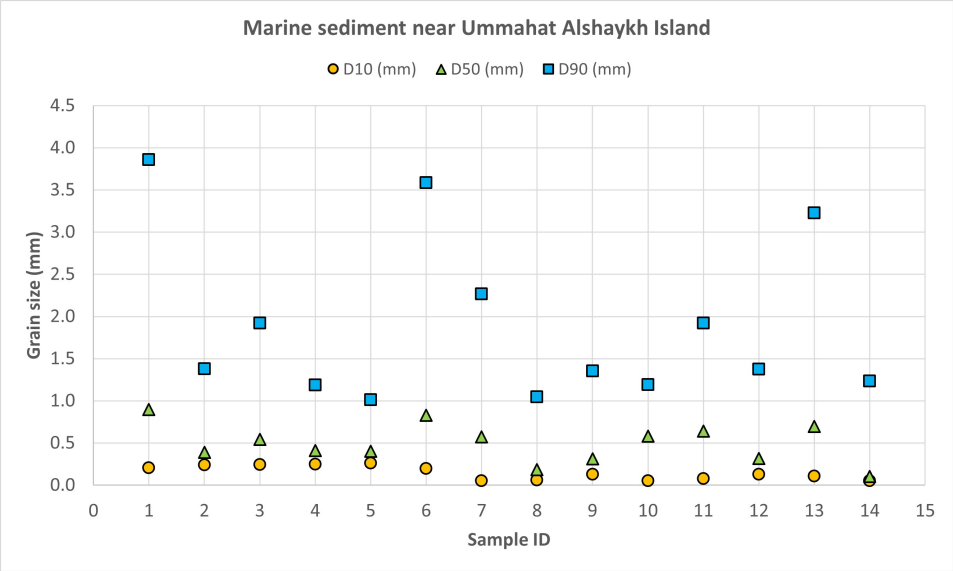

Figure 2.19: D10, D50, D90 in mm of Samples near Ummahat Al Shaykh Island

samples were from four islands in the central and southern part of Al Wajh Bank where very few or no turtle nests are found. Thus, this data mainly related to non-nesting locations at Al Wajh in southern part of lagoon. The analysis revealed poorly or well graded sand with D_{50} values ranging from 0.2 to 0.5 mm. Some of the samples have course sand mixed with gravel. The grain size D_{n10}, D_{n50} and D_{n90} values for the samples are shown Figure 2.19, Table 3.1; Figure 2.20, Table 3.3; and Figure 3.6,Table 3.2 for Umm Al Shaykh island, Sheybarah South island and Shurayrat island respectively.

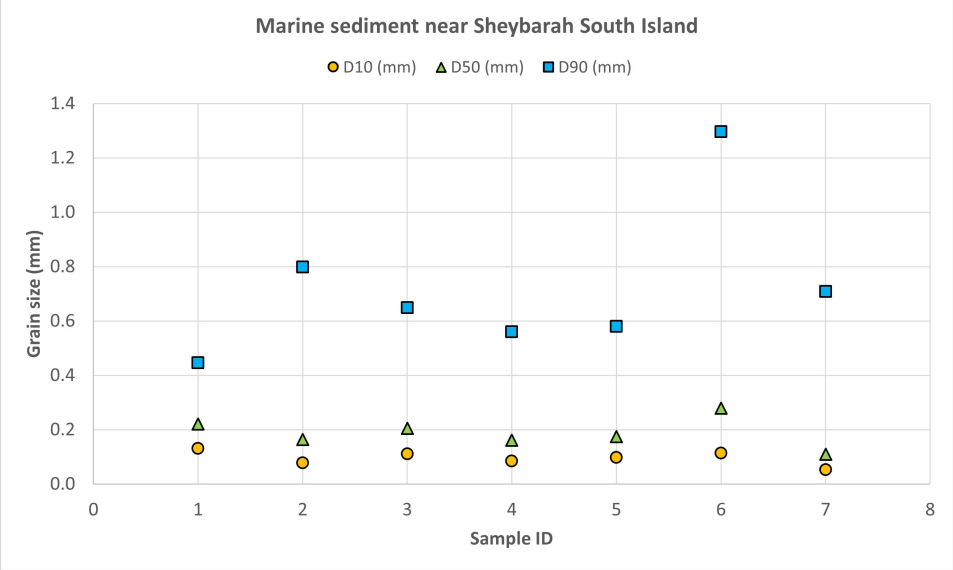

Figure 2.20: D10, D50, D90 in mm of Samples near Sheybarah South island

3

Geomorphology and Vegetation Ecology of Al Wajh Bank

3.1. Introduction

The Al Wajh Bank is dominated by a rimmed coral reef shelf. The shelf and reef bathymetry are highly complex with submerged reef flats, raised islands and plateaus. It is dominated by a large, sheltered lagoon, which contains extensive non-reefal seabed near the coastline and a number of islands. Inter-reef channels cut through the reef complex which are pathways for strong tidal currents and exchange of Red Sea water with lagoon waters. The turtle nesting sites are located on the sandy beaches of the islands, both at the outer rim and inside the lagoon.

The morphodynamics of sandy coasts where turtles prefer to nest for breeding have some unique features that will provide conditions ensuring safe and successful hatching of eggs and return of the hatchlings to the sea. Beach slope is one of the important factors for nest site selection in addition to other beach factors such as sand texture, moisture, salinity, and temperature for breeding of sea turtles [97]. It is established through systematic studies that beach sediment size and sorting, affect turtle nesting and the incubation normally depends on sediment with a mean diameter in the range 0.063-2.0 mm (+4 to -1 ϕ) [72, 68, 34]. This also determines the levels of porosity, air flow, and moisture suitable for incubation [72]. On the other hand, well sorted course sediment exposes the nests to low moisture levels causing embryonic mortality [72, 1]. Presence of more than 5-10% of silt or clay in the sand can enhance compaction of the sediment and pose problems for hatchlings to dig out of the egg chamber [72, 71].

There are a few studies in literature investigating the relationship between vegetation and the nesting habits of sea turtles. In the coral reef environment, the geomorphological evolution is a result of biotic and abiotic processes with large temporal and spatial timescales. In the relatively small time scales the coastal processes dominated by wind, waves and tides determine the type of sediments forming the morphological features along the coastline and the vegetation that will thrive in this environment. The relatively high energy regions dominated by wave action will have sandy coastlines with sparse vegetation, generally in the backshore. The shallow, sheltered and flat areas dominated by tidal circulation with low or no wave activity will have, in addition to sand, fine silt or clay sediments where mangroves and other vegetation are observed. These sheltered areas may not be suitable for turtle

nesting and are not preferred by the sea turtles. At Al Wajh Bank the islands at the edge of the reefs and inside the lagoon have both sandy beaches and muddy coastlines with nearshore vegetation.

3.2. Geomorphological characterization

The beach profiles and slopes determine the inundation of the turtle nesting sites due to wave runup and setup in the swash zone. Under extreme wave conditions due to storm and associated storm surge can cause erosion and changes to the beach morphology. It is observed that the turtle nesting sites are located in zones where the sudden changes in the bottom gradients at the edge of the reef crest and the presence of reef flat where high dissipation of wave energy occurs. The surf and swash zone dynamics and associated sediments that shape the beach profiles in addition to other factors determining successful nesting like sediment sorting, consolidation, moisture, aeration, temperature which are interdependent. The geomorphological setup favouring the above conditions can be also determined from the foreshore and backshore beach profiles.

3.2.1. Beach cross-sections

Two of the islands one at the edge of the barrier reef and one inside the lagoon are selected and higher interpolation of bathymetry and topographic data was done to get the profiles with higher resolution. Three sections corresponding to nesting, non-nesting and sheltered area with vegetation were selected at Birrim and Qummaan Islands and shown below. The Figure 3.1 shows the transect locations.

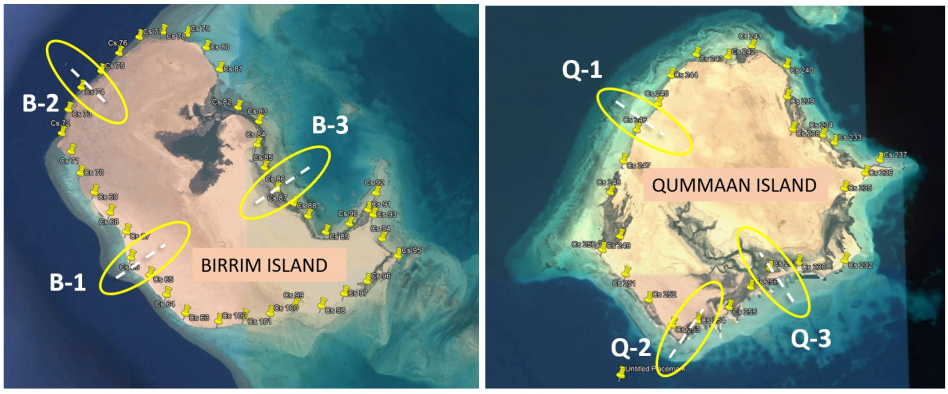

Figure 3.1: Location of transects for the cross section plots at Birrim island (B1, B2, B3) and Qummaan island (Q1, Q2, Q3)

The sections B-1, B-2 and B-3 shown for Birrim Island correspond to nesting, non-nesting and nearshore vegetation areas respectively. Similarly, the sections Q-1, Q-2 and Q-3 are for Qummaan island corresponding to nesting, non-nesting and nearshore vegetation areas respectively.

The bed profile in the foreshore and nearshore are shown in Figure 3.2. The profile in Figure 3.2a located on the seaside of Birrim is for Section 66 and is a nesting site in a narrow strip of beach close to highwater line. The beach appears to have dune or rocky face in the backshore. The foreshore between high water line and the reef crest is wide and shallow with almost flat slope. The geomorphological features in this section are windward coral crests, carbonate hard ground, reef flats and shallow sand sheets.

The profile in Figure 3.2b which is also located on the seaside of Birrim is Section 73, a non-nesting site at the edge of the reef with very steep slope. The edge of the shoreline is presumably rocky and has high wave energy exposure. The geomorphology corresponds to steep edge windward crest with

carbonate hard rock.

The profile in Figure 3.2c which is located on the lagoon side of Birrim, Section 87 is a non-nesting site in the shallow sheltered zone with very low wave activity and influenced by tidal circulation. The shoreline is presumably biologically active zone with prominent vegetation. Due to the low wave energy and mild tidal circulation the morphology will be dominated by fine sediments like silt and clay. The geomorphological features are sand and mud flats with mangroves and other vegetation.

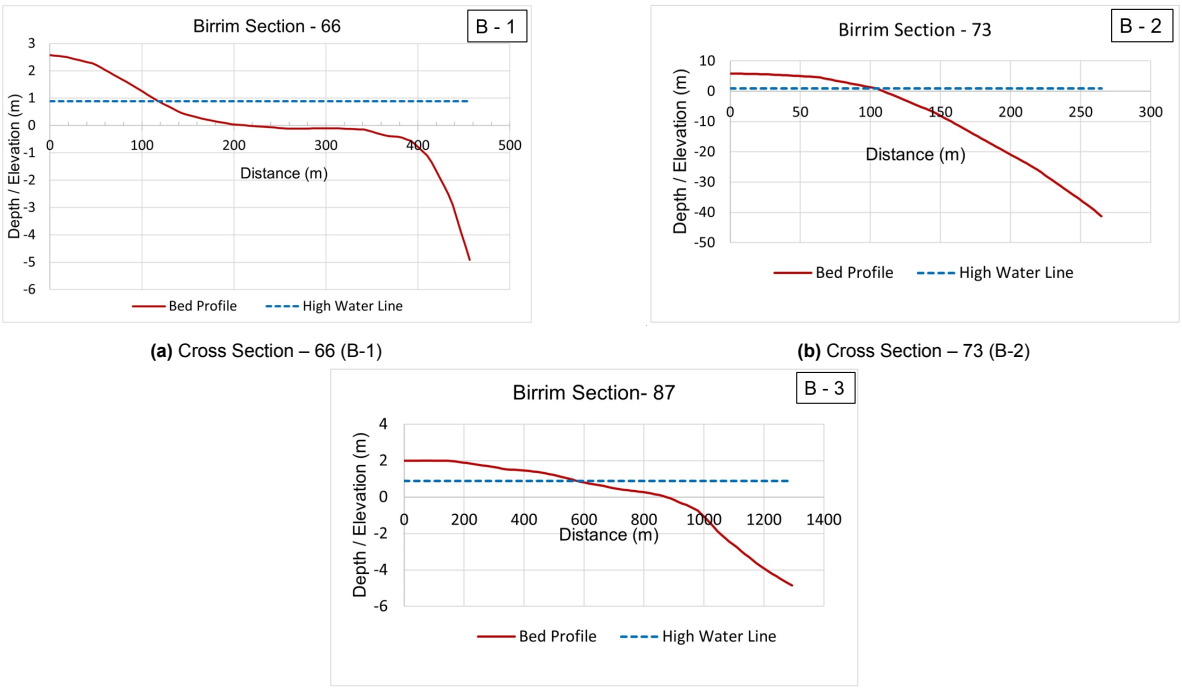

(a) Cross Section – 66 (B-1)

(b) Cross Section – 73 (B-2)

(c) Cross Section – 87 (B-3)

Figure 3.2: Profiles at Birrim island: B1 (nesting), B2 (non-nesting), B3 (sheltered area with near shore vegetation). The red line represents elevation w.r.t. LAT and the blue line represents the highwater line (0.89).

The Qummaan island is located inside the lagoon. The profile in Figure 3.3a located on the windward side is for Section 246 which is a nesting site in a sandy beach close to highwater line. The beach appears to have dune in the backshore. Like what has been observed for Birrim nesting site, the foreshore between high water line and the reef crest is wide and shallow with almost flat slope. This flat profile helps in the dissipation of wave energy under stormy wind conditions. The geomorphological features in this section are coral crests, shallow sand sheets, reef flats and deep lagoon sands.

The profile in Figure 3.3b which is located on the leeside of Qummaan belongs to Section 253 is a non-nesting site at the edge of the reef flat with very gentle slope. The edge of the shoreline is having sand and mud flats and has mangroves and other vegetation. The geomorphology corresponds to steep edge fringing reef covered with sand and mudflats in the intertidal zone.

The profile in Figure 3.3c, which is located in the shallow part of lagoon, is in the leeside side of Qummaan. Section 257 is a non-nesting site in the shallow sheltered zone exposed to very low wave activity but influenced by tidal circulation. The Google imagery indicates that the section falls in a shallow creek network which extends to the centre of island and flanked by mud flats. This may be functioning as a drainage channel for the freshwater during occasional rainfall. The shoreline is biologically active zone with prominent vegetation. Due to the low wave energy and mild tidal circulation the morphology will be dominated by fine sediments. The geomorphological features are sand and mud

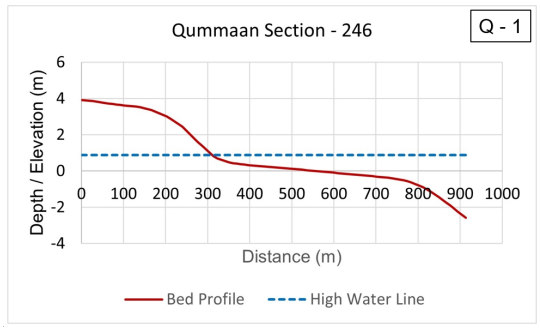

(a) Cross Section – 246 (Q-1)

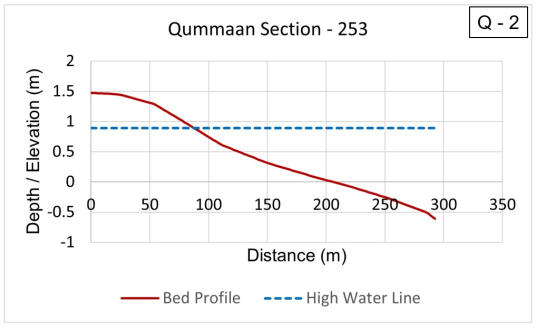

(b) Cross Section – 253 (Q-2)

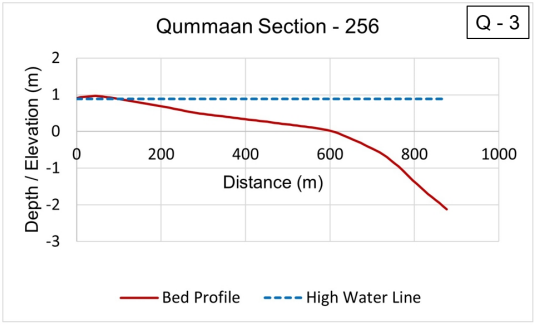

(c) Cross Section – 256 (Q-3)

Figure 3.3: Profiles at Qummaan island: Q1 (nesting), Q2 (non-nesting), Q3 (sheltered area with near shore vegetation). The red line represents elevation w.r.t. LAT and the blue line represents the highwater line (0.89 m).

flats with mangroves and other vegetation.

3.2.2. Beach slopes

Slopes were also computed at 31 nesting and 35 non-nesting sites using bed profile data. The seabed slopes close to high water line for nesting and non-nesting sites are shown in Figure 3.4 and Figure 3.5 respectively. The gentle beach slopes for nesting sites are evident. It is generally observed that slopes are below 0.10 (1/10) at the nesting sites. The non-nesting sites where slopes are similar may not be preferred for nesting by sea turtles due to other reasons like presence of fine sediments and vegetation. It is also evident that the non-nesting sites with gentle slopes are, in general, located inside the lagoon. These sections are similar to the profiles shown for Birrim (Figure 3.2c) and Qummaan (Figure 3.3c) located in the sheltered zone, towards lagoon, with low wave energy.

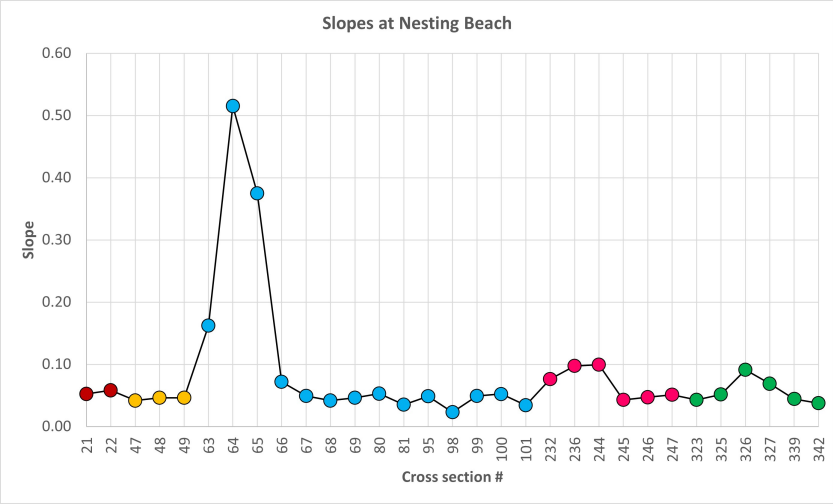

Figure 3.4: Slopes at the Nesting sites. The islands are represented by different colours, Maroon: Um Rumah island; Yellow: Ghawar island; Blue: Birrim island; Pink: Qummaan island; Green: Sheybarah south island. For exact location of the cross-section see Table 1.1

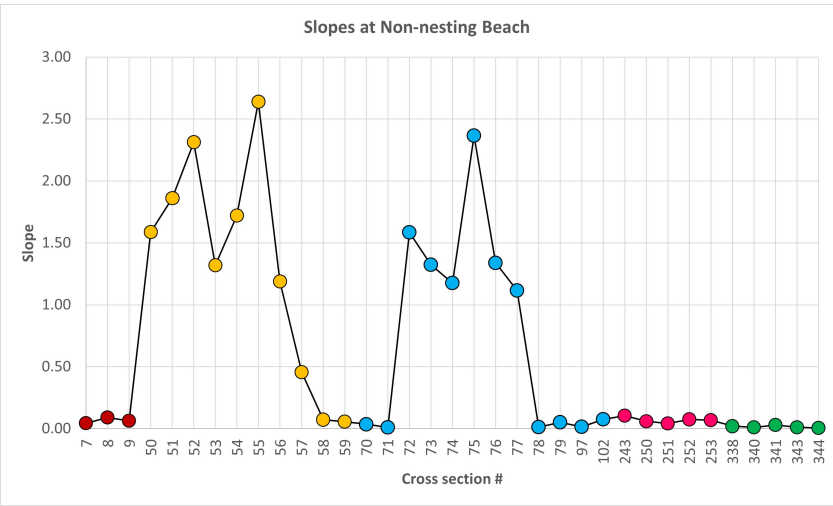

Figure 3.5: Slopes at the Non-nesting sites. The islands are represented by different colours, Maroon: Um Rumah island; Yellow: Ghawar island; Blue: Birrim island; Pink: Qummaan island; Green: Sheybarah south island. For exact location of the cross-section see Table 1.1

3.2.3. Sediment Characteristics

Turtles prefer to dig their nests in deep, fine, moist sand located above the high tide levels [73]. Once the egg chamber is made ready inside the pit the turtle lays the eggs and fills the hole with sand and returns to the ocean [73]. Thus, the unique features of the sediments at the sandy shoreline are of primary importance for turtles to make site selection. The data on sediment characteristics available for Al Wajh Bank is limited to a few islands which are not prominent nesting grounds for sea turtles.

Because different organisms require different grain sizes, sediment structure is critical for benthic populations. Grain size and sorting makes a difference in the ability of turtles to dig a stable egg chamber for nesting. Coral reef sands are made up of skeletal material from corals, macroalgae, phytoplankton, foraminifera, radiolarians, mollusks, and other organisms. Suspended sediments have been shown to stress fish and harm their gills, as well as smother coral reefs and lower benthic primary production. Sediment characteristics can reveal source materials, the deposition environment that can

explain the amount of energy in waves and currents, as well as other physical and chemical properties.

One way to characterize a sediment is to determine the sizes of grains in that sediment running through representative samples in a set of sieves. Based on the distribution of different size classes statistical analysis can be done to know population size characteristics like mean, median, mode, standard deviation, skewness and kurtosis. These can help in identifying the sorting of the sediments. Well sorted sand grains favour nesting activity. High silt content results in a mixed sorting and more compacted soil that does not favour successful nesting. High percentage of fine material does not allow oxygen to penetrate freely [16] and water does not drain.

The sediment characteristics of samples collected at Shurayrat island which does not have nesting sites is shown in Figure 3.6 and Table 3.2 below. The sediment is poorly graded sand. Similarly, the sediment characteristics for Ummahat Alshaykh island and Sheybarah South are shown in Figure 2.19, Table 3.1 and Figure 2.20, Table 3.3 respectively. Sample location map is shown in Figure 2.18.

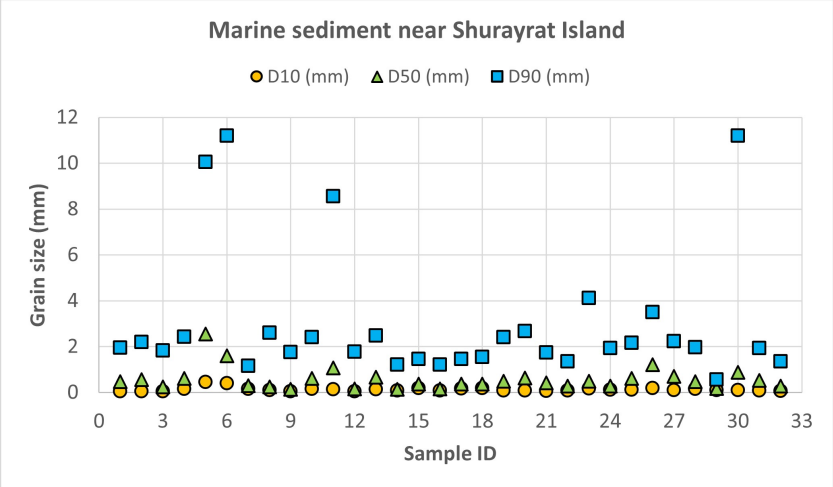

Figure 3.6: D10, D50, D90 of marine sediments near Shurayrat island

Table 3.1: Sediment Characteristics for samples collected near Ummahat Alshaykh island

Sr. no.	Sample_ID	Latitude	Longitude	Grading	Dn10 (mm)	Dn50 (mm)	Dn90 (mm)
1	SP1.1	25.55	36.75	SP	0.21	0.90	3.86
2	SP1.2	25.55	36.75	SP	0.24	0.39	1.38
3	SP1.3	25.55	36.75	SP	0.24	0.54	1.92
4	SP1.4	25.54	36.76	SP	0.25	0.41	1.19
5	SP1.5	25.55	36.75	SP	0.26	0.40	1.01
6	SP1.6	25.55	36.75	SP	0.20	0.83	3.58
7	SP1.7	25.55	36.75	SP	0.05	0.57	2.27
8	SP2.1	25.52	36.78	SP	0.06	0.18	1.05
9	SP2.2	25.52	36.78	SP	0.13	0.31	1.35
10	SP2.3	25.52	36.78	SP	0.05	0.58	1.19
11	SP2.4	25.53	36.78	SW	0.08	0.64	1.92
12	SP2.5	25.53	36.79	SP	0.13	0.32	1.37
13	SP2.6	25.52	36.78	SP	0.11	0.70	3.23
14	SP2.7	25.52	36.78	SP	0.05	0.10	1.23

Table 3.2: Sediment Characteristics for samples collected near Shurayrat island

Sr. no.	Sample_ID	Latitude	Longitude	Grading	Dn10 (mm)	Dn50 (mm)	Dn90 (mm)
1	BS4	25.49	36.99	SP	0.05	0.48	1.96
2	BS5	25.50	36.99	SP	0.05	0.56	2.20
3	BS6	25.50	36.99	SP	0.05	0.25	1.82
4	BS7	25.50	36.99	SP	0.16	0.62	2.43
5	BS8	25.50	37.00	SW	0.45	2.55	10.05
6	BS9	25.50	37.00	SP	0.41	1.60	11.20
7	BS10	25.50	37.00	SW	0.16	0.30	1.15
8	BS11	25.50	37.00	SW	0.11	0.24	2.61
9	BS16	25.49	36.99	SP	0.05	0.14	1.76
10	BS17	25.49	36.99	SP	0.16	0.62	2.41
11	BS18	25.49	36.99	SP	0.14	1.07	8.56
12	BS19	25.49	36.99	SP	0.05	0.15	1.77
13	BS20	25.49	37.00	SW	0.13	0.67	2.48
14	SP5.1	25.49	37.02	SP	0.08	0.14	1.21
15	SP5.2	25.49	37.01	SP	0.19	0.37	1.45
16	SP5.3	25.49	37.02	SP	0.09	0.15	1.21
17	SP5.4	25.49	37.02	SP	0.18	0.37	1.47
18	SP5.5	25.49	37.02	SP	0.18	0.37	1.55
19	SP5.6	25.49	37.02	SP	0.09	0.49	2.41
20	SP5.7	25.49	37.02	SP	0.08	0.63	2.67
21	SP NB1	25.50	36.97	SP	0.08	0.42	1.75
22	SP NB2	25.50	36.97	SP	0.09	0.28	1.35
23	SP NB3	25.51	36.98	SP	0.17	0.48	4.12
24	SP NB4	25.51	36.98	SP	0.13	0.28	1.94
25	SP NB5	25.51	36.98	SP	0.12	0.61	2.16
26	SP NB6	25.51	36.99	SP	0.19	1.20	3.50
27	SP NB7	25.51	36.99	SW	0.11	0.69	2.24
28	SP NB8	25.50	37.00	SP	0.15	0.47	1.98
29	SP NB9	25.51	37.00	SP	0.10	0.18	0.56
30	SP NB10	25.51	36.98	SP	0.10	0.88	11.20
31	SP NB11	25.50	36.98	SP	0.08	0.53	1.94
32	SP NB12	25.50	36.98	SP	0.06	0.27	1.36

Table 3.3: Sediment Characteristics for samples collected near Sheybarah South

Sr. no.	Sample_ID	Latitude	Longitude	Grading	Dn10 (mm)	Dn50 (mm)	Dn90 (mm)
1	SP4.1	25.36	36.91	SP	0.13	0.22	0.45
2	SP4.2	25.36	36.91	SP	0.08	0.16	0.80
3	SP4.4	25.36	36.91	SP	0.11	0.21	0.65
4	SP4.5	25.36	36.91	SP	0.08	0.16	0.56
5	SP4.6	25.37	36.91	SP	0.10	0.17	0.58
6	SP4.7	25.36	36.91	SP	0.11	0.28	1.30
7	SP4.7			SP	0.05	0.11	0.71

3.2.4. Nest distance from waterline

The location of the nest site on the beach relative to the high tide line is also considered as an important criterion for successful hatching of the eggs. Nests placed closer to the high tide line have lesser chances of survival of hatchlings compared to nests placed at farther away from the high tide line [84, 96]. Studies, however, could not find any correlation between selection of nesting sites and preference

to a particular zone across the beach [7, 8, 84].

The data on nest site coordinates were used to approximately estimate the position of the nests relative to the high water line at Al Wajh Bank using Google Earth imagery. The Figure 3.7 shows the distance between the nesting site and high water line at various nesting sites identified by nesting site section number. The nesting sites at a particular island fall in a band width across the beach which is specific to that island due to local geomorphology. This will depend on the location of the island exposed to sea or inside the lagoon. The nests are generally closer to the water line inside the lagoon (Qummaan, Mudra, Abu Laheq). It is assumed that the water line depicted in google earth is high water line. Therefore there is uncertainty in the measured values as the measurements could be from high water line, low water line or somewhere in-between. Therefore, in-situ measurements are required for finding the relation between the preferred nest location and distance from the high water line.

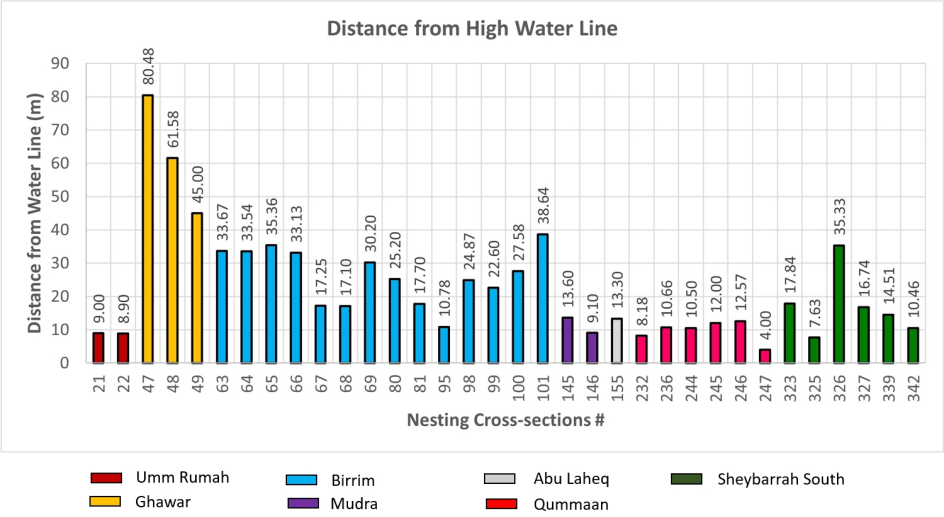

Figure 3.7: This figure shows distance of nesting site from High Water Line with different colours representing different nesting cross sections. The graph shows distances in the same band width for a particular island

3.2.5. Coastal Erosion Trends at Al Wajh Bank

The dynamics of sediment transport and erosion / accretion of islands with reef are poorly understood though waves in association with tides are known to play a major role. The source of beach sands in the reef islands is from biophysical processes unlike the coastal beaches where the sediment inputs are from fluvial rivers, eroding cliffs and aeolian deposits. Coral reef sands are produced by bioerosion of limestone skeletal material of marine organisms (skeletal fragments of foraminifera, calcareous algae, molluscs and crustaceans). Historically the sediment constituents influencing the development of reef islands is derived from primary contribution of the founding platforms by corals and the secondary contribution from benthic carbonate sources like foraminifera and calcareous green algae [49]. The development of reef islands and associated ongoing morphological changes are influenced by several factors [75]. The historical sea level changes and its influence on the growth of reefs and development of platforms is of primary importance which will also impact the future stability of the islands. The second factor is the available space for accommodating the sediment volume which is a function of the substrate slope, elevation and sea level. The factor controlling the vertical growth of the island are the storm wave runup processes, which will be in turn influenced by the relative sea level. The reef platform elevation and the lagoon depth will decide the lower limit of the available space. The other important factor is the sediment supply which is related to the benthic sediment budget dynamics

and the rates of sediment generation. The hydrodynamic regime comprising wind, wave and currents along with the frequency of extreme storm events will have a major role on the transport and deposition of sediments. The energy distribution in the barrier reef and lagoon system generally determines the nature of sediments in the beaches along the edges of the islands. The outer edge of the barrier reef and the windward side of the lagoon islands will be dominated by sandy sediments. Whereas the low energy sheltered areas on the inner reef shelf and leeward side of islands will have deposition of fine sediments of mud mixed with sand where mangroves and other vegetation will grow. Similar trends have been observed for the Al Wajh Bank habitats. The sandy beaches may have net erosion or deposition based on their location and orientation whereas the mud and sand flats with vegetation are more likely to have net accretion.

The reef crests and reef flats of the fringing reefs at the edge of the islands dissipate a major part of the destructive energy of the large waves associated with storms and cyclones. About 90% of the incident wave energy is dissipated by breaking process. The radiation stress gradients generated by waves breaking at the reef crests induce raising of the water surface elevation, above mean sea level, over the reef flats in the form of wave setup and swash uprush along the beach. The formation of low frequency infra gravity waves on the reef flats and generation of bores through resonant amplification [35] influence flooding of the beaches and the morphology through overwash. The onshore movement of the sediments produced in the forereef and reef flats helps in the deposition and growth of beach sediments. Whereas the alongshore sediment transport gradients and overwash can erode the beach sediments. Several ongoing studies are focused on the influence of sea level rise on the reef islands. Some of the studies depict an optimistic picture based on the observed changes during the last century which indicated a net increase or no change in the area of the islands [48, 50]. The Red Sea is reported to have large evaporation rates with seasonal changes in the sea level with net loss of water and increased density and salinity. The climate change may further enhance the evaporation rates in the Red Sea. The presence and influence of net sea level rise and the impact on the morphological processes at Al Wajh Bank may need to be investigated.

There are no systematic data collection or studies available in literature on the erosion and accretion trends for the Al Wajh Bank islands. However, a study carried out by [59] in respect of sandy beaches, on a global scale, based on satellite images for the period 1984-2016 provides quantitative information on the net erosion and accretion rates at transects taken at every 500 m. The study also covered the Al Wajh Bank region. The study uses sophisticated and automated image interrogation and analysis methods along with pixel based supervised classification to identify the global scale occurrence of sandy beaches and rates of shoreline changes. The study classified the shoreline change rates with class intervals of 0.5 m/yr to identify the trends at the beach transects covering six class intervals from accretion to extreme erosion. The study highlights the global prevalence of sandy beaches; global quantitative assessment of the rate of erosion and accretion; analysis of selected locations for observed natural and human induced impacts; and global hot-spots of erosion and accretion. The analysis of this study for Al Wajh Bank is presented below.

The identification of chronic erosion spots at Al Wajh Bank identified by the study is shown in Figure 3.8. The figure indicates that chronic erosion (< -3.0 m/yr.) are located along the northern coastline of Al Wajh Bank and in the Sheybarrah island. The Sheybarrah island have about 2% of the turtle nesting sites in the Al Wajh Bank. A few erosion sections are also indicated for Umm Khud and Ghawar islands in the northern part of the outer reef shelf.

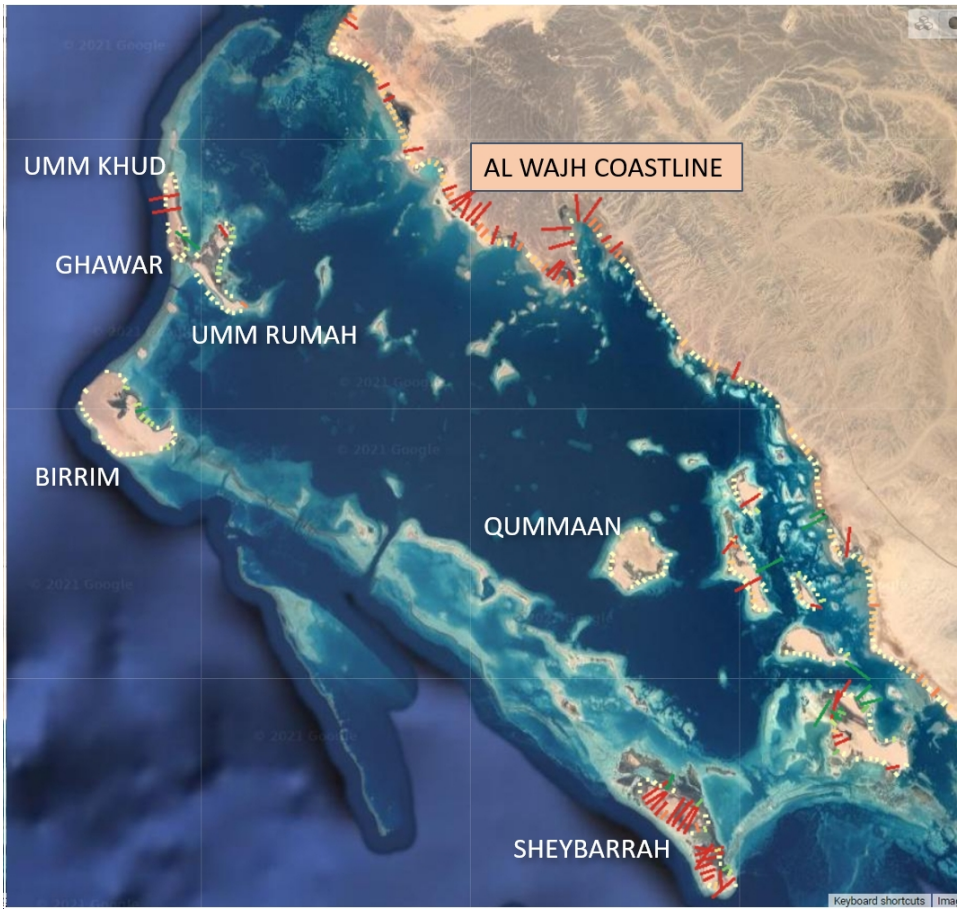

Figure 3.8: The figure shows the beach transects at 500 m at the Al wajh coastline and the islands at the reef edge and inside the lagoon. The red colour of the transects indicates chronic erosion spots with < -3 m/yr erosion rates. (source: https://aqua-monitor.appspot.com/?datasets=shoreline)

The highest number of nesting sites are found in the Birrim island with 50.62% of the total turtle nests in Al wajh Bank. The beach along the western face on the reef edge has the highest density of nests where erosion from 0.1 m/yr to 0.4 m/yr is indicated by the said study. The Al Waqadi island which has long coastline with continuous sandy beaches south of Al Wajh has next highest i.e., 27.7% of the nesting sites but this island is not covered by the study as this island could not be properly resolved on the computational grid used. The erosion and accretion rates at transect near the nesting and non-nesting sites for islands along the edge of the reef and the lagoon are given Table 3.4. The values have been also plotted separately for nesting and non-nesting sites and shown in Figure 3.9 to Figure 3.12. Figure 3.9 shows the erosion / accretion rates at transects near the nesting sites for lagoon side islands. The erosion rates or accretion rates are low (-0.3 to 0.7 m/yr.). Figure 3.10 shows the erosion / accretion rates at transect near the nesting sites for seaside islands. The erosion rates or accretion rates are very low (0.1 to 0.4 m/yr) for all the islands except for Sheybarrah South island which has chronic erosion rates but has only 2% of nesting sites. Figure 3.11 shows the erosion / accretion rates at transect near the non-nesting sites for lagoon side islands. The net erosion rates or accretion rates are stable (-0.5 to 0.5 m/yr.). Figure 3.12 shows the erosion / accretion rates at transect near the non-nesting sites for sea side islands. The erosion rates or accretion rates are stable (-0.5 to 0.3 m/yr) for most of the nesting sites except for sites at Ghawar and Sheybarrah islands where erosion rates are high (-30 m/yr to -5 m/yr). The trend indicates that the nesting is preferred at sites with stable conditions of erosion / accretion. Similar stable conditions are also observed at non-nesting sites on

the seaside islands but the other conditions for turtle nesting may not be fulfilled.

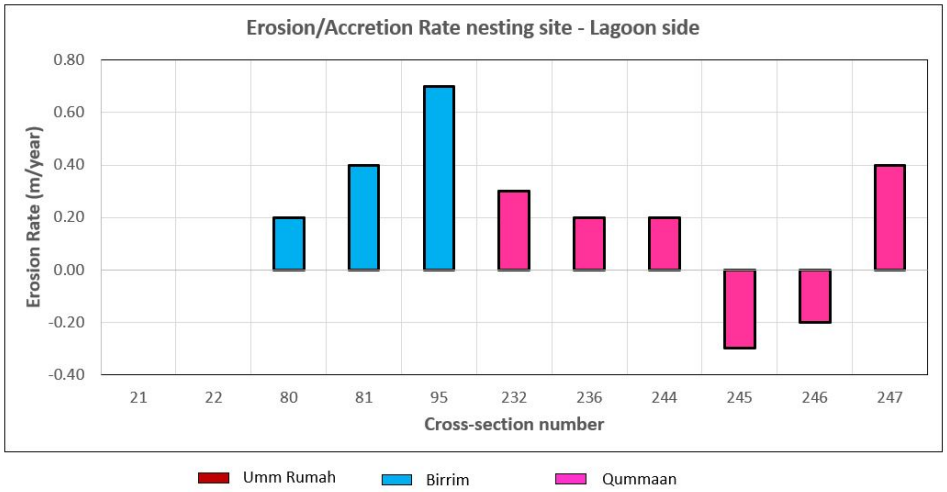

Figure 3.9: The erosion / accretion rates are depicted at transects near the nesting sites for Lagoon side islands. The erosion rates or accretion rates are low (-0.3 - 0.7 m/yr)

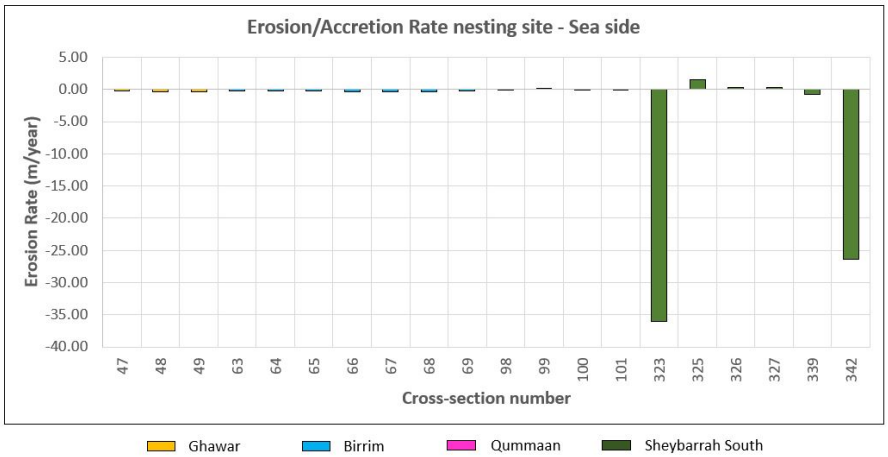

Figure 3.10: The erosion / accretion rates are depicted at transects near the nesting sites for seaside islands. The erosion rates or accretion rates are very low (0.1 - 0.4 m/yr) for all the islands except for Sheybarrah South island which has chronic erosion rates but has about 2% nesting sites.

Table 3.4: The Erosion / Accretion rates for Nesting and Non-Nesting sites at various islands located at the edge of the reef and inside the Lagoon.

Cross-section no.	Island Name	Nesting (N) or Non-Nesting (NN)	Location	Erosion Rate (m/yr)	
7	Um Rumah 1 Island	NN	Lagoon side	-0.20	+/-0.1
8	Um Rumah 1 Island	NN	Lagoon side	-0.10	+/-0.2
9	Um Rumah 1 Island	NN	Lagoon side	0.20	+/-0.2
21	Um Rumah 1 Island	N	Lagoon side	NAN	NAN
22	Um Rumah 1 Island	N	Lagoon side	NAN	NAN
47	Ghawar Island	N	Sea side	-0.20	+/-0.1
48	Ghawar Island	N	Sea side	-0.40	+/-0.1
49	Ghawar Island	N	Sea side	-0.40	+/-0.4
50	Ghawar Island	NN	Sea side	-29.70	+/-8.1
51	Ghawar Island	NN	Sea side	-0.30	+/-0.6
52	Ghawar Island	NN	Sea side	-32.90	+/-7.6
53	Ghawar Island	NN	Sea side	-0.20	+/-0.6
54	Ghawar Island	NN	Sea side	-0.20	+/-0.6
55	Ghawar Island	NN	Sea side	-0.60	+/-0.8
56	Ghawar Island	NN	Sea side	-0.70	+/-0.7
57	Ghawar Island	NN	Sea side	-0.30	+/-0.1
58	Ghawar Island	NN	Sea side	-0.50	+/-0.2
59	Ghawar Island	NN	Sea side	-0.10	+/-0.1
63	Breem Island	N	Sea side	-0.30	+/-0.2
64	Breem Island	N	Sea side	-0.20	+/-0.1
65	Breem Island	N	Sea side	-0.30	+/-0.2
66	Breem Island	N	Sea side	-0.40	+/-0.1
67	Breem Island	N	Sea side	-0.40	+/-0.5
68	Breem Island	N	Sea side	-0.40	+/-0.5
69	Breem Island	N	Sea side	-0.20	+/-0.2
70	Breem Island	NN	Sea side	-0.70	+/-0.2
71	Breem Island	NN	Sea side	-0.40	+/-0.2
72	Breem Island	NN	Sea side	-0.40	+/-1.3
73	Breem Island	NN	Sea side	-0.30	+/-0.3
74	Breem Island	NN	Sea side	-0.60	+/-0.4
75	Breem Island	NN	Sea side	-0.10	+/-0.3
76	Breem Island	NN	Sea side	-0.10	+/-0.3
77	Breem Island	NN	Sea side	-0.10	+/-0.3
78	Breem Island	NN	Sea side	0.30	+/-0.3
79	Breem Island	NN	Lagoon side	0.30	+/-0.2
80	Breem Island	N	Lagoon side	0.20	+/-0.1
81	Breem Island	N	Lagoon side	0.40	+/-0.1
95	Breem Island	N	Lagoon side	0.70	+/-0.3
97	Breem Island	NN	Lagoon side	0.50	+/-0.2
98	Breem Island	N	Sea side	-0.10	+/-0.1
99	Breem Island	N	Sea side	0.10	+/-0.2
100	Breem Island	N	Sea side	-0.10	+/-0.1
101	Breem Island	N	Sea side	-0.10	+/-0.1
102	Breem Island	NN	Sea side	-0.30	+/-0.1
232	Quman Island	N	Lagoon side	0.30	+/-0.1
236	Quman Island	N	Lagoon side	0.20	+/-0.1
243	Quman Island	NN	Lagoon side	0.20	+/-0.2
244	Quman Island	N	Lagoon side	0.20	+/-0.2
245	Quman Island	N	Lagoon side	-0.30	+/-0.1
246	Quman Island	N	Lagoon side	-0.20	+/-0.1
247	Quman Island	N	Lagoon side	0.40	+/-0.1
250	Quman Island	NN	Lagoon side	-0.60	+/-0.2

Cross-section no.	Island Name	Nesting (N) or Non-Nesting (NN)	Location	Erosion Rate (m/yr)	
251	Quman Island	NN	Lagoon side	-0.20	+/-0.2
252	Quman Island	NN	Lagoon side	0.20	+/-0.2
253	Quman Island	NN	Lagoon side	-0.10	+/-0.1
323	Sheybarah South Island	N	Sea side	-36.00	+/-7.5
325	Sheybarah South Island	N	Sea side	1.50	+/-0.2
326	Sheybarah South Island	N	Sea side	0.30	+/-0.2
327	Sheybarah South Island	N	Sea side	0.30	+/-0.2
338	Sheybarah South Island	NN	Sea side	-1.80	+/-1.3
339	Sheybarah South Island	N	Sea side	-0.80	+/-0.5
340	Sheybarah South Island	NN	Sea side	-4.70	+/-1
341	Sheybarah South Island	NN	Sea side	-26.40	+/-4
342	Sheybarah South Island	N	Sea side	-26.40	+/-4
343	Sheybarah South Island	NN	Sea side	-14.40	+/-2.8
344	Sheybarah South Island	NN	Sea side	-17.70	+/-3.5

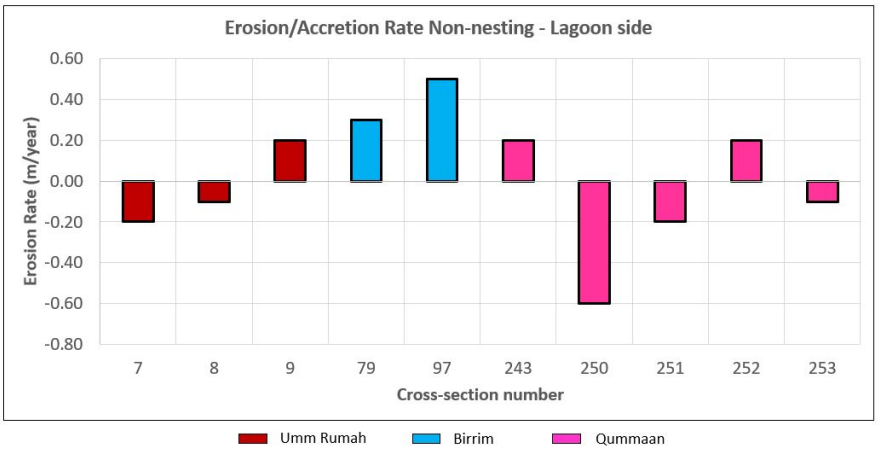

Figure 3.11: The erosion / accretion rates are depicted at transect near the non-nesting sites for lagoon side islands. The erosion rates or accretion rates are low (-0.5 - 0.5 m/yr)

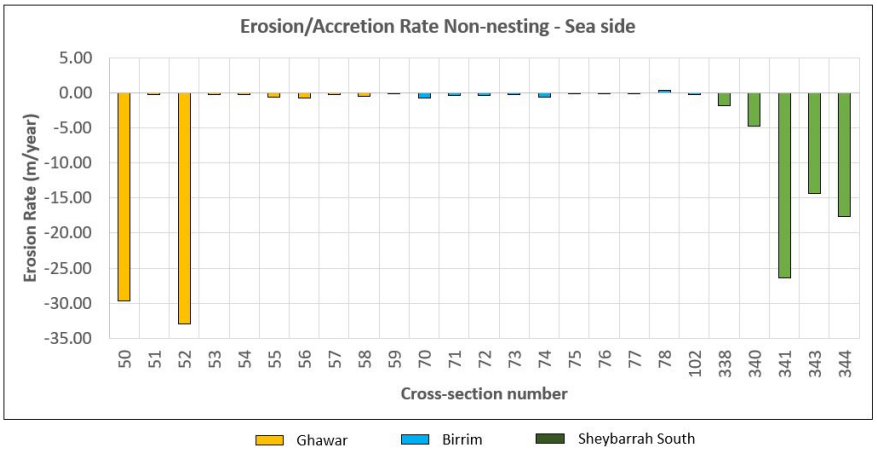

Figure 3.12: The erosion / accretion rates are depicted at transect near the non-nesting sites for seaside islands. The erosion rates or accretion rates are low (-0.5 - 0.3 m/yr.) for most of the nesting sites except for sites at Ghawar and Sheybarrah islands with erosion rates are high.

3.3. Vegetation characterization

The spatial distribution of vegetation was analysed on the lagoon side in relation to the nesting and non-nesting sites. The data is extracted from the “Atlas of Saudi Arabia Red Sea Marine Habitats” [12]. An example of data provided in “Atlas of Saudi Arabia Red Sea Marine Habitats” is shown in Figure 3.13. The nest construction by sea turtles can be blocked by the presence of vegetation [15, 14, 19]. Vegetation can cause drying of sand, affecting nest construction due to collapse of egg chamber [14]. The spread of roots around the nests can destroy eggs, damage eggshells, and disrupt hatching [15, 32, 56, 95, 57]. The development and survival of embryo can be disrupted by the roots due to reduced pore space between sand particles and hindered gas exchange between the egg and surrounding sand [2].

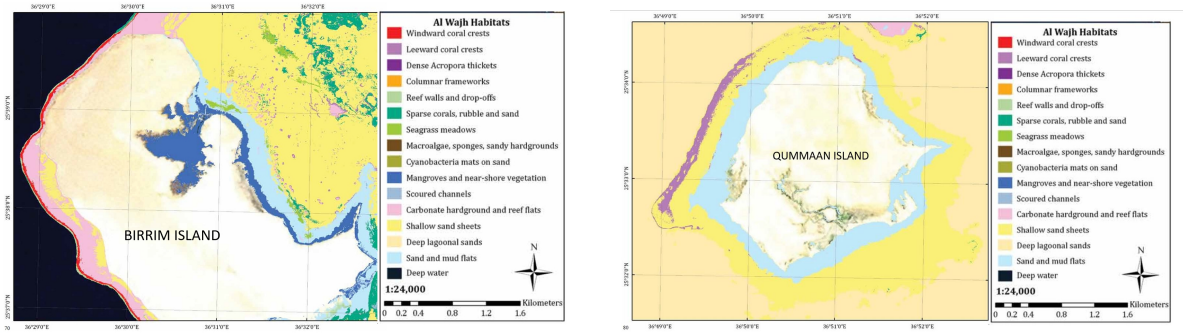

(a) Marine Habitat near Birrim island

(b) Marine Habitat near Qummaan island

Figure 3.13: Example of marine habitats at the seaward end and inside the lagoon. These maps were used for finding the nearshore habitat at each cross-section. Soruce:[12]

In the reef lagoon system vegetation is more prevalent in sheltered zones with little or no wave exposure and mild tidal circulation where suspended sediments can slowly settle forming soft beds. These areas are biologically active and the vegetation like mangroves sea bed grass provides nursery grounds for marine species. The vast area inside the protected lagoon at Al Wajh Bank has widespread mangroves mainly in sheltered areas behind reef flats, in bays or creeks, and on the leeward side of offshore islands. They are more prevalent in inner protected lagoons and sheltered embayments where water depths range from 0.5-1.5 m [12].The leeward side of the islands has soft bottom habitats where sea bed grass grows extensively. Habitat analysis of the nesting and non-nesting sites was carried out in relation to the geomorphological features and vegetation. The Figure 3.14 shows the percentage occurrence of nesting and non-nesting sites in different habitats. The prevalence of nesting sites in areas without mangroves and nearshore vegetation is evident. Similar trend can be seen from the pie chart distribution shown in Figure 3.15 and Figure 3.16.

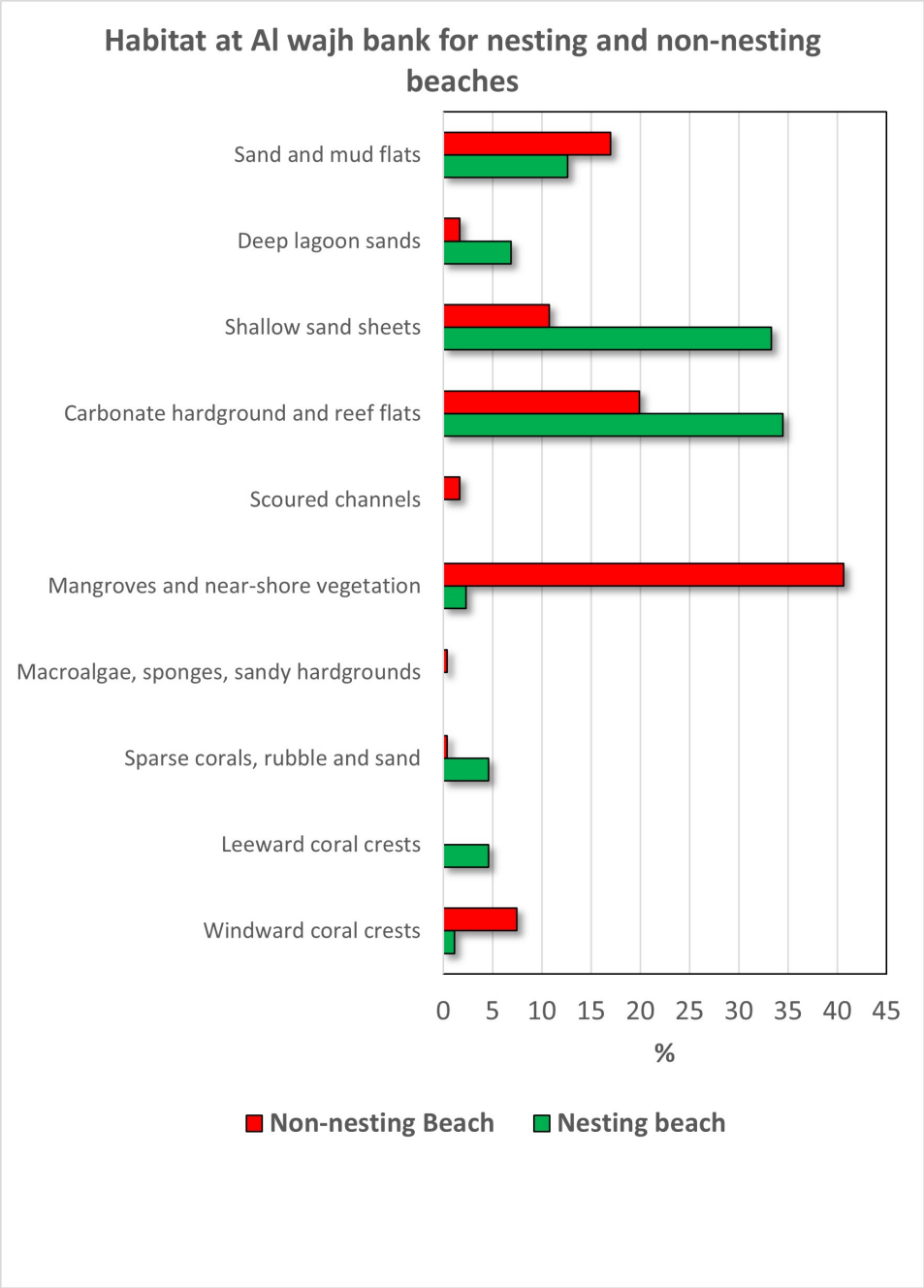

Figure 3.14: Marine habitat at Al Wajh bank for nesting and non-nesting beaches. The graph shows percentage occurrence of nesting and non-nesting beaches at specific habitat. Nesting beaches and non-nesting beaches are represented by Green and red bars respectively.

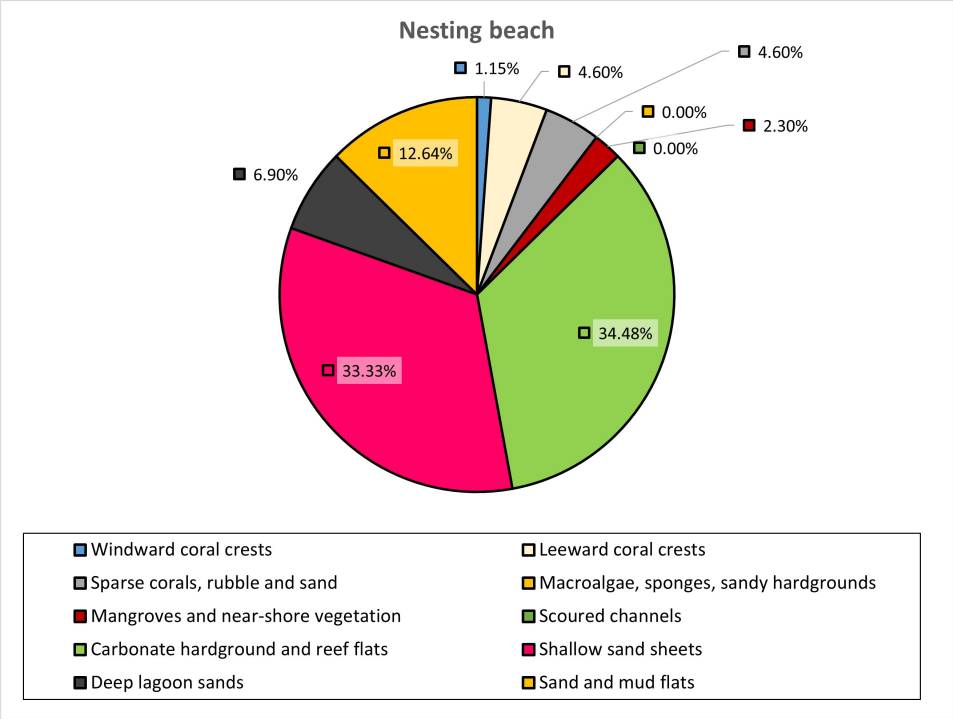

Figure 3.15: Pie chart showing distribution of beach features at Nesting beaches with percentage of occurrence at each habitat

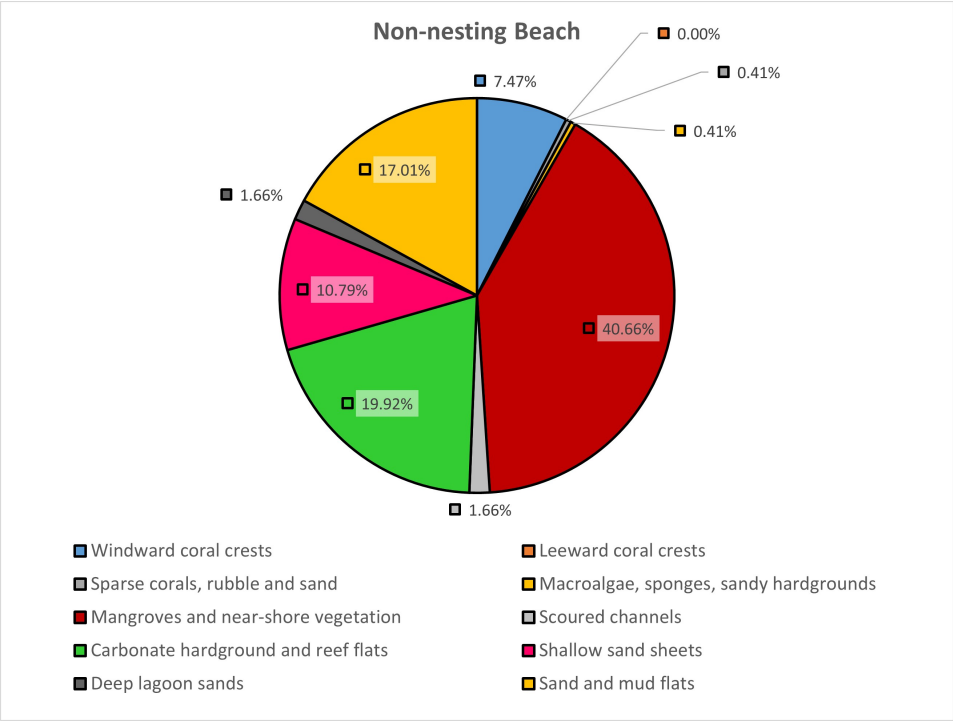

Figure 3.16: Pie chart showing distribution of beach features at Non-nesting beaches with percentage of occurrence at each habitat

3.4. Summary of Results

The geomorphological features, sediment characteristics and vegetation characteristics were examined in relation to the turtle nesting and non-nesting sites at Al Wajh Bank. The Birrim Island at the edge of the reef has more than 50% of the nesting sites for the Al Wajh Bank region. The beach and foreshore profiles were examined at this and other islands for the nesting, non-nesting sites with mud flats and vegetation. The analysis shows that the nesting sites have very distinct gently sloping beaches with a wide and flat reef in the foreshore. These features are absent at the non-nesting sites. The sites with mud flats and vegetation which are on the inner shelf of the reef shelf have similar gentle slopes but have large amounts of fine sediments. The nesting sites are not found in these areas.

The beach slopes for the nesting sites were in the range of 1 in 10 to 1 in 20. In the islands inside the lagoon the nesting sites have also beach slopes in the above range but some of them are not preferred due reasons of unfavorable sediment parameters. The available sediment data is poorly represented for the nesting sites and the data was available for Sheybarah south Island which is having only 2% of the nesting sites. The island is identified as having chronic erosion rates and highly unstable. The island is dominated by fine sediments.

A comparison of the extensive sediment data available from Shurayrat Island which has no turtle nests indicated that the sediments are course and poorly graded.

The analysis of the distance of the nesting sites from the water line showed varying conditions for the different islands both outside and inside the lagoon. The nesting sites at a particular island fall in a band width across the beach which is specific to that island due to local geomorphology. This will depend on the location of the island exposed to sea or inside the lagoon. The nests are generally closer to the water line inside the lagoon (Qummaan, Mudra, Abu Laheq).

The erosion and accretions trends indicated chronic erosion (< 3.0 m/yr.) are located along the northern coastline of Al Wajh Bank and in the Sheybarrah island in the south. A few erosion sections are also indicated for Umm Khud and Ghawar islands in the northern part of the outer reef shelf. The Sheybarrah island have about 2% of the turtle nesting sites in the Al Wajh Bank. The turtle nesting sites are found at stable beaches with marginal erosion / accretion rates (+/- 0.5 m/year).

The vast area inside the protected lagoon at Al Wajh Bank has widespread mangroves mainly in sheltered areas behind reef flats, in bays or creeks, and on the leeward side of offshore islands. They are more prevalent in inner protected area of the lagoon and sheltered embayments where water depths range from 0.5 - 1.5 m. The prevalence of nesting sites in areas without mangroves and nearshore vegetation is observed for the Al Wajh Bank.

4

Hydrodynamics of Al Wajh Bank

4.1. Introduction

To get a preliminary idea on the characteristics of the wave conditions and the rate of wave energy dissipation taking place across the reefs at the Al Wajh Bank, numerical modelling of the spectral waves transformation from offshore to nearshore is carried out. The effect of the normal and extreme waves and wind approaching from the northwest were simulated in the model to get the conditions inside and outside the lagoon, at the sea turtle nesting and non-nesting sites. The study will also provide estimates of wave runup using HyCReWW metamodel at the nesting and non-nesting sites to examine the inundation risks for nesting grounds at Al Wajh Bank. The propagation of waves from offshore to nearshore will undergo the process of refraction, diffraction and shoaling. In the deep ocean the wave growth due to wind and dissipation will take place due to white capping and non-linear quadruplet wave-wave interactions which transfer energy from lower frequencies to higher frequencies. The directional spreading of the wave energy will also occur. In the nearshore the presence of reefs, islands and lagoon will present a complex bathymetry condition [88]. The waves will be influenced by non-linear triad wave-wave interactions, bottom friction and wave breaking due to shallow depths along the reefs and islands [98, 70]. Unlike the gently sloping sandy beach environment found along coastlines, the wave transformation across the nearshore coral reef barriers is influenced by steep fore reef slope and strong bottom friction [9, 91, 70]. The energy entering the lagoon behind the reefs is influenced by the water depths over the reefs. The lower the depths the higher will be the wave attenuation and only a moderate amount of wave energy is allowed to pass over the reef. This filtering effect of the reefs on the waves creates conditions for unique ecological environment.

Very few studies are published on the wave climate near reef environment along the Red Sea coastline. Most of the model studies on waves are in the regional scale covering the whole of Red Sea and often use very course grid. Some of the studies which covered areas close to the coastline have focused in areas in the South Red Sea, far south of Al Wajh, near Jeddah where in situ data on wave measurements using wave rider buoy are available [33, 54]. No such measured wave data is available for the Al Wajh Bank for validation of the wave model in the present study. Though this is a major setback for simulating the correct wave conditions at Al Wajh Bank, the present study will be useful in the qualitative assessment of the wave conditions and a relative analysis of the model results

are expected to identify the future strategy for detailed data collection and further research on this topic. The study is expected to give an idea of the rate of energy dissipation occurring across the barrier reef system at Al Wajh Bank forming a major contribution from this study. Therefore, the present exercise is considered as a preliminary study for modelling wave conditions at Al Wajh Bank and a first step in understanding the preferential conditions for sea turtle nesting.

The numerical wave model is proposed to be setup in the Delft3D-WAVE model version 3.04.01.757 of Deltares which basically uses the SWAN model version swan_4072ABCDE. The bathymetry input is available at a very high resolution of 50 cm for the Al Wajh Bank made available by KAUST through GCS which is supplemented by a relatively course resolution data for the offshore area from GEBCO. The data for specifying the offshore boundary conditions of wind and wave were sourced from 'Wave-climate.com'. It is proposed to model the transformation of spectral waves from offshore to nearshore derived from the analysis of 27 years 3 hourly daily wind and wave data at an offshore location north-west of Al Wajh Bank. The model area was chosen sufficiently large to establish the boundary covering the wave data location. An introduction to Delft3D model is given in Section 4.2 and the details of the model setup and the results are given in the following sections.

4.2. Delft3D Wave Model

4.2.1. Introduction

The Delft3D-Wave module is a standalone wave model to simulate the evolution of wind generated waves in deep ocean and coastal waters. It uses the third-generation phase averaged SWAN (Simulating Wave Nearshore; Version 4072 ABCDE) model developed by TU Delft [10, 80]. SWAN is a fully spectral (in all directions and frequencies) and is based on the discrete spectral action balance equation. The evolution of random short-crested waves including interactions with currents can be computed using SWAN for the coastal regions in the offshore and nearshore region including whitecapping and depth induced wave breaking. The SWAN model incorporates the following physics:

- wave refraction due to variable depth and spatially varying ambient currents
- shoaling due to changes in depth and currents
- dissipation by whitecapping
- dissipation by depth-induced breaking
- dissipation due to bottom friction
- non-linear wave-wave interactions
- wave blocking by flow
- transmission through, blockage or reflection against obstacles
- diffraction

A provision is there for dynamic interaction of the wave model with Delft3D FLOW module to account for two-way wave-current interactions. This is accomplished both in the online or offline mode of coupling. The SWAN model of Delft3D-WAVE is typically used for projects related to harbours, offshore installations and for wave hind casting. In general, the areas of model applicability include estuaries, tidal inlets, lakes, barrier islands, tidal flats, channels and coastal regions.

4.2.2. Physical background of SWAN

The two dimensional wave action density spectrum N(σ, θ) is used to describe waves in SWAN and this spectral moment of second order is able to handle non-linear phenomena with reasonable accuracy.

The action density spectrum N(σ, θ) is used instead of the energy density spectrum E(σ, θ) to conserve action density in the presence of currents. Here σ and θ are independent variables relative frequency and wave direction respectively. The action density is obtained by dividing the energy density by the relative frequency i.e. N(σ, θ) = E(σ, θ)/σ. The spectrum may vary in space and time in SWAN.

The spectral action balance equation describes the evolution of wave spectrum in SWAN and the equation in Cartesian coordinates is given by [42]:

$$\frac{\partial N}{\partial t} + \frac{\partial C_x N}{\partial x} + \frac{\partial C_y N}{\partial y} + \frac{\partial C_\sigma N}{\partial \sigma} + \frac{\partial C_\theta N}{\partial \theta} = \frac{S}{\sigma}$$

The local change of action density in time is represented by the first term. The second and the third term represent propagation of action in the x and y direction with propagation velocity of C_x and C_y. The shifting of relative frequency due to variations in depth and currents is handled by the fourth term with propagation velocity C_σ in σ – space. The depth and current induced refraction is represented by the fifth term with propagation velocity C_θ in θ – space. The propagation speed expressions are based on linear wave theory [94, 65, 27] The S term on the right side is the source term representing the effects of generation, dissipation and non-linear wave-wave interactions. The various source terms are

$$S(\sigma, \theta) = S_{in}(\sigma, \theta) + S_{ds,w}(\sigma, \theta) + S_{ds,b}(\sigma, \theta) + S_{ds,br}(\sigma, \theta) + S_{nl4}(\sigma, \theta) + S_{nl3}(\sigma, \theta)$$

The source term $S(\sigma, \theta)$ accounts for the processes related to the generation by wind $S_{in}(\sigma, \theta)$, dissipation by whitecapping $S_{wc}(\sigma, \theta)$, bottom friction $S_{ds,b}(\sigma, \theta)$ and depth induced breaking $S_{ds,br}(\sigma, \theta)$. It also includes the non-linear wave-wave interactions quadruplets $S_{nl4}(\sigma, \theta)$ and triads $S_{nl3}(\sigma, \theta)$. The transfer of wind energy through wind input is based on resonance mechanism [76] and feed-back mechanism [67] The steepness of waves controls the dissipation by whitecapping. The whitecapping formula is based on the pulse-based model [41], which WAMDI group [39] modified for the WAM model. Alternative whitecapping formulations are also provided in SWAN.

Implementation of depth induced breaking in spectral wave modelling is not well understood. The dissipation due to breaking is applied in the form similar to dissipation of a bore applied to breaking waves in a random field [5, 89] A spectral version of the bore model is also formulated in terms of rate of dissipation of total energy [30]

Bottom friction, moving beds, percolation in porous beds, and back scattering by sea bed irregularities can all generate depth-induced dissipation [85]. Bottom friction is the dominant mechanism for both continental shelf seas and in barrier reefs. A number of formulations for bottom friction are available in literature and some are very complex to implement or not effective for real natural conditions. The empirical mode of JONSWAP [42], the drag law model [22], and the eddy viscosity model [62] are the bottom friction models implemented in SWAN.

The evolution of the spectrum in deep water is dominated by quadruplet wave-wave interactions which transfer energy from the spectral peak to the lower frequencies and to higher frequencies in the event of whitecapping. Whereas the transfer of energy from lower frequencies to higher frequencies occurs in shallow water by the triad wave-wave interactions. The computation of quadruplet wave-wave interactions in SWAN is implemented with the Discrete Interaction Approximation (DIA) [43]. The Lumped Triad Approximation (LTA) is used for computing the Triad wave-wave interactions in SWAN [31].

4.2.3. Model Implementation

The Finite Difference Schemes have been used in the implementation of the integration of action balance equation in SWAN in all the five dimensions (time, geographical space (x,y) and spectral space (σ, θ)). Due to application in stationary mode for SWAN in Delft3D-WAVE, the time is omitted from the equations. A rectangular grid is used to discretise the geographical space with constant resolution in Δx and Δy. The spectrum is discretised by constant directional resolution $\Delta\theta$ and relative frequency resolution $\Delta\sigma/\sigma$. In SWAN the discrete frequencies are defined between fixed low frequency and fixed high frequency cut off. For computing wave-wave interactions a diagnostic f^{-m} tail is added above the high frequency cut off. The implementation of implicit schemes permits large time steps and the model is unconditionally stable. The downwave boundary conditions in the direction of wave propagation in SWAN are fully absorbing for waves leaving the boundary and crossing the land. The boundary conditions are specified along the deep water geographic boundary conditions. In Delft3D-WAVE user can specify different sets of wave boundary conditions and wind conditions. Four options are provided in the spatial and temporal domain:

1. Time varying and uniform wave conditions.
2. Time varying and space varying wave boundary.
3. Space varying boundary condition for use with UNIBEST coupling.
4. Space varying boundary condition: spectral input and output files.

Nesting of grids is implemented in SWAN and several grid resolutions can be included in one model run. The idea of nesting is to have a coarse grid for larger area and more fine grid for the smaller area of interest. The coarse grids and fine grids have to be properly connected in the model input specification. The model requires providing independent bathymetry files for the main and nested grids.

The outputs from the model simulations can be obtained in different formats for water depth (m), significant wave height (m), mean wave direction (deg.), peak wave period (s), directional spreading of waves (deg.), root mean square value of the maximum of the orbital motion near the bottom (m/s).

4.3. Model Setup

4.3.1. Computational Grid and Bathymetry

The computational grid was chosen sufficiently larger than the area of interest. The up-wave boundary is located in sufficiently deep water. The resolution for the spatial grid has to be chosen properly to resolve all the relevant details of the reefs, islands and the lagoon. The model domain for simulating the wave climate at Al Wajh Bank covered an area 198 km X 90 km as shown in Figure 4.1. A course rectangular grid with resolution of 1500 m was set up for this area. Further two stage nesting of finer grid was done for covering the Al Wajh bank with higher resolution. The two stage nesting adopted grid size of 500 and 100 m. The grid size of 100 m was used to resolved the Al Wajh bank features with reasonable economy for the computation time and memory space, though a third nesting by adopting grid size of 50 m or less could have been better. The grid layout and nesting adopted in the model are shown in Figure 4.2.

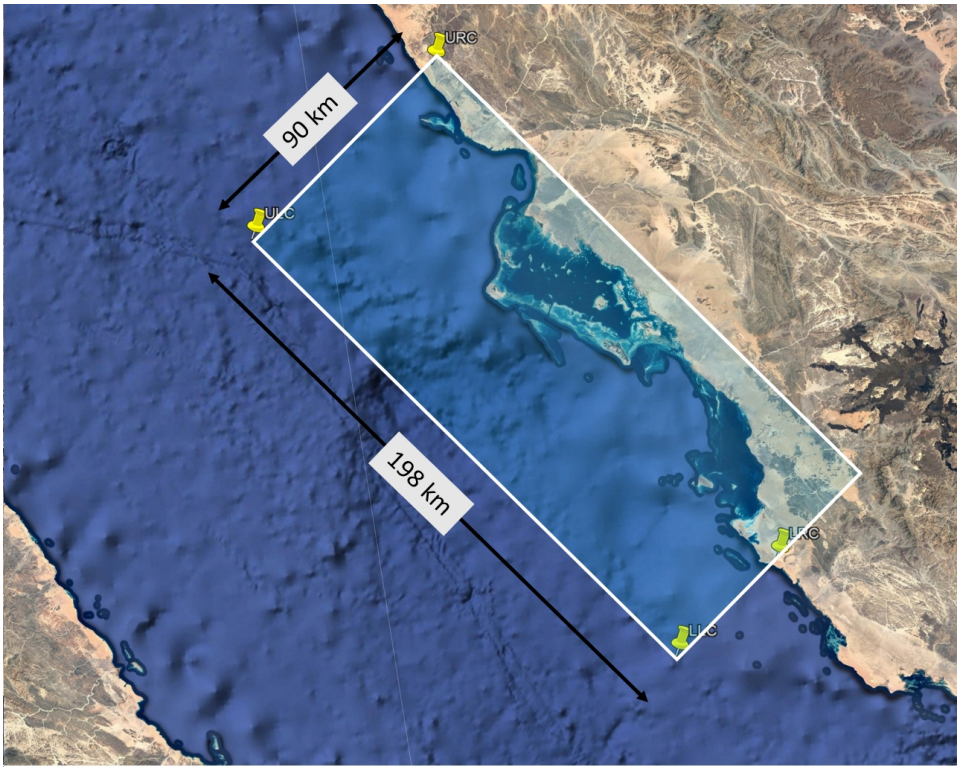

Figure 4.1: Extent of the area covered by the coarser grid in the Model.

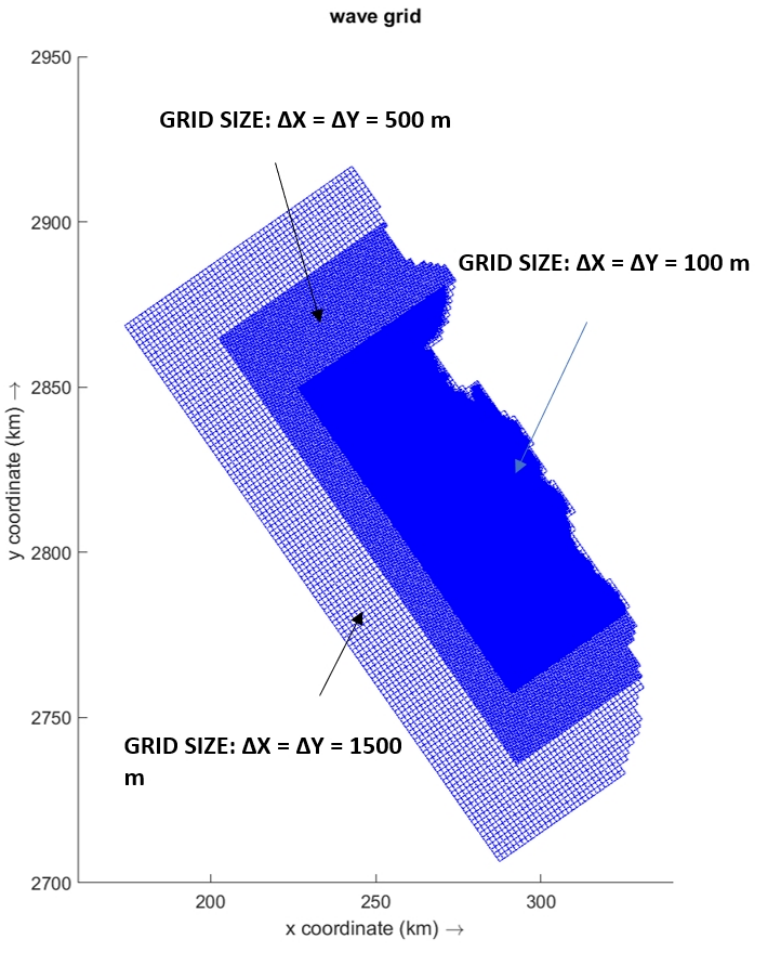

Figure 4.2: This figure shows grids with two stage nesting and corresponding gird cell size.The grids have three open boundaries and one land boundary. Boundary conditions were specified on Northwest and Southwest boundary.

The spectral resolution in both direction and frequency space must be defined for each computational grid in the Delft3D-WAVE model. A minimum and maximum frequency outside the expected lowest and peak frequency for the modelled area define the frequency space. The number of frequencies to be considered in this range for computations needs to be given as input apart from the frequency range. In the present study 40 frequencies were specified. In the directional space full $360°$ range can be specified. In addition, the number discrete directions also need to be specified. In the present study a resolution of $10°$ was chosen.

Delft3D-WAVE model specifies separate grids for the computations and input of bathymetry currents as well as for the output. For the proposed model grid the bathymetry was interpolated utilising the GCS and GEBCO data. The nesting of grids in SWAN model requires separate bathymetry input for the course grid and the nested grids. The model bathymetry for the course grid and the fine grid are shown in Figure 4.3 and Figure 4.4. The difference in resolution of bathymetry due to the grid spacing can be observed.

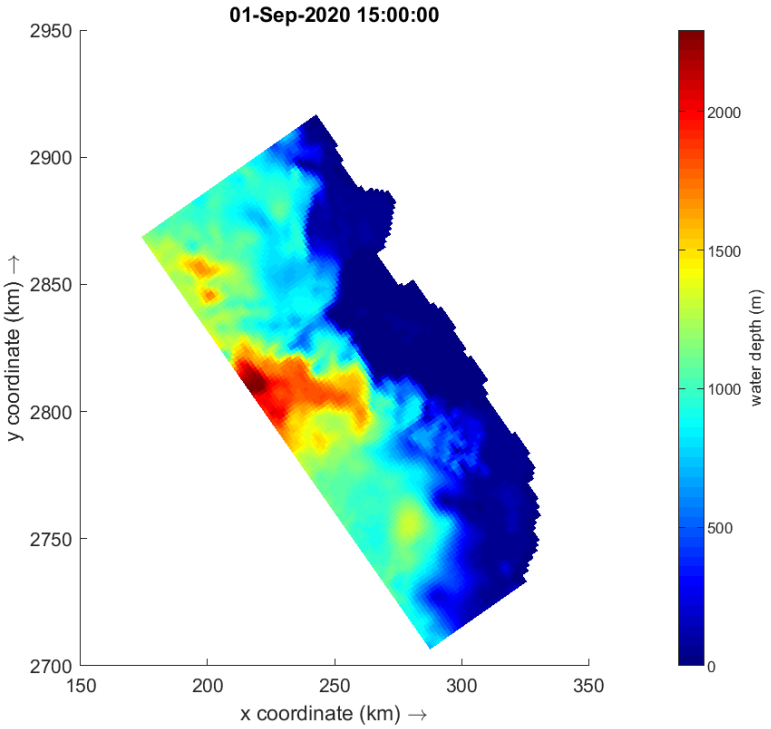

Figure 4.3: Representation of water depth on the Course Grid (1500 x 1500 m). The island features are not clearly resolved on this grid

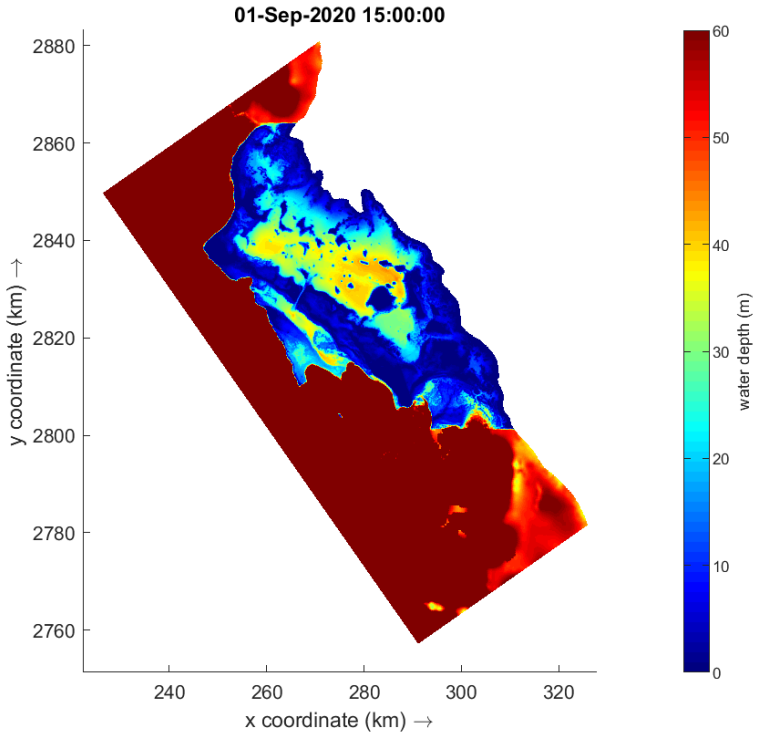

Figure 4.4: Representation of water depth on the fine Grid (100 x 100 m). Distinct islands could be seen in dark blue colour with shallow lagoon surrounded by islands; Red represents deep waters.

4.3.2. Boundary Conditions

The boundary definitions in SWAN can be specified in two ways – 1. By orientation of the full side (north, northeast, southwest etc.) and 2. By segment from the corner along a side (defined by grid or x-y coordinates). In the present study the boundary conditions are specified on the two sides of the top left corner of computational grid which is located on the up-wave side of wave propagation. The boundary along the southwest is specified by orientation and has uniform wave boundary conditions. The lateral boundary on northwest side between the land and deep water is specified by segments and has space varying wave boundary conditions.

The objective of the present study is to investigate the nearshore wave conditions based on satellite derived offshore wind and wave data and also understand the energy dissipation characteristics of the reef at Al Wajh in providing the preferential hydrodynamic conditions for turtle nesting. The analysis of the offshore data indicated that the directions of propagation of wind and waves lie in a narrow sector from 300^o to 330^o in the north-west quadrant (see Figure 2.10 and Figure 2.13. The directional distribution is in a narrow band. The estimate of the mean direction for the nesting and non-nesting season gave values of equal magnitude. The estimate of the significant wave heights for the nesting and non-nesting season are 1.34 and 1.41 respectively with very marginal difference. The wave periods are falling in the range of 4 to 6 seconds which indicate that these are short period waves and mostly locally generated. The wind conditions corresponding to the normal and extreme conditions were used to examine the effect of variability in wind.

For the preferential conditions of sea turtle nesting at Al Wajh Bank it is also proposed to investigate the expected inundation risk to the nesting conditions due to wave runup using simulations in HyCReWW metamodel. Therefore, extreme wave conditions were also estimated for 1 in 1 year and

1 in 100 year return period wave conditions and included in the numerical wave model simulations. The mean range of tidal fluctuations at the Al Wajh bank is 0.59 m and simulations were also done in numerical model to assess the effect of tides in the wave propagation and transformation across the reef flats and inside the lagoon.

In the absence of observed data for Al Wajh Bank, the present study uses available offshore wave and wind data to make a relative assessment of the wave hydrodynamics at Al Wajh Bank. Therefore, the default numerical and physical parameters were used for the model simulations. The inclusion of nearshore non-linear wave interactions by triads posed problems of model instability hence this was not included.

Table 4.1: Boundary conditions for model simulations

Sr. No.	Season/ Return Period	H_s (m)	T_p (s)	Mean Wave Direction (deg.)	Mean Wind Speed, $U_{10}(m/s)$	Mean Wind Direction (deg.)
Normal Conditions						
1	Nesting	1.34	5.56	315	6.83	324
2	Non-Nesting	1.41	5.65	316	6.85	323
Extreme Conditions						
1	1 in 1 year	2.65	6.11	315	13.06	318.5
2	1 in 100 years	3.66	6.98	315	15.35	318.5

4.3.3. Inputs for Numerical and Physical Parameters

Computational Model	Stationary
Frequency Space	40 bins between 0.03 Hz and 1.42 Hz
Directional Space	36 bins 10°
Generation by Wind	Komen et al. (1984), wave cycle 3
Whitecapping	Komen et al. (1984)
Refraction	Activated
Diffraction	Activated
Triads	Not Activated
Quadruplets	Discrete Interaction, Hasselmann (1983)
Bottom Friction	JONSWAP Model, Hasselmann et al. (1973)
Depth Induced breaking	Model after Battjes and Janssen (1978)

4.4. Model Results

The Delft3D WAVE (SWAN) model gives output for important wave parameters in the model area at the computational grid points in the model domain. The results of significant wave heights, mean wave direction, peak period, dissipation rate, 1-D spectrum and curve output of the above parameters along transects at specified nesting and non-nesting sites were analysed for the present study. The model simulations were carried out for the normal and extreme conditions and the results are initially presented individually for these conditions and later a comparative analysis is done as per context and relevance. In this study, the main focus is on the nearshore wave conditions and the wave energy dissipation across the barrier reef and the lagoon. Outside the barrier the energy dissipation due to wave breaking and bottom friction will be dominating at the rim of the reefs. Inside the lagoon some energy dissipation will occur on the up wave side of the islands. The shape and orientation of the Al Wajh bank to the approaching waves from North west and the nearshore depth contours will influence

the refraction and diffraction of the waves and transfer of energy on the southwest and southeast edge of the barrier. The rate of energy dissipation is examined from the output of significant wave heights, 1-D spectrum, dissipation rate and the curve plots of the above parameters along transects near the islands having turtle nests at the outer rim of the barrier island and inside the lagoon. The model simulations were carried out for normal (average) waves (Hs = 1.34 m (nesting) and 1.41 m (non-nesting)) and extreme waves of 1 in 1 year (2.65 m) and 1 in 100 year (3.66 m) return period. Though the initial model simulations were carried out for normal wave conditions for the nesting and non-nesting season separately. The wave conditions in the two seasons are similar and there was no noticeable difference in the model results. Therefore, this approach was discarded and only nesting season conditions are discussed here.

4.4.1. Distribution of Wave Heights

The spatial distribution of significant wave heights for the incident offshore wave conditions were analysed using 2-D vector plots of the wave heights in the Al Wajh Bank. Figure 4.5, Figure 4.6 and Figure 4.7 show the distribution of wave heights and wave vectors for the normal condition, 1 in 1 year and 1 in 100 years return period waves respectively. The waves from the offshore approach from the northwest with mean direction of $315°$. The alignment of the longitudinal axis of the Al Wajh Bank is also roughly along the wave approach. It is observed that after the transformation the waves to the nearshore, directly approach the northern part with little dissipation and thus this part of the reef is fully exposed to the waves. Whereas on the western side the wave incidence is due to lateral spreading of wave energy by refraction and diffraction. The major dissipation of wave energy across the reefs is clear with substantial reduction in the wave heights inside the lagoon. The mean wave heights inside the lagoon are in the range of 0.2 m to 0.6 m which increase to up to 1.25 m for the extreme wave conditions.

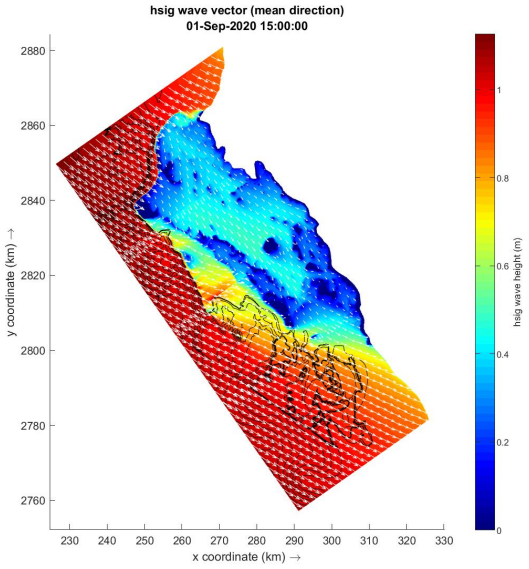

Figure 4.5: Wave height distribution near the Al Wajh bank for normal condition (H_s = 1.34 m). The vectors (white) show mean wave propagation direction. The black lines represent the depth contours.

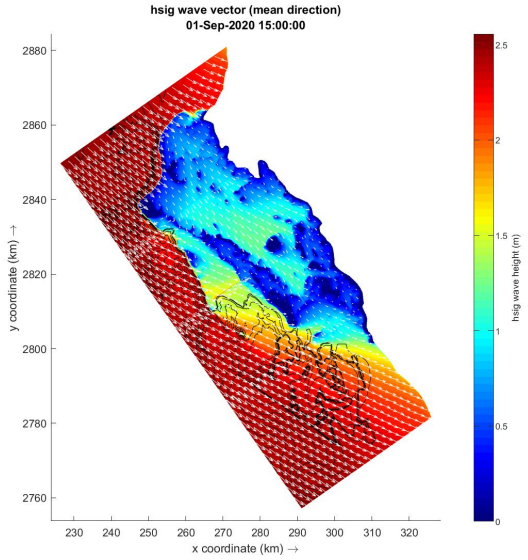

Figure 4.6: Wave height distribution near the Al Wajh bank for 1 in 1 year return period condition (H_s = 2.65 m). The vectors (white) show mean wave propagation direction. The black lines represent the depth contours.

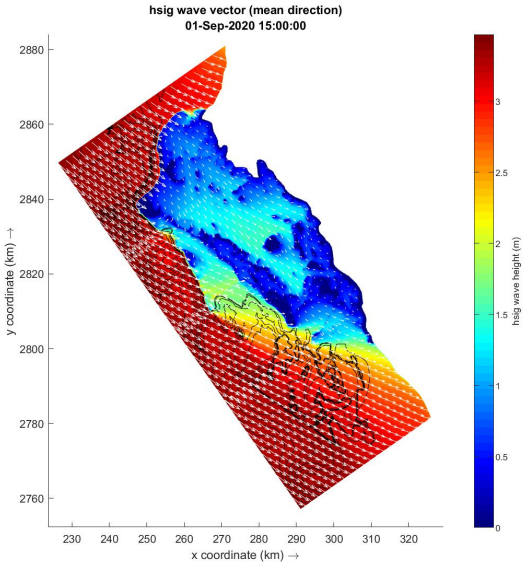

Figure 4.7: Wave height distribution near the Al Wajh bank for 1 in 100 year return period condition (H_s = 3.66 m). The vectors (white) show mean wave propagation direction. The black lines represent the depth contours.

In order to get a better idea on the variation of wave heights in the nearshore the enlarged view of the spatial distribution of wave vectors at the prominent islands along the rim of the barrier reef and the lagoon are shown in Figure 4.8, Figure 4.9 and Figure 4.10. In ‘A’ the wave vectors at the islands Birrim, Umm Rumah and Ghawar are shown. In ‘B’ and ‘C’ the wave vectors at the islands Qummaan and Sheybarah South respectively are shown. For the offshore wave of 1.34 m (normal), 2.65 m (1 in 1 year) and 3.66 m (1 in 100 years) have reduced to approximately 1.0 m, 2.0 m and 2.5 m respectively on the up-wave side of the reefs (nearshore) in the north and west. A major reduction in wave heights is observed at Sheybarah South as it is located in the sheltered area. After dissipation of the wave energy across the reef similar trend is observed inside the lagoon.

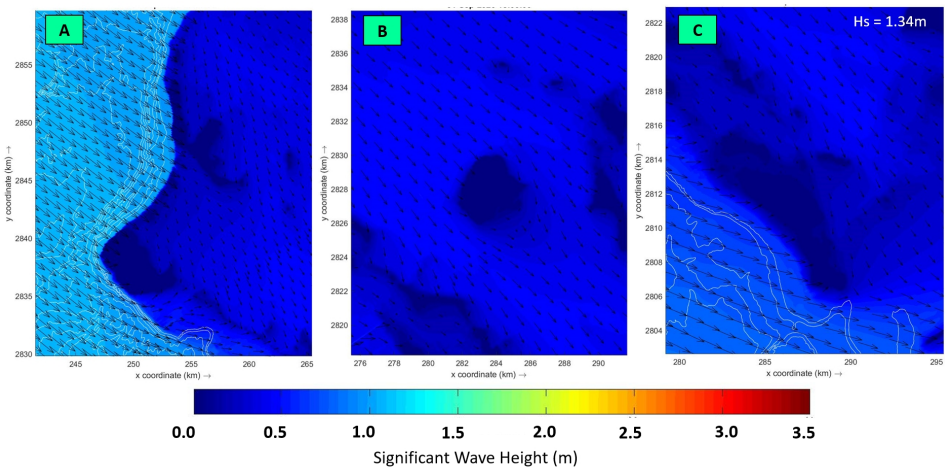

Figure 4.8: Distribution of Waves and vectors near major islands in Al Wajh Bank for normal condition (H_s = 1.37 m). The vectors (black) show mean wave propagation direction. The white lines represent the depth contours.

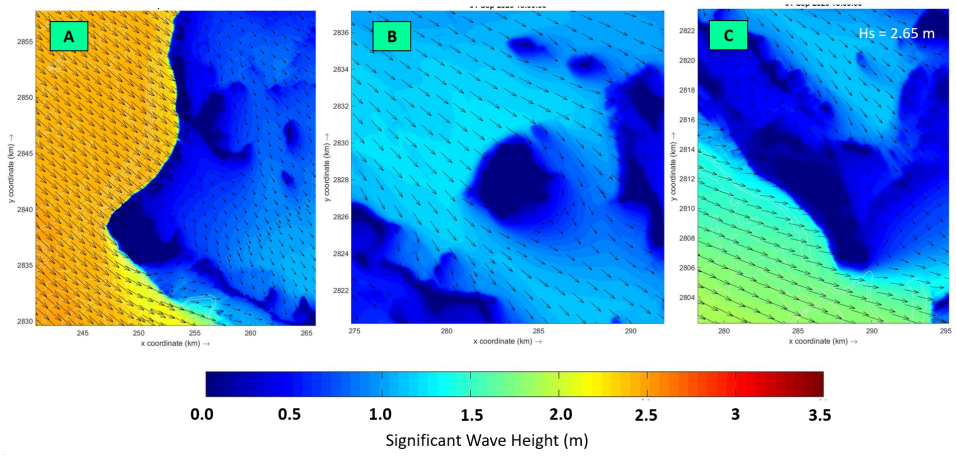

Figure 4.9: Distribution of Waves and vectors near major islands in Al Wajh Bank for 1 in 1 year condition (H_s = 2.65 m). The vectors (black) show mean wave propagation direction. The white lines represent the depth contours.

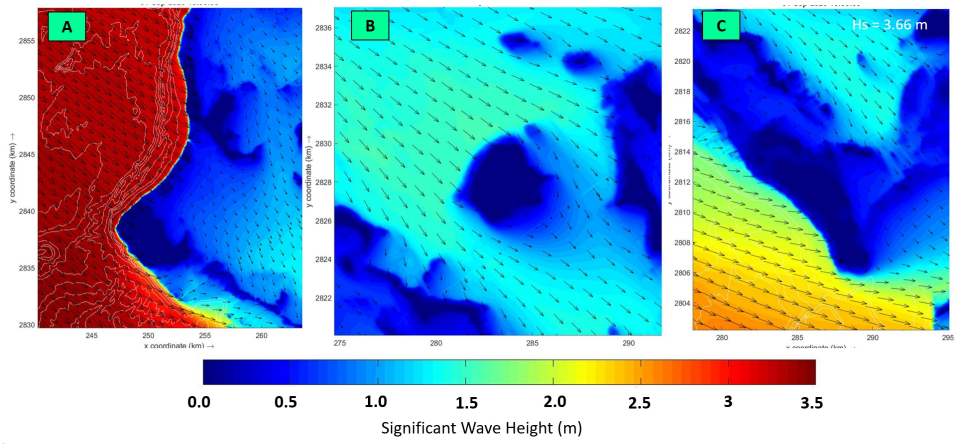

Figure 4.10: Distribution of Waves and vectors near major islands in Al Wajh Bank for 1 in 100 year condition (H_s = 3.66 m). The vectors (black) show mean wave propagation direction. The white lines represent the depth contours.

4.4.2. Analysis of Spectral Wave Distribution

The spectral waves form of the offshore were modelled and transformed to Al wajh Bank to understand the energy dissipation at the reef system and the prevailing wave conditions at the outer rim and inside the lagoon. The spectral wave distribution outside and inside the reef system was examined by extracting 1-D wave spectrum at specified locations along the rim of the reef and inside the lagoon. The analysis was carried out to estimate the relative dissipation of energy by comparing the spectra on the seaside and lagoon side across the reefs due to bottom friction and wave breaking. The nearshore wave spectrum is also analysed at the turtle nesting sites of some of the important islands at the edge of the reefs and inside the lagoon. The 1-D spectrum was obtained from the model simulations at a few points in the north and south of the reef system. The analysis for the area around the Birrim island is given below followed by Qummaan and Seybarrah South islands.

Birrim Island

The index of locations around the Birrim and the contiguous reef where the wave spectrum data is taken for analysis is shown in Figure 4.11.

Figure 4.11: Index map for Wave Spectrums described near Birrim island

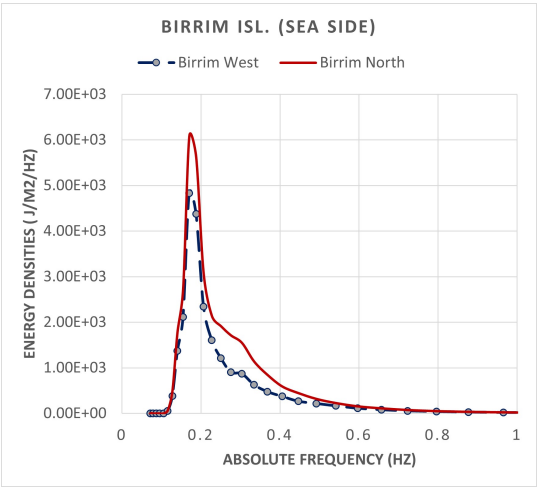

Figure 4.12: Comparison of Spectral Energy Density ($J/m^2/Hz$) at North and West side of Birrim island for normal condition. North side of the island has non-nesting stretches and west side has nesting stretches

A comparison of the 1-D spectra at two points located in the west and north of Birrim Island, on the sea side, for normal wave conditions is shown in Figure 4.12. The north side is directly exposed to the approaching waves and has very steep gradient and depths at the edge of the island. The west side where turtle nesting sites are located the wave energy reaches there after refraction and the site has some gently sloping foreshore with sandy beach. The reduction in the peak energy density is about 20% and the respective values of significant Wave Heights are 1.04 and 0.87 for north and west side of the island.

For the comparison of spectra across the reef between Birrim and Ghawar islands two points were taken close to Mizab island and inside the reef (lagoon side). The 1-D spectra for the two locations, for normal wave conditions, are shown in Figure 4.13(A). There is a vast difference (> 95%) in the peak energy density and shift in the peak frequency inside the lagoon. The enlarged view of the spectrum inside the lagoon is shown in Figure 4.13(B). The significant wave heights in the sea and lagoon are 1.01 m and 0.29 m respectively.

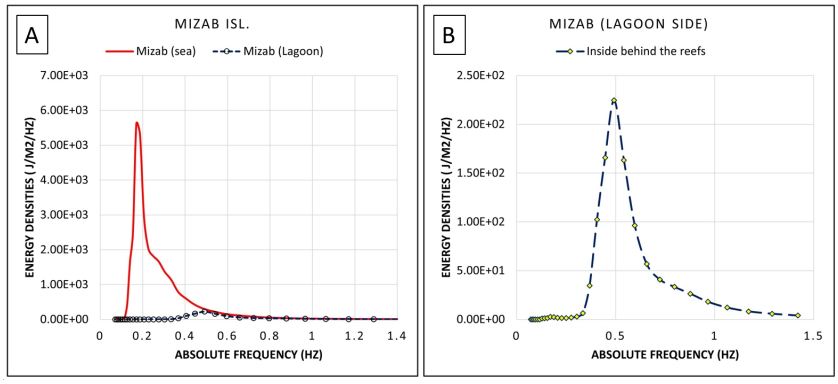

Figure 4.13: (A) Comparison of Spectral Energy Density ($J/m^2/Hz$) across the reef near Mizab island (between Birrim and Ghawar islands) for normal condition. (B) Enlarged view of Spectral Energy Density ($J/m^2/Hz$) inside the lagoon depicted by Reef (lagoon) in index map

In Figure 4.11, the barrier reef on the southwest side is wide and shallow. In the central part on the seaside additional narrow and elongated reef is located (see Figure 2.1). This part of the reef is expected to dissipate substantial energy due to bottom friction and wave breaking. Therefore, two points were chosen, one on the seaside and other on lagoon side of the barrier. The 1-D spectra for the two locations, for normal wave conditions, are shown in Figure 4.14(A). The large difference in peak energy density (> 77%) is observed and a shift in the peak frequency inside the lagoon. The enlarged view of the spectrum inside the lagoon is shown in Figure 4.14(B).The significant wave heights in the sea and lagoon are 0.73 m and 0.42 m respectively.

A comparison for the extreme wave conditions of 1 in 1 year and 1 in 100 years is also done across the Barrier and shown in Figure 4.15 and Figure 4.16. Similar trend is observed indicating large dissipation of energy across the reefs. An important observation is that the significant wave height inside the lagoon is of similar magnitude for 1 in 1 year (0.92 m) and 1 in 100 years (1.13 m) wave conditions. This implies that the waves inside the lagoon are entirely wind generated and the barrier reef system is able to completely dissipate the energy of the waves from offshore waves from the Red Sea.

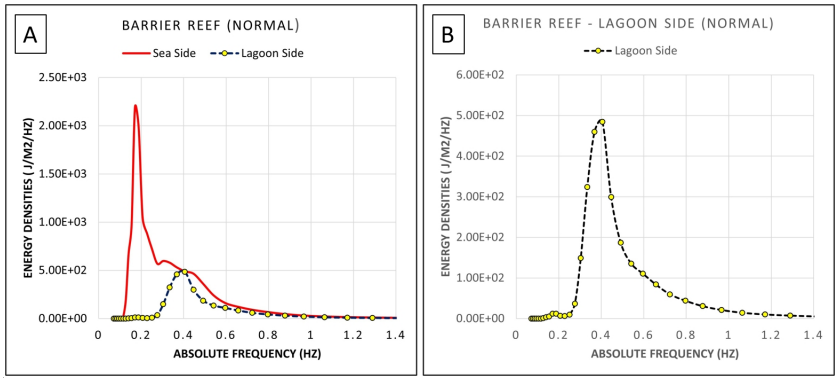

Figure 4.14: (A) Comparison of Spectral Energy Density ($J/m^2/Hz$) across the barrier reef for normal condition. (B) Enlarged view of Spectral Energy Density ($J/m^2/Hz$) inside the lagoon depicted by barrier (lagoon) in index map

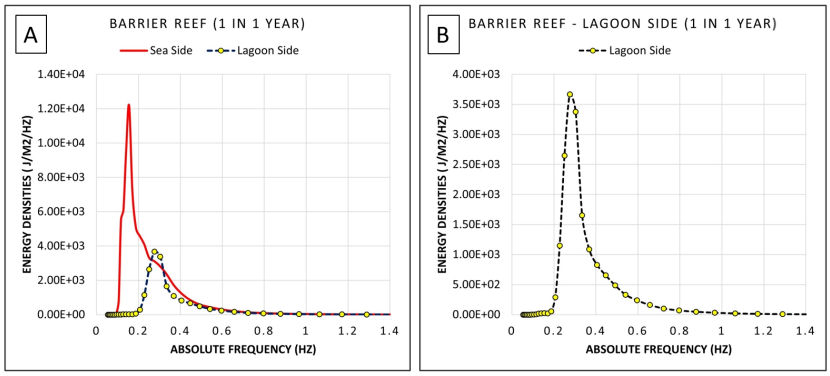

Figure 4.15: (A) Comparison of Spectral Energy Density ($J/m^2/Hz$) across the barrier reef for 1 in 1 year return period condition. (B) Enlarged view of Spectral Energy Density ($J/m^2/Hz$) inside the lagoon depicted by barrier (lagoon) in index map

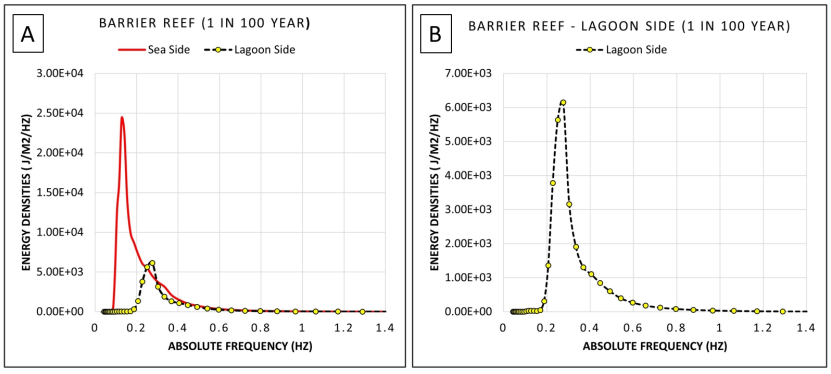

Figure 4.16: (A) Comparison of Spectral Energy Density ($J/m^2/Hz$) across the barrier reef for 1 in 100 year return period condition. (B) Enlarged view of Spectral Energy Density ($J/m^2/Hz$) inside the lagoon depicted by barrier (lagoon) in index map

The spring tidal range at Al Wajh Bank is 0.59 m. The model simulations were carried out for MHWS tidal level of 0.89 m. The effect of tidal levels on wave transformation and energy dissipation over the reefs was examined by carrying out model simulations with MLWS level of 0.3 m. The wave spectra across the barrier reef were compared for High Water and Low Water and shown in Figure 4.17. The Figure 4.17(A) gives the comparison of spectra on the seaside and lagoon side. The enlarged view on the lagoon side is shown in Figure 4.17(B). The marginal effect of the tide is seen inside the lagoon where apparently dominance of wind generated waves is observed.

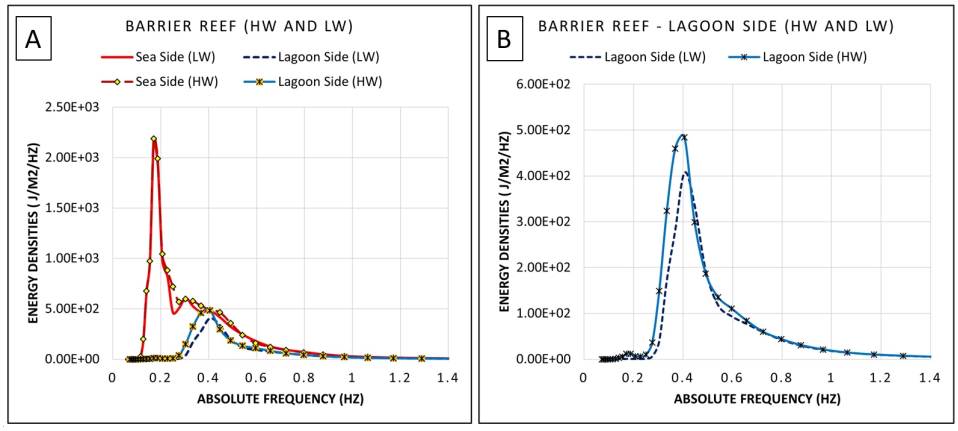

Figure 4.17: (A) Comparison of Spectral Energy Density ($J/m^2/Hz$) across the barrier reef for normal conditions with Low water (0.3 m LAT) and High water (0.89 m LAT). (B) Enlarged view of Spectral Energy Density ($J/m^2/Hz$) for low and high water inside the lagoon depicted by barrier (lagoon) in index map

Qummaan Island

The index of locations around the Qummaan and Sheybarrah South island where the wave spectrum data is taken for analysis is shown in Figure 4.18 The comparison of wave spectra is given below:

Figure 4.18: Index for Wave Spectrum near Qummaan and Sheybarrah South islands

Qummaan is the largest island at the centre of the lagoon where some turtle nesting sites are located on the windward or up-wave side. The wave spectra for HW and LW tidal levels is shown in Figure 4.19 for normal wave conditions. The difference in the spectra is almost negligible. The significant wave height for LW and HW were 0.465 m and 0.478 m respectively.

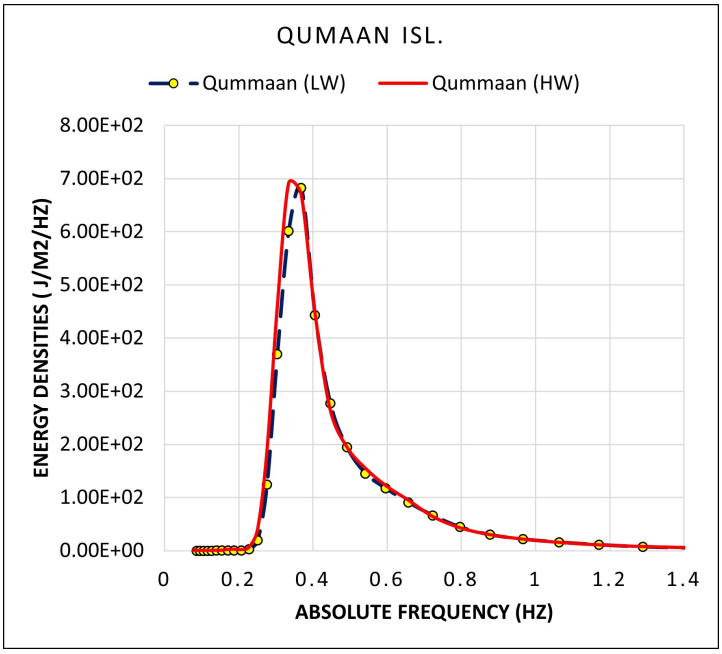

Figure 4.19: Comparison of Spectral Energy Density ($J/m^2/Hz$) near Qummaan island for HW = 0.89 m LAT and LW = 0.3 m LAT

The comparison of wave spectra for the offshore extreme wave conditions is done for 1 in 1 year (2.65 m) and 1 in 100 years (3.66 m) waves and wind speeds of 13.06 m/s and 15.35 m/s respectively. The results are shown in Figure 4.20. The wave height at Qummaan were 1.16 m and 1.42 m for 1 in 1 year and 1 in 100 year return period respectively. These waves are local wind generated waves.

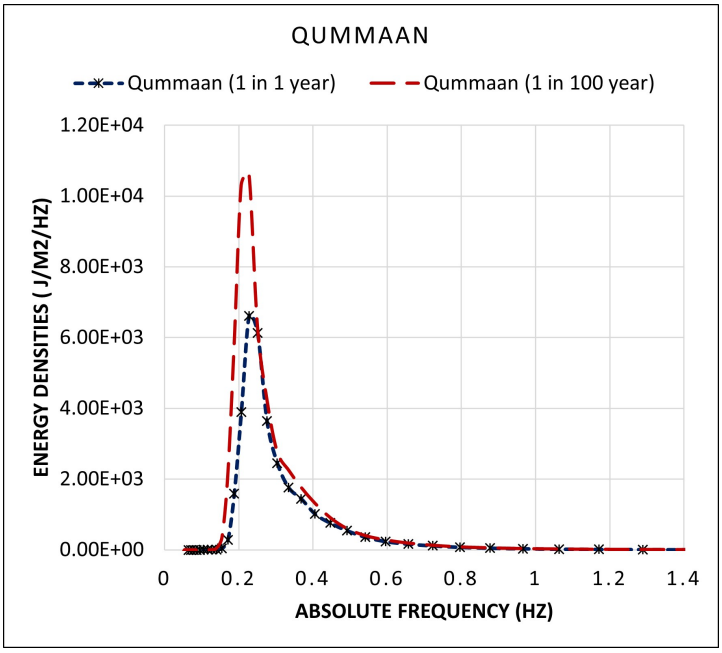

Figure 4.20: Comparison of Spectral Energy Density ($J/m^2/Hz$) near Sheybarrah island for Extreme Waves

Sheybarrah South island

The Sheybarrah island is in the southern end of the Al Wajh Bank (see Figure 4.18) and has some turtle nesting sites. The island is at the outer edge of the sheltered area of the reef and is partially exposed

to the northwest waves. The spectra for the normal wave conditions and the extreme wave conditions have been compared and shown in Figure 4.21(A). The enlarged view of the spectrum for the normal wave conditions is shown in Figure 4.21(B). For the normal wave conditions two peaks are seen in the spectrum indicating energy due to offshore waves and local wind generated waves. Similar trend is seen not seen for the extreme wave conditions. The significant wave heights at Sheybarrah for normal, 1 in 1 year and 1 in 100 years are 0.698 m, 1.61 m and 2.09 m respectively.

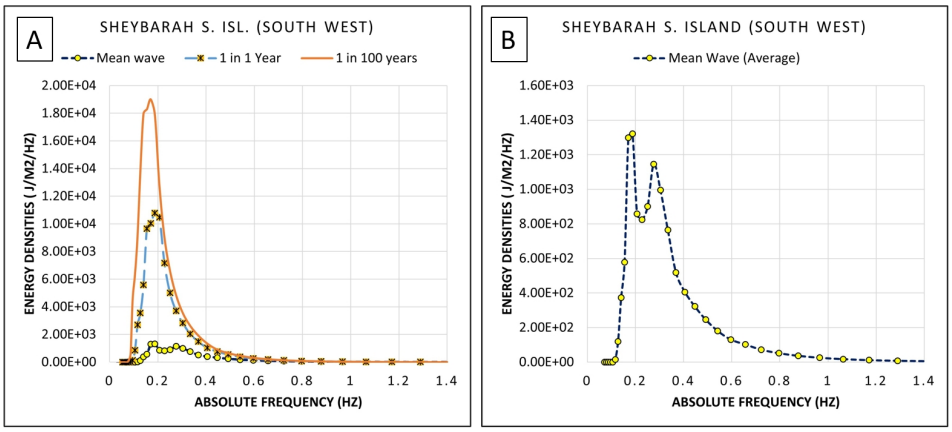

Figure 4.21: (A)Comparison of Spectral Energy Density ($J/m^2/Hz$) near Sheybarrah island for normal and extreme Waves. (B) Enlarged view of Wave Spectrum at Sheybarrah island for normal conditions

4.4.3. Comparison of wave parameters at nesting and non-nesting sites

In the foreshore, the surf zone and the swash zone will not be correctly resolved in the present spectral wave model as the grid size taken in the nearshore nested model is 100 m. The surf zone and swash zone dynamics are recommended to be investigated in a separate study using X-Beach model taking input from the Delft3D-WAVE model. Transects were, however, taken for model output for constructing curves of significant wave heights and the dissipation rates, along the foreshore cross sections, near nesting and non-nesting sites. This data is taken at every 10 m along the transect and the model gives interpolated data at these points. The locations at the turtle nesting and non-nesting sites were taken at the three islands at the rim of the barrier reef and two islands inside the lagoon. The islands at the rim are Ghawar, Birrim and Sheybarrah (South) and that in the lagoon are Umm Rumah and Qummaan. The analysis of the curves at each of these islands is presented below.

Ghawar Island

The locations for the transects taken at Ghawar are shown in Figure 4.22. The plots for the curves of significant wave heights and dissipation rates for nesting sites are shown in Figure 4.23. The plots for non-nesting sites are shown in Figure 4.24.

The depth profile and the high waterline is shown in the figures. At Ghawar island the depth profile at the nesting sites is distinctly different from the non-nesting sites. There is a wide, shallow and almost flat foreshore after the reef crest where the dissipation rate is maximum. A very high rate of dissipation is observed above the reef crest. The significant wave height gradually reduces from about 1.0 m to 0.2 m. At the non-nesting sites the depth profile shows a very steep and short foreshore where relatively large depths with very low energy dissipation is observed. The uniform wave height of 1.0 m is maintained before the breaking.

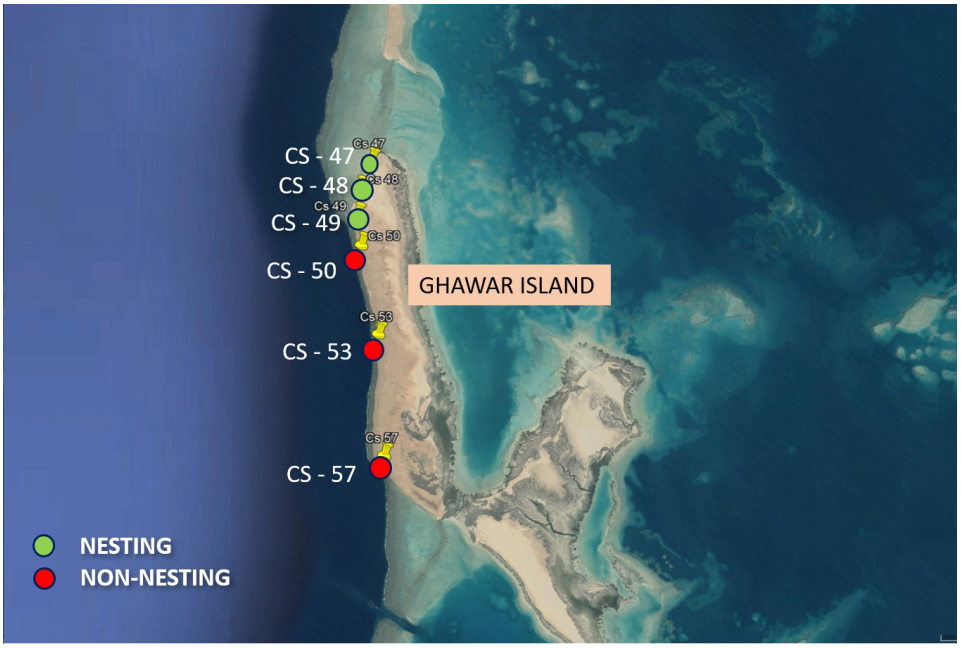

Figure 4.22: Index of transect locations at Ghawar island. Green dots represent Nesting locations and Red dots represent non-nesting locations

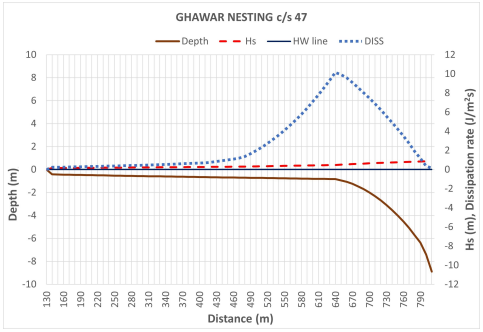

(a) Section 47

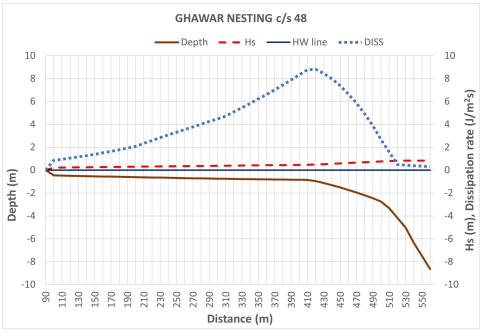

(b) Section 48

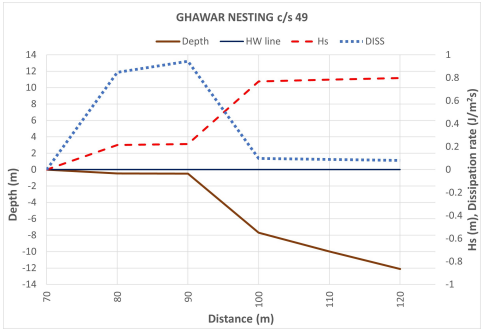

(c) Section 49

Figure 4.23: Significant wave height and dissipation rate curves at Nesting locations - Ghawar island. The x-axis represents distance from nearshore to offshore. The y-axis(left) shows scale for depths (m) (brown) and y-axis (right) scale is for significant wave height (m) (red) and dissipation rate ($J/m^2/s$) (blue). Note: neglect the negative values on y-axis(right), this was done only to match 0 value on both sides.

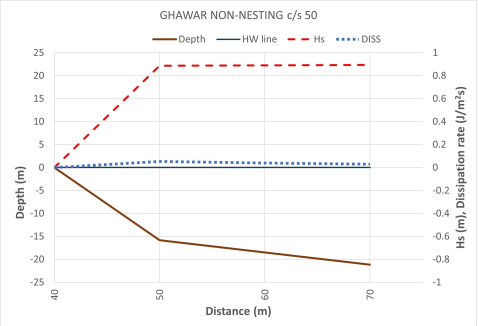

(a) Section 50

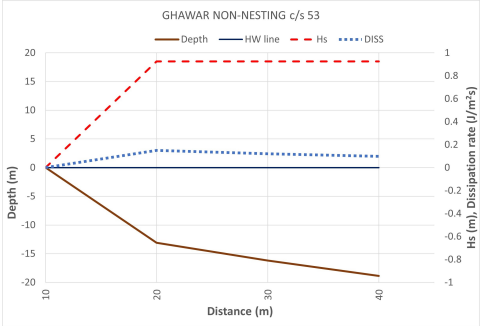

(b) Section 53

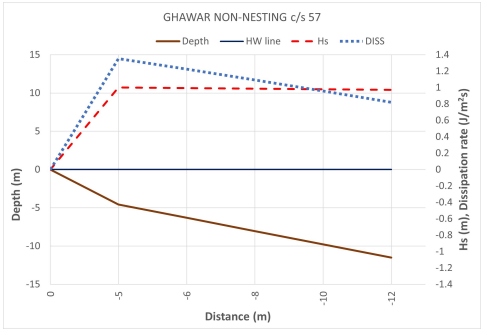

(c) Section 57

Figure 4.24: Significant wave height and dissipation rate curves at Non-nesting locations - Ghawar island. The x-axis represents distance from nearshore to offshore. The y-axis(left) shows scale for depths (m) (brown) and y-axis (right) scale is for significant wave height (m) (red) and dissipation rate ($J/m^2/s$) (blue). Note: neglect the negative values on y-axis(right), this was done only to match 0 value on both sides.

Birrim Island

The locations for the transects taken at Birrim island are shown in Figure 4.25. The plots for the curves of significant wave heights and dissipation rates for nesting sites are shown in Figure 4.26. The plots for non-nesting sites are shown in Figure 4.27.

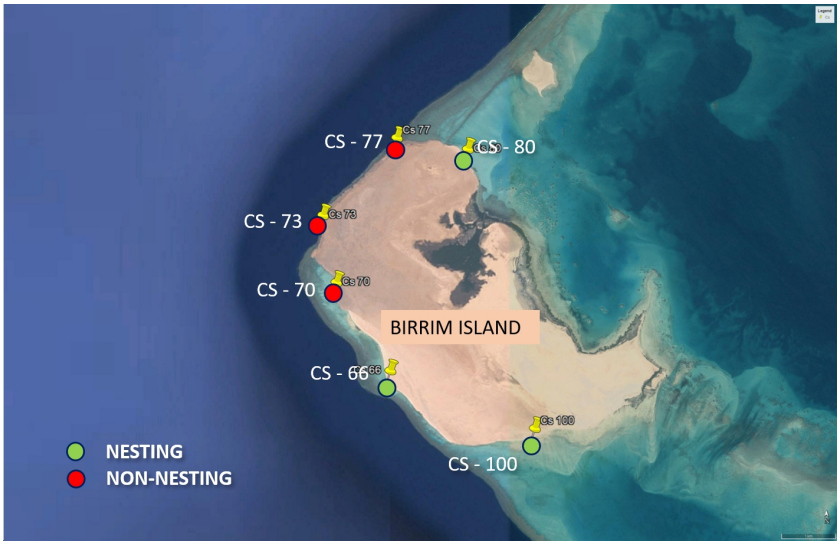

Figure 4.25: Index of transect locations at Birrim island. Green dots represent Nesting locations and Red dots represent non-nesting locations

Similar to the observations at Ghawar island the depth profile at the nesting sites of Birrim island are distinctly different from the non-nesting sites. There are wide, shallow and gentle slopes in the

foreshore after the reef crest where the dissipation rate is maximum. There is gradual reduction in the significant wave height from about 1.0 m to 0.2 m. At the non-nesting sites the depth profile shows a very steep foreshore of small width where relatively large depths with very low to high energy dissipation is observed. The wave height at the non-nesting sites is around 1.0 m before breaking. Moreover at Birrim the non-nesting sites are located at the steepest side of reef where it is directly exposed to the incoming waves from northwest.

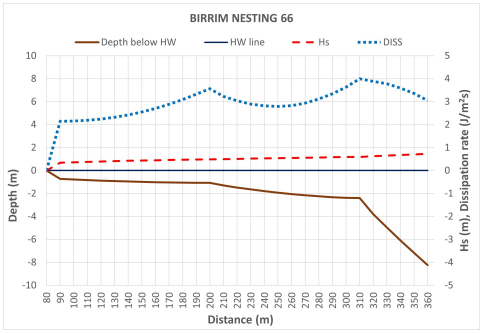

(a) Section 66

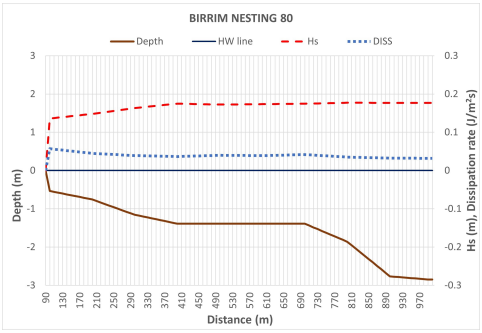

(b) Section 80

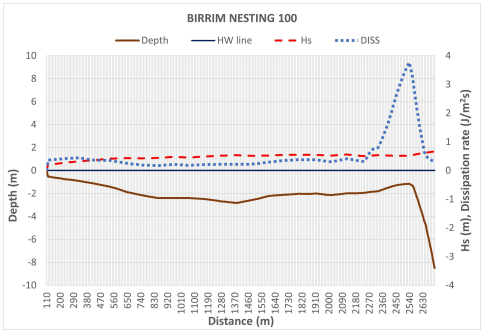

(c) Section 100

Figure 4.26: Significant wave height and dissipation rate curves at Nesting locations - Birrim island. The x-axis represents distance from nearshore to offshore. The y-axis(left) shows scale for depths (m) (brown) and y-axis (right) scale is for significant wave height (m) (red) and dissipation rate ($J/m^2/s$) (blue). Note: neglect the negative values on y-axis(right), this was done only to match 0 value on both sides.

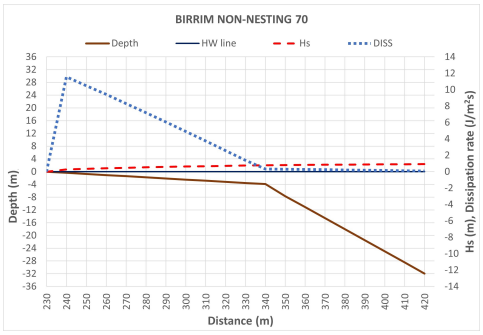

(a) Section 70

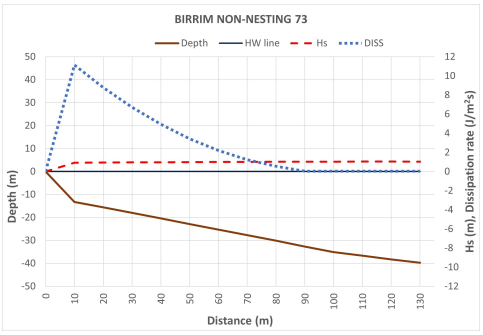

(b) Section 73

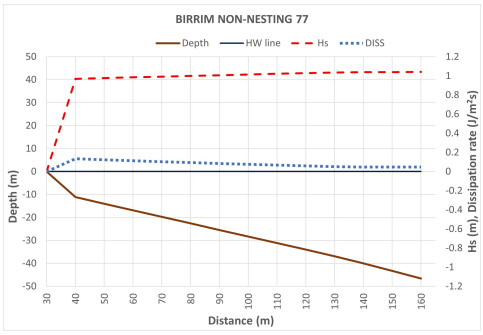

(c) Section 77

Figure 4.27: Significant wave height and dissipation rate curves at Non-nesting locations - Birrim island. The x-axis represents distance from nearshore to offshore. The y-axis(left) shows scale for depths (m) (brown) and y-axis (right) scale is for significant wave height (m) (red) and dissipation rate ($J/m^2/s$) (blue). Note: neglect the negative values on y-axis(right), this was done only to match 0 value on both sides.

Sheybarrah South Island

The locations for the transects taken at Sheybarrah South island are shown in Figure 4.28. The plots for the curves of significant wave heights and dissipation rates for nesting sites are shown in Figure 4.29. The plots for non-nesting sites are shown in Figure 4.30.

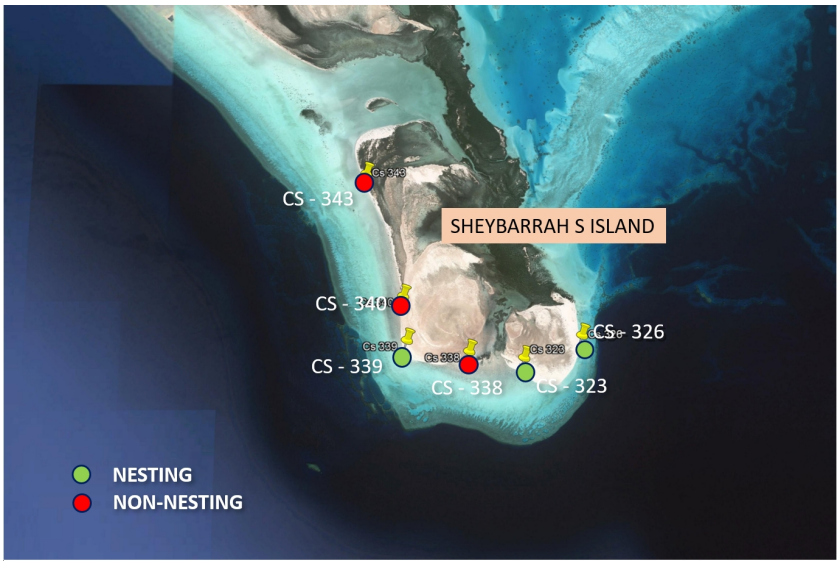

Figure 4.28: Index of transect locations at Sheybarrah island. Green dots represent Nesting locations and Red dots represent non-nesting locations.

At Sheybarrah island the depth profile at the nesting and non-nesting sites is similar. There is a

wide, shallow and almost flat foreshore after the reef crest where the dissipation rate is maximum. The wave heights at the nesting and non-nesting sites is less than 0.5 m. The difference could be beach sediments where shallow sand sheets may be interrupted by mud flats or vegetation.

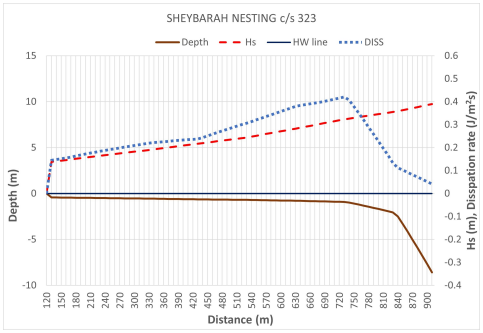

(a) Section 323

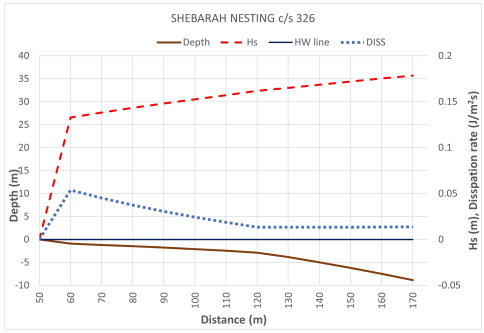

(b) Section 326

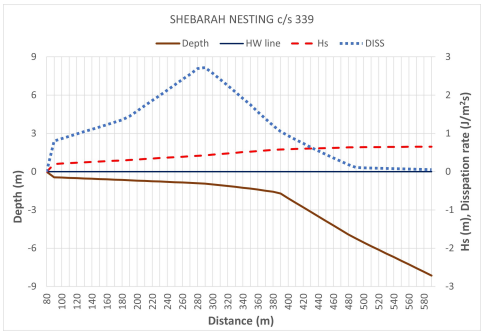

(c) Section 339

Figure 4.29: Significant wave height and dissipation rate curves at Nesting locations - Sheybarrah island. The x-axis represents distance from nearshore to offshore. The y-axis(left) shows scale for depths (m) (brown) and y-axis (right) scale is for significant wave height (m) (red) and dissipation rate ($J/m^2/s$) (blue). Note: neglect the negative values on y-axis(right), this was done only to match 0 value on both sides.

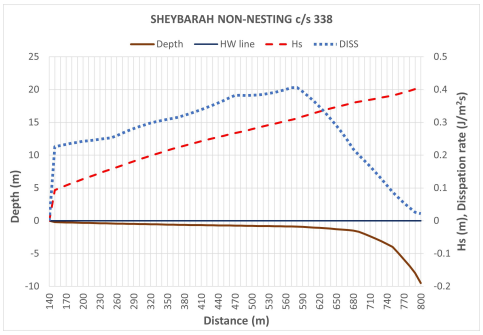

(a) Section 338

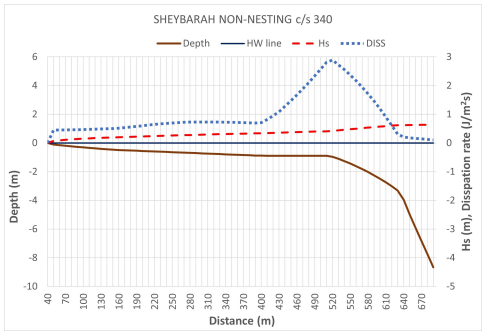

(b) Section 340

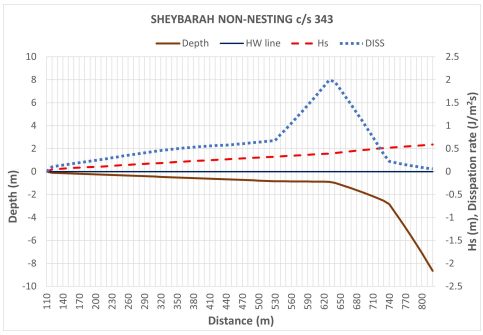

(c) Section 343

Figure 4.30: Significant wave height and dissipation rate curves at Non-nesting locations - Sheybarrah island. The x-axis represents distance from nearshore to offshore. The y-axis(left) shows scale for depths (m) (brown) and y-axis (right) scale is for significant wave height (m) (red) and dissipation rate ($J/m^2/s$) (blue). Note: neglect the negative values on y-axis(right), this was done only to match 0 value on both sides.

Qummaan Island

Some transects were taken for islands located inside the lagoon. The analysis of the curves at each of these islands is presented. The locations for the transects taken at Qummaan island are shown in Figure 4.31. The plots for the curves of significant wave heights and dissipation rates for nesting sites are shown in Figure 4.32. The plots for non-nesting sites are shown in Figure 4.33.

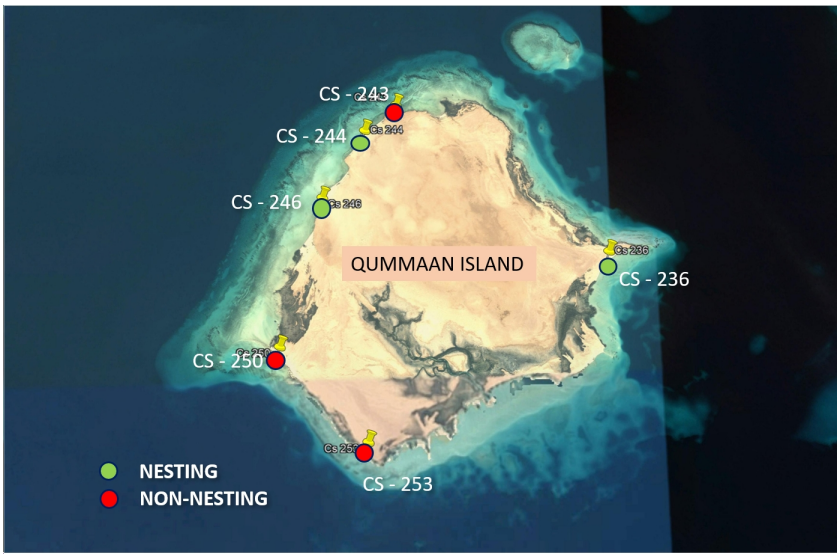

Figure 4.31: Index of transect locations at Qummaan island. Green dots represent Nesting locations and Red dots represent non-nesting locations.

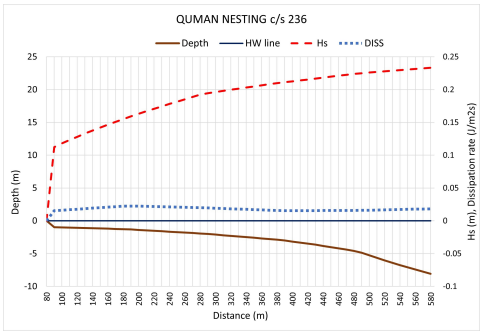

(a) Section 236

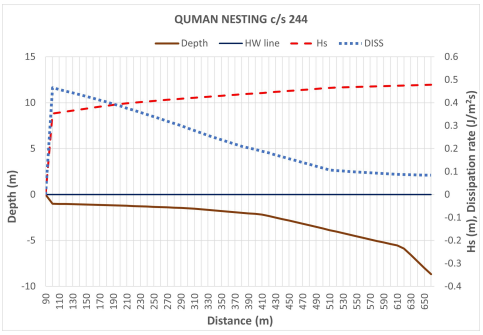

(b) Section 244

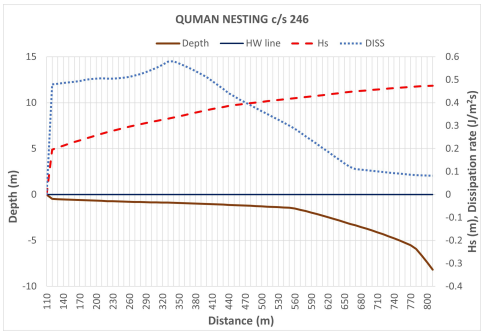

(c) Section 246

Figure 4.32: Significant wave height and dissipation rate curves at Nesting locations - Qummaan island. The x-axis represents distance from nearshore to offshore. The y-axis(left) shows scale for depths (m) (brown) and y-axis (right) scale is for significant wave height (m) (red) and dissipation rate ($J/m^2/s$) (blue). Note: neglect the negative values on y-axis(right), this was done only to match 0 value on both sides.

In the analysis carried out for the spectra outside and inside the lagoon it has been established that the energy of the waves from offshore waves is entirely dissipated by the barrier reef and islands at the outer rim of the reef. The comparison of the wave spectra for the normal and extreme wave conditions also clearly established the exclusive presence of wind generated waves inside the lagoon. The significant waves inside the lagoon for the normal wind conditions is below 0.8 m. The waves are incident from the windward side and the lee side has less than 0.2 m significant wave height. At Qummaan island the depth profile at the nesting and non-nesting sites is similar. There is a wide, shallow and almost flat foreshore after the reef crest where the dissipation rate is maximum. The wave heights at the nesting and non-nesting sites is less than 0.5 m. The difference in the nesting and non-nesting could be beach sediments where sandy beach sediments may be interrupted by mud flats or vegetation.

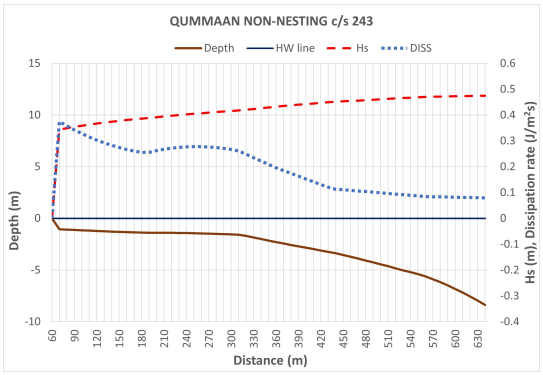

(a) Section 243

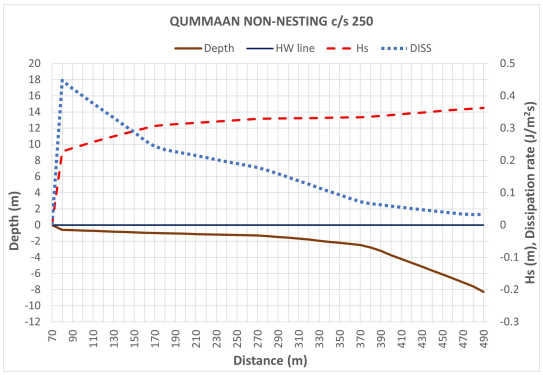

(b) Section 250

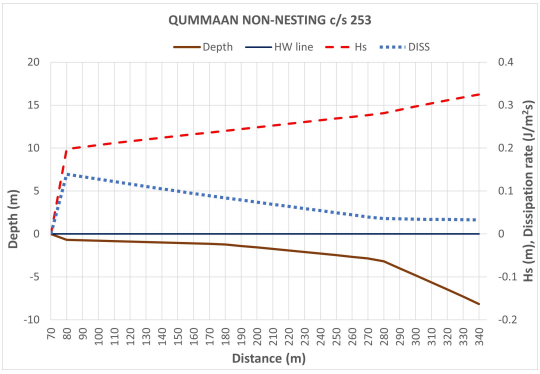

(c) Section 253

Figure 4.33: H_s and Dissipation rate curves at Non-nesting locations - Qummaan island

Umm Rumah Island

The other island selected for analysis inside the lagoon is Umm Rumah. The locations for the transects taken at Umm Rumah island are shown in Figure 4.34. The plots for the curves of significant wave heights and dissipation rates for nesting sites are shown in Figure 4.35. The plots for non-nesting sites are shown in Figure 4.36.

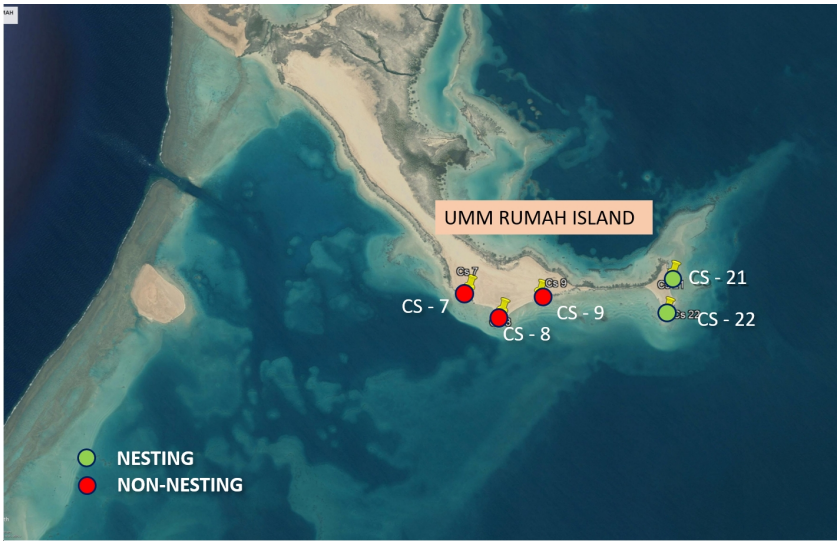

Figure 4.34: Index of transect locations at Umm Rumah island. Green dots represent Nesting locations and Red dots represent non-nesting locations.

The Umm Rumah island has vegetation and mangroves in a large portion along the high waterline. There are certain stretches where vegetation is absent and shallow sandy sheets or sand and mud flats with carbonate hard grounds are existing. The depth profile is similar for the nesting and non-nesting sites. The significant wave heights are less than 0.2 m. The energy dissipation rates are also similar for the two types of sites. The difference appears to be in the nature of sediments in the preference for nesting by the sea turtles.

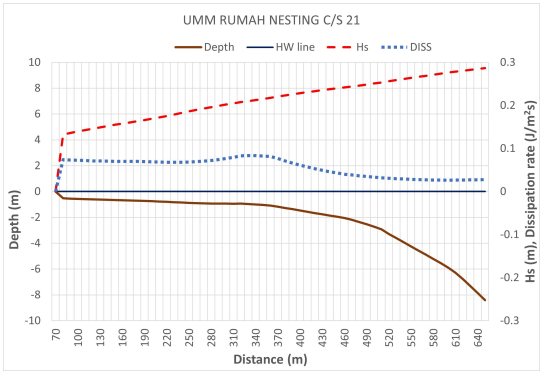

(a) Section 21

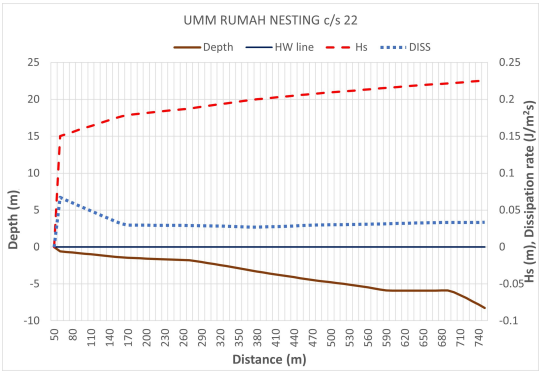

(b) Section 22

Figure 4.35: H_s and Dissipation rate curves at Nesting locations - Umm Rumah island

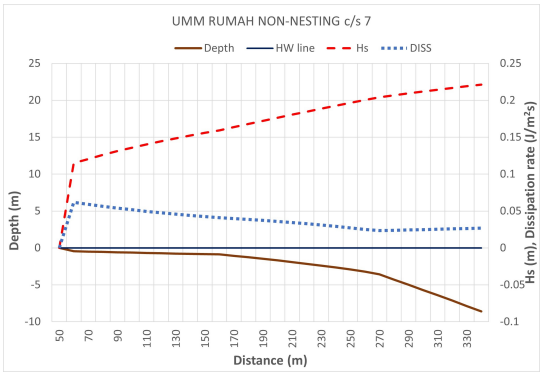

(a) Section 7

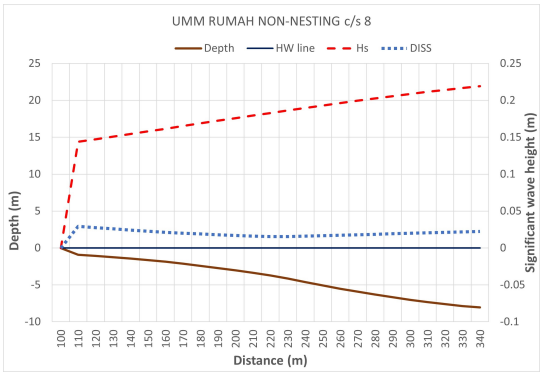

(b) Section 8

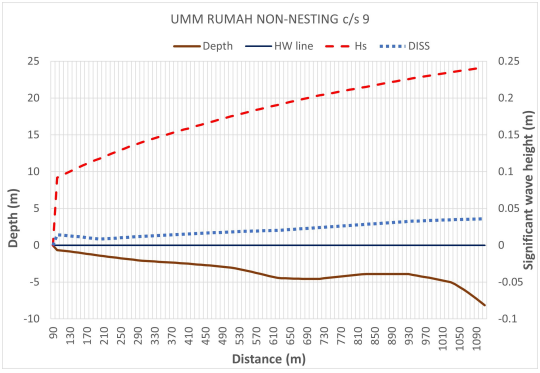

(c) Section 9

Figure 4.36: H_s and Dissipation rate curves at Non-nesting locations - Umm Rumah island

4.4.4. Sensitivity Analysis

The validation of model results is essential to ensure that the trends of the significant wave heights, the mean wave period and the mean wave direction are well captured by the model. For this exercise simultaneous measurements are needed from the field site both for the boundary conditions and for calibration and validation. The boundary conditions are taken from the offshore and the data for validation is taken in the nearshore region close to the area of interest. A comparison is then made with the observed data and the modelled data. A good match between the two will confirm the model performance and the validity of the predicted data. The following statistical parameters used for verification of model performance and other comparison:

1. Correlation coefficient (r)

$$r = \frac{\sum_i (x_i - \bar{x})(y_i - \bar{y})}{\sqrt{(\sum_i (x_i - \bar{x})^2)(\sum_i (y_i - \bar{y})^2)}}$$

2. Bias

$$Bias = \frac{1}{n} \sum_i (y_i - x_i)$$

3. Root Mean Square Error (RMSE)

$$RMSE = \frac{1}{n} \sqrt{\sum_i (y_i - x_i)^2}$$

4. Scatter Index

$$S = \frac{RMSE}{\bar{x}}$$

Where,
xi = Observed value (measurements),
yi = Model predicted value,
i = Corresponding time step,
n = length of record

The validation of the model results could not be carried out as there are no measured wave data in the nearshore or inside the lagoon at Al Wajh. There is no published literature or references on the wave climate at Al Wajh Bank. Perhaps the present study is the first of its kind which attempts to examine the wave transformation and energy dissipation aspects at the vicinity and inside the reef system in the Al Wajh Bank area.

A sensitive analysis was done for important tuning parameters for the model simulations. The focus in the present study is the dissipation of wave energy. Therefore, the model sensitivity to the parameters related to white capping, bottom friction, non-linear triad interactions, higher resolution for directional bins and wave breaking parameters was examined. Previous studies on comparison of wave models have demonstrated that the tuning of the wave breaking parameter in SWAN improves the model predictions in reef environment [13].

Figure 4.37 shows the spectral energy distribution at three locations for the formulations by Van er Westhuysen and Kommen et al. for whitecapping. The plot shows some differences in the energy for the waves from offshore and local wind waves, the former being higher and the latter being lower in the Van der Westhuysen formulation.

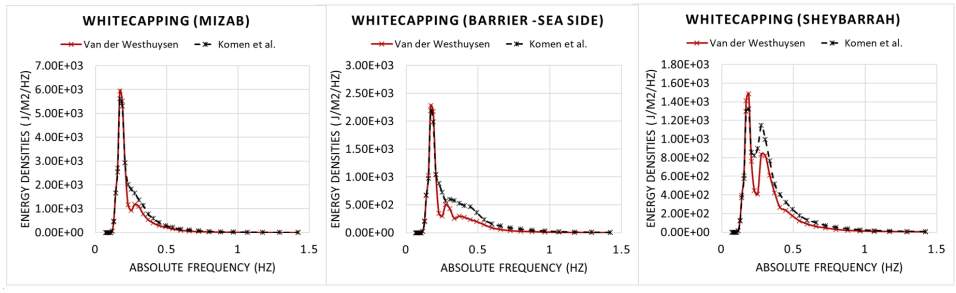

Figure 4.37: Sensitivity Analysis for Whitecapping formula. (Van der Westhuysen and Komen et. al)

Figure 4.38 shows the spectral energy distribution at three locations for the two values of recommended for JONSWAP based friction factors. The plot shows minor difference in the spectral peak energy but overall the results appear not very sensitive to the two recommended values under JONSWAP.

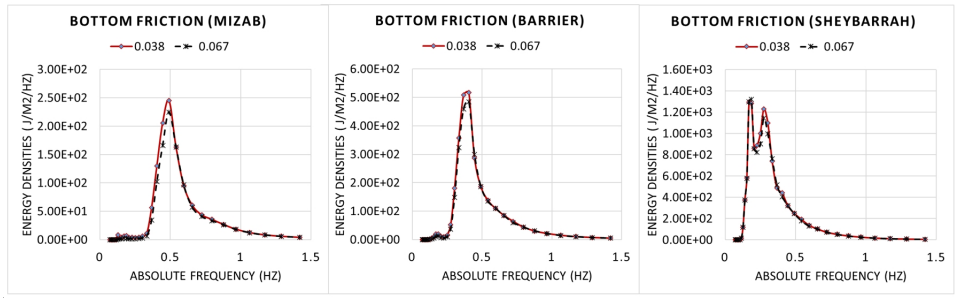

Figure 4.38: Sensitivity Analysis for Bottom friction coefficient.(0.038 m^2/s^3, 0.067 m^2/s^3)

Figure 4.39 shows the spectral energy distribution at three locations for the case of shallow water nonlinear interactions of triads. The plots show that there no perceivable difference in the energy for the waves from offshore and local wind waves. It appears that the results are not sensitive to triad interactions in the barrier reef environment.

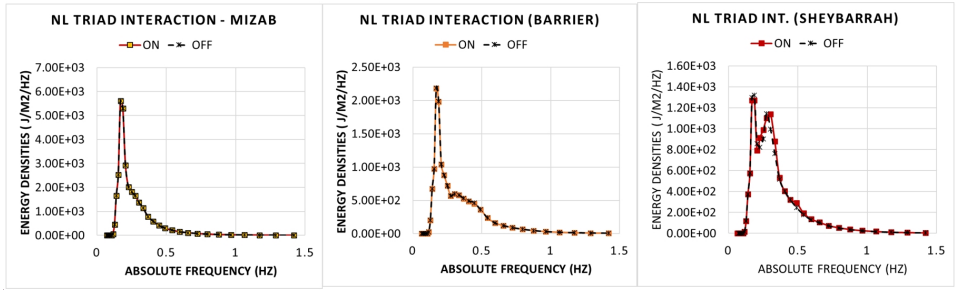

Figure 4.39: Sensitivity Analysis for Non-linear triad interactions (Activated, Deactivated)

The significant wave heights predicted for the above conditions are shown in Table 4.2. Some marginal difference in the computed wave heights is observed.

Figure 4.40 shows the spectral energy distribution at a seaside location for the for higher spectral resolution in the directional space. The plot shows some shift in the energy but not very significant. A more detailed analysis could not be carried out as this posed stability problems at most of the nested computational grids.

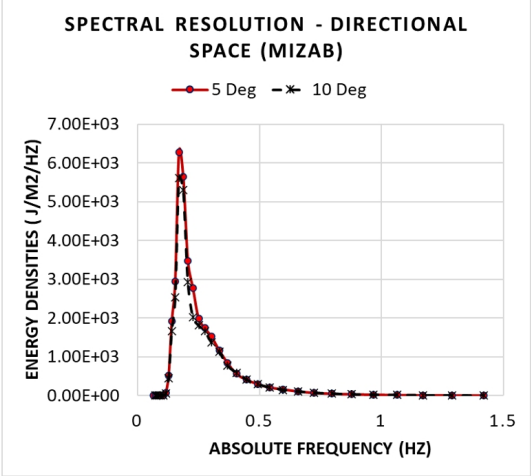

Figure 4.40: Sensitivity Analysis for directional space resolution (5 deg and 10 deg)

Figure 4.41 compares the spectral wave energy distribution for wave breaker parameter (0.55 and 0.73). The results have been plotted for three locations (Mizab, Barrier reef and Sheybarrah) and it is observed that there is very marginal difference in the results.

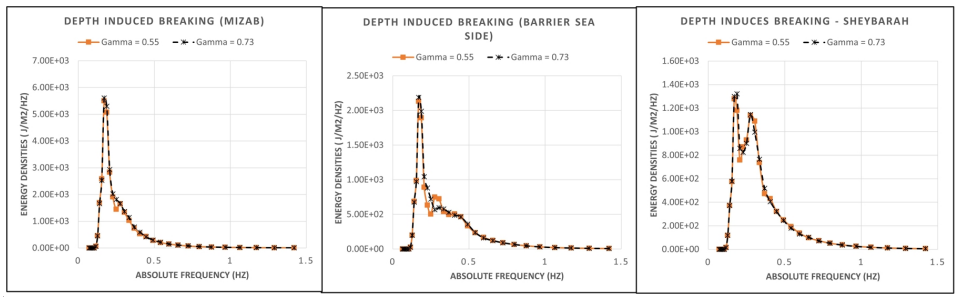

Figure 4.41: Sensitivity Analysis for depth induced breaking parameter (γ = 0.55 and 0.73)

Table 4.2: Sensitivity Analysis for Friction, Whitecapping, Nonlinear Triads, Directional Space, and depth induced breaking.

Parameter		Significant wave height (m)		
		Barrier reef	Mizab	Sheybarrah
JONSWAP bottom friction cofficient	0.067 m^2/s^3	0.42	0.34	0.70
	0.038 m^2/s^3	0.43	0.36	0.71
Whitecapping formulation	Komen et. Al	0.73	1.04	0.70
	Van der Westhuysen	0.62	0.95	0.61
Non-linear triad interactions	Not Activated	0.73	1.04	0.70
	Activated	0.73	1.04	0.71
Directional space resolution	10 deg	-	1.04	-
	5 deg	-	1.10	-
Depth induced breaking	Gamma = 0.73	0.73	1.04	0.70
	Gamma = 0.55	0.72	1.00	0.70

4.5. Estimation of Wave Run-up

Wave runup is the combined effect of wave setup and the swash uprush and rundown. The wave setup is defined as the superelevation of the mean water level and the swash uprush and run down is the fluctuation around the mean [89, 45]. Several empirical relations have been developed for estimating

the wave setup and the swash uprush [11, 6, 46, 87]. Most of the empirical formulas relate beach slope, wave height, deep water wavelength and are derived using laboratory and field measurements, generally, for simplified and idealised conditions. The application of these formulas to natural beaches often poses complications due to specifying various definitions for wave height and wave period; difficulty in obtaining a single beach slope; presence of offshore sandbar etc. The Stockdon formula is common and considered dependable for estimation of wave setup. The coral reef hydrodynamics, morphology and geometry present more complex and wide range of input data values for the application of these empirical formulations for reliable evaluation of the wave runup.

The estimation of wave runup for the reef island beaches is important for understanding the nesting site selection of sea turtles. The flooding of the beaches by wave runup, storm surge and sea level rise are a hazard for the turtle nests. The inundation exposure of sea turtle nesting sites influence the hatching success of the sea turtles [34, 77]. Numerical models like X-Beach can be successfully applied to the reef environment for computing the wave runup. However, the availability of alternative and easy to use tools for cost effective quick and reliable estimates of runup for reef island based beaches can help in the management of sea turtle nesting sites. One such tool is the Hybrid Coral Reef Wave and Water (HyCReWW) level metamodel and its implementation using MATLAB facilitates estimates of runup for reef environments [83]. The metamodel uses interpolation techniques based on Radial Basis Functions (RBFs) to obtain runup estimates for a combination of reef hydrodynamic and morphological parameters. The hydrodynamic parameters are offshore water level (η_0), significant wave height (H_0), offshore wave length (L_0), wave steepness (H_0/L_0); the morphological parameters are forereef slope (β_f), beach slope (β_b), seabed roughness (c_f). The metamodel uses a range of values for the above parameters and the model computes the runup computations for values falling in the specified range.

The HyCReWW metamodel was used to estimate the wave run up at the nesting and non-nesting sites of Al Wajh Bank using the wave parameters from the Delft3D WAVE model. The bounds for wave height input in HyCreWW metamodel is 1 m to 5 m. But the wave heights obtained inside the lagoon are in the range of 0.1 m to 0.5 m which are generated by local wind. This was mainly the case for normal wave conditions for nesting and non-nesting season. Therefore, wave heights above 0.5 and below 1.0 m were rounded off to 1.0 m, the lower bound specified for HyCReWW metamodel. Similarly reef width was adjusted to 1500 m for values above 1500 m (the upper bound for reef width). Beach slope and reef slope were also adjusted to the nearest value within specified bounds in HyCReWW metamodel. These adjustments were not done for the cross sections which were way out of bounds (e.g. Hs = 0.1 to 0.4 m) and were disregarded in the simulation. This analysis for the adjusted values may give approximate runup values. Run up ($R_{2\%}$) values for different conditions and corresponding wave heights can be found in Table 4.3. The computed rupup for nesting and non-nesting sites varied from 0.14 to 0.93 m for wave heights in the range of 0.5 to 1.04 m. For sections with very steep slope and negligible reef width, the metamodel gives very high values (about 70-90% of wave height).

Table 4.3: The runup values obtained from the HyCReWW model with corresponding wave heights obtained from the Delft3D model

Cross-section no.	RUN UP (R2%)							
	Nesting season		Non-nesting season		1 year RP		100 year RP	
	Hs	RUNUP	Hs	RUNUP	Hs	RUNUP	Hs	RUNUP
7	0.28	-	0.27	-	0.55	0.19	0.66	0.19
8	0.30	-	0.29	-	0.61	0.28	0.72	0.28
9	0.26	-	0.26	-	0.54	0.26	0.63	0.26
21	0.32	-	0.32	-	0.60	0.16	0.70	0.16
22	0.24	-	0.24	-	0.48	-	0.57	0.35
47	0.93	0.36	0.95	0.36	2.14	0.68	2.85	-
48	0.90	0.30	0.92	0.30	2.06	0.60	2.75	0.82
49	0.85	0.45	0.87	0.45	1.92	0.85	2.55	-
50	0.89	0.57	0.92	0.55	2.05	1.11	2.71	-
51	0.90	0.91	0.93	0.88	2.08	-	2.74	-
52	0.91	0.91	0.93	0.89	2.09	2.03	2.76	2.75
53	0.92	0.55	0.95	0.55	2.15	1.15	2.79	1.54
54	0.94	0.57	0.97	0.56	2.16	-	2.81	1.60
55	0.95	0.91	0.97	0.89	2.22	2.17	2.92	2.92
56	0.97	0.56	1.00	0.56	2.14	1.16	2.80	1.58
57	0.93	0.54	0.95	0.53	2.09	-	2.73	1.46
58	0.90	0.46	0.93	0.45	2.05	-	2.71	1.28
59	0.92	0.33	0.94	0.32	2.10	0.61	2.80	0.79
63	0.71	0.50	0.72	0.50	1.47	0.71	1.95	0.96
64	0.70	0.55	0.71	0.55	1.44	0.77	1.92	1.03
65	0.62	0.48	0.63	0.48	1.28	0.63	1.69	0.90
66	0.89	0.45	0.91	0.45	1.95	0.80	2.67	1.18
67	0.82	0.33	0.84	0.33	1.76	0.61	2.37	0.87
68	0.76	0.42	0.77	0.42	1.59	0.67	2.09	0.90
69	0.74	0.35	0.75	0.35	1.60	0.62	2.17	0.91
70	0.88	0.48	0.89	0.47	1.86	-	2.43	1.16
71	0.95	0.41	0.96	0.41	2.07	0.83	2.77	1.15
72	1.01	0.52	1.02	0.54	2.29	1.20	3.09	-
73	0.97	0.56	0.99	0.56	2.15	1.15	2.86	-
74	1.01	0.58	1.03	0.58	2.20	1.21	2.89	1.66
75	1.03	0.93	1.04	0.91	2.32	2.28	3.08	-
76	0.98	0.56	0.99	0.57	2.18	-	2.84	-
77	1.00	0.57	1.01	0.56	2.29	1.27	3.05	-
78	1.02	0.42	1.04	0.43	2.33	-	3.09	-
79	0.99	0.24	0.99	0.24	2.21	-	2.86	-
80	0.18	-	0.22	-	0.42	-	0.50	0.32
81	0.26	-	0.26	-	0.53	0.32	0.63	0.32
95	0.38	-	0.38	-	0.60	0.32	0.66	0.32
97	0.50	0.32	0.50	0.32	0.82	0.32	0.97	0.32
98	0.71	0.19	0.72	0.19	1.48	0.22	1.97	0.26
99	0.74	0.23	0.75	0.23	1.54	-	2.10	0.32
100	0.73	0.17	0.74	0.17	1.49	0.20	1.97	0.23
101	0.75	0.32	0.76	0.32	1.60	0.46	2.18	0.61
102	0.67	0.47	0.68	0.47	1.37	0.59	1.83	0.78
232	0.27	-	0.27	-	0.57	0.28	0.70	0.28
236	0.26	-	0.26	-	0.54	0.15	0.64	0.15
243	0.48	-	0.48	-	1.22	-	1.50	-
244	0.48	-	0.49	-	1.23	0.21	1.52	0.26
245	0.48	-	0.49	-	1.22	0.36	1.51	0.43
246	0.48	-	0.49	-	1.21	0.35	1.49	0.43

Cross-section no.	RUN UP (R2%)							
	Nesting season		Non-nesting season		1 year RP		100 year RP	
	Hs	RUNUP	Hs	RUNUP	Hs	RUNUP	Hs	RUNUP
246	0.48	-	0.49	-	1.21	0.35	1.49	0.43
247	0.48	-	0.48	-	1.21	0.36	1.49	0.43
250	0.40	-	0.40	-	0.85	0.26	1.01	0.26
251	0.36	-	0.37	-	0.79	0.16	0.95	0.16
252	0.39	-	0.40	-	0.89	0.41	1.08	0.43
253	0.41	-	0.41	-	0.95	0.38	1.15	0.42
323	0.44	-	0.45	-	0.90	0.34	1.15	0.37
325	0.27	-	0.27	-	0.56	0.17	0.69	0.17
326	0.20	-	0.20	-	0.38	-	0.47	-
327	0.45	-	0.46	-	0.95	0.41	1.22	-
338	0.46	-	0.47	-	0.97	0.36	1.25	0.44
339	0.69	0.25	0.72	0.25	1.58	0.39	2.05	-
340	0.66	0.16	0.69	0.16	1.53	0.25	1.97	-
341	0.65	0.23	0.68	0.23	1.50	0.34	1.92	0.44
342	0.65	0.25	0.67	0.25	1.49	0.36	1.89	0.46
343	0.65	0.17	0.68	0.17	1.50	-	1.92	0.33
344	0.56	0.14	0.57	0.14	1.25	-	1.57	0.15

Wave runup distance from the mean water line were calculated for the nesting and non-nesting sites based on the wave runup estimates. The wave runup distance plots for the nesting sites and the comparison with the distance of the nests from the mean waterline are depicted in the Figure 4.42 and Figure 4.43 separately for the seaside and lagoon side nests. The results for seaside nesting sites (Figure 4.42) indicated that for normal conditions and the extreme conditions most of the nesting sites are located at sufficient distance away (5 – 60 m) from the estimated wave runup distance along the beach. The nest location at cross section, 67 and 68, located on the west side of Birrim island are close to the estimated runup distance for 1 in 100 year return period wave height and are vulnerable for inundation.

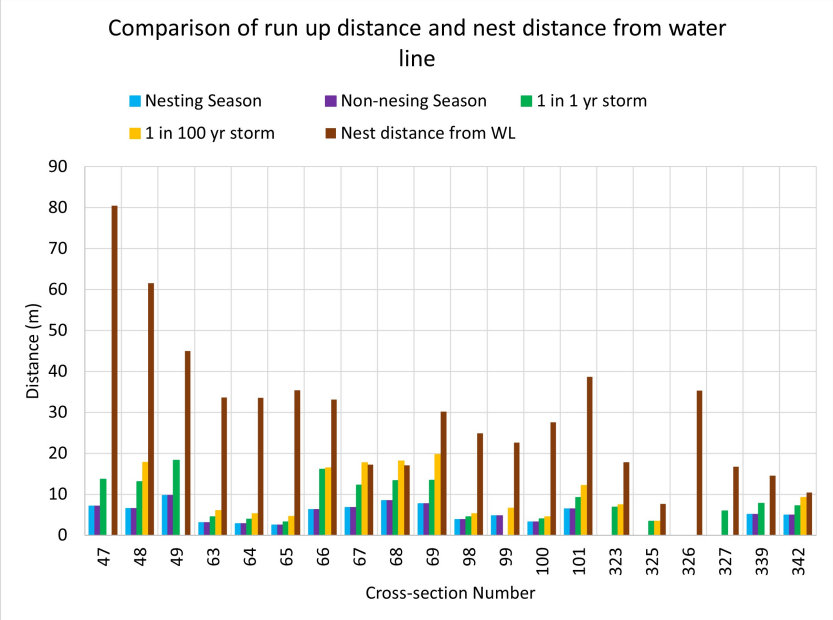

Figure 4.42: Plots for wave runup distance and nesting distance from mean water line for sea side nesting sites (nesting sites on islands at the edge of the reef)

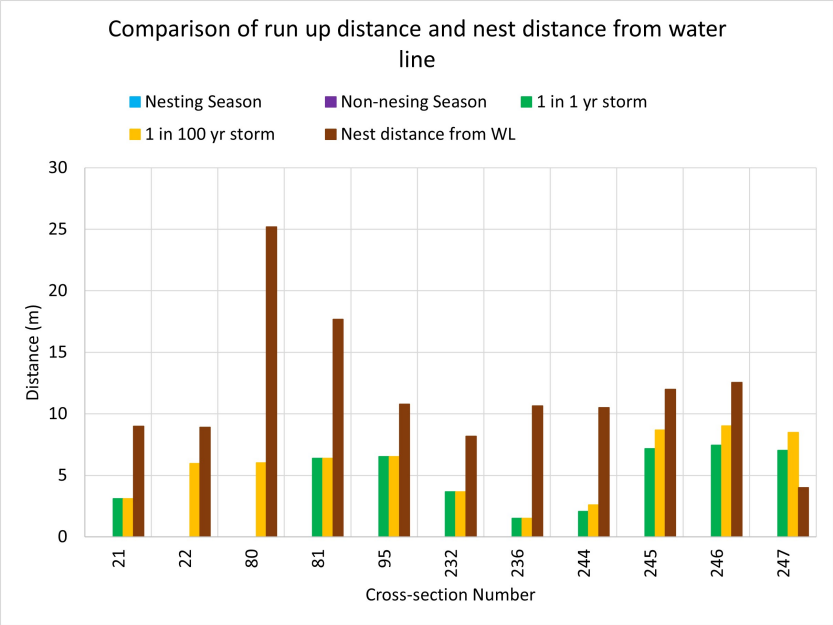

Figure 4.43: Plots for wave runup distance and nesting distance from mean water line for lagoon side nesting sites (nesting sites on islands inside the lagoon)

The wave runup distance plots for the non-nesting sites are shown in Figure 4.44 and Figure 4.45 for seaside and lagoon side respectively. The wave run up distance estimated for non-nesting sites on the seaside and lagoon side were of similar magnitude found in some of the nesting sites. There is no distinct correlation between the runup and the preference for nesting and non-nesting sites though it is clearly established that the sea turtles at Al Wajh Bank are able to locate their nesting sites in the safe zone in relation to the estimated wave runup.

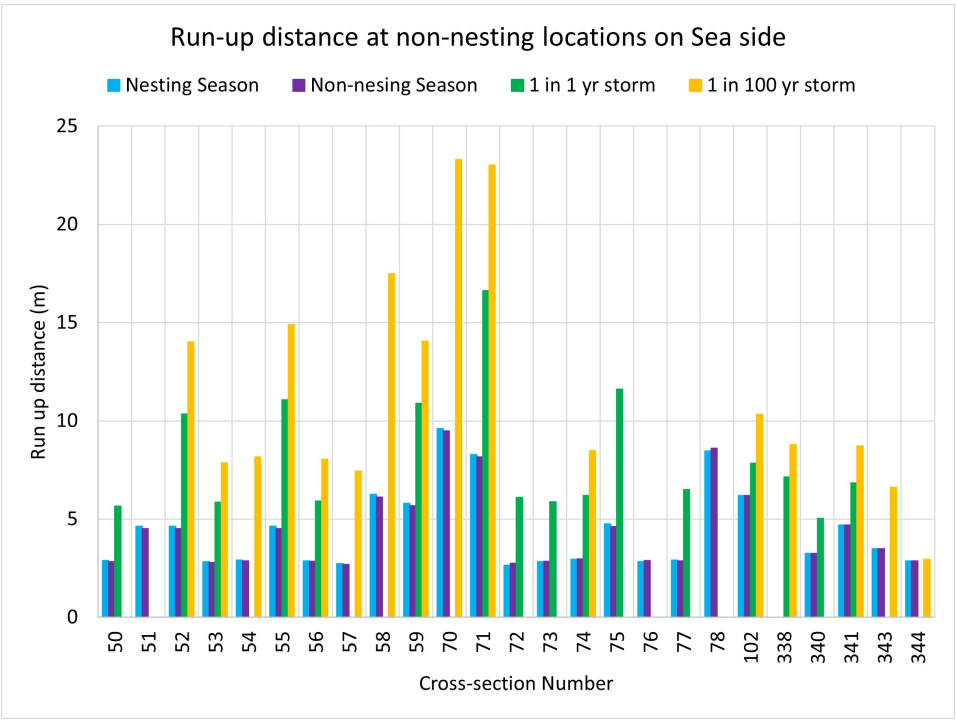

Figure 4.44: Plots for wave runup distance from mean water line for seaside non-nesting sites (nesting sites on islands at the edge of the reef)

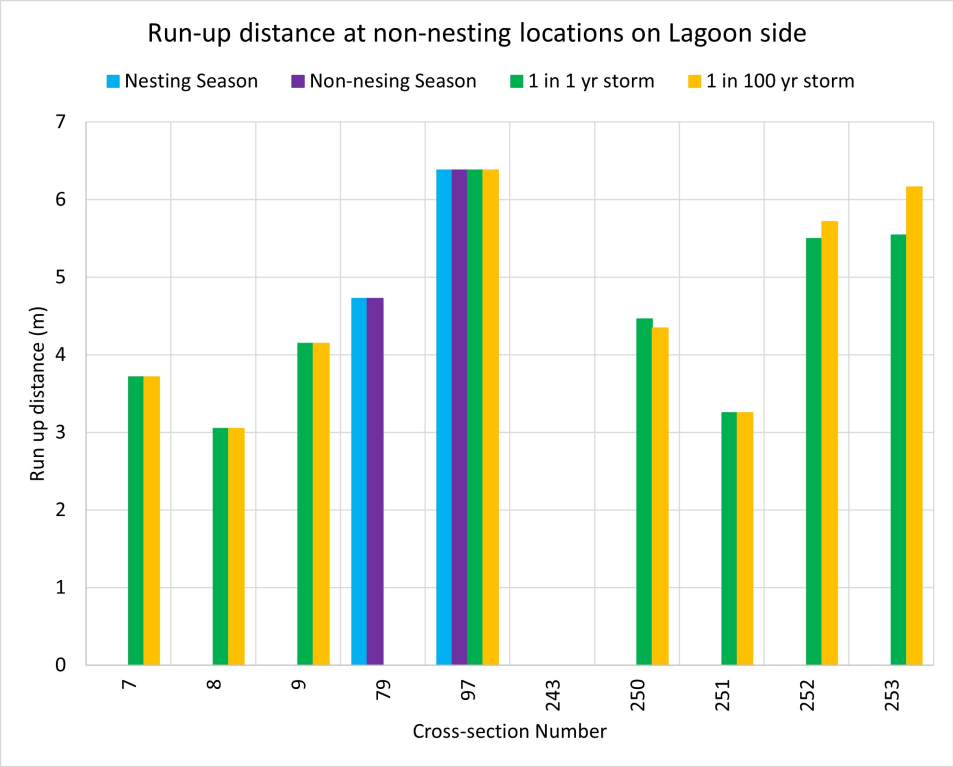

Figure 4.45: Plots for wave runup distance from mean water line for lagoon side non-nesting sites (nesting sites on islands inside the lagoon)

4.6. Summary of Results

The objective of the present study is to investigate the nearshore wave conditions using satellite derived offshore wind and wave data and also understand the energy dissipation characteristics of the reef at Al Wajh Bank in providing the preferential hydrodynamic conditions for turtle nesting. The wind and wave data analysis indicates that the directional spread of the data is in a narrow sector ($300^o to 330^o$) from the northwest quadrant. The wave periods are in the range of 2 to 6 seconds which implies that most of the waves are wind generated short period waves. The numerical model simulations were carried out for the normal (average), 1 in I year and 1 in 100 year return period significant wave heights of 1.34 m, 2.65 m and 3.66 m respectively. For the preferential conditions of sea turtle nesting at Al Wajh Bank the expected inundation risk to the nesting sites due to wave runup using HyCReWW metamodel simulations were carried also carried out. The key results of the model simulations are given below:

- The spatial distribution of the nearshore significant wave heights is analysed and it is observed that the offshore significant wave height of 1.35 m and wind speed of 6.8 m/s generates nearshore wave heights in the range of 0.4 m to 1.0 m at the outer edge of the Al Wajh bank. The higher wave heights are in the northern edge which is directly exposed to waves and lower wave heights are in the southern relatively sheltered area. The 1 in 1 year wave height of 2.65 m and 1 in 100 year wave height of 3.66 m generated maximum nearshore wave height of 2.0 m and 2.5 m respectively. The wave heights observed inside the lagoon were of the order of 0.2 to 0.6 m for normal conditions. The 1 in 1 year and 1 in 100 year conditions generated maximum significant wave heights of 1 m and 1.5 m respectively.
- The analysis of the 1-D spectral wave distribution outside and inside the lagoon gave important insight about the energy dissipation across the reef and the transmission of energy from outside

into the lagoon. An important conclusion is that the waves transformed from offshore to nearshore retained the short period wave characteristics with wave periods in the range of 4 to 6 seconds and appeared more like locally generated wind waves. The results also indicated that the reef flats at Al Wajh Bank completely dissipate the nearshore wave energy with almost negligible transmission of energy into the lagoon. The analysis clearly established through a range of wind speeds 6.8 m/s to 15.3 m/s that the waves inside the lagoon are exclusively wind generated waves. Due to the limitations of the SWAN model the presence of infra gravity waves could not be identified from the results. A comparison of the energy density was also made for the nesting and non-nesting sites at the edge of the reef. The results indicated lesser energy density at the nesting sites compared to the non-nesting sites.Similar trends are found for the nesting and non-nesting sites inside the lagoon.

- The energy dissipation on the reef flat was also analyzed utilizing the numerical model by plotting the curves of wave heights and the dissipation rates across the fore reef and reef flats. The results are computed by the model at closely spaced discrete points (10 m in present case) by interpolation and therefore are approximate. The large dissipation of energy at reef edge and at transitions in the slopes and the reef flat were evident from these results. The reduction of nearshore wave heights of 0.9 m to 0.2 m at the inner edge of the reef flat was demonstrated by the model. The nesting sites are abundant in beaches with flat and wide reef in the foreshore having high rates of energy dissipation. The nesting and non-nesting sites inside the lagoon have similar energy dissipation rates. But the non-nesting sites inside the lagoon are dominated by mud flats, Mangroves and other vegetation and are not preferred by Turtles for nesting.
- The HyCReWW metamodel developed specifically for application to reef environments was used to estimate the wave runup for the nesting and non-nesting sites utilizing the wave data from the numerical model. The input at some of the nesting and non-nesting sites did not fall in the range parameter (the upper and lower bounds) for which the model simulations are not possible. Very low values of wave heights at the nesting and non-nesting sites were discarded and the values closer to the lower and upper bounds were rounded off to the nearest value. The estimated results for the wave setup for normal wave conditions were in the range of 0.14 to 0.25 m and were in the range of 0.15 to 0.43 for 1 in 1 year and 1 in 100 year return period wave conditions. The wave setup results were used to estimate the runup distance along the beach to compare with the nesting site location from the mean water line. The comparison indicates that the nesting site locations are sufficiently away (5 to 60 m) from the estimated wave runup.

5

Discussion and Limitations

For the conservation and protection of the sea turtle nesting sites at Al Wajh Bank it is fundamental to understand the hydrodynamics of the coral reef system and the associated geomorphological features. The present study is a first step in understanding the wave hydrodynamics and the geomorphological features at the nesting and non-nesting sites at Al Wajh Bank based on available data, to a large extent, from secondary sources. The Delft3D WAVE standalone phase averaged spectral wave model which is based on SWAN [10] was used in this study to transform waves from offshore to nearshore. In the absence of any measured data on waves in the nearshore and inside the lagoon the study provides a quantitative and relative assessment of the distribution of significant wave heights and wave energy density using default model parameters with focus on the dissipation of wave energy across the reef.

Delft3D WAVE model was run in a stationary mode with generation by wind, white-capping, refraction, diffraction, Quadruplets, bottom friction and depth induced wave breaking activated. The wave setup was deactivated due to grid size resolution issues. The simulations were performed with 36 directional bins from 0 to 360° and 40 logarithmically distributed frequency bins from 0.03 to 1.42 Hz. Depth-limited wave-breaking was modeled using the Battjes and Janssen (1978) formulation [5] with the default γ=0.73. The model study identified that the main source of energy for the waves at the edge of the reef is from the waves propagating from offshore whereas the waves inside the lagoon are local wind generated waves. The study established that the waves propagating from offshore have no effect on the lagoon wave climate and undergo almost total dissipation at the reef barrier due to bottom friction and wave breaking. In shallow water the triads redistribute energy from lower frequencies to higher frequencies through non-linear interactions. The sensitivity analysis by including triads did not alter the energy distribution in the nearshore and increased the computational time and hence not included.

The validation of the model results could not be carried out due to lack of wave measurements at Al Wajh Bank. The lack of site-specific data on the hydrodynamic and geomorphological parameters has been a major limitation for the present study. The nesting seasons of Green Turtles and Hawksbill Turtles differ. Therefore the data on nearshore wave climate for the nesting and non-nesting seasons would have helped to identify the preferred wave conditions for nesting. The model simulations based on offshore data did not show any difference in the normal wave conditions for the nesting and non-nesting seasons.

The sensitivity analysis of the wave model was caried out for variations in the parameters and for-

mulations for directional spectral resolution, non-linear Triad interactions, bottom friction, whitecapping and wave breaking parameter. Study by Buckley [13] demonstrated that the tuning of the wave breaking parameter in SWAN improves the model predictions in reef environment. The sensitivity analysis was not very exhaustive in the present study due to lack of measured data for detailed analysis and comparison. The limited analysis was carried out which indicated that the sensitivity of results to spectral resolution and whitecapping but demonstrated negligible difference in the significant wave heights and minor difference in spectral peak and energy density.

A course grid global model covering offshore area with a two-stage nesting for regional fine grid resolution for the Al Wajh Bank was used for the wave simulations. Due to computational time and memory constraints the fine grid size of 100 m was chosen for the computations. Though the phase averaged models do not have restriction of grid resolution a finer grid will provide more accurate results if reef lagoon system is better resolved. The outputs of water depth, significant waves heights, wave dissipation rates were obtained in the shallow fore reef zone in a fine resolution output grid from the model. Due to the course resolution of the computational grid the model gives this output by spatial interpolation and therefore is less accurate. The output, however, illustrates the relative wave dissipation rates at the reef crest and reef flat and useful for qualitative assessment. Similarly, the course resolution of computational grid is not suitable to simulation of wave set up and runup.

Unlike mild slope sandy beaches, the coral reef systems are unique and complex with very steep and nearly vertical slope and therefore the available numerical wave models can have limitations in their applications to reef environment. The Delft3D WAVE model results did not simulate presence of low frequency infragravity (IG) waves at the edge of the reefs. In the study done by Buckley [13], three commonly used models (SWASH, SWAN and X-Beach) for reef environment were reviewed and compared using laboratory data. The study brought out the limitations of SWAN model in simulating IG waves. The X-Beach [82], which is a coupled phase-averaged spectral wave model and a non-linear shallow water phase resolving model for modeling sea swell waves and infragravity waves respectively, can resolve the low frequency IG waves and the associated wave runup and setup.

For extreme value analysis of wave data Peak over threshold (POT) is preferred over Annual Maxima Method (AMM). The AMM uses only one data per year disregarding the information in the remaining data. POT is considered to be better than AMM for independent and identically distributed random variables [26]. In the present study the extreme value analysis was carried out using the POT/GPD method.

The Figure 4.14 showed the spectral energy density on the seaside and lagoon side of the barrier reef south of Birrim Island. The frequency distribution of energy inside the lagoon coincides with the energy distribution in this frequency band on the sea side of the barrier. This gives the impression that there is transfer of energy into the lagoon from the seaside. To investigate this further a model simulation was carried out for no wind condition in the model domain. The result of the frequency distribution of spectral energy density on either side of the Barrier Reef is shown with and without wind (no wind) is shown in Figure 5.1. The independent effect of wind on either side of the barrier reef can be clearly seen. On the sea side a shift of energy from peak frequency to higher frequency is also indicated in addition to contribution due to wind. On the lagoon side very little or negligible energy is seen in the absence of wind (no wind condition). The nearshore waves and the lagoon side waves are short period waves and appear to be generated by local wind conditions. The model results for extreme waves show similar trends of energy dissipation at the reef edge and do not transfer energy to the wind generated waves inside the lagoon. The long period swell waves could not be identified at Al Wajh Bank. Field observations will be needed at Al Wajh Bank to identify the swell and sea components.

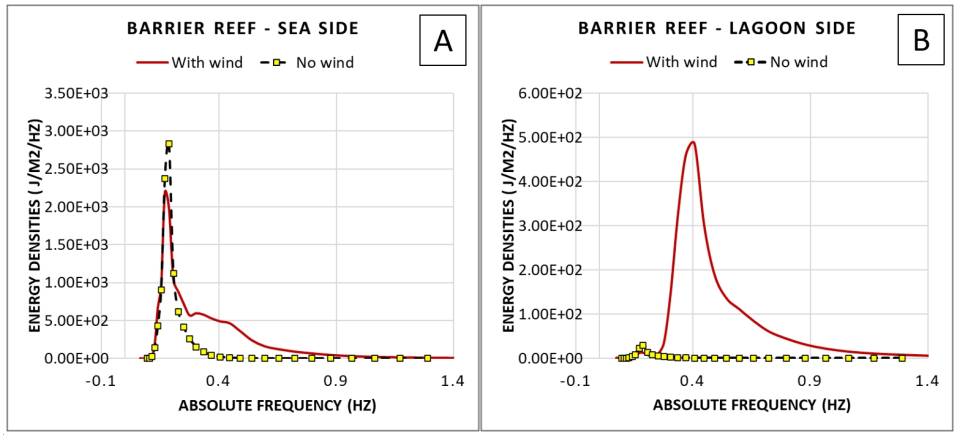

Figure 5.1: Wind effect across the Barrier reef

The wave runup was estimated using the HyCReWW metamodel. The metamodel had some limitations with respect to the range of input parameters that can be used for the simulation of output. For this reason the metamodel could not be effectively used in the runup estimation for many of the sites at Al Wajh Bank. The numerical models like SWASH or XBeach may be useful in overcoming these limitations.

The erosion and accretion rates for Al Wajh Bank were identified using the satellite image based shoreline monitoring database. It is observed that the data base identified some of the mud flats with vegetation around the islands located at the seaside and inside the lagoon as sandy beaches. It appears that the database has some limitations for the coral reef island coastlines.

The analysis of the geomorphological features at the sea turtle nesting and non-nesting sites was done using data from secondary sources. Systematic in-situ data on beach sediments and beach slopes was not available for this study, especially for the nesting sites. The more systematic and accurate analysis of beach slopes, widths, sediment data and other parameters like moisture content, temperature are essential to clearly identify the dominating factors for sea turtle nesting at a particular site. The data indicated differences in nest densities of Green and Hawksbill turtles with dominance of one over the other at different islands.

6

Conclusion

In the analysis of the preferential conditions for sea turtle nesting conditions at Al Wajh Bank the wave hydrodynamics play a pivotal role. The waves not only influence the reef geomorphology but also indirectly affect the microclimate conditions for the turtle nests. The Delft3D WAVE standalone phase averaged spectral wave model was successfully applied for transformation of offshore waves to the nearshore reef system at Al Wajh Bank with available bathymetric data and the offshore data derived from wave hindcast models and satellite altimetry. The lack of wave data in the nearshore and inside the lagoon at Al Wajh Bank is a major limitation but the present study provided quantitative information for relative assessment of the hydrodynamic conditions. A number of preferential conditions for sea turtle related to geomorpholgy and vegetation ecology were identified at Al Wajh Bank including the conditions not favourable for turtle nesting sites at the non-nesting locations. The conclusions drawn for each sub-research question to answer the main research question **'What are the preferential hydrodynamic, geomorphologic and vegetation features influencing the selection of turtle nesting at the Al Wajh Bank?'** are given below.

How is the wave propagation taking place at the seaward end islands and islands in the lagoon?

The analysis of offshore wave data and the transformation of the waves from offshore to nearshore clearly established that the waves at Al Wajh Bank are short period waves and appear to be dominated by locally generated wind waves. The model results gave important insight into the dissipation of wave energy due to depth induced wave breaking and bottom friction effects at the outer edge of the barrier reef. Model results for a range of wind conditions confirm that local winds are responsible for the generation of waves inside the lagoon. The extensive barrier reef on the seaward side of the Al Wajh Bank is able to completely prevent and dissipate the energy of the nearshore waves providing ideal conditions for turtle nesting at seaside Islands. The important hydrodynamic results are summarised below:

- The offshore significant wave height of 1.35 m and wind speed of 6.8 m/s generate nearshore wave heights in the range of 0.4 m to 1.0 m at the outer edge of the Al Wajh bank. The higher wave heights are in the northern edge which is directly exposed to waves and lower wave heights

are in the southern relatively sheltered area. The 1 in 1 year return period wave height of 2.65 m and 1 in 100 year return period wave height of 3.66 m generated maximum nearshore wave height of 2.0 m and 2.5 m respectively. The wave heights observed inside the lagoon were of the order of 0.2 to 0.6 m for normal conditions. The 1 in 1 year and 1 in 100 year return period conditions generated maximum significant wave heights of 1 m and 1.5 m respectively.

- 1-D spectral wave distribution revealed that the waves transformed from offshore to nearshore retained the short period wave characteristics with wave periods in the range of 4 to 6 seconds and appeared more like locally generated wind waves. The results also indicated that the reef flats at Al Wajh Bank completely dissipate the nearshore wave energy with almost negligible transmission of energy into the lagoon. The analysis clearly established through a range of wind speeds 6.8 m/s to 15.3 m/s that the waves inside the lagoon are exclusively wind generated waves. Due to the limitations of the SWAN model the presence of infra gravity waves could not be identified from the study.
- The analysis of energy dissipation on the reef flat using the Delft3D WAVE model interpolated data of wave heights and the dissipation rates across the fore reef and reef flats indicate large dissipation of energy at reef edge, at transitions in the slopes and the reef flats. The reduction of nearshore wave heights of 0.9 m to 0.2 m at the inner edge of the reef flat was demonstrated by the model.
- Estimates of the wave runup using HyCReWW metamodel for normal wave conditions gave values in the range of 0.14 to 0.25 m for the nesting and non-nesting sites. The same were in the range of 0.15 to 0.43 for 1 in 1 year and 1 in 100 year return period wave conditions respectively.

How are the different conditions (hydrodynamic, vegetation and beach features) influencing the turtle nesting sites at Al Wajh Bank?

The numerical wave model demonstrated the large energy dissipation rates across the reef at Al Wajh Bank. A comparison of the energy density for the nesting and non-nesting sites at the edge of the reef indicated lesser energy density at the nesting sites compared to the non-nesting sites. Similar trends are found for the nesting and non-nesting sites inside the lagoon. The abundance of nesting sites in beaches with flat and wide reef in the foreshore are observed having high rates of energy dissipation. whereas the nesting and non-nesting sites inside the lagoon have similar energy dissipation rates. The non-nesting sites inside the lagoon are dominated by mud flats, mangroves and other nearshore vegetation therefore not preferred by turtles for nesting. The comparison of the runup distance along the beach with the nesting site location from the mean water line indicated that the nesting site locations are sufficiently away (5 to 60 m) from the estimated wave runup.

In the absence of relevant data on sediments for the nesting and non-nesting beaches no specific conclusions could be drawn. The beach slopes where sea turtle nests were abundant had slopes in the range of 1:10 and 1:20. The study indicated that the non-nesting sites inside the lagoon are located in the sheltered zones of inner reef shelfs and behind the islands where mud flats with mangrove and other nearshore vegetation are present.The analysis of erosion and accretion trends at Al Wajh Bank identified Ghawar and Sheybarrah Island as having chronic erosion (erosion > 3 m/year) which have limited nesting sites (about 2%). The analysis indicates that the sea turtle prefer beaches with stable conditions of erosion/accretion (+/- 0.5 m/year). The areas with large accretion areas are in leeside of islands where there is extensive growth of vegetation where non-nesting sites are found.

Why are turtle choosing one beach over the other in this area?

Most of the sea turtle nests have been found on the up wave or windward side of beaches with flat and wide fore reefs or fringing reefs between the reef crest and the high-water line. The preference of a particular nesting sites at Al Wajh is clearly for areas with high energy dissipation rates. The nests were more prevalent in areas with shallow sand sheets and carbonate hard grounds and reef flats. Beaches with steep slopes appear to be not preferred for nesting as these may have higher percentage of coarse sand affecting the stability and moisture of the egg chamber and steep slopes are more exposed to waves. The sandy beaches in the neighbourhood of mud flats and associated vegetation are not preferred for nesting as the eggs may get affected by the invasion of roots in and around the nests. Higher density of nests is found at beaches on the outer rim of the barrier reef compared to the nesting sites inside the lagoon. This can be attributed to the fact that hatchlings may find it easier to return to the sea at the reef edge than from inside the lagoon. There could be also higher chances of predation inside the lagoon. Though under stormy wind conditions, the lagoon can offer better nesting conditions as the beaches on the outer rim may get inundated.

7

Recommendation

This study is a first step in understanding the nearshore wave conditions and energy dissipation across the barrier reef and to a limited extent the geomorphological features favouring nesting of sea turtles at Al Wajh Bank. The study is useful in providing guidance for further research and the recommendations for the same are presented below. The thesis is part of a larger study to identify the preferential hydrodynamic and geomorphological conditions for sea turtle nesting at Al Wajh Bank under the Red Sea Development Project of Kingdom of Saudi Arabia.

Regional Data on Hydrodynamic Parameters

The present study could not verify and validate the model results due to lack of wave data in the nearshore or inside the lagoon. The Delft3D WAVE model simulations, however, gave useful quantitative information of the relative distribution of wave field and the dissipation of wave energy outside the lagoon. The study also established the influence of wind on the wave distribution inside the lagoon and the absence of swell component. Under the broader study this study is expected to provide inputs to a separate model investigation using X-Beach in the nearshore surf and swash zone with higher resolution. Therefore, the validation of the models is essential, and it may also be necessary to give spatially varied input data on wind and bottom friction. A detailed systematic data acquisition programme of regional wind, waves, tides and currents in the nearshore and inside the lagoon has to be devised for further research. The measurements for reef friction affects will help in better simulation and understanding of the energy dissipation across the barrier reef. The data also needs to be collected on wave runup, wave setup at selected sites of nesting and non-nesting beaches.

Delft3D WAVE model limitations

Published studies on comparison of commonly used wave models have brought out the limitations of the SWAN model used in the Delft3D WAVE in the simulation of infragravity (IG) waves. The X-Beach model or similar which have a coupled model with phase resolving capability will be capable in simulating the IG waves. IG waves are important for the wave setup in the context of turtle nests and their distribution across the beach slopes. The present model could not get any result on wave setup due to the course resolution of the computational grid. The HyCReWW metamodel had some limitations in the application to some of the nesting sites at Al Wajh Bank due very low magnitude of

wave heights. The metamodel failed to provide results for some combinations of input parameters. It is expected that future research on these aspects will have to use either SWASH or X-Beach models.

Geomorphological data and Statistical Analysis

The geomorphological data on sediment characteristics, beach slopes, beach profiles, distance of nesting sites from high tide line was very limited for the present study. This posed a major limitation for the application of statistical methods like ANOVA / logistic regression analysis. Some of this information was obtained indirectly or from secondary sources but was very limited. A large number of nesting site locations identified by KAUST survey but the survey did nor cover the above geomorphological data. A limited and manageable set of sites can be selected based on the present study to plan a detailed data acquisition programme for a more elaborate statistical analyis to identify the set of dominating hydrodynamic and geomorphological features and their inter relations.

References

[1] Ralph A Ackerman. “The nest environment and the embryonic development of sea turtles”. In: *The biology of sea turtles* 1 (1997), pp. 83–106.

[2] Ralph A Ackerman et al. “Water and heat exchange between parchment-shelled reptile eggs and their surroundings”. In: *Copeia* (1985), pp. 703–711.

[3] Jose-Henrique Alves et al. “Wave modelling - The state of the art”. In: *Progress In Oceanography* 75 (Sept. 2007), pp. 603–674. DOI: 10.1016/j.pocean.2007.05.005.

[4] Fabrice Ardhuin and Alastair D. Jenkins. “On the Interaction of Surface Waves and Upper Ocean Turbulence”. In: *Journal of Physical Oceanography* 36.3 (2006), pp. 551–557. DOI: 10.1175/JPO2862.1. URL: https://journals.ametsoc.org/view/journals/phoc/36/3/jpo2862.1.xml.

[5] Jurjen A Battjes and JPFM Janssen. “Energy loss and set-up due to breaking of random waves”. In: *Coastal engineering 1978*. 1978, pp. 569–587.

[6] Jurjen Anno Battjes. “Computation of set-up, longshore currents, run-up and overtopping due to wind-generated waves”. In: (1974).

[7] Karen A Bjorndal and Alan B Bolten. “Spatial distribution of green turtle (Chelonia mydas) nests at Tortuguero, Costa Rica”. In: *Copeia* (1992), pp. 45–53.

[8] Sean J Blamires, MICHAEL L Guinea, and ROBERT IT Prince. “Influence of nest site selection on predation of flatback sea turtle (Natator depressus) eggs by varanid lizards in northern Australia”. In: *Chelonian Conservation and Biology* 4.3 (2003), pp. 557–563.

[9] Philippe Bonneton et al. “Tidal modulation of wave-setup and wave-induced currents on the Aboré coral reef, New Caledonia”. In: *Journal of Coastal Research* (2007), pp. 762–766.

[10] NRRC Booij, Roeland C Ris, and Leo H Holthuijsen. “A third-generation wave model for coastal regions: 1. Model description and validation”. In: *Journal of geophysical research: Oceans* 104.C4 (1999), pp. 7649–7666.

[11] A. Bowen, D. Inman, and V. Simmons. “Wave ‘set-down’ and set-Up”. In: *Journal of Geophysical Research* 73 (1968), pp. 2569–2577.

[12] Andrew Bruckner et al. “Atlas of Saudi Arabian Red Sea Marine Habitats”. In: *Khaled bin Sultan Living Ocean s Foundation p* 273 (2012).

[13] Mark Buckley, Ryan Lowe, and Jeff Hansen. “Evaluation of nearshore wave models in steep reef environments”. In: *Ocean Dynamics* 64.6 (2014), pp. 847–862.

[14] H Robert Bustard and Peter Greenham. “Physical and chemical factors affecting hatching in the green sea turtle, Chelonia mydas (L.)” In: *Ecology* 49.2 (1968), pp. 269–276.

[15] DK Caldwell. “The loggerhead turtles of Cape Romain, South Carolina”. In: *Bulletin of the Florida State Museum* 4.4 (1959), pp. 320–348.

[16] RR Carthy. “Loggerhead nest morphology: effects of female body size, clutch size and nesting medium on nest chamber size”. In: *Proceedings of the 14 th Annual Symposium on Sea Turtle Biology and Conservation. NOAA Technical Memorandum NMFS SEFSC*. Vol. 351. 1994, pp. 25–28.

[17] Enrique Castillo et al. “Extreme value and related models with applications in engineering and science”. In: (2005).

[18] Vasiliki I Chalastani et al. “Reconciling tourism development and conservation outcomes through marine spatial planning for a Saudi giga-project in the Red Sea (The Red Sea Project, Vision 2030)”. In: *Frontiers in Marine Science* 7 (2020), p. 168.

[19] Ho-Chang Chen, I-Jiunn Cheng, and Eason Hong. “The influence of the beach environment on the digging success and nest site distribution of the green turtle, Chelonia mydas, on Wan-an Island, Penghu Archipelago, Taiwan”. In: *Journal of Coastal Research* 23.5 (2007), pp. 1277–1286.

[20] John B Christoffersen and Ivar G Jonsson. “Bed friction and dissipation in a combined current and wave motion”. In: *Ocean Engineering* 12.5 (1985), pp. 387–423.

[21] Stuart Coles and Emil Simiu. “Estimating uncertainty in the extreme value analysis of data generated by a hurricane simulation model”. In: *Journal of engineering mechanics* 129.11 (2003), pp. 1288–1294.

[22] J Ian Collins. “Prediction of shallow-water spectra”. In: *Journal of Geophysical Research* 77.15 (1972), pp. 2693–2707.

[23] William R Dally, Robert George Dean, and Robert A Dalrymple. *Modeling Wave Transformation in the Surf Zone.* Tech. rep. COASTAL ENGINEERING RESEARCH CENTER VICKSBURG MS, 1984.

[24] Robin Davidson-Arnott, Bernard Bauer, and Chris Houser. *Introduction to coastal processes and geomorphology*. Cambridge university press, 2019.

[25] AG Davies and C Villaret. “Eulerian drift induced by progressive waves above rippled and very rough beds”. In: *Journal of Geophysical Research: Oceans* 104.C1 (1999), pp. 1465–1488.

[26] Anthony C Davison and Richard L Smith. “Models for exceedances over high thresholds”. In: *Journal of the Royal Statistical Society: Series B (Methodological)* 52.3 (1990), pp. 393–425.

[27] Maarten W Dingemans. *Water wave propagation over uneven bottoms: Linear wave propagation*. Vol. 13. World Scientific, 1997.

[28] Mark A. Donelan, William M. Drennan, and Kristina B. Katsaros. “The Air Sea Momentum Flux in Conditions of Wind Sea and Swell”. In: *Journal of Physical Oceanography* 27.10 (1997), pp. 2087–2099. DOI: 10.1175/1520-0485(1997)027<2087:TASMFI>2.0.CO;2. URL: https://journals.ametsoc.org/view/journals/phoc/27/10/1520-0485_1997_027_2087_tasmfi_2.0.co_2.xml.

[29] Ahmed Eladawy et al. “Characterization of the northern Red Sea’s oceanic features with remote sensing data and outputs from a global circulation model”. In: *Oceanologia* 59.3 (2017), pp. 213–237. ISSN: 0078-3234. DOI: https://doi.org/10.1016/j.oceano.2017.01.002. URL: https://www.sciencedirect.com/science/article/pii/S0078323417300039.

[30] Ya Eldeberky. “Parameterization of triad interaction in wave energy model”. In: *Proc. Coastal Dynamics Conf. Gdansk, Poland, 1995*. 1995.

[31] Yasser Eldeberky and Jurjen A Battjes. “Spectral modeling of wave breaking: Application to Boussinesq equations”. In: *Journal of Geophysical Research: Oceans* 101.C1 (1996), pp. 1253–1264.

[32] Michael A Ewert. “The embryo and its egg: development and natural history”. In: *Turtles: perspectives and research* (1979), pp. 333–413.

[33] N Fery et al. “Evaluation of the sea state near Jeddah based on recent observations and model results”. In: *Journal of Operational Oceanography* 8.1 (2015), pp. 1–10.

[34] Allen M Foley, Sue A Peck, and Glenn R Harman. “Effects of sand characteristics and inundation on the hatching success of loggerhead sea turtle (Caretta caretta) clutches on low-relief mangrove islands in southwest Florida”. In: *Chelonian Conservation and Biology* 5.1 (2006), pp. 32–41.

[35] Matthijs Gawehn et al. “Identification and classification of very low frequency waves on a coral reef flat”. In: *Journal of Geophysical Research: Oceans* 121.10 (2016), pp. 7560–7574.

[36] J. GEISTER. “The influence of wave exposure on the ecological zonation of Caribbean coral reefs. 3rd Int”. In: *Coral Reef Symp. Miami, Proc.* 1 (Jan. 1977), pp. 23–30.

[37] William D Grant and Ole Secher Madsen. “Combined wave and current interaction with a rough bottom”. In: *Journal of Geophysical Research: Oceans* 84.C4 (1979), pp. 1797–1808.

[38] Peter Groenewoud, C de Valk, and M Williams. “Overview of the Service and Validation of the Database”. In: *Reference: RP_A870* (2011).

[39] The Wamdi Group. “The WAM model—A third generation ocean wave prediction model”. In: *Journal of Physical Oceanography* 18.12 (1988), pp. 1775–1810.

[40] Emil Julius Gumbel. *Statistics of extremes*. Columbia university press, 1958.

[41] Klaus Hasselmann. “On the spectral dissipation of ocean waves due to white capping”. In: *Boundary-Layer Meteorology* 6.1 (1974), pp. 107–127.

[42] Klaus F Hasselmann et al. “Measurements of wind-wave growth and swell decay during the Joint North Sea Wave Project (JONSWAP).” In: *Ergaenzungsheft zur Deutschen Hydrographischen Zeitschrift, Reihe A* (1973).

[43] Susanne Hasselmann et al. “Computations and parameterizations of the nonlinear energy transfer in a gravity-wave spectrum. Part II: Parameterizations of the nonlinear energy transfer for application in wave models”. In: *Journal of Physical Oceanography* 15 (1985), pp. 1378–1391.

[44] *Hatching amp; Care of Young*. URL: `https://seaworld.org/animals/all-about/sea-turtles/care-of-young/`.

[45] K_T Holland et al. “Runup kinematics on a natural beach”. In: *Journal of Geophysical Research: Oceans* 100.C3 (1995), pp. 4985–4993.

[46] Rob A Holman and AH Sallenger Jr. “Setup and swash on a natural beach”. In: *Journal of Geophysical Research: Oceans* 90.C1 (1985), pp. 945–953.

[47] Stephanie Jill Kamel. “Vegetation cover predicts temperature in nests of the hawksbill sea turtle: implications for beach management and offspring sex ratios”. In: *Endangered Species Research* 20.1 (2013), pp. 41–48.

[48] Paul S Kench, Murray R Ford, and Susan D Owen. “Patterns of island change and persistence offer alternate adaptation pathways for atoll nations”. In: *Nature communications* 9.1 (2018), pp. 1–7.

[49] Paul S Kench and Thomas Mann. “Reef island evolution and dynamics: Insights from the Indian and Pacific oceans and perspectives for the Spermonde Archipelago”. In: *Frontiers in Marine Science* 4 (2017), p. 145.

[50] Paul S Kench et al. “Coral islands defy sea-level rise over the past century: Records from a central Pacific atoll”. In: *Geology* 43.6 (2015), pp. 515–518.

[51] Sabique Langodan et al. “The climatology of the Red Sea–part 1: the wind”. In: *International Journal of Climatology* 37.13 (2017), pp. 4509–4517.

[52] Sabique Langodan et al. “The climatology of the Red Sea–part 2: the waves”. In: *International Journal of Climatology* 37.13 (2017), pp. 4518–4528.

[53] Sabique Langodan et al. “The Red Sea: a natural laboratory for wind and wave modeling”. In: *Journal of Physical Oceanography* 44.12 (2014), pp. 3139–3159.

[54] Sabique Langodan et al. “Wave modeling of a reef-sheltered coastal zone in the Red Sea”. In: *Ocean Engineering* 207 (2020), p. 107378.

[55] Sabique Langodan et al. “Wind-wave source functions in opposing seas”. In: *Journal of geophysical research: Oceans* 120.10 (2015), pp. 6751–6768.

[56] James D Lazell. “Predation on diamondback terrapin (Malaclemys terrapin) eggs by dunegrass (Ammophila breviligulata)”. In: (1981).

[57] A Leslie et al. “Leatherback turtle, Dermochelys coriacea, nesting and nest success at Tortuguero, Costa Rica, in 1990–1991. Tortuga baula, Dermochelys coriacea, anidamiento y éxito en el nido en Tortuguero, Costa Rica, en 1990–1991”. In: *Chelonian Conserv Biol* 2 (1996), pp. 159–168.

[58] K Lohmann and C Lohmann. “Orientation and open-sea navigation in sea turtles”. In: *The Journal of Experimental Biology* 199.1 (1996), pp. 73–81.

[59] Arjen Luijendijk et al. “The state of the world’s beaches”. In: *Scientific reports* 8.1 (2018), pp. 1–11.

[60] Marta P Lyons et al. “Quantifying the impacts of future sea level rise on nesting sea turtles in the southeastern United States”. In: *Ecological Applications* 30.5 (2020), e02100.

[61] Derek Madden et al. “Sea turtle nesting as a process influencing a sandy beach ecosystem”. In: *Biotropica* 40.6 (2008), pp. 758–765.

[62] Ole Secher Madsen, Ying-Keung Poon, and Hans C Graber. “Spectral wave attenuation by bottom friction: Theory”. In: *Coastal Engineering 1988*. 1989, pp. 492–504.

[63] Adolfo Marco et al. “Female nesting behaviour affects hatchling survival and sex ratio in the loggerhead sea turtle: implications for conservation programmes”. In: *Ethology Ecology & Evolution* 30.2 (2018), pp. 141–155. DOI: 10.1080/03949370.2017.1330291. eprint: https://doi.org/10.1080/03949370.2017.1330291. URL: https://doi.org/10.1080/03949370.2017.1330291.

[64] François Marin. “Eddy viscosity and Eulerian drift over rippled beds in waves”. In: *Coastal Engineering* 50.3 (2004), pp. 139–159. ISSN: 0378-3839. DOI: https://doi.org/10.1016/j.coastaleng.2003.10.001. URL: https://www.sciencedirect.com/science/article/pii/S0378383903001108.

[65] Chiang C Mei. *The applied dynamics of ocean surface waves*. Vol. 1. World scientific, 1989.

[66] M Miche. “Mouvements ondulatoires de la mer en profondeur constante ou décroissante”. In: *Annales de Ponts et Chaussées, 1944, pp (1) 26-78,(2) 270-292,(3) 369-406* (1944).

[67] John W Miles. “On the generation of surface waves by shear flows”. In: *Journal of Fluid Mechanics* 3.2 (1957), pp. 185–204.

[68] Sarah L Milton et al. “Effects of Hurricane Andrew on the sea turtle nesting beaches of South Florida”. In: *Bulletin of Marine Science* 54.3 (1994), pp. 974–981.

[69] Hamid Mirfenderesk and Ian R. Young. “Direct measurements of the bottom friction factor beneath surface gravity waves”. In: *Applied Ocean Research* 25.5 (2003), pp. 269–287. ISSN: 0141-1187. DOI: https://doi.org/10.1016/j.apor.2004.02.002. URL: https://www.sciencedirect.com/science/article/pii/S0141118704000045.

[70] Stephen G Monismith et al. “Wave transformation and wave-driven flow across a steep coral reef”. In: *Journal of Physical Oceanography* 43.7 (2013), pp. 1356–1379.

[71] Clay L Montague. “Ecological engineering of inlets in southeastern Florida: design criteria for sea turtle nesting beaches”. In: *Journal of Coastal Research* (1993), pp. 267–276.

[72] Jeanne A Mortimer. “The influence of beach sand characteristics on the nesting behavior and clutch survival of green turtles (Chelonia mydas)”. In: *Copeia* (1990), pp. 802–817.

[73] Catharine Muir and Sea Sense. “The status of marine turtles in the United Republic of Tanzania, East Africa”. In: *Sea sense (Tanzania Turtle & Dugong Conservation Programme)* (2005).

[74] Peter Nielsen. *Coastal bottom boundary layers and sediment transport*. Vol. 4. World scientific, 1992.

[75] CT Perry et al. “Time scales and modes of reef lagoon infilling in the Maldives and controls on the onset of reef island formation”. In: *Geology* 41.10 (2013), pp. 1111–1114.

[76] Owen M Phillips. “On the generation of waves by turbulent wind”. In: *Journal of fluid mechanics* 2.5 (1957), pp. 417–445.

[77] David A Pike, Elizabeth A Roznik, and Ian Bell. “Nest inundation from sea-level rise threatens sea turtle population viability”. In: *Royal Society Open Science* 2.7 (2015), p. 150127.

[78] Najeeb MA Rasul, Ian CF Stewart, and Zohair A Nawab. “Introduction to the Red Sea: its origin, structure, and environment”. In: *The Red Sea*. Springer, 2015, pp. 1–28.

[79] Matthew A Reidenbach et al. “Boundary layer turbulence and flow structure over a fringing coral reef”. In: *Limnology and oceanography* 51.5 (2006), pp. 1956–1968.

[80] RC Ris, LH Holthuijsen, and N Booij. “A third-generation wave model for coastal regions: 2. Verification”. In: *Journal of Geophysical Research: Oceans* 104.C4 (1999), pp. 7667–7681.

[81] N.J. Robinson and F.V. Paladino. “Sea Turtles□”. In: (2013). DOI: https://doi.org/10.1016/B978-0-12-409548-9.04352-9. URL: https://www.sciencedirect.com/science/article/pii/B9780124095489043529.

[82] Dano Roelvink et al. “Modelling storm impacts on beaches, dunes and barrier islands”. In: *Coastal engineering* 56.11-12 (2009), pp. 1133–1152.

[83] Ana Rueda Zamora et al. “HyCReWW: A Hybrid Coral Reef Wave and Water level metamodel”. In: *Computers Geosciences* 127 (Mar. 2019). DOI: 10.1016/j.cageo.2019.03.004.

[84] Thiago Zagonel Serafini, Gustave Gilles Lopez, and Pedro Luís Bernardo da Rocha. “Nest site selection and hatching success of hawksbill and loggerhead sea turtles (Testudines, Cheloniidae) at Arembepe Beach, northeastern Brazil”. In: *Phyllomedusa: Journal of Herpetology* 8.1 (2009), pp. 03–17.

[85] O Shemdin et al. “Nonlinear and linear bottom interaction effects in shallow water”. In: *Turbulent fluxes through the sea surface, wave dynamics, and prediction*. Springer, 1978, pp. 347–372.

[86] James R Spotila et al. “Temperature dependent sex determination in the green turtle (Chelonia mydas): effects on the sex ratio on a natural nesting beach”. In: *Herpetologica* (1987), pp. 74–81.

[87] Hilary F Stockdon et al. “Empirical parameterization of setup, swash, and runup”. In: *Coastal engineering* 53.7 (2006), pp. 573–588.

[88] Graham Symonds, Kerry P Black, and Ian R Young. “Wave-driven flow over shallow reefs”. In: *Journal of Geophysical Research: Oceans* 100.C2 (1995), pp. 2639–2648.

[89] Edward B Thornton and RT Guza. “Transformation of wave height distribution”. In: *Journal of Geophysical Research: Oceans* 88.C10 (1983), pp. 5925–5938.

[90] Susan M Tuxbury and Michael Salmon. “Competitive interactions between artificial lighting and natural cues during seafinding by hatchling marine turtles”. In: *Biological Conservation* 121.2 (2005), pp. 311–316.

[91] AP Van Dongeren et al. “Numerical modeling of low-frequency wave dynamics over a fringing coral reef”. In: *Coastal Engineering* 73 (2013), pp. 178–190.

[92] WallpapersHome. *turtle*. 2021. URL: https://wallpapershome.com/animals/aquatic/turtle-beach-4k-15293.html.

[93] Matthew Ware, Joseph W. Long, and Mariana M.P.B. Fuentes. “Using wave runup modeling to inform coastal species management: An example application for sea turtle nest relocation”. In: *Ocean Coastal Management* 173 (2019), pp. 17–25. ISSN: 0964-5691. DOI: https://doi.org/10.1016/j.ocecoaman.2019.02.011. URL: https://www.sciencedirect.com/science/article/pii/S0964569118310202.

[94] Gerald Beresford Whitham. *Linear and nonlinear waves*. Vol. 42. John Wiley & Sons, 2011.

[95] Clare P Whitmore and Peter H Dutton. “Infertility, embryonic mortality and nest-site selection in leatherback and green sea turtles in Suriname”. In: *Biological conservation* 34.3 (1985), pp. 251–272.

[96] Blair Witherington, Shigetomo Hirama, and Andrea Mosier. “Sea turtle responses to barriers on their nesting beach”. In: *Journal of Experimental Marine Biology and Ecology* 401.1-2 (2011), pp. 1–6.

[97] Daniel W Wood and Karen A Bjorndal. “Relation of temperature, moisture, salinity, and slope to nest site selection in loggerhead sea turtles”. In: *Copeia* 2000.1 (2000), pp. 119–119.

[98] Ian R Young. “Wave transformation over coral reefs”. In: *Journal of Geophysical Research: Oceans* 94.C7 (1989), pp. 9779–9789.

[99] Leonel Zavaleta-Lizárraga and Jorge E Morales-Mávil. “Nest site selection by the green turtle (Chelonia mydas) in a beach of the north of Veracruz, Mexico”. In: *Revista Mexicana de Biodiversidad* 84.3 (2013), pp. 927–937.

A

Survey Data

Table A.1: Distribution of Hawksbill and Green Turtle Nests at Al Wajh Bank

Sr. No.	Name of Island	Number of Nests	
		Hawksbill	Green
1	Al Shaykh Murbat	20	10
2	Ghawar	32	6
3	Um Kud	13	8
4	Mizab	2	-
5	Um Rumah	13	3
6	Mirid	1	-
7	Hur	27	-
8	Qaed Alzawraq	14	-
9	Safayih 2	1	4
10	Abu Khalid	22	3
11	Al osh Al Sharqi	2	-
12	Al – Diyar – 1	2	-
13	Al – Diyar – 2	1	-
14	Al – Diyar – 3	3	-
15	Al – Diyar – 4	8	-
16	Al – Diyar – 5	5	-
17	Al – Diyar – 6	12	-
18	Al – Diyar – 8	2	-
19	Um Al Uqum	1	1
20	Birrim	126	660
21	Shimmujah - 1	5	-
22	Shimmujah – 2	1	-
23	Ummahat Al Shaykh - 1	3	-
24	Ummahat Al Shaykh - 2	3	-
25	Al Samdaniat – 1	1	-
26	Al Samdaniat – 2	1	1
27	Quman	23	3
28	Abu Laheq	2	-
29	Mudra	4	-
30	Suwayhill	1	-
31	Al Radeem	5	17
32	Ummairat	2	-
33	Sheybarah South	34	2
34	Al Waqadi	397	37
35	Alaweel	19	2
36	Awaeel	4	-
37	Al Munqalab	3	1
	Total	**815**	**758**

B

Wind Data

In this section wind rose diagrams for monthly distribution of wind speed and direction are shown with corresponding frequency distribution table for 27 years data from 1992 to 2018.

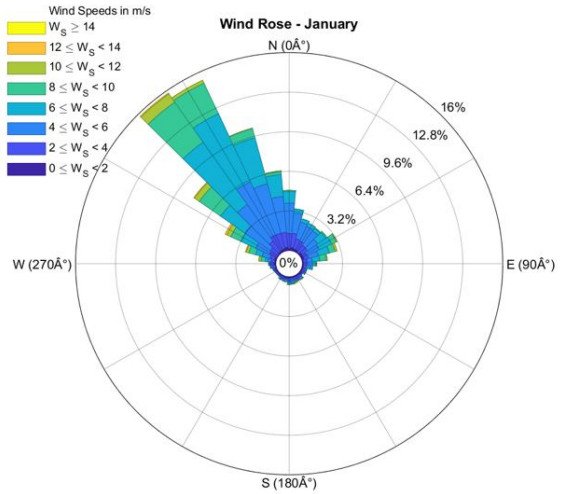

Frequencies (%)		Wind Speed Interval								
Direction Interval (Â°)	Avg. Direction	(0 , 2)	[2 , 4)	[4 , 6)	[6 , 8)	[8 , 10)	[10 , 12)	[12 , 14)	[14 , Inf)	TOTAL
[355 , 5)	0	0.07	1.29	2.47	0.93	0.09	0.01	0.00	0.00	4.86
[5 , 15)	10	0.22	1.17	1.66	0.31	0.01	0.00	0.00	0.00	3.38
[15 , 25)	20	0.16	0.85	1.39	0.28	0.00	0.00	0.00	0.00	2.69
[25 , 35)	30	0.12	0.82	1.30	0.30	0.00	0.00	0.00	0.00	2.54
[35 , 45)	40	0.03	0.72	1.42	0.27	0.04	0.00	0.00	0.00	2.48
[45 , 55)	50	0.15	0.57	0.99	0.79	0.12	0.00	0.00	0.00	2.62
[55 , 65)	60	0.12	0.34	1.12	1.09	0.42	0.04	0.00	0.00	3.14
[65 , 75)	70	0.15	0.39	0.81	0.91	0.46	0.16	0.00	0.00	2.89
[75 , 85)	80	0.04	0.33	0.42	0.60	0.52	0.07	0.00	0.00	1.99
[85 , 95)	90	0.04	0.31	0.45	0.22	0.06	0.04	0.00	0.00	1.14
[95 , 105)	100	0.06	0.27	0.31	0.16	0.01	0.00	0.00	0.00	0.82
[105 , 115)	110	0.09	0.19	0.10	0.03	0.00	0.00	0.00	0.00	0.42
[115 , 125)	120	0.06	0.22	0.12	0.01	0.00	0.00	0.00	0.00	0.42
[125 , 135)	130	0.12	0.09	0.03	0.01	0.00	0.00	0.00	0.00	0.25
[135 , 145)	140	0.09	0.21	0.16	0.03	0.01	0.00	0.00	0.00	0.51
[145 , 155)	150	0.07	0.21	0.12	0.01	0.01	0.03	0.00	0.00	0.46
[155 , 165)	160	0.07	0.18	0.09	0.09	0.06	0.04	0.00	0.00	0.54
[165 , 175)	170	0.09	0.19	0.21	0.09	0.01	0.00	0.00	0.00	0.60
[175 , 185)	180	0.09	0.24	0.10	0.13	0.04	0.00	0.00	0.00	0.61
[185 , 195)	190	0.09	0.10	0.16	0.06	0.00	0.00	0.00	0.00	0.42
[195 , 205)	200	0.09	0.13	0.10	0.03	0.01	0.00	0.00	0.00	0.37
[205 , 215)	210	0.01	0.21	0.13	0.00	0.00	0.00	0.00	0.00	0.36
[215 , 225)	220	0.06	0.12	0.04	0.00	0.00	0.00	0.00	0.00	0.22
[225 , 235)	230	0.04	0.13	0.03	0.00	0.00	0.00	0.00	0.00	0.21
[235 , 245)	240	0.06	0.15	0.01	0.00	0.00	0.00	0.00	0.00	0.22
[245 , 255)	250	0.09	0.13	0.04	0.03	0.00	0.00	0.00	0.00	0.30
[255 , 265)	260	0.03	0.27	0.12	0.01	0.00	0.03	0.00	0.00	0.46
[265 , 275)	270	0.12	0.30	0.09	0.03	0.03	0.00	0.00	0.00	0.57
[275 , 285)	280	0.07	0.30	0.28	0.19	0.34	0.16	0.01	0.00	1.38
[285 , 295)	290	0.12	0.39	0.66	0.54	0.57	0.21	0.06	0.00	2.54
[295 , 305)	300	0.03	0.63	1.21	1.32	0.90	0.34	0.13	0.01	4.58
[305 , 315)	310	0.04	0.72	2.48	2.38	2.08	0.46	0.06	0.00	8.22
[315 , 325)	320	0.10	1.06	3.60	6.15	3.95	0.82	0.07	0.00	15.76
[325 , 335)	330	0.12	1.38	4.74	6.07	2.72	0.25	0.00	0.00	15.28
[335 , 345)	340	0.16	1.32	4.14	3.84	0.76	0.04	0.00	0.00	10.27
[345 , 355)	350	0.24	1.23	2.92	1.79	0.25	0.03	0.00	0.00	6.46
(0 , 360)	TOTAL	3.36	17.17	34.07	28.74	13.52	2.78	0.34	0.01	100.00
No Direction	Wind Speed = 0									0.00

Figure B.1: Wind Rose and frequency distribution - January

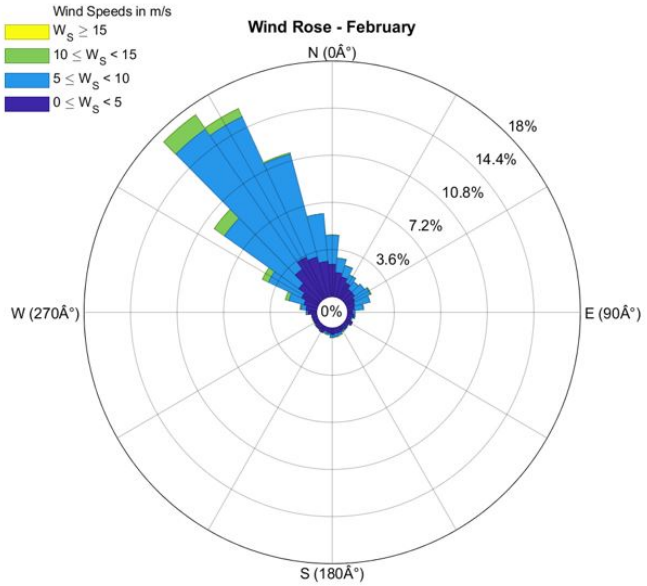

Frequencies (%)		Wind Speed Interval				
Direction Interval (Â°)	Avg. Direction	(0 , 5)	[5 , 10)	[10 , 15)	[15 , Inf)	TOTAL
[355 , 5)	0	2.46	2.23	0.02	0.00	4.71
[5 , 15)	10	1.85	1.10	0.02	0.00	2.97
[15 , 25)	20	1.59	0.90	0.02	0.00	2.51
[25 , 35)	30	1.26	0.69	0.00	0.00	1.95
[35 , 45)	40	0.93	0.72	0.00	0.00	1.66
[45 , 55)	50	0.92	0.92	0.00	0.00	1.84
[55 , 65)	60	0.72	1.33	0.07	0.00	2.12
[65 , 75)	70	0.61	1.21	0.00	0.00	1.82
[75 , 85)	80	0.51	0.71	0.03	0.00	1.25
[85 , 95)	90	0.36	0.21	0.00	0.00	0.57
[95 , 105)	100	0.48	0.10	0.00	0.00	0.57
[105 , 115)	110	0.30	0.08	0.00	0.00	0.38
[115 , 125)	120	0.51	0.02	0.00	0.00	0.52
[125 , 135)	130	0.31	0.05	0.00	0.00	0.36
[135 , 145)	140	0.34	0.08	0.00	0.00	0.43
[145 , 155)	150	0.31	0.13	0.03	0.00	0.48
[155 , 165)	160	0.41	0.18	0.02	0.00	0.61
[165 , 175)	170	0.41	0.23	0.05	0.00	0.69
[175 , 185)	180	0.48	0.23	0.00	0.00	0.71
[185 , 195)	190	0.39	0.13	0.00	0.00	0.52
[195 , 205)	200	0.30	0.16	0.00	0.00	0.46
[205 , 215)	210	0.49	0.02	0.00	0.00	0.51
[215 , 225)	220	0.41	0.02	0.00	0.00	0.43
[225 , 235)	230	0.39	0.03	0.00	0.00	0.43
[235 , 245)	240	0.33	0.05	0.00	0.00	0.38
[245 , 255)	250	0.34	0.03	0.02	0.00	0.39
[255 , 265)	260	0.38	0.02	0.00	0.00	0.39
[265 , 275)	270	0.64	0.18	0.00	0.00	0.82
[275 , 285)	280	0.82	0.41	0.07	0.00	1.30
[285 , 295)	290	1.05	1.21	0.28	0.00	2.54
[295 , 305)	300	1.39	2.84	0.52	0.00	4.76
[305 , 315)	310	1.94	7.04	0.97	0.00	9.94
[315 , 325)	320	2.82	13.07	1.33	0.00	17.22
[325 , 335)	330	3.46	11.82	0.69	0.00	15.97
[335 , 345)	340	3.18	8.13	0.10	0.00	11.41
[345 , 355)	350	2.71	3.66	0.00	0.00	6.36
[0 , 360)	TOTAL	35.80	59.94	4.21	0.00	99.95
No Direction	Wind Speed = 0					0.05

Figure B.2: Wind Rose and frequency distribution - February

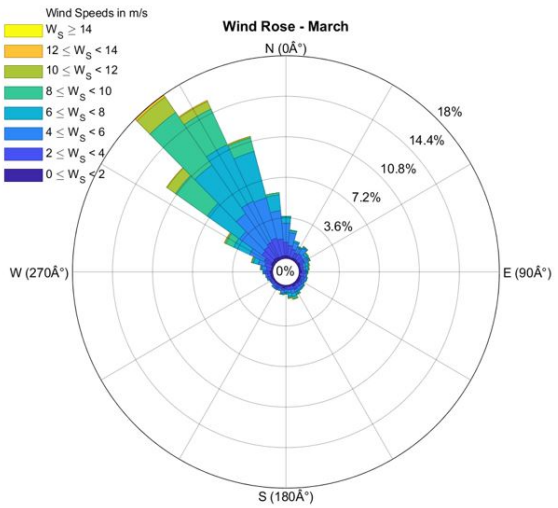

Frequencies (%)		Wind Speed Interval								
Direction Interval (Â°)	Avg. Direction	(0 , 2)	[2 , 4)	[4 , 6)	[6 , 8)	[8 , 10)	[10 , 12)	[12 , 14)	[14 , Inf)	TOTAL
[355 , 5)	0	0.22	1.21	1.68	0.57	0.04	0.00	0.00	0.00	3.73
[5 , 15)	10	0.21	0.94	1.14	0.19	0.03	0.01	0.00	0.00	2.53
[15 , 25)	20	0.13	0.76	0.61	0.13	0.00	0.00	0.00	0.00	1.65
[25 , 35)	30	0.15	0.49	0.54	0.10	0.03	0.00	0.00	0.00	1.32
[35 , 45)	40	0.19	0.58	0.63	0.10	0.03	0.01	0.00	0.00	1.56
[45 , 55)	50	0.13	0.54	0.30	0.22	0.01	0.04	0.00	0.00	1.26
[55 , 65)	60	0.18	0.48	0.37	0.12	0.03	0.01	0.00	0.00	1.20
[65 , 75)	70	0.13	0.27	0.27	0.21	0.07	0.03	0.00	0.00	0.99
[75 , 85)	80	0.12	0.25	0.22	0.21	0.07	0.01	0.00	0.00	0.90
[85 , 95)	90	0.19	0.40	0.06	0.07	0.04	0.00	0.00	0.00	0.78
[95 , 105)	100	0.04	0.39	0.18	0.06	0.03	0.00	0.00	0.00	0.70
[105 , 115)	110	0.19	0.34	0.22	0.01	0.00	0.00	0.00	0.00	0.78
[115 , 125)	120	0.16	0.25	0.21	0.04	0.01	0.00	0.00	0.00	0.69
[125 , 135)	130	0.22	0.33	0.19	0.07	0.00	0.00	0.00	0.00	0.82
[135 , 145)	140	0.13	0.36	0.24	0.10	0.00	0.00	0.00	0.00	0.84
[145 , 155)	150	0.19	0.34	0.25	0.16	0.07	0.00	0.00	0.00	1.03
[155 , 165)	160	0.09	0.34	0.34	0.30	0.18	0.06	0.00	0.00	1.32
[165 , 175)	170	0.10	0.28	0.28	0.31	0.10	0.04	0.01	0.01	1.17
[175 , 185)	180	0.09	0.22	0.30	0.07	0.07	0.00	0.00	0.00	0.76
[185 , 195)	190	0.22	0.21	0.27	0.09	0.01	0.01	0.00	0.00	0.82
[195 , 205)	200	0.10	0.22	0.18	0.03	0.00	0.00	0.00	0.00	0.54
[205 , 215)	210	0.09	0.34	0.13	0.00	0.00	0.00	0.00	0.00	0.57
[215 , 225)	220	0.10	0.28	0.16	0.00	0.00	0.00	0.00	0.00	0.55
[225 , 235)	230	0.10	0.18	0.12	0.00	0.00	0.00	0.00	0.00	0.40
[235 , 245)	240	0.09	0.28	0.04	0.00	0.00	0.00	0.00	0.00	0.42
[245 , 255)	250	0.18	0.24	0.13	0.01	0.00	0.00	0.00	0.00	0.57
[255 , 265)	260	0.16	0.30	0.16	0.00	0.00	0.00	0.00	0.00	0.63
[265 , 275)	270	0.21	0.45	0.13	0.06	0.00	0.00	0.00	0.00	0.85
[275 , 285)	280	0.12	0.43	0.42	0.06	0.06	0.03	0.00	0.00	1.12
[285 , 295)	290	0.10	0.66	0.61	0.45	0.12	0.06	0.01	0.00	2.02
[295 , 305)	300	0.24	0.70	1.47	1.57	0.78	0.10	0.04	0.00	4.91
[305 , 315)	310	0.24	1.17	2.47	3.55	3.49	0.94	0.04	0.00	11.90
[315 , 325)	320	0.30	1.23	3.58	5.28	5.70	1.66	0.21	0.00	17.96
[325 , 335)	330	0.24	1.48	4.01	5.54	3.49	0.75	0.09	0.00	15.60
[335 , 345)	340	0.19	1.71	3.70	4.27	1.26	0.10	0.03	0.00	11.26
[345 , 355)	350	0.22	1.51	2.51	1.42	0.18	0.00	0.00	0.00	5.85
[0 , 360)	TOTAL	5.85	20.22	28.17	25.43	15.94	3.91	0.45	0.01	100.00
No Direction	Wind Speed = 0									0.00

Figure B.3: Wind Rose and frequency distribution - March

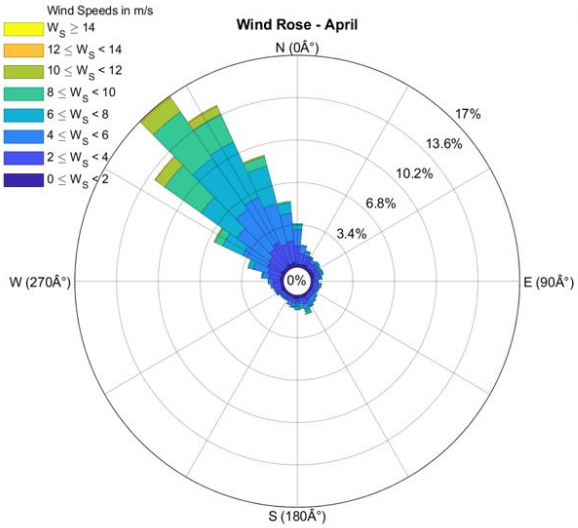

Frequencies (%)		Wind Speed Interval								
Direction Interval (Â°)	Avg.Direction	(0 , 2)	[2 , 4)	[4 , 6)	[6 , 8)	[8 , 10)	[10 , 12)	[12 , 14)	[14 , Inf)	TOTAL
[355 , 5)	0	0.22	1.47	1.33	0.39	0.08	0.00	0.00	0.00	3.48
[5 , 15)	10	0.22	0.88	0.57	0.11	0.00	0.00	0.00	0.00	1.78
[15 , 25)	20	0.26	0.74	0.31	0.06	0.02	0.00	0.00	0.00	1.39
[25 , 35)	30	0.28	0.66	0.11	0.05	0.00	0.00	0.00	0.00	1.10
[35 , 45)	40	0.19	0.46	0.26	0.02	0.00	0.00	0.00	0.00	0.93
[45 , 55)	50	0.25	0.57	0.17	0.09	0.00	0.00	0.00	0.00	1.08
[55 , 65)	60	0.23	0.40	0.17	0.14	0.03	0.00	0.00	0.00	0.97
[65 , 75)	70	0.28	0.46	0.22	0.06	0.03	0.00	0.00	0.00	1.05
[75 , 85)	80	0.22	0.46	0.11	0.08	0.02	0.00	0.00	0.00	0.88
[85 , 95)	90	0.14	0.26	0.15	0.02	0.00	0.00	0.00	0.00	0.57
[95 , 105)	100	0.15	0.45	0.15	0.06	0.00	0.02	0.00	0.00	0.83
[105 , 115)	110	0.17	0.37	0.11	0.05	0.02	0.02	0.00	0.00	0.73
[115 , 125)	120	0.15	0.31	0.19	0.02	0.00	0.00	0.00	0.00	0.66
[125 , 135)	130	0.12	0.37	0.31	0.02	0.02	0.00	0.00	0.00	0.83
[135 , 145)	140	0.11	0.40	0.36	0.08	0.03	0.00	0.00	0.00	0.97
[145 , 155)	150	0.20	0.37	0.46	0.09	0.02	0.02	0.00	0.00	1.16
[155 , 165)	160	0.23	0.51	0.43	0.22	0.17	0.03	0.00	0.00	1.59
[165 , 175)	170	0.17	0.29	0.23	0.23	0.12	0.03	0.00	0.00	1.08
[175 , 185)	180	0.25	0.29	0.32	0.29	0.00	0.00	0.00	0.00	1.16
[185 , 195)	190	0.26	0.36	0.29	0.06	0.02	0.00	0.00	0.00	0.99
[195 , 205)	200	0.17	0.36	0.28	0.03	0.00	0.00	0.00	0.00	0.83
[205 , 215)	210	0.11	0.37	0.11	0.00	0.00	0.00	0.00	0.00	0.59
[215 , 225)	220	0.17	0.36	0.09	0.00	0.00	0.00	0.00	0.00	0.62
[225 , 235)	230	0.17	0.31	0.14	0.00	0.00	0.00	0.00	0.00	0.62
[235 , 245)	240	0.25	0.45	0.11	0.00	0.00	0.00	0.00	0.00	0.80
[245 , 255)	250	0.22	0.49	0.14	0.00	0.00	0.00	0.00	0.00	0.85
[255 , 265)	260	0.19	0.68	0.17	0.00	0.00	0.00	0.00	0.00	1.04
[265 , 275)	270	0.19	0.63	0.36	0.05	0.00	0.00	0.00	0.00	1.22
[275 , 285)	280	0.28	0.91	0.49	0.09	0.02	0.00	0.00	0.00	1.79
[285 , 295)	290	0.22	1.13	1.24	0.40	0.03	0.00	0.00	0.00	3.01
[295 , 305)	300	0.32	1.22	2.21	1.81	0.70	0.08	0.00	0.00	6.34
[305 , 315)	310	0.25	1.41	3.23	3.52	3.63	0.96	0.03	0.00	13.03
[315 , 325)	320	0.23	1.81	3.86	5.01	4.54	1.41	0.12	0.00	16.99
[325 , 335)	330	0.34	1.99	3.99	4.87	2.46	0.70	0.08	0.00	14.42
[335 , 345)	340	0.29	1.65	3.37	3.11	0.79	0.11	0.00	0.00	9.32
[345 , 355)	350	0.40	1.72	2.21	0.82	0.14	0.00	0.00	0.00	5.29
[0 , 360)	TOTAL	7.88	25.60	28.25	21.82	12.86	3.35	0.23	0.00	100.00
No Direction	Wind Speed = 0									0.00

Figure B.4: Wind Rose and frequency distribution - April

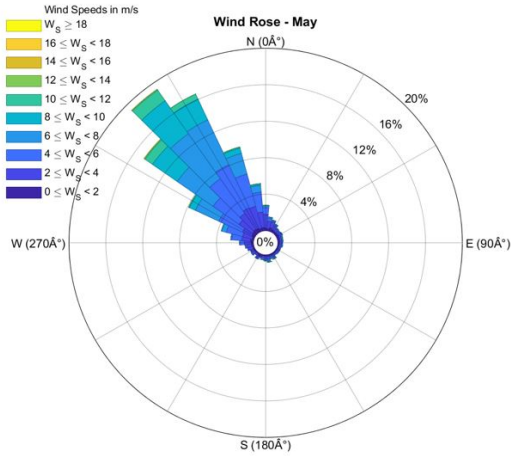

Frequencies (%)		Wind Speed Interval										
Direction Interval (Â°)	Avg. Direction	(0 , 2)	[2 , 4)	[4 , 6)	[6 , 8)	[8 , 10)	[10 , 12)	[12 , 14)	[14 , 16)	[16 , 18)	[18 , Inf)	TOTAL
[355 , 5)	0	0.25	1.52	0.75	0.18	0.06	0.00	0.00	0.01	0.00	0.00	2.78
[5 , 15)	10	0.21	0.82	0.34	0.10	0.03	0.00	0.00	0.00	0.00	0.00	1.51
[15 , 25)	20	0.36	0.69	0.10	0.09	0.03	0.00	0.00	0.00	0.00	0.00	1.27
[25 , 35)	30	0.22	0.54	0.15	0.04	0.00	0.00	0.00	0.00	0.00	0.00	0.96
[35 , 45)	40	0.19	0.34	0.07	0.04	0.00	0.00	0.00	0.00	0.00	0.00	0.66
[45 , 55)	50	0.21	0.24	0.10	0.01	0.01	0.00	0.00	0.00	0.00	0.00	0.58
[55 , 65)	60	0.24	0.37	0.04	0.01	0.00	0.00	0.00	0.00	0.00	0.00	0.67
[65 , 75)	70	0.21	0.21	0.12	0.03	0.01	0.00	0.00	0.00	0.00	0.00	0.58
[75 , 85)	80	0.18	0.21	0.07	0.04	0.04	0.00	0.00	0.00	0.00	0.00	0.55
[85 , 95)	90	0.13	0.28	0.07	0.01	0.00	0.00	0.00	0.00	0.00	0.00	0.51
[95 , 105)	100	0.13	0.24	0.07	0.03	0.03	0.00	0.00	0.00	0.00	0.00	0.51
[105 , 115)	110	0.09	0.18	0.09	0.01	0.00	0.00	0.00	0.00	0.00	0.00	0.37
[115 , 125)	120	0.12	0.19	0.07	0.00	0.00	0.00	0.00	0.00	0.00	0.00	0.39
[125 , 135)	130	0.09	0.19	0.07	0.03	0.00	0.00	0.00	0.00	0.00	0.00	0.39
[135 , 145)	140	0.10	0.12	0.06	0.03	0.00	0.00	0.00	0.00	0.00	0.00	0.31
[145 , 155)	150	0.13	0.30	0.13	0.06	0.00	0.01	0.00	0.00	0.00	0.00	0.64
[155 , 165)	160	0.12	0.12	0.12	0.07	0.04	0.01	0.01	0.00	0.00	0.00	0.51
[165 , 175)	170	0.16	0.31	0.15	0.10	0.06	0.01	0.00	0.00	0.00	0.00	0.81
[175 , 185)	180	0.10	0.28	0.10	0.09	0.06	0.00	0.00	0.00	0.00	0.00	0.64
[185 , 195)	190	0.10	0.30	0.12	0.01	0.00	0.00	0.00	0.00	0.00	0.00	0.54
[195 , 205)	200	0.21	0.13	0.03	0.01	0.01	0.00	0.00	0.00	0.00	0.00	0.40
[205 , 215)	210	0.25	0.24	0.10	0.01	0.01	0.00	0.00	0.00	0.00	0.00	0.63
[215 , 225)	220	0.07	0.21	0.03	0.00	0.00	0.00	0.00	0.00	0.00	0.00	0.31
[225 , 235)	230	0.13	0.31	0.12	0.00	0.00	0.00	0.00	0.00	0.00	0.00	0.57
[235 , 245)	240	0.13	0.30	0.04	0.03	0.00	0.00	0.00	0.00	0.00	0.00	0.51
[245 , 255)	250	0.12	0.46	0.13	0.00	0.00	0.00	0.00	0.00	0.00	0.00	0.72
[255 , 265)	260	0.19	0.55	0.15	0.00	0.00	0.00	0.00	0.00	0.00	0.00	0.90
[265 , 275)	270	0.22	0.76	0.48	0.01	0.00	0.00	0.00	0.00	0.00	0.00	1.48
[275 , 285)	280	0.31	0.96	1.09	0.10	0.00	0.00	0.00	0.00	0.00	0.00	2.46
[285 , 295)	290	0.18	1.08	1.82	0.51	0.04	0.01	0.00	0.00	0.00	0.00	3.64
[295 , 305)	300	0.28	1.14	2.84	2.82	0.72	0.09	0.00	0.00	0.00	0.00	7.89
[305 , 315)	310	0.39	1.79	3.45	4.75	3.27	0.99	0.10	0.00	0.01	0.00	14.76
[315 , 325)	320	0.48	2.12	4.64	6.02	4.41	1.42	0.10	0.00	0.00	0.00	19.19
[325 , 335)	330	0.40	2.49	5.21	5.42	2.51	0.61	0.00	0.00	0.00	0.00	16.65
[335 , 345)	340	0.28	2.52	3.66	2.36	0.60	0.10	0.01	0.00	0.00	0.00	9.54
[345 , 355)	350	0.34	1.70	2.20	0.75	0.15	0.03	0.01	0.00	0.00	0.00	5.18
[0 , 360)	TOTAL	7.39	24.24	28.84	23.84	12.11	3.30	0.25	0.01	0.01	0.00	100.00
No Direction	Wind Speed = 0											0.00

Figure B.5: Wind Rose and frequency distribution - May

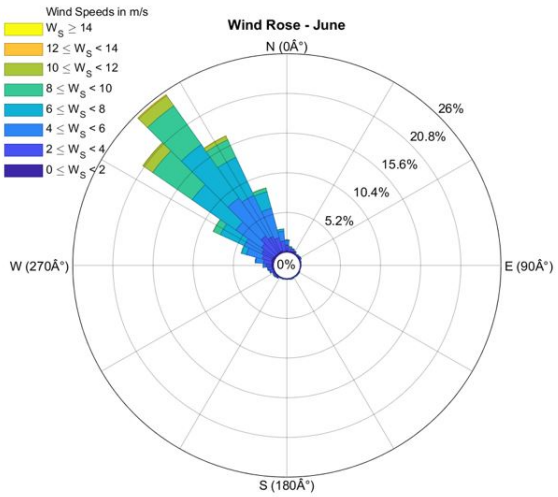

Frequencies (%)		Wind Speed Interval								
Direction Interval (Â°)	Avg. Direction	(0 , 2)	[2 , 4)	[4 , 6)	[6 , 8)	[8 , 10)	[10 , 12)	[12 , 14)	[14 , Inf)	TOTAL
[355 , 5)	0	0.19	0.74	0.59	0.09	0.00	0.00	0.00	0.00	1.60
[5 , 15)	10	0.08	0.45	0.19	0.03	0.02	0.00	0.00	0.00	0.76
[15 , 25)	20	0.14	0.37	0.06	0.00	0.00	0.00	0.00	0.00	0.57
[25 , 35)	30	0.19	0.15	0.03	0.00	0.00	0.00	0.00	0.00	0.37
[35 , 45)	40	0.05	0.11	0.00	0.00	0.00	0.00	0.00	0.00	0.15
[45 , 55)	50	0.05	0.11	0.08	0.00	0.00	0.00	0.00	0.00	0.23
[55 , 65)	60	0.12	0.15	0.02	0.00	0.00	0.00	0.00	0.00	0.29
[65 , 75)	70	0.08	0.06	0.00	0.00	0.00	0.00	0.00	0.00	0.14
[75 , 85)	80	0.09	0.02	0.00	0.00	0.00	0.00	0.00	0.00	0.11
[85 , 95)	90	0.05	0.03	0.02	0.00	0.00	0.00	0.00	0.00	0.09
[95 , 105)	100	0.05	0.02	0.00	0.00	0.00	0.00	0.00	0.00	0.06
[105 , 115)	110	0.03	0.00	0.00	0.00	0.00	0.00	0.00	0.00	0.03
[115 , 125)	120	0.05	0.05	0.02	0.00	0.00	0.00	0.00	0.00	0.11
[125 , 135)	130	0.05	0.06	0.02	0.00	0.00	0.00	0.00	0.00	0.12
[135 , 145)	140	0.02	0.08	0.00	0.00	0.00	0.00	0.00	0.00	0.09
[145 , 155)	150	0.02	0.02	0.02	0.00	0.00	0.00	0.00	0.00	0.05
[155 , 165)	160	0.05	0.08	0.03	0.00	0.00	0.00	0.00	0.00	0.15
[165 , 175)	170	0.05	0.03	0.00	0.00	0.00	0.00	0.00	0.00	0.08
[175 , 185)	180	0.03	0.06	0.00	0.00	0.00	0.00	0.00	0.00	0.09
[185 , 195)	190	0.03	0.06	0.00	0.00	0.00	0.00	0.00	0.00	0.09
[195 , 205)	200	0.00	0.08	0.03	0.00	0.00	0.00	0.00	0.00	0.11
[205 , 215)	210	0.03	0.02	0.02	0.00	0.00	0.00	0.00	0.00	0.06
[215 , 225)	220	0.17	0.11	0.02	0.00	0.00	0.00	0.00	0.00	0.29
[225 , 235)	230	0.11	0.19	0.09	0.02	0.00	0.00	0.00	0.00	0.40
[235 , 245)	240	0.09	0.19	0.03	0.00	0.00	0.00	0.00	0.00	0.31
[245 , 255)	250	0.11	0.42	0.08	0.00	0.00	0.00	0.00	0.00	0.60
[255 , 265)	260	0.17	0.48	0.14	0.00	0.00	0.00	0.00	0.00	0.79
[265 , 275)	270	0.19	0.76	0.39	0.02	0.00	0.00	0.00	0.00	1.34
[275 , 285)	280	0.19	1.11	1.02	0.08	0.00	0.00	0.00	0.00	2.39
[285 , 295)	290	0.31	1.22	2.15	0.68	0.02	0.00	0.00	0.00	4.37
[295 , 305)	300	0.26	1.57	2.52	3.41	1.00	0.02	0.00	0.00	8.78
[305 , 315)	310	0.19	2.08	4.03	6.93	6.25	1.51	0.03	0.00	21.02
[315 , 325)	320	0.17	2.81	6.06	8.53	6.20	1.64	0.14	0.00	25.56
[325 , 335)	330	0.15	2.30	5.93	5.49	2.55	0.52	0.03	0.00	16.98
[335 , 345)	340	0.25	1.77	3.98	2.25	0.48	0.02	0.00	0.00	8.75
[345 , 355)	350	0.08	1.40	1.28	0.29	0.00	0.00	0.00	0.00	3.06
[0 , 360)	TOTAL	3.83	19.14	28.80	27.82	16.51	3.70	0.20	0.00	100.00
No Direction	Wind Speed = 0									0.00

Figure B.6: Wind Rose and frequency distribution - June

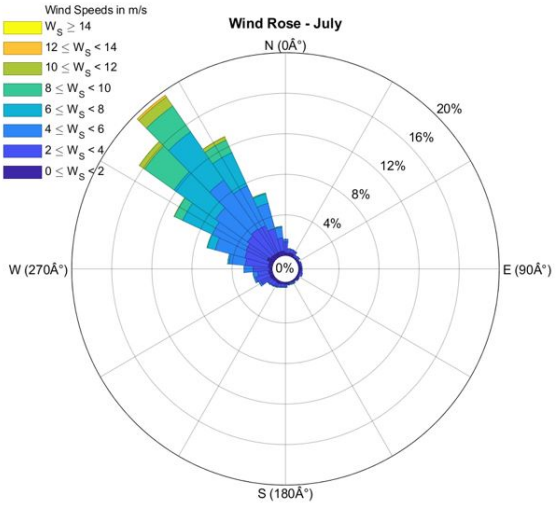

Frequencies (%)		Wind Speed Interval								
Direction Interval (Â°)	Avg. Direction	(0 , 2)	[2 , 4)	[4 , 6)	[6 , 8)	[8 , 10)	[10 , 12)	[12 , 14)	[14 , Inf)	TOTAL
[355 , 5)	0	0.22	1.12	0.22	0.03	0.00	0.00	0.00	0.00	1.60
[5 , 15)	10	0.22	0.43	0.03	0.00	0.00	0.00	0.00	0.00	0.69
[15 , 25)	20	0.30	0.37	0.00	0.00	0.00	0.00	0.00	0.00	0.67
[25 , 35)	30	0.27	0.34	0.00	0.00	0.00	0.00	0.00	0.00	0.61
[35 , 45)	40	0.09	0.21	0.01	0.00	0.00	0.00	0.00	0.00	0.31
[45 , 55)	50	0.13	0.22	0.01	0.00	0.00	0.00	0.00	0.00	0.37
[55 , 65)	60	0.12	0.06	0.00	0.00	0.00	0.00	0.00	0.00	0.18
[65 , 75)	70	0.15	0.15	0.01	0.00	0.00	0.00	0.00	0.00	0.31
[75 , 85)	80	0.18	0.12	0.00	0.00	0.00	0.00	0.00	0.00	0.30
[85 , 95)	90	0.21	0.12	0.00	0.00	0.00	0.00	0.00	0.00	0.33
[95 , 105)	100	0.16	0.16	0.01	0.00	0.00	0.00	0.00	0.00	0.34
[105 , 115)	110	0.12	0.27	0.01	0.00	0.00	0.00	0.00	0.00	0.40
[115 , 125)	120	0.07	0.15	0.00	0.00	0.00	0.00	0.00	0.00	0.22
[125 , 135)	130	0.21	0.07	0.00	0.00	0.00	0.00	0.00	0.00	0.28
[135 , 145)	140	0.10	0.04	0.01	0.00	0.00	0.00	0.00	0.00	0.16
[145 , 155)	150	0.10	0.15	0.04	0.00	0.00	0.00	0.00	0.00	0.30
[155 , 165)	160	0.04	0.13	0.01	0.03	0.00	0.00	0.00	0.00	0.22
[165 , 175)	170	0.15	0.12	0.00	0.00	0.00	0.00	0.00	0.00	0.27
[175 , 185)	180	0.15	0.30	0.01	0.00	0.00	0.00	0.00	0.00	0.46
[185 , 195)	190	0.13	0.30	0.04	0.01	0.00	0.00	0.00	0.00	0.49
[195 , 205)	200	0.22	0.30	0.03	0.00	0.00	0.00	0.00	0.00	0.55
[205 , 215)	210	0.22	0.39	0.04	0.00	0.00	0.00	0.00	0.00	0.66
[215 , 225)	220	0.19	0.49	0.06	0.00	0.00	0.00	0.00	0.00	0.75
[225 , 235)	230	0.25	0.54	0.04	0.00	0.00	0.00	0.00	0.00	0.84
[235 , 245)	240	0.31	1.08	0.19	0.00	0.00	0.00	0.00	0.00	1.58
[245 , 255)	250	0.30	1.40	0.16	0.01	0.00	0.00	0.00	0.00	1.88
[255 , 265)	260	0.34	1.11	0.46	0.00	0.00	0.00	0.00	0.00	1.91
[265 , 275)	270	0.19	1.70	0.91	0.00	0.00	0.00	0.00	0.00	2.81
[275 , 285)	280	0.37	2.30	1.63	0.13	0.00	0.00	0.00	0.00	4.44
[285 , 295)	290	0.36	2.49	3.06	0.82	0.03	0.00	0.00	0.00	6.77
[295 , 305)	300	0.66	2.34	3.72	3.26	0.91	0.03	0.00	0.00	10.92
[305 , 315)	310	0.46	2.82	3.91	5.02	3.61	0.63	0.00	0.00	16.46
[315 , 325)	320	0.42	3.05	5.90	5.81	3.11	1.09	0.21	0.00	19.58
[325 , 335)	330	0.37	2.99	4.35	3.63	1.36	0.34	0.01	0.00	13.05
[335 , 345)	340	0.42	2.37	2.57	0.97	0.07	0.00	0.00	0.00	6.41
[345 , 355)	350	0.42	1.31	1.05	0.07	0.01	0.00	0.00	0.00	2.87
[0 , 360)	TOTAL	8.68	31.54	28.55	19.80	9.11	2.09	0.22	0.00	100.00
No Direction	Wind Speed = 0									0.00

Figure B.7: Wind Rose and frequency distribution - July

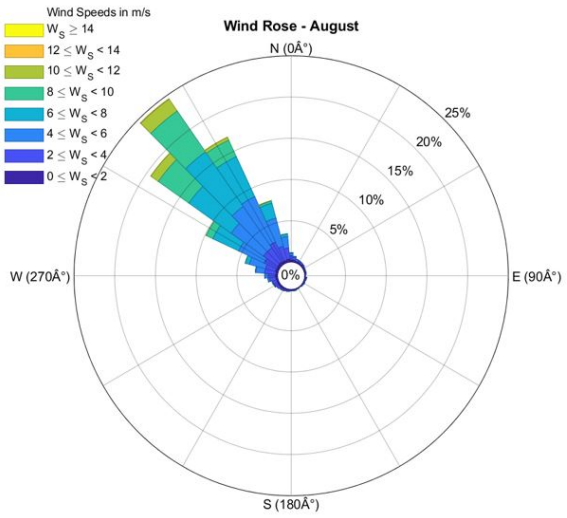

Frequencies (%)		Wind Speed Interval								
Direction Interval (Â°)	Avg. Direction	[0 , 2)	[2 , 4)	[4 , 6)	[6 , 8)	[8 , 10)	[10 , 12)	[12 , 14)	[14 , Inf)	TOTAL
[355 , 5)	0	0.21	0.54	0.33	0.04	0.00	0.00	0.00	0.00	1.12
[5 , 15)	10	0.24	0.37	0.10	0.00	0.00	0.00	0.00	0.00	0.72
[15 , 25)	20	0.12	0.30	0.01	0.00	0.00	0.00	0.00	0.00	0.43
[25 , 35)	30	0.15	0.22	0.00	0.00	0.00	0.00	0.00	0.00	0.37
[35 , 45)	40	0.10	0.22	0.00	0.00	0.00	0.00	0.00	0.00	0.33
[45 , 55)	50	0.19	0.10	0.00	0.00	0.00	0.00	0.00	0.00	0.30
[55 , 65)	60	0.10	0.10	0.00	0.00	0.00	0.00	0.00	0.00	0.21
[65 , 75)	70	0.09	0.07	0.00	0.00	0.00	0.00	0.00	0.00	0.16
[75 , 85)	80	0.10	0.07	0.01	0.00	0.00	0.00	0.00	0.00	0.19
[85 , 95)	90	0.04	0.03	0.01	0.00	0.00	0.00	0.00	0.00	0.09
[95 , 105)	100	0.13	0.09	0.00	0.00	0.00	0.00	0.00	0.00	0.22
[105 , 115)	110	0.03	0.09	0.03	0.00	0.00	0.00	0.00	0.00	0.15
[115 , 125)	120	0.07	0.10	0.00	0.00	0.00	0.00	0.00	0.00	0.18
[125 , 135)	130	0.04	0.07	0.01	0.00	0.00	0.00	0.00	0.00	0.13
[135 , 145)	140	0.03	0.01	0.00	0.00	0.00	0.00	0.00	0.00	0.04
[145 , 155)	150	0.03	0.01	0.01	0.01	0.00	0.00	0.00	0.00	0.07
[155 , 165)	160	0.06	0.00	0.04	0.00	0.00	0.00	0.00	0.00	0.10
[165 , 175)	170	0.07	0.07	0.03	0.00	0.00	0.00	0.00	0.00	0.18
[175 , 185)	180	0.10	0.03	0.04	0.00	0.00	0.00	0.00	0.00	0.18
[185 , 195)	190	0.07	0.07	0.04	0.01	0.00	0.00	0.00	0.00	0.21
[195 , 205)	200	0.10	0.15	0.03	0.00	0.00	0.00	0.00	0.00	0.28
[205 , 215)	210	0.09	0.22	0.04	0.00	0.00	0.00	0.00	0.00	0.36
[215 , 225)	220	0.18	0.19	0.03	0.00	0.00	0.00	0.00	0.00	0.40
[225 , 235)	230	0.19	0.30	0.01	0.00	0.00	0.00	0.00	0.00	0.51
[235 , 245)	240	0.16	0.46	0.07	0.00	0.00	0.00	0.00	0.00	0.70
[245 , 255)	250	0.16	0.51	0.10	0.00	0.00	0.00	0.00	0.00	0.78
[255 , 265)	260	0.21	0.76	0.22	0.00	0.00	0.00	0.00	0.00	1.19
[265 , 275)	270	0.25	0.88	0.45	0.00	0.00	0.00	0.00	0.00	1.58
[275 , 285)	280	0.21	1.39	1.09	0.07	0.00	0.00	0.00	0.00	2.76
[285 , 295)	290	0.31	1.27	2.06	0.51	0.03	0.00	0.00	0.00	4.18
[295 , 305)	300	0.24	1.75	3.46	3.49	0.91	0.01	0.00	0.00	9.87
[305 , 315)	310	0.31	2.17	4.84	6.35	4.58	1.12	0.01	0.00	19.38
[315 , 325)	320	0.36	2.11	6.12	8.08	6.05	1.75	0.06	0.00	24.52
[325 , 335)	330	0.27	2.58	6.06	5.35	2.21	0.37	0.01	0.00	16.86
[335 , 345)	340	0.25	1.78	3.54	1.88	0.25	0.04	0.01	0.00	7.77
[345 , 355)	350	0.34	1.36	1.39	0.31	0.03	0.00	0.00	0.00	3.43
[0 , 360)	TOTAL	5.68	20.49	30.24	26.12	14.07	3.30	0.10	0.00	100.00
No Direction	Wind Speed = 0									0.00

Figure B.8: Wind Rose and frequency distribution - August

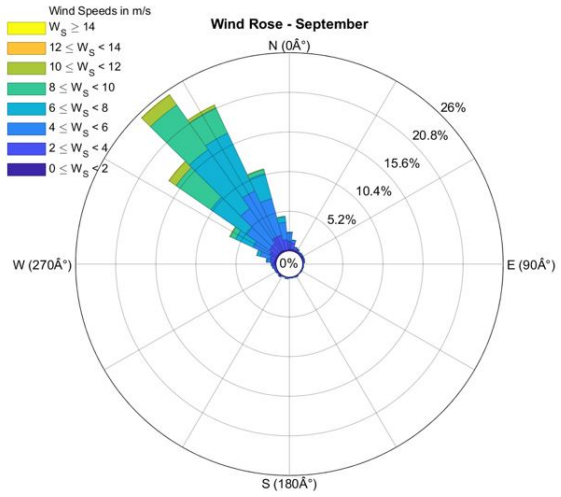

Frequencies (%)		Wind Speed Interval								
Direction Interval (Â°)	Avg. Direction	[0 , 2)	[2 , 4)	[4 , 6)	[6 , 8)	[8 , 10)	[10 , 12)	[12 , 14)	[14 , Inf)	TOTAL
[355 , 5)	0	0.19	1.08	1.10	0.11	0.00	0.00	0.00	0.00	2.47
[5 , 15)	10	0.20	0.82	0.37	0.03	0.03	0.00	0.00	0.00	1.45
[15 , 25)	20	0.14	0.42	0.03	0.00	0.00	0.00	0.00	0.00	0.59
[25 , 35)	30	0.12	0.28	0.08	0.00	0.00	0.00	0.00	0.00	0.48
[35 , 45)	40	0.09	0.12	0.05	0.00	0.00	0.00	0.00	0.00	0.26
[45 , 55)	50	0.06	0.22	0.03	0.02	0.00	0.00	0.00	0.00	0.32
[55 , 65)	60	0.11	0.09	0.09	0.00	0.00	0.00	0.00	0.00	0.29
[65 , 75)	70	0.08	0.15	0.06	0.00	0.00	0.00	0.00	0.00	0.29
[75 , 85)	80	0.08	0.12	0.03	0.00	0.00	0.00	0.00	0.00	0.23
[85 , 95)	90	0.03	0.03	0.00	0.00	0.00	0.00	0.00	0.00	0.06
[95 , 105)	100	0.02	0.06	0.03	0.00	0.00	0.00	0.00	0.00	0.11
[105 , 115)	110	0.02	0.06	0.00	0.00	0.00	0.00	0.00	0.00	0.08
[115 , 125)	120	0.00	0.06	0.03	0.00	0.00	0.00	0.00	0.00	0.09
[125 , 135)	130	0.02	0.03	0.00	0.00	0.00	0.00	0.00	0.00	0.05
[135 , 145)	140	0.02	0.02	0.00	0.00	0.00	0.00	0.00	0.00	0.03
[145 , 155)	150	0.11	0.03	0.02	0.00	0.00	0.00	0.00	0.00	0.15
[155 , 165)	160	0.02	0.08	0.00	0.00	0.00	0.00	0.00	0.00	0.09
[165 , 175)	170	0.00	0.08	0.00	0.00	0.00	0.00	0.00	0.00	0.08
[175 , 185)	180	0.05	0.02	0.00	0.00	0.00	0.00	0.00	0.00	0.06
[185 , 195)	190	0.06	0.12	0.02	0.00	0.00	0.00	0.00	0.00	0.20
[195 , 205)	200	0.00	0.03	0.00	0.00	0.00	0.00	0.00	0.00	0.03
[205 , 215)	210	0.05	0.03	0.00	0.00	0.00	0.00	0.00	0.00	0.08
[215 , 225)	220	0.17	0.12	0.02	0.00	0.00	0.00	0.00	0.00	0.31
[225 , 235)	230	0.05	0.11	0.00	0.00	0.00	0.00	0.00	0.00	0.15
[235 , 245)	240	0.05	0.20	0.02	0.00	0.00	0.00	0.00	0.00	0.26
[245 , 255)	250	0.05	0.23	0.02	0.00	0.00	0.00	0.00	0.00	0.29
[255 , 265)	260	0.03	0.37	0.06	0.00	0.00	0.00	0.00	0.00	0.46
[265 , 275)	270	0.12	0.34	0.14	0.00	0.00	0.00	0.00	0.00	0.60
[275 , 285)	280	0.22	0.51	0.45	0.09	0.00	0.00	0.00	0.00	1.27
[285 , 295)	290	0.15	0.68	1.34	0.45	0.02	0.00	0.00	0.00	2.64
[295 , 305)	300	0.11	0.96	2.39	2.48	0.79	0.06	0.00	0.00	6.79
[305 , 315)	310	0.15	1.27	3.61	5.65	5.53	1.11	0.02	0.00	17.33
[315 , 325)	320	0.17	1.36	5.65	9.43	7.13	1.62	0.03	0.00	25.39
[325 , 335)	330	0.19	1.96	6.70	8.37	3.67	0.39	0.00	0.00	21.27
[335 , 345)	340	0.15	2.02	4.97	3.41	0.56	0.06	0.00	0.00	11.17
[345 , 355)	350	0.11	1.36	2.30	0.73	0.06	0.00	0.00	0.00	4.55
[0 , 360)	TOTAL	3.15	15.43	29.59	30.76	17.78	3.24	0.05	0.00	100.00
No Direction	Wind Speed = 0									0.00

Figure B.9: Wind Rose and frequency distribution - September

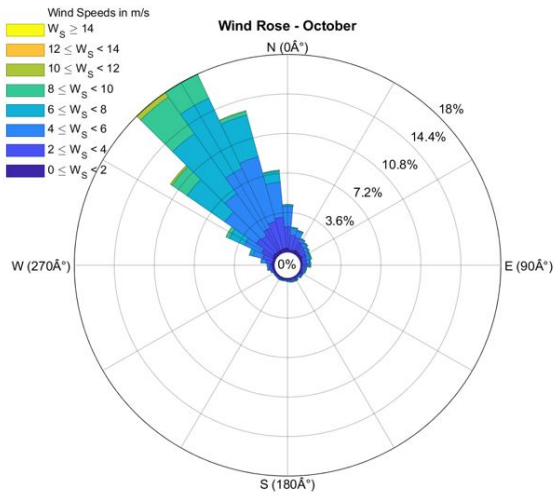

Frequencies (%)		Wind Speed Interval								
Direction Interval (Â°)	Avg. Direction	(0 , 2)	[2 , 4)	[4 , 6)	[6 , 8)	[8 , 10)	[10 , 12)	[12 , 14)	[14 , Inf)	TOTAL
[355 , 5)	0	0.31	1.99	1.87	0.13	0.01	0.00	0.00	0.00	4.32
[5 , 15)	10	0.18	1.39	0.61	0.09	0.00	0.00	0.00	0.00	2.27
[15 , 25)	20	0.21	1.21	0.58	0.09	0.00	0.00	0.01	0.00	2.11
[25 , 35)	30	0.30	0.81	0.36	0.01	0.03	0.00	0.00	0.00	1.51
[35 , 45)	40	0.25	0.67	0.34	0.07	0.00	0.00	0.00	0.00	1.34
[45 , 55)	50	0.22	0.55	0.28	0.09	0.01	0.00	0.00	0.00	1.16
[55 , 65)	60	0.22	0.40	0.34	0.04	0.03	0.00	0.00	0.00	1.05
[65 , 75)	70	0.15	0.42	0.30	0.12	0.04	0.00	0.00	0.00	1.03
[75 , 85)	80	0.13	0.36	0.30	0.07	0.01	0.00	0.00	0.00	0.88
[85 , 95)	90	0.10	0.46	0.18	0.09	0.03	0.00	0.00	0.00	0.87
[95 , 105)	100	0.07	0.25	0.12	0.06	0.03	0.00	0.00	0.00	0.54
[105 , 115)	110	0.10	0.18	0.12	0.07	0.03	0.00	0.00	0.00	0.51
[115 , 125)	120	0.13	0.18	0.07	0.00	0.00	0.00	0.00	0.00	0.39
[125 , 135)	130	0.10	0.21	0.09	0.00	0.00	0.00	0.00	0.00	0.40
[135 , 145)	140	0.06	0.06	0.12	0.03	0.00	0.00	0.00	0.00	0.27
[145 , 155)	150	0.09	0.18	0.06	0.06	0.01	0.00	0.00	0.00	0.40
[155 , 165)	160	0.07	0.19	0.06	0.01	0.04	0.00	0.00	0.00	0.39
[165 , 175)	170	0.10	0.09	0.10	0.04	0.00	0.00	0.00	0.00	0.34
[175 , 185)	180	0.06	0.15	0.04	0.00	0.00	0.00	0.00	0.00	0.25
[185 , 195)	190	0.07	0.10	0.01	0.00	0.00	0.00	0.00	0.00	0.19
[195 , 205)	200	0.13	0.07	0.04	0.00	0.00	0.00	0.00	0.00	0.25
[205 , 215)	210	0.09	0.15	0.04	0.00	0.00	0.00	0.00	0.00	0.28
[215 , 225)	220	0.07	0.12	0.06	0.00	0.00	0.00	0.00	0.00	0.25
[225 , 235)	230	0.09	0.10	0.04	0.00	0.00	0.00	0.00	0.00	0.24
[235 , 245)	240	0.07	0.12	0.03	0.00	0.00	0.00	0.00	0.00	0.22
[245 , 255)	250	0.12	0.16	0.09	0.00	0.00	0.00	0.00	0.00	0.37
[255 , 265)	260	0.16	0.30	0.15	0.00	0.00	0.00	0.00	0.00	0.61
[265 , 275)	270	0.16	0.21	0.24	0.00	0.00	0.00	0.00	0.00	0.61
[275 , 285)	280	0.19	0.58	0.39	0.03	0.00	0.00	0.00	0.00	1.19
[285 , 295)	290	0.15	0.96	0.94	0.28	0.01	0.00	0.00	0.00	2.34
[295 , 305)	300	0.24	1.11	1.75	1.49	0.31	0.00	0.00	0.00	4.90
[305 , 315)	310	0.33	1.90	3.43	4.18	1.66	0.16	0.00	0.00	11.66
[315 , 325)	320	0.27	1.81	4.69	6.66	4.08	0.49	0.00	0.00	18.00
[325 , 335)	330	0.27	2.26	5.99	7.08	2.37	0.03	0.00	0.00	18.00
[335 , 345)	340	0.28	2.64	6.09	3.94	0.36	0.03	0.00	0.00	13.35
[345 , 355)	350	0.36	2.82	3.21	1.00	0.09	0.00	0.00	0.00	7.48
[0 , 360)	TOTAL	5.97	25.16	33.17	25.78	9.18	0.72	0.01	0.00	100.00
No Direction	Wind Speed = 0									0.00

Figure B.10: Wind Rose and frequency distribution - October

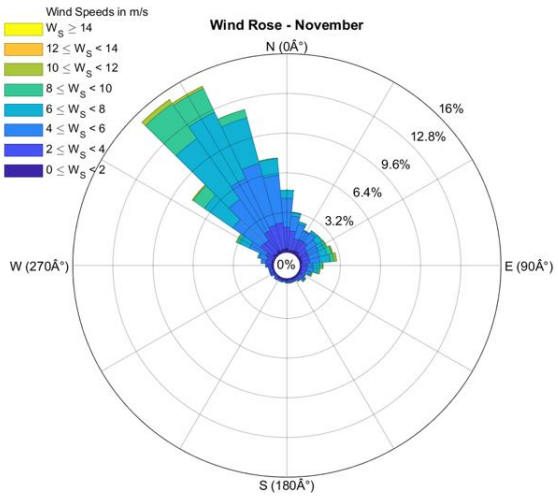

Frequencies (%)		Wind Speed Interval								
Direction Interval (Â°)	Avg. Direction	(0 , 2)	[2 , 4)	[4 , 6)	[6 , 8)	[8 , 10)	[10 , 12)	[12 , 14)	[14 , Inf)	TOTAL
[355 , 5)	0	0.31	1.70	2.33	0.65	0.02	0.00	0.00	0.00	5.00
[5 , 15)	10	0.15	1.57	1.20	0.28	0.03	0.00	0.00	0.00	3.24
[15 , 25)	20	0.19	0.97	1.23	0.19	0.00	0.00	0.00	0.00	2.58
[25 , 35)	30	0.25	0.99	0.76	0.08	0.00	0.00	0.00	0.00	2.07
[35 , 45)	40	0.28	0.94	0.91	0.20	0.00	0.02	0.00	0.00	2.35
[45 , 55)	50	0.15	0.74	0.94	0.52	0.02	0.00	0.00	0.00	2.38
[55 , 65)	60	0.15	0.65	0.90	0.51	0.22	0.03	0.00	0.00	2.45
[65 , 75)	70	0.15	0.62	0.85	0.63	0.37	0.06	0.03	0.00	2.72
[75 , 85)	80	0.15	0.62	0.80	0.83	0.31	0.19	0.00	0.00	2.90
[85 , 95)	90	0.05	0.49	0.43	0.57	0.23	0.03	0.02	0.00	1.82
[95 , 105)	100	0.11	0.46	0.49	0.32	0.17	0.02	0.02	0.00	1.59
[105 , 115)	110	0.12	0.39	0.28	0.14	0.06	0.02	0.03	0.02	1.05
[115 , 125)	120	0.11	0.22	0.17	0.03	0.03	0.03	0.00	0.02	0.60
[125 , 135)	130	0.11	0.45	0.12	0.06	0.02	0.00	0.02	0.00	0.77
[135 , 145)	140	0.14	0.20	0.08	0.05	0.00	0.00	0.03	0.00	0.49
[145 , 155)	150	0.08	0.15	0.09	0.02	0.00	0.00	0.00	0.00	0.34
[155 , 165)	160	0.12	0.15	0.05	0.02	0.00	0.00	0.00	0.00	0.34
[165 , 175)	170	0.09	0.17	0.03	0.05	0.02	0.02	0.00	0.00	0.37
[175 , 185)	180	0.12	0.11	0.08	0.02	0.00	0.00	0.00	0.00	0.32
[185 , 195)	190	0.09	0.09	0.05	0.02	0.00	0.00	0.00	0.00	0.25
[195 , 205)	200	0.15	0.11	0.05	0.00	0.00	0.00	0.00	0.00	0.31
[205 , 215)	210	0.05	0.15	0.05	0.00	0.00	0.00	0.00	0.00	0.25
[215 , 225)	220	0.08	0.20	0.06	0.00	0.00	0.00	0.00	0.00	0.34
[225 , 235)	230	0.02	0.15	0.05	0.00	0.00	0.00	0.00	0.00	0.22
[235 , 245)	240	0.09	0.28	0.03	0.00	0.00	0.00	0.00	0.00	0.40
[245 , 255)	250	0.06	0.26	0.06	0.00	0.00	0.00	0.00	0.00	0.39
[255 , 265)	260	0.11	0.20	0.08	0.00	0.00	0.00	0.00	0.00	0.39
[265 , 275)	270	0.14	0.32	0.11	0.03	0.00	0.00	0.00	0.00	0.60
[275 , 285)	280	0.12	0.52	0.31	0.02	0.02	0.00	0.00	0.00	0.99
[285 , 295)	290	0.15	0.40	0.63	0.12	0.02	0.00	0.00	0.00	1.33
[295 , 305)	300	0.05	0.69	1.48	0.85	0.29	0.02	0.00	0.00	3.38
[305 , 315)	310	0.25	1.22	2.70	2.78	1.10	0.08	0.02	0.00	8.13
[315 , 325)	320	0.14	1.27	4.04	5.97	3.44	0.39	0.00	0.00	15.25
[325 , 335)	330	0.28	1.76	4.65	5.88	2.11	0.19	0.00	0.00	14.86
[335 , 345)	340	0.19	2.11	5.14	3.81	0.68	0.00	0.00	0.00	11.93
[345 , 355)	350	0.25	2.13	3.86	1.34	0.05	0.00	0.00	0.00	7.62
[0 , 360)	TOTAL	5.05	23.47	35.08	25.97	9.18	1.06	0.15	0.03	100.00
No Direction	Wind Speed = 0									0.00

Figure B.11: Wind Rose and frequency distribution - November

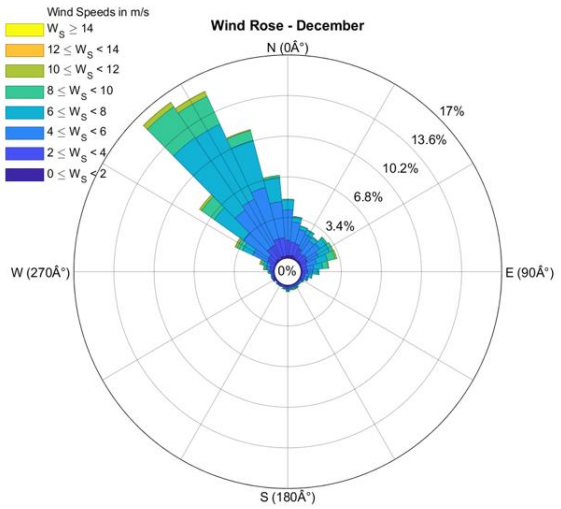

Frequencies (%)		Wind Speed Interval								
Direction Interval (Â°)	Avg. Direction	(0 , 2)	[2 , 4)	[4 , 6)	[6 , 8)	[8 , 10)	[10 , 12)	[12 , 14)	[14 , Inf)	TOTAL
[355 , 5)	0	0.19	1.28	2.55	0.85	0.03	0.00	0.00	0.00	4.91
[5 , 15)	10	0.19	1.15	1.70	0.45	0.01	0.00	0.00	0.00	3.51
[15 , 25)	20	0.25	1.03	1.24	0.30	0.01	0.00	0.00	0.00	2.84
[25 , 35)	30	0.10	0.90	1.31	0.40	0.01	0.00	0.01	0.00	2.75
[35 , 45)	40	0.07	0.63	1.31	0.39	0.04	0.00	0.00	0.00	2.45
[45 , 55)	50	0.12	0.70	1.36	0.63	0.15	0.00	0.00	0.00	2.96
[55 , 65)	60	0.07	0.63	1.05	1.05	0.30	0.00	0.00	0.00	3.09
[65 , 75)	70	0.06	0.46	0.87	0.97	0.66	0.13	0.00	0.00	3.15
[75 , 85)	80	0.07	0.40	0.60	0.75	0.48	0.04	0.00	0.00	2.34
[85 , 95)	90	0.09	0.45	0.43	0.43	0.12	0.00	0.00	0.00	1.52
[95 , 105)	100	0.07	0.25	0.33	0.24	0.04	0.00	0.00	0.00	0.94
[105 , 115)	110	0.07	0.24	0.25	0.06	0.03	0.00	0.00	0.00	0.66
[115 , 125)	120	0.06	0.18	0.10	0.03	0.00	0.00	0.00	0.00	0.37
[125 , 135)	130	0.03	0.07	0.15	0.01	0.00	0.00	0.00	0.00	0.27
[135 , 145)	140	0.01	0.12	0.07	0.00	0.04	0.01	0.00	0.00	0.27
[145 , 155)	150	0.03	0.13	0.10	0.10	0.03	0.00	0.00	0.00	0.40
[155 , 165)	160	0.06	0.12	0.07	0.10	0.04	0.03	0.00	0.00	0.43
[165 , 175)	170	0.03	0.12	0.09	0.06	0.07	0.00	0.00	0.00	0.37
[175 , 185)	180	0.09	0.15	0.10	0.10	0.07	0.00	0.00	0.00	0.52
[185 , 195)	190	0.10	0.12	0.10	0.00	0.00	0.00	0.00	0.00	0.33
[195 , 205)	200	0.01	0.12	0.06	0.01	0.00	0.00	0.00	0.00	0.21
[205 , 215)	210	0.03	0.13	0.03	0.01	0.00	0.00	0.00	0.00	0.21
[215 , 225)	220	0.09	0.06	0.06	0.00	0.00	0.00	0.00	0.00	0.21
[225 , 235)	230	0.06	0.03	0.01	0.00	0.00	0.00	0.00	0.00	0.10
[235 , 245)	240	0.12	0.13	0.00	0.01	0.00	0.00	0.00	0.00	0.27
[245 , 255)	250	0.07	0.13	0.09	0.01	0.00	0.00	0.00	0.00	0.31
[255 , 265)	260	0.03	0.18	0.06	0.00	0.01	0.00	0.00	0.00	0.28
[265 , 275)	270	0.04	0.18	0.12	0.06	0.12	0.00	0.00	0.00	0.52
[275 , 285)	280	0.07	0.30	0.25	0.07	0.15	0.06	0.01	0.00	0.93
[285 , 295)	290	0.06	0.36	0.30	0.28	0.19	0.12	0.00	0.00	1.31
[295 , 305)	300	0.04	0.70	1.40	0.94	0.52	0.15	0.03	0.00	3.79
[305 , 315)	310	0.10	0.75	2.60	3.02	1.31	0.19	0.00	0.00	7.97
[315 , 325)	320	0.16	1.15	3.85	7.39	3.15	0.43	0.01	0.00	16.16
[325 , 335)	330	0.04	1.28	4.23	6.93	2.57	0.43	0.01	0.00	15.50
[335 , 345)	340	0.19	1.52	4.45	4.06	0.87	0.06	0.01	0.00	11.17
[345 , 355)	350	0.15	1.57	3.03	2.00	0.19	0.00	0.00	0.00	6.94
[0 , 360)	TOTAL	3.11	17.74	34.36	31.75	11.26	1.67	0.10	0.00	100.00
No Direction	Wind Speed = 0									0.00

Figure B.12: Wind Rose and frequency distribution - December

C

Monthly Mean daily distribution of Wave and wind parameters

The daily mean values are found by taking the mean of the measurement of each day for 27 years from 1st January 1992 to 31st December 2018. The mean wave height, wave period, wave direction, wind speed and wind direction for each month are represented in Figure C.1 to Figure C.12. The monthly standard deviation for wind speed (u_{10}), wind direction (u_{10d}), significant wave height (H_s), wave direction (H_{sd}) and wave period (T_p) are given in Table C.1.

Table C.1: Monthly mean and standard deviations of 27 years for wind sped (u10), wind direction (u10d), significant wave height (Hs), wave direction (Hsd), wave period (Tp)

Month	u10 (m/s)		u10d (deg)		Hs (m)		Hsd (deg)		Tp (s)	
	Mean	St. Dev.	Mean	St. Dev.	Mean	St. Dev.	Mean	St. Dev.	Mean	St. Dev.
January	5.72	2.18	241.98	125.34	0.79	0.48	274.53	88.70	4.72	1.12
February	5.81	2.37	258.68	115.61	0.84	0.53	287.50	75.68	4.80	1.12
March	5.68	2.47	263.89	107.51	0.86	0.55	292.72	63.68	4.84	1.07
April	5.24	2.47	267.68	99.39	0.77	0.52	293.76	58.71	4.71	1.03
May	5.30	2.44	282.94	88.68	0.78	0.50	303.99	43.65	4.66	0.94
June	5.82	2.33	304.38	58.29	0.95	0.49	314.98	11.27	4.95	0.88
July	4.83	2.34	289.74	68.44	0.70	0.47	310.80	22.70	4.55	0.91
August	5.56	2.34	302.08	58.54	0.86	0.49	312.89	18.77	4.78	0.91
September	5.98	2.20	303.61	69.31	0.95	0.46	314.49	15.84	4.94	0.84
October	5.10	2.09	274.15	106.78	0.74	0.40	298.18	55.24	4.68	0.83
November	5.19	2.08	243.63	125.00	0.71	0.40	276.19	82.88	4.67	0.97
December	5.61	2.01	240.42	127.78	0.77	0.43	273.41	89.41	4.69	1.02

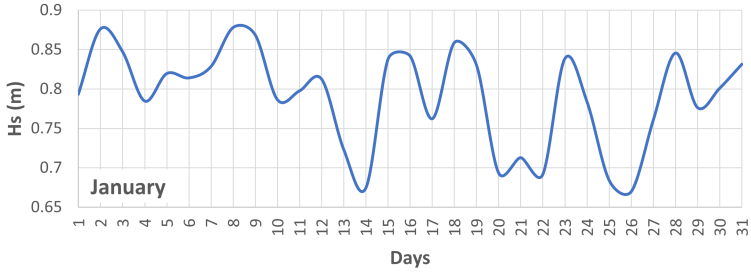

(a) Wave Height (m)

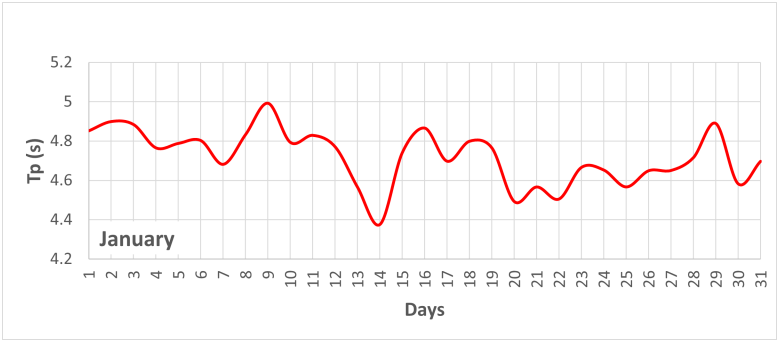

(b) Wave Period (s)

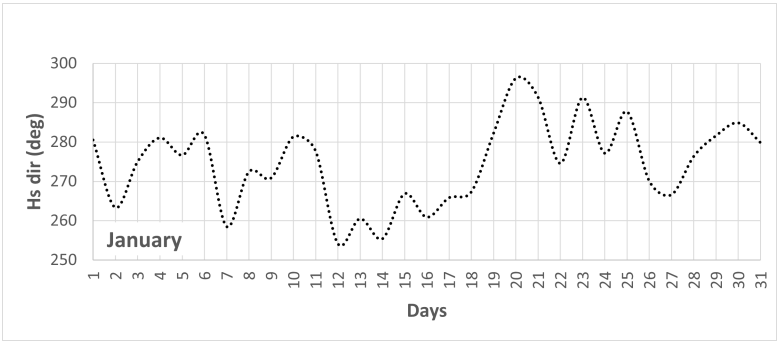

(c) Wave direction (deg)

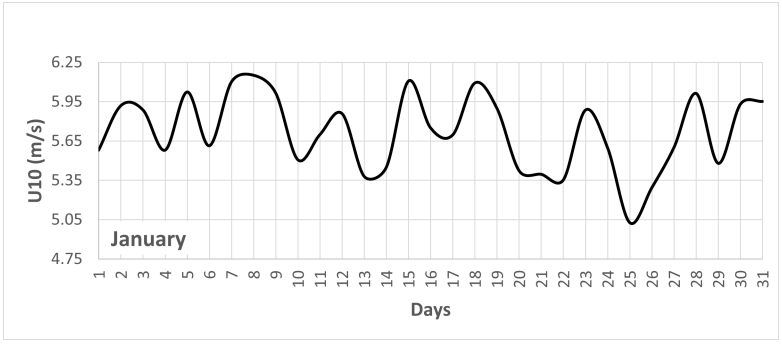

(d) Wind Speed (m/s)

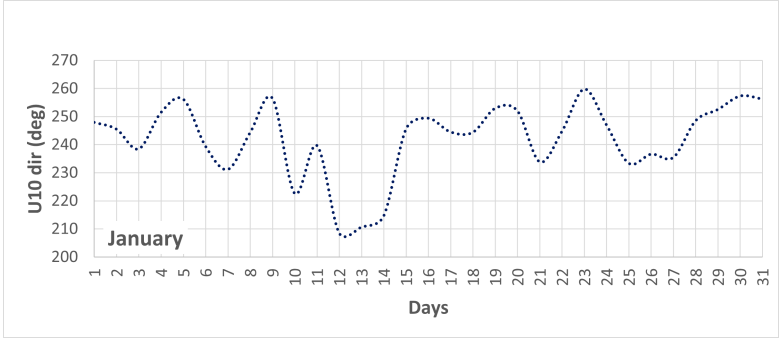

(e) Wind direction (deg)

Figure C.1: 27 years daily mean wave and wind characteristics for January

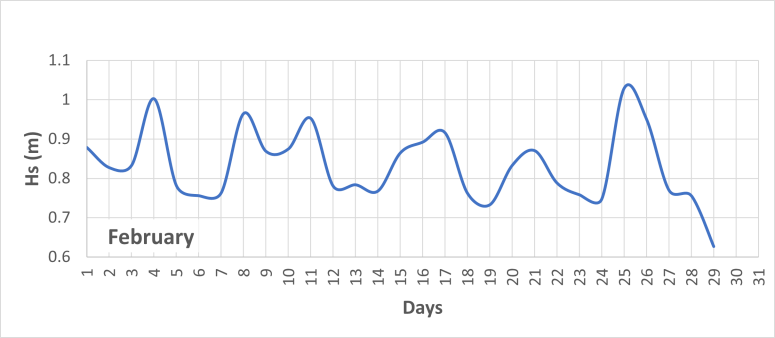

(a) Wave Height (m)

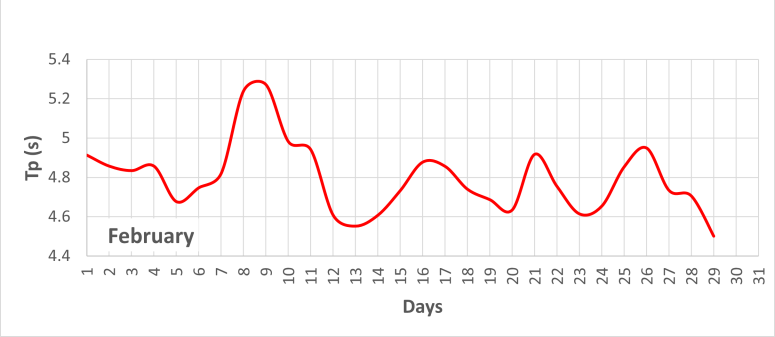

(b) Wave Period (s)

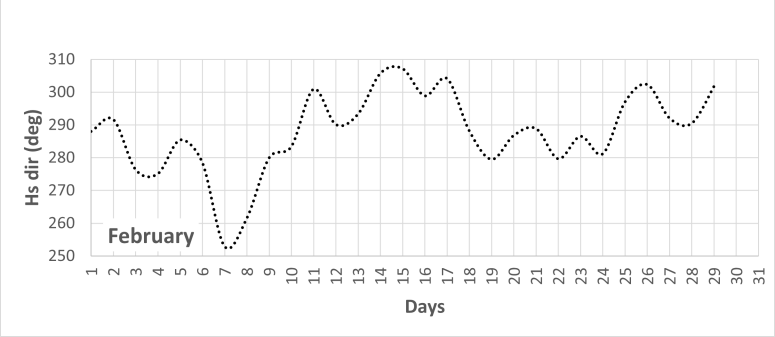

(c) Wave direction (deg)

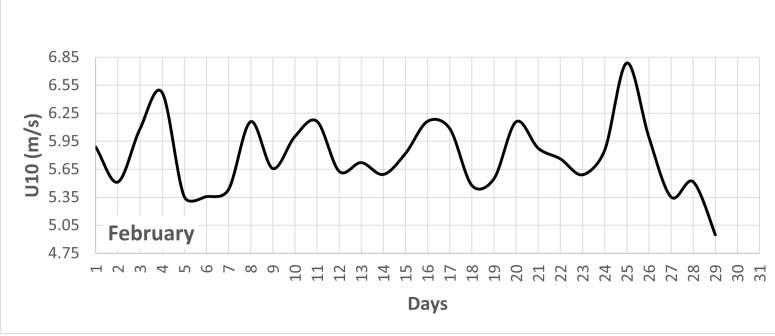

(d) Wind Speed (m/s)

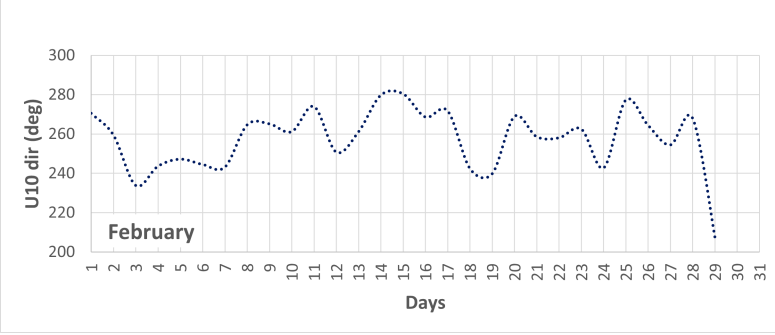

(e) Wind direction (deg)

Figure C.2: 27 years daily mean wave and wind characteristics for February

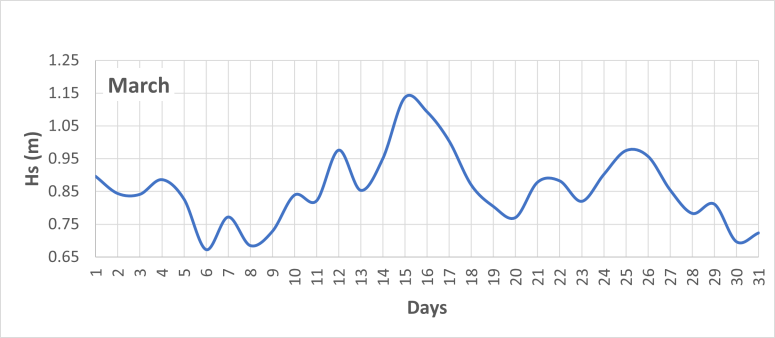

(a) Wave Height (m)

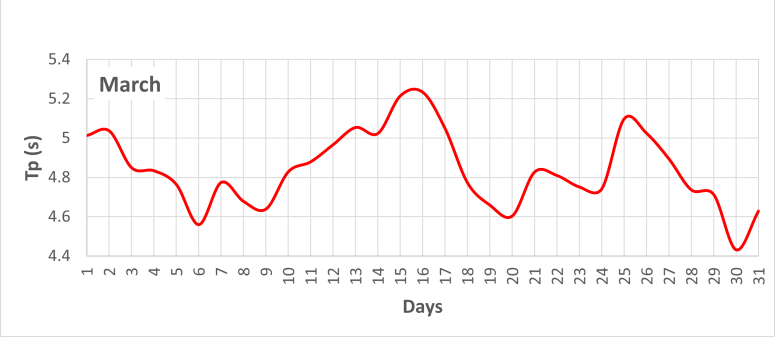

(b) Wave Period (s)

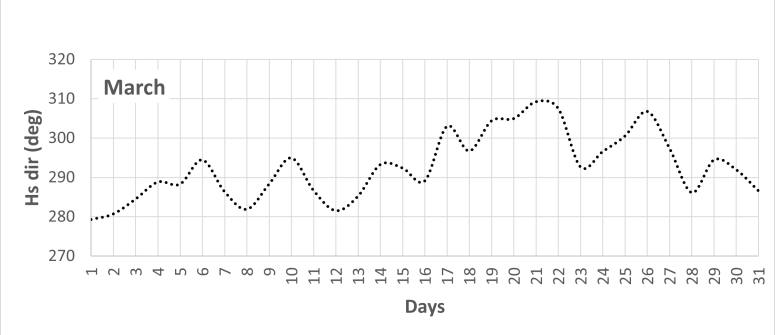

(c) Wave direction (deg)

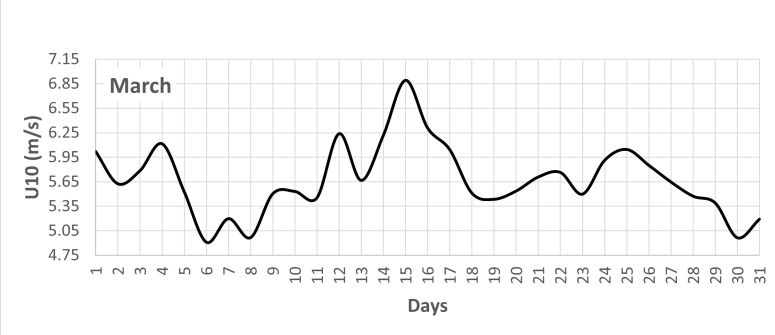

(d) Wind Speed (m/s)

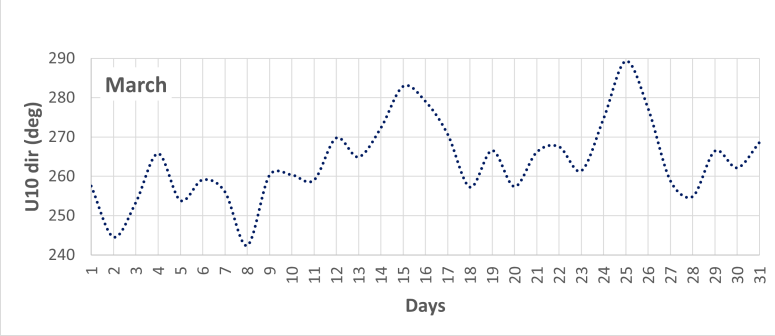

(e) Wind direction (deg)

Figure C.3: 27 years daily mean wave and wind characteristics for March

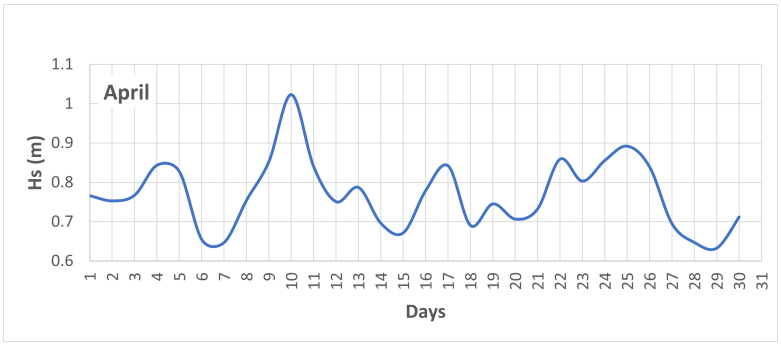

(a) Wave Height (m)

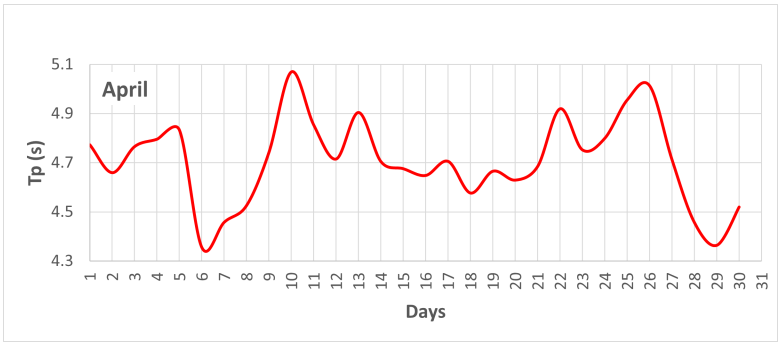

(b) Wave Period (s)

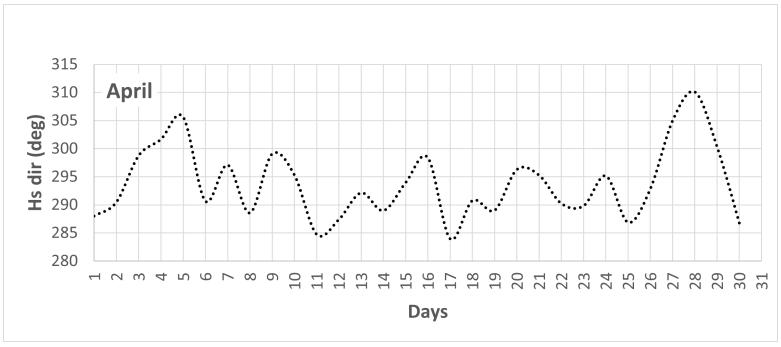

(c) Wave direction (deg)

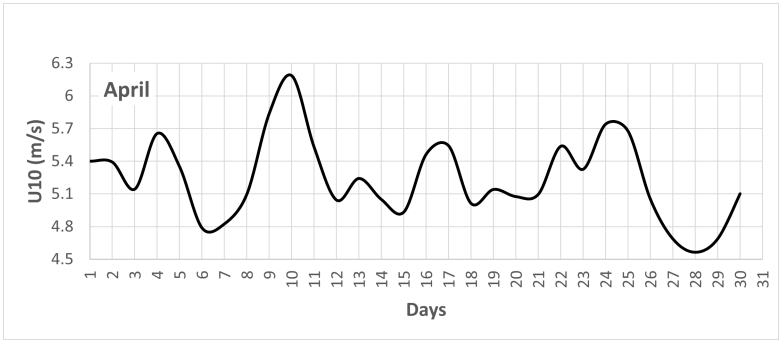

(d) Wind Speed (m/s)

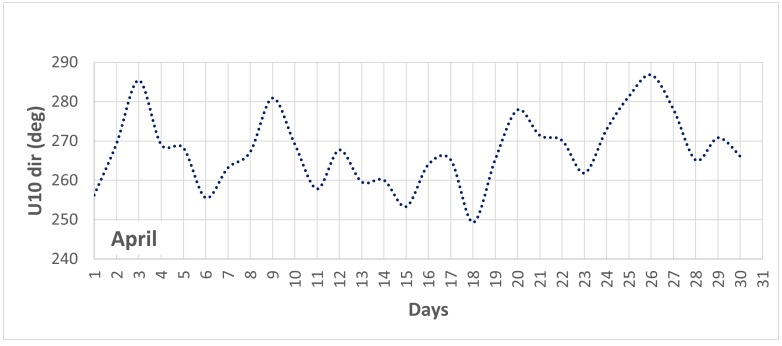

(e) Wind direction (deg)

Figure C.4: 27 years daily mean wave and wind characteristics for April

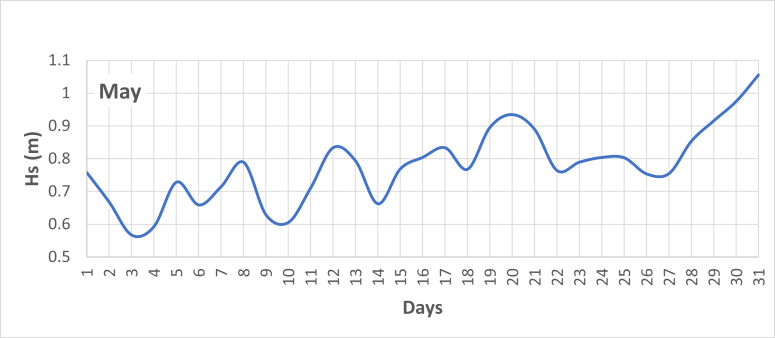

(a) Wave Height (m)

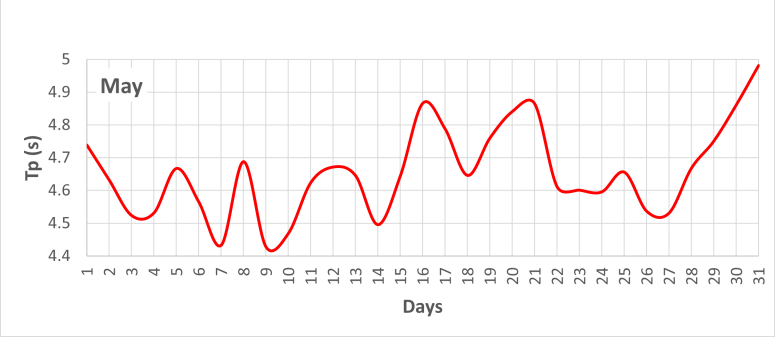

(b) Wave Period (s)

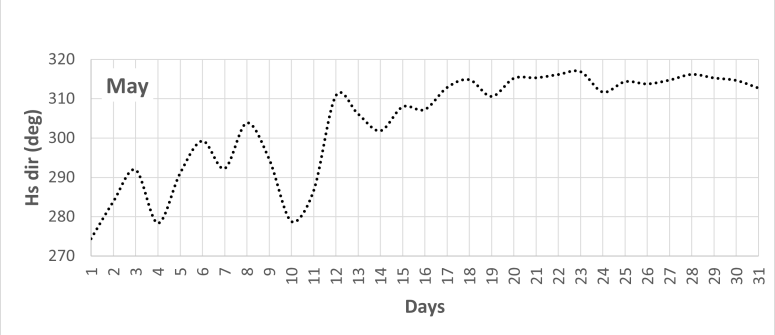

(c) Wave direction (deg)

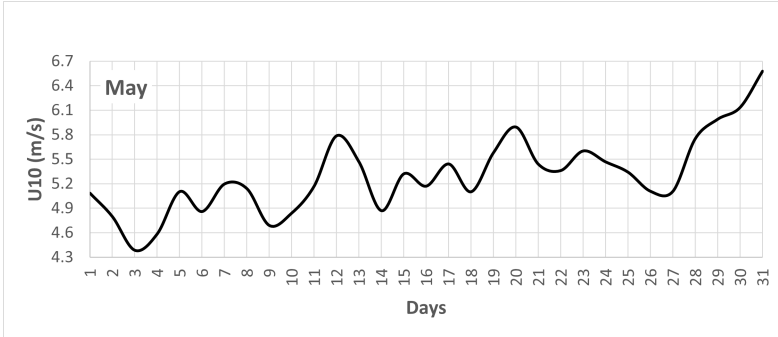

(d) Wind Speed (m/s)

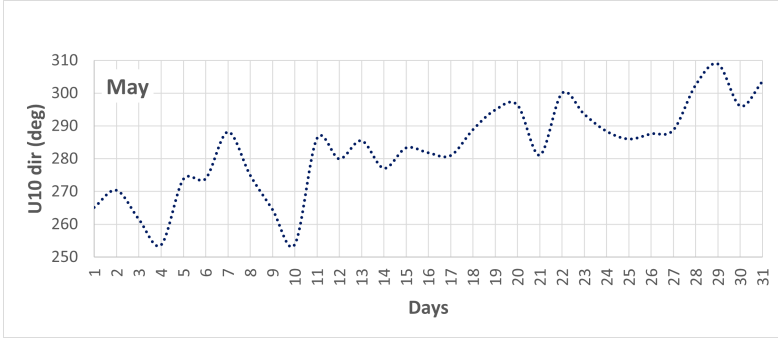

(e) Wind direction (deg)

Figure C.5: 27 years daily mean wave and wind characteristics for May

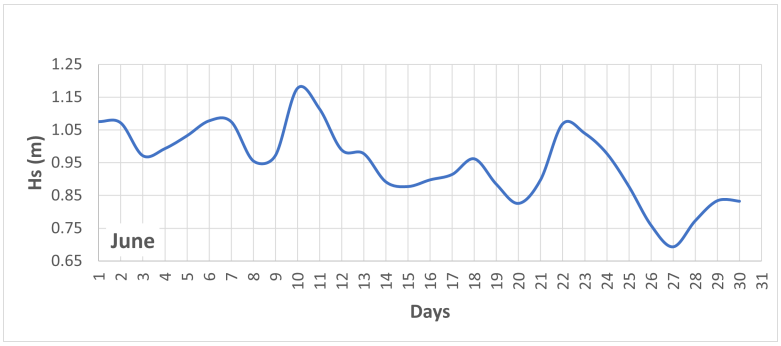

(a) Wave Height (m)

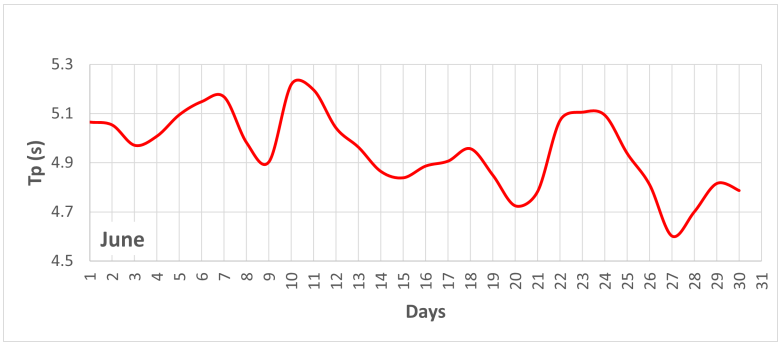

(b) Wave Period (s)

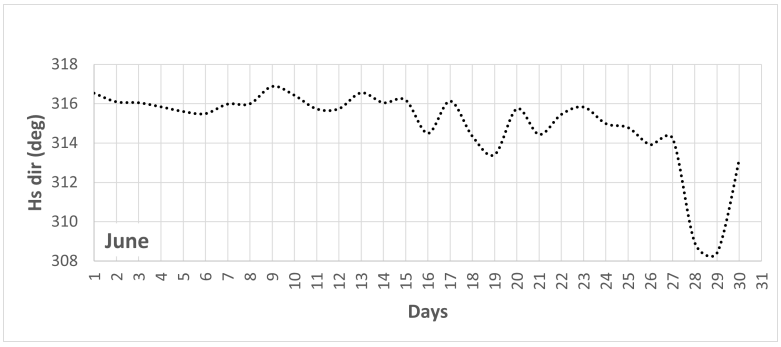

(c) Wave direction (deg)

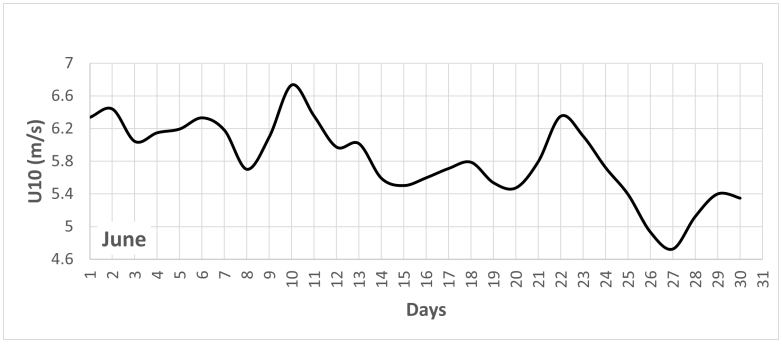

(d) Wind Speed (m/s)

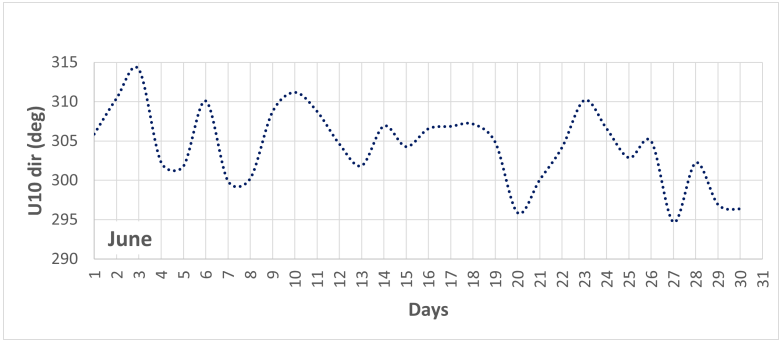

(e) Wind direction (deg)

Figure C.6: 27 years daily mean wave and wind characteristics for June

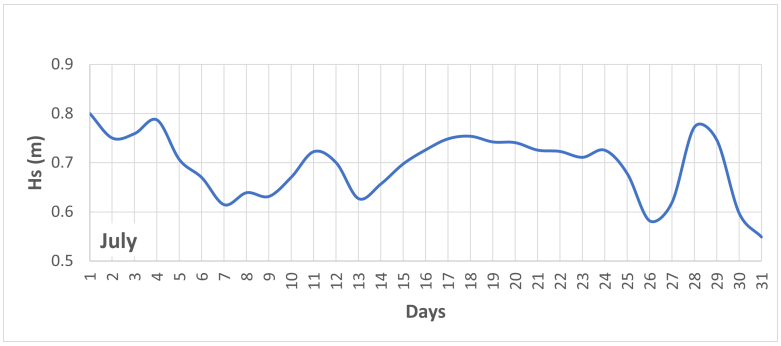

(a) Wave Height (m)

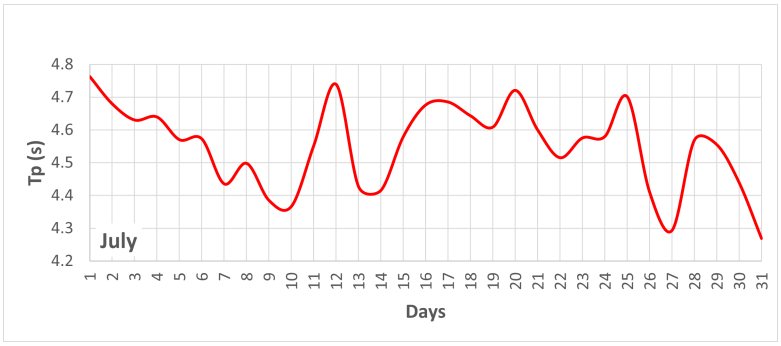

(b) Wave Period (s)

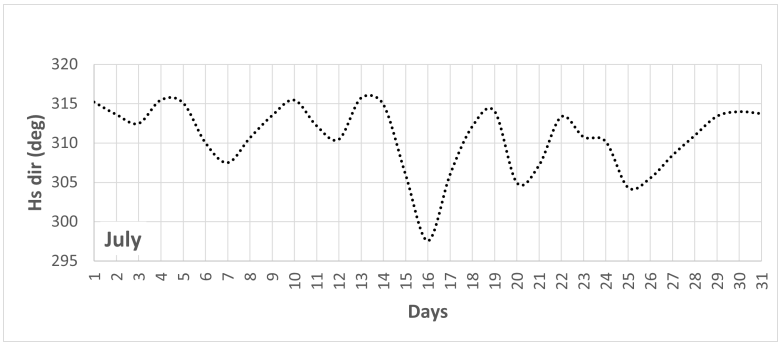

(c) Wave direction (deg)

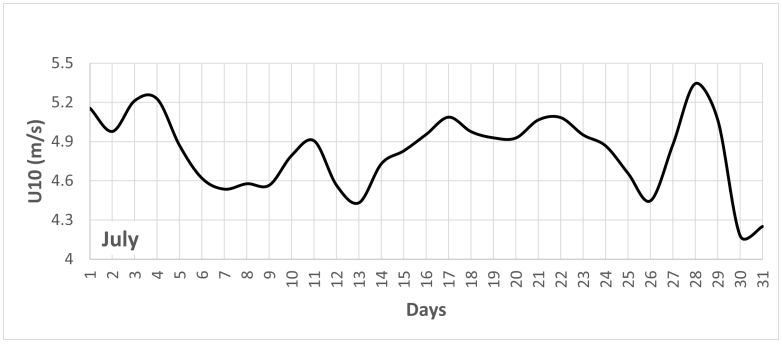

(d) Wind Speed (m/s)

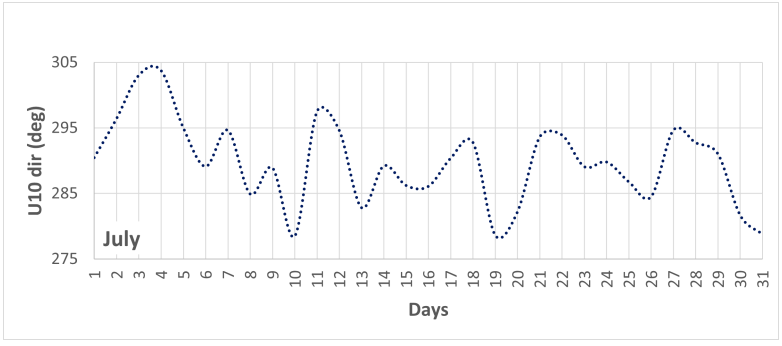

(e) Wind direction (deg)

Figure C.7: 27 years daily mean wave and wind characteristics for July

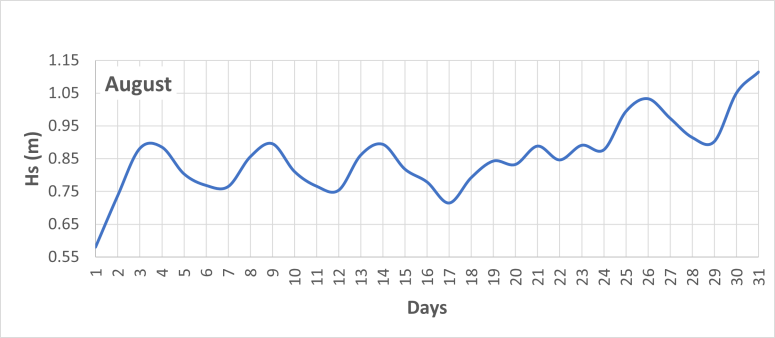

(a) Wave Height (m)

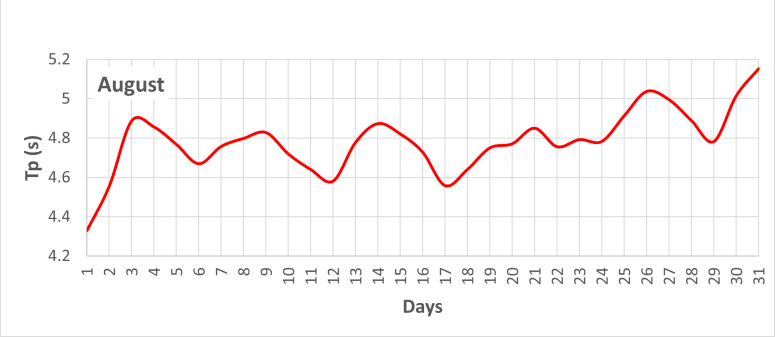

(b) Wave Period (s)

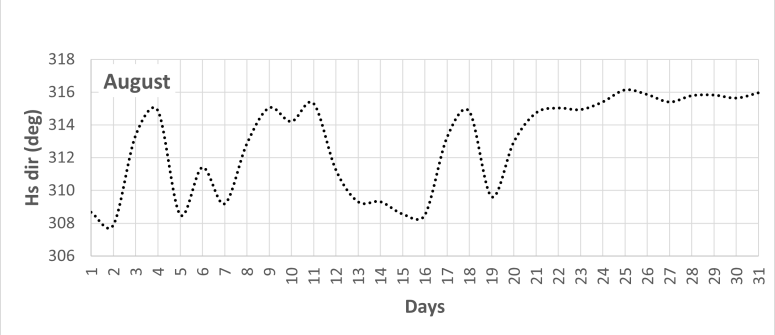

(c) Wave direction (deg)

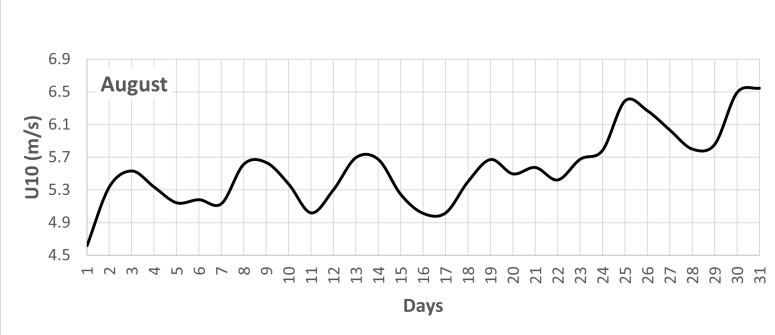

(d) Wind Speed (m/s)

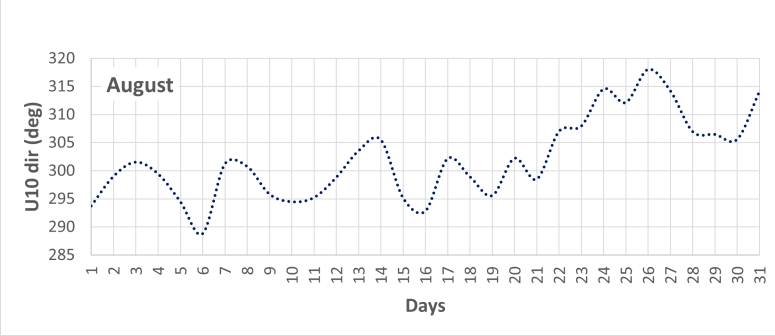

(e) Wind direction (deg)

Figure C.8: 27 years daily mean wave and wind characteristics for August

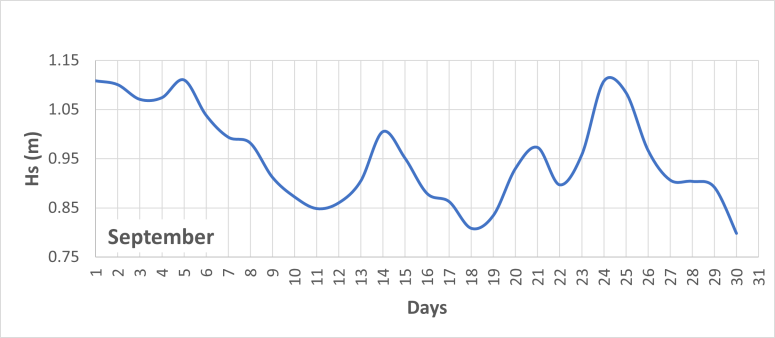

(a) Wave Height (m)

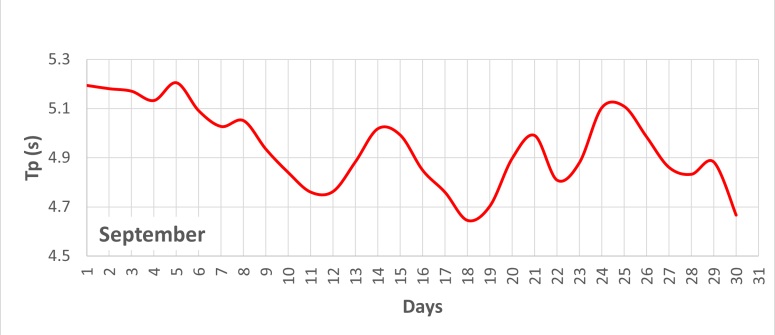

(b) Wave Period (s)

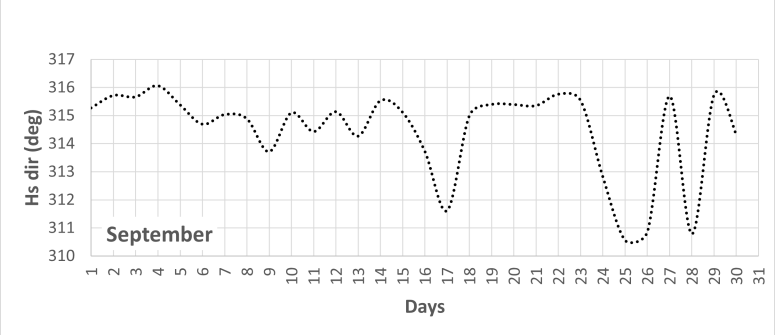

(c) Wave direction (deg)

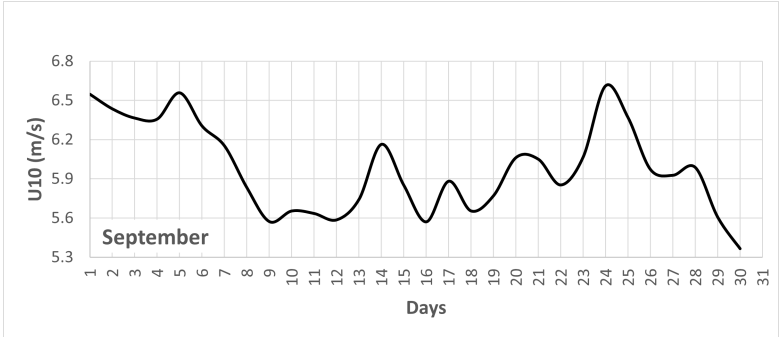

(d) Wind Speed (m/s)

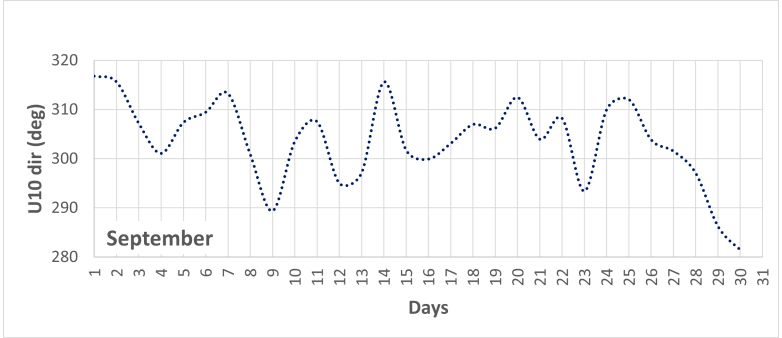

(e) Wind direction (deg)

Figure C.9: 27 years daily mean wave and wind characteristics for September

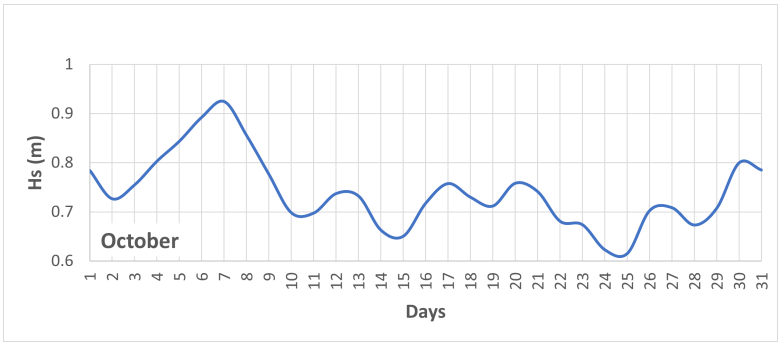

(a) Wave Height (m)

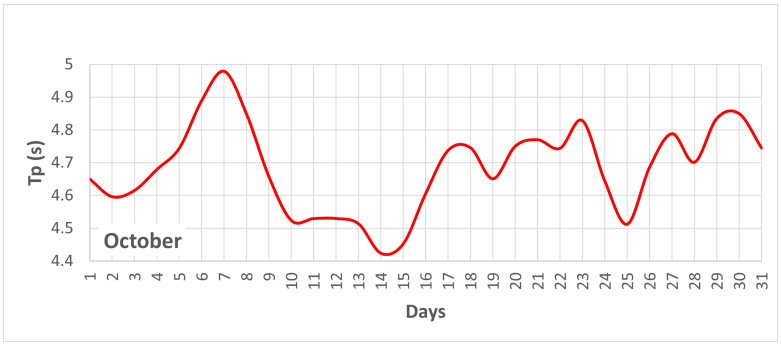

(b) Wave Period (s)

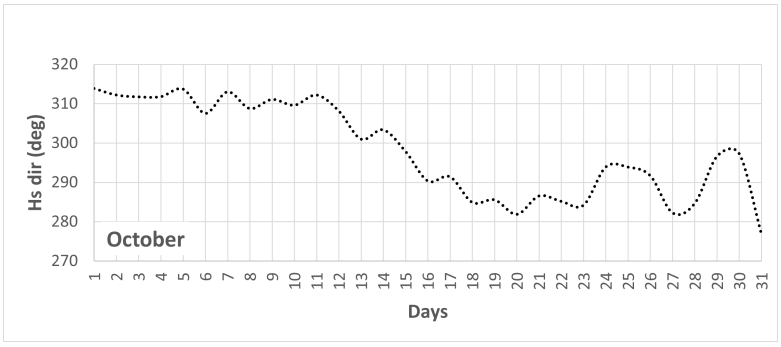

(c) Wave direction (deg)

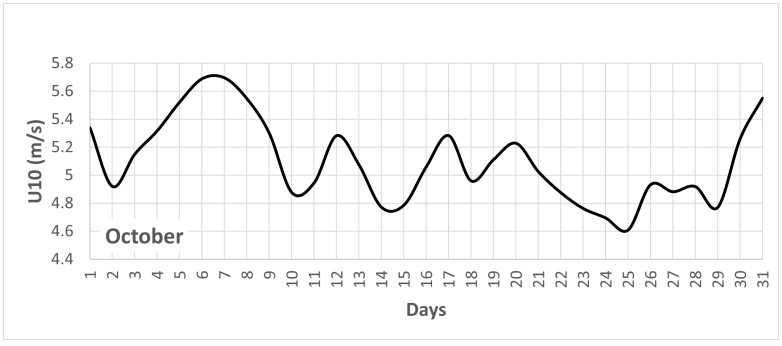

(d) Wind Speed (m/s)

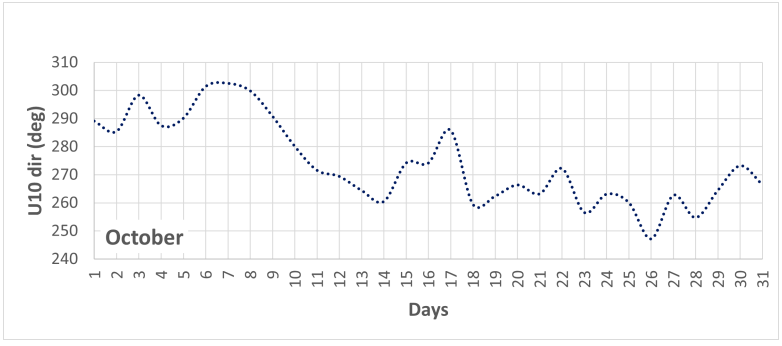

(e) Wind direction (deg)

Figure C.10: 27 years daily mean wave and wind characteristics for October

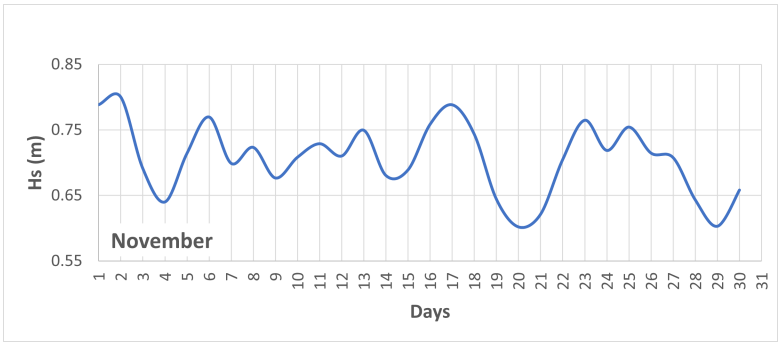

(a) Wave Height (m)

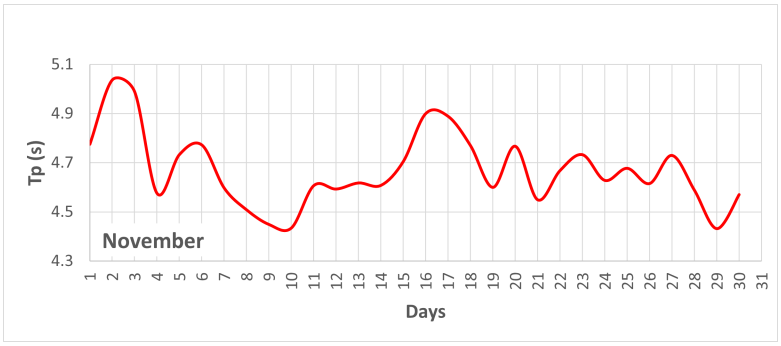

(b) Wave Period (s)

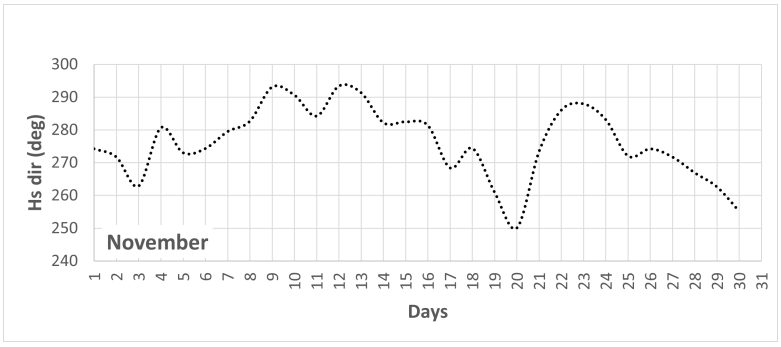

(c) Wave direction (deg)

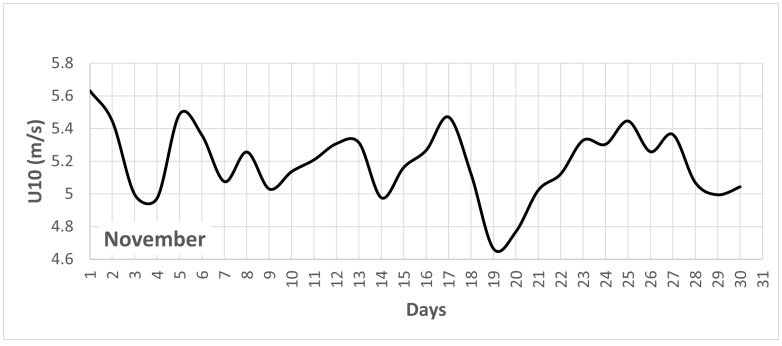

(d) Wind Speed (m/s)

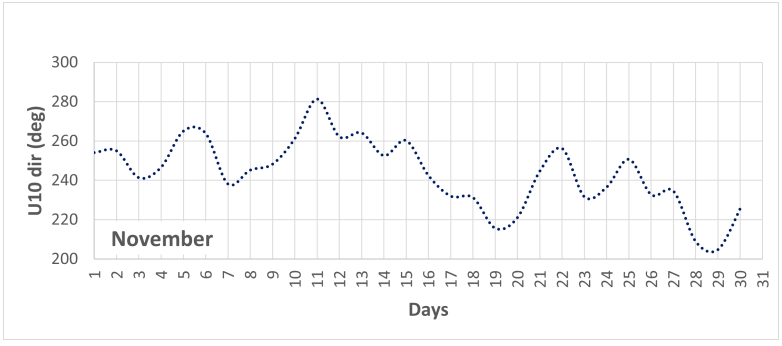

(e) Wind direction (deg)

Figure C.11: 27 years daily mean wave and wind characteristics for November

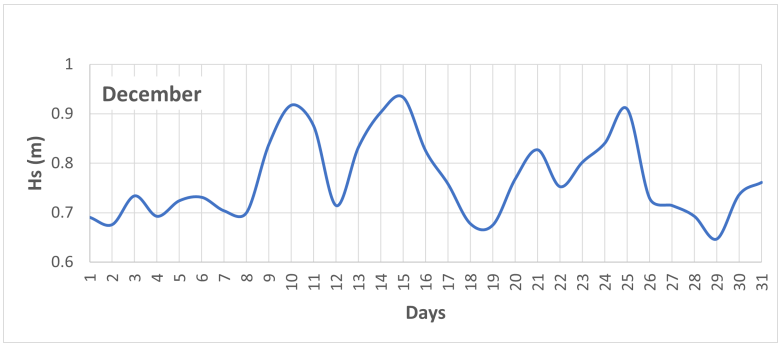

(a) Wave Height (m)

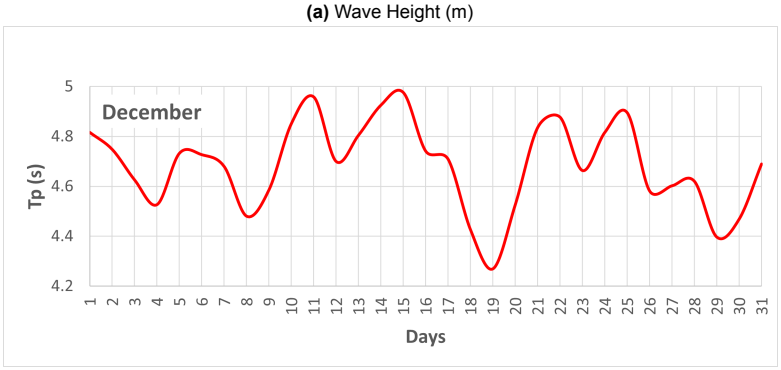

(b) Wave Period (s)

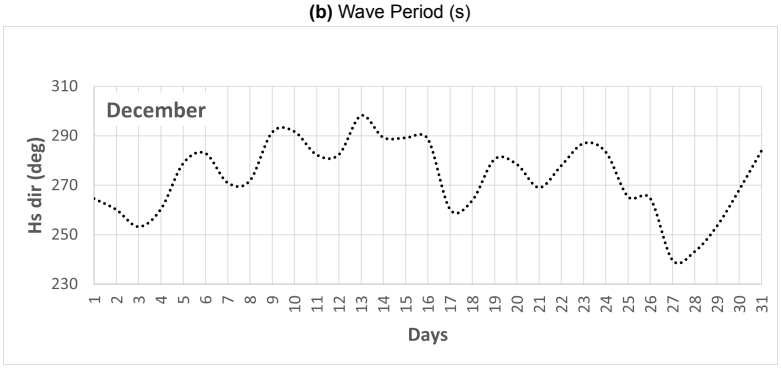

(c) Wave direction (deg)

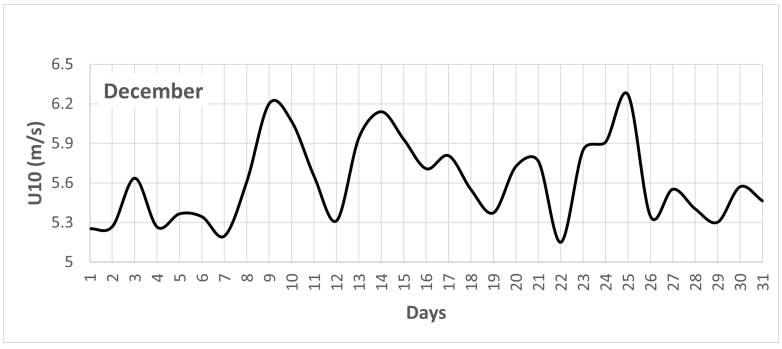

(d) Wind Speed (m/s)

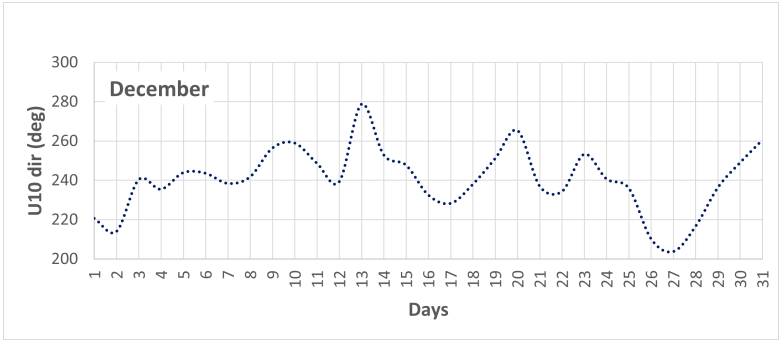

(e) Wind direction (deg)

Figure C.12: 27 years daily mean wave and wind characteristics for December

D

Storms

Table D.1: 59 storms obtained from the peak over threshold method for Extreme wave analysis. This table contains date, time and corresponding wind speed (u_{10}), wind direction (u_{10d}), significant wave height (H_s), wave direction (H_{sd}) and peak wave period (T_p)

Year	Month	Day	Hour	u_{10} (m/s)	u_{10d} (deg)	H_s (m)	H_{sd} (deg)	T_p (s)
1992	1	2	6	12.00	308	3.01	313	6.93
1992	2	10	6	11.40	316	2.69	315	6.93
1992	2	24	6	10.60	296	2.52	310	6.93
1992	6	1	0	12.20	326	3.57	318	7.62
1993	2	4	12	12.00	318	2.81	313	6.93
1994	4	8	9	12.00	320	2.65	316	6.93
1995	4	3	3	11.40	320	2.73	317	6.93
1996	3	7	3	10.80	304	2.74	310	6.93
1998	1	12	6	13.40	320	2.87	314	6.93
1998	3	18	9	11.40	314	2.57	317	6.93
1998	3	24	15	11.60	314	2.57	313	6.93
1998	5	31	9	11.80	314	2.61	312	6.93
1998	6	22	9	12.20	316	2.83	314	6.93
1998	7	10	6	11.60	318	2.70	315	6.93
1999	5	29	15	12.60	322	2.63	315	6.93
1999	5	30	9	11.60	314	2.54	313	6.93
1999	6	15	12	11.60	318	2.52	313	6.93
2000	1	28	9	12.20	304	3.03	312	7.62
2000	2	27	9	11.00	316	2.63	312	6.93
2000	3	24	3	11.00	314	2.52	314	6.30
2003	1	16	0	11.00	332	2.51	318	6.93
2004	3	6	18	7.40	326	2.60	315	6.93
2004	3	15	6	9.00	328	2.55	317	6.93
2004	3	30	15	11.60	320	2.52	316	6.93
2004	11	23	3	10.60	316	2.51	315	6.93
2006	3	9	9	10.60	310	2.71	314	7.62
2006	4	16	9	11.20	310	2.58	312	6.93
2006	6	11	9	12.00	322	2.54	313	6.93
2006	12	27	21	11.20	312	2.60	314	6.93
2007	2	4	3	11.40	294	2.54	308	6.93
2007	6	7	12	11.80	316	2.70	312	6.93
2009	2	11	3	10.80	328	2.63	319	6.93
2009	3	24	12	12.80	316	2.79	314	6.93
2010	2	4	3	13.00	328	2.84	318	6.93
2010	2	26	3	13.80	302	2.55	310	6.30
2010	3	18	12	13.80	316	3.37	315	7.62
2010	5	19	12	10.60	314	2.64	311	6.93

Year	Month	Day	Hour	u10 (m/s)	u10d (deg)	Hs (m)	Hsd (deg)	Tp (s)
2012	1	20	3	11.40	330	2.69	320	6.93
2012	2	25	9	12.60	314	3.37	317	7.62
2012	3	17	15	12.20	324	2.72	320	6.93
2012	4	19	12	13.00	318	3.00	317	7.62
2012	8	4	12	11.60	312	2.64	317	6.93
2013	3	17	12	13.00	318	2.87	317	6.93
2013	5	27	15	11.20	324	2.51	318	6.93
2013	7	1	15	11.40	326	2.53	318	6.93
2013	7	10	6	11.00	326	2.67	318	6.93
2013	7	18	12	12.20	318	2.79	319	6.93
2013	7	30	9	13.20	316	2.79	319	6.93
2014	5	19	3	9.80	326	2.53	317	6.93
2015	1	4	3	11.20	324	2.53	320	6.93
2015	1	12	0	12.40	322	2.88	318	6.93
2015	4	23	15	9.80	332	2.51	318	6.93
2015	6	10	12	12.40	320	2.62	315	6.93
2016	7	23	12	11.60	324	2.59	318	6.93
2016	8	1	9	11.60	318	2.62	317	6.93
2016	12	20	6	12.20	338	2.56	320	6.93
2017	1	27	6	11.40	328	2.60	321	6.93
2017	4	24	9	11.40	324	2.85	317	7.62
2018	3	29	18	11.20	330	2.58	324	6.93